

DESIGN OF AMPHIPHILIC NANOCAPSULES BASED ON HYPERBRANCHED STAR-BLOCK COPOLYMERS FOR THE ENCAPSULATION AND THE CONTROLLED RELEASE OF OLFACTORY COMPOUNDS

THÈSE N° 3770 (2007)

PRÉSENTÉE LE 4 MAI 2007

À LA FACULTÉ DES SCIENCES ET TECHNIQUES DE L'INGÉNIEUR
Laboratoire de technologie des composites et polymères
SECTION DE SCIENCE ET GÉNIE DES MATÉRIAUX

ÉCOLE POLYTECHNIQUE FÉDÉRALE DE LAUSANNE

POUR L'OBTENTION DU GRADE DE DOCTEUR ÈS SCIENCES

PAR

Céline TERNAT

DEA en polymères fonctionnels, Université Paris XII, France
et de nationalité française

acceptée sur proposition du jury:

Prof. H. J. Mathieu, président du jury
Prof. J.-A. E. Manson, Dr C.J.G Plummer, directeurs de thèse
Dr A. Herrmann, rapporteur
Prof. H.-A. Klok, rapporteur
Prof. E. Malmström, rapporteur



ÉCOLE POLYTECHNIQUE
FÉDÉRALE DE LAUSANNE

Lausanne, EPFL
2007

Acknowledgements

Je tiens à remercier ici les personnes qui ont contribué scientifiquement et humainement à l'aboutissement de ce travail. Je souhaiterais tout d'abord remercier le Professeur Jan-Anders Månson de m'avoir accueillie au sein de son laboratoire (Laboratoire de Technologie des Composites et Polymères) et m'avoir donné la possibilité de mener à bien ce projet. Je tiens également à remercier « l'agence de la confédération pour la promotion de l'innovation » (CTI) pour son support financier.

Sans le soutien continu du Dr. Christopher Plummer, la qualité de ce travail aurait assurément été moindre, et je tiens donc vivement à le remercier pour le suivi scientifique de mon travail ainsi que pour ses conseils pertinents et sa disponibilité tout au long de ces quatre années, et tout particulièrement lors de la rédaction de ce manuscrit. Je tiens également à remercier le Prof. Harm-Anton Klok, du Laboratoire des Polymères (LP), pour ses précieux conseils et nombreuses discussions scientifiques ainsi que pour son chaleureux accueil dans son laboratoire pour la synthèse des polymères. Je souhaiterais aussi particulièrement remercier Tuan NGuyen pour les très nombreuses analyses GPC effectuées.

Par ailleurs, je tiens à remercier spécialement Maria-Inès Velazco Senior Vice Président R&D chez Firmenich de m'avoir accueillie au sein du département « Analysis, Physical Chemistry and Human Bioresponse » et m'avoir donné la possibilité de côtoyer des chimistes et physico-chimistes spécialisés dans l'encapsulation et la délivrance de molécules olfactives. Aussi, je souhaiterais vivement remercier Dr. Andreas Herrmann pour sa grande disponibilité et ses pertinents conseils scientifiques et rédactionnels ainsi que Dr. Lahoussine Ouali de m'avoir accueillie dans son laboratoire et pour son intérêt envers ce travail. Je souhaiterais aussi remercier Dr. Wolfgang Fieber et Dr. Horst Sommer pour leur grand investissement et les résultats de diffusion apportés à ce travail.

Je tiens également à remercier Dr. Georg Kreutzer et Dr Damien Berthier pour leur aide technique, leur disponibilité et les nombreuses et enrichissantes discussions scientifiques ainsi que Pascal Beaussoubre et Dr. Guillaume Lamarque pour leurs judicieux conseils et leur précieux savoir faire.

Ces quatre années de thèse m'ont donné l'opportunité de rencontrer des personnes qui ont pris une place importante dans ma vie et qui par leur présence m'ont permis de conclure ce travail. Je tiens aujourd'hui à leur exprimer toute ma gratitude et mon amitié pour leur soutien et pour tous ces moments inoubliables. A ce titre je remercie vivement Xavier, Laurence, Christian, Dima, Joëlle, Loïc, Gil, Gaby, Chrystèle, et Laure.

Je remercie aussi mes collègues du LP, Harald, Nadja, Seb, Eric... et ceux de Firmenich Géraldine, Nathalie, Alexandrine et Djamila qui m'ont tous chaleureusement accueillie à leur côté et avec qui travailler fut un réel plaisir.

Surtout, j'adresse un grand merci à ma famille, mes parents et mes sœurs qui m'ont soutenue tout au long de ces années de thèse et d'études en générale ainsi qu'à la famille Rion pour leur présence durant cette dernière année et leur grand intérêt porté à mon travail.

Enfin, un grand merci à Julien pour son infinie patience. Je souhaiterais lui exprimer toute ma reconnaissance pour sa présence et son soutien quotidien et sans faille qui m'ont permis d'achever sereinement ce travail. Qu'il reçoive tous mes remerciements et mon amour.

Abstract

Effective encapsulation of small, volatile, weakly water-soluble molecules such as flavors and fragrances is necessary to protect them from degradation, to increase their lifetime, and to improve their water dispersion and fixation depending on the substrate of interest. The aim of this project has been to improve encapsulation and release in order to optimize the performance of fragrance molecules in water-based household (detergents, softeners, etc.) and body care applications (shampoos, lotions, etc.), and fine perfumery applications. More specifically, the aim has been to investigate the effectiveness of “unimolecular micelles” based on amphiphilic multi-arm star-block copolymers with a hyperbranched core with more than 26 functional groups, a hydrophobic inner and a hydrophilic outer shell. These have been prepared from a commercial hyperbranched polyester macroinitiator (HBP) by ring-opening polymerization of ϵ -caprolactone, followed by the atom transfer radical polymerization (ATRP) of *tert*-butyl acrylate (*t*BuA). Hydrolysis of the *tert*-butyl groups has then been used to convert the poly(*t*BuA) blocks to poly(acrylic acid) (PAA), resulting in HBP-(PCL)_p-(PAA)_q pH-dependent amphiphilic star-block copolymers with good control of the molecular weight distribution. These were shown to form stable nanocapsules with a well defined core-shell architecture, as confirmed by thermal and microstructural characterization.

The necessity of the core-shell architecture for the effective encapsulation of fragrance molecules in aqueous dispersion has been demonstrated by NMR (nuclear magnetic resonance). The extent of encapsulation reflects the dynamic equilibrium between the free molecules and the fragrance/polymer complex and is dependent on the octanol/water partition coefficient ($\log P$) of the fragrance compounds, as demonstrated with a similar non ionic core-shell architecture HBP-(PBMA)₃₇-(PPEGMA)₃₉ composed of a hydrophobic poly(butyl methacrylate) (PBMA) core and a hydrophilic poly(polyethylene glycol) methyl ether methacrylate (PPEGMA) shell (provided by the Polymer Laboratory of the EPFL). The

fragrance loadings in the polymer (HBP-(PCL)_p-(PAA)_q and HBP-(PBMA)₃₇-(PPEGMA)₃₉), which reached up to 30 wt% depending on the type of the fragrance molecule, were argued to be linked to their solubility in the hydrophobic core of the star-block copolymer. Moreover, under conditions representative of real applications (fine perfumery and softener applications) the star-block copolymers significantly extended the time over which the concentration of certain volatiles remained above the human olfactory threshold. Effective encapsulation and delayed release of small hydrophobic molecules was hence demonstrated to be possible with the present systems. The straightforward synthesis, tailorable chemistry and globular architecture of the star-block copolymers investigated here therefore offer promise for the development of relatively cheap encapsulants with affinities for specific components in fragrance packages, and release triggered by selected substrates according to their surface chemistry.

Keywords: Star-block copolymer, amphiphilic nanocapsules, core-shell architecture, hyperbranched polymer, ring-opening polymerization, atom transfer polymerization, delivery systems, encapsulation, fragrances

Version abrégée

Les médicaments, colorants, arômes et molécules odorantes sont généralement de petites molécules actives peu solubles dans l'eau. Afin de les protéger contre d'éventuelles dégradations (hydrolyse ou oxydation) ainsi que pour contrôler leur relargage et optimiser leurs performances en fonction de l'application, il est nécessaire de les encapsuler de façon efficace. Dans l'industrie des arômes et des parfums, les odeurs sont rapidement évaporées du fait de la grande volatilité des molécules olfactives. L'objectif de ce travail était d'améliorer l'encapsulation et le relargage des molécules olfactives pour optimiser leur perception dans des compositions à base d'eau telles que les produits ménagés (les détergents, les adoucissants,...) et les produits pour le corps (shampooing, lotion ...), ainsi que pour la parfumerie. Le but était plus spécialement d'étudier l'efficacité de nouveaux copolymères à blocs amphiphiles étoilés, tels des micelles unimoléculaires, comprenant un corps hyperbranché, une couche interne hydrophobe et une écorce externe hydrophile. Ces copolymères ont été préparés à partir d'un polyester hyperbranché commercial (HBP), par une polymérisation par ouverture de cycle (ROP) d' ϵ -caprolactone suivi d'une polymérisation par transfert d'atome (ATRP) de l'acrylate de *tert*-butyle (*t*BuA). Après hydrolyse des groupements *tert*-butyle du poly(acrylate de *tert*-butyle) (*Pt*BuA) en acide acrylique (PAA), un copolymère à blocs amphiphile et sensible au pH (HBP-(PCL)_p-(PAA)_q) est obtenu avec un bon contrôle des masses molaires. Selon les mesures des propriétés thermiques et l'observation de la microstructure, les copolymères amphiphiles à blocs étoilés obtenus se présentent sous la forme de nanocapsules stables avec une architecture cœur-écorce.

L'utilité de la structure cœur-écorce pour l'encapsulation de molécules olfactives en milieu aqueux a été démontrée par spectroscopie RMN. Le processus d'encapsulation consiste en un équilibre dynamique du polymère et des molécules olfactives entre leur forme libre et encapsulée. Cet équilibre est dépendant du coefficient de partition octanol/eau ($\log P$) des molécules olfactives tel que démontré avec un copolymère à blocs étoilé amphiphile non

ionique de même architecture HBP-(PBMA)₃₇-(PPEGMA)₃₉ composé d'un cœur hydrophobe de poly(*n*-butyle méthacrylate) (PBMA) et d'une écorce hydrophile de poly(méthacrylate de poly(éthylène glycol)) (PPEGMA) (fournit par le laboratoire des polymères (LP) de l'EPFL). La proportion de molécules olfactives dans les polymères (HBP-(PCL)_p-(PAA)_q et HBP-(PBMA)₃₇-(PPEGMA)₃₉) peut atteindre jusqu'à 30 % en poids (selon les molécules olfactives), et est liée à la solubilité des fragrances dans le cœur hydrophobe du copolymère à blocs étoilé. De plus, dans des conditions semblables à celles rencontrées lors des applications (parfumerie fine et adoucissants) le copolymère à blocs étoilé prolonge de façon significative la durée pendant laquelle la concentration des volatiles est supérieure au seuil de perception humain.

La possibilité d'encapsuler efficacement et de prolonger le relargage de petites molécules hydrophobes a ainsi été démontrée avec ce système. La structure globulaire et la possibilité de contrôler chimiquement les groupements terminaux des copolymères à blocs étoilés développés au cours de ce travail, leur confèrent une grande flexibilité permettant d'optimiser leur affinité avec les fragrances et de cibler le relargage en accord avec les fonctions chimiques présentes sur les surfaces sélectionnées.

Mots-clé: copolymère à blocs étoilé, nanocapsules amphiphiles, architecture cœur-écorce, polymère hyperbranché, polymérisation par ouverture de cycle, polymérisation radicalaire par transfert d'atome, système de délivrance, encapsulation, fragrance

List of acronyms

AFM	Atomic Force Microscopy
ATRA	Atom Transfer Radical Addition
ATRP	Atom Transfer Radical Polymerization
BHT	2,6-Di-tert-butyl-4-methylphenol
BSA	Bovine Serum Albumin
<i>bis</i> -MPA	2,2-Bis (hydroxymethyl)propionic acid
β -CD	β -Cyclodextrin
BMA	<i>n</i> -Butyl methacrylate
CDCl ₃	Deuterated chloroform
cmc	Critical micellar concentration
CRP	Controlled Radical Polymerization
DB	Degree of Branching
DEGMA	Diethylene glycol methyl ether methacrylate
DLS	Dynamic Light Scattering
DMAEMA	2-(N,N-dimethylamino)ethyl methacrylate
DMSO	Dimethylsulfoxide
DNA	Desoxyribo Nucleic Acid
DSC	Differential Scanning Calorimetry
e.c.	Ethylene carbonate
FID	Flame Ionization Detector
FT-IR	Fourier transform infra red spectroscopy
GC	Gas Chromatography
GPC	Gel Permeation Chromatography
HBP	Hyperbranched polymer
HEA	Hydroxyethyl acrylate
HEMA	Hydroxyethyl methacrylate
HMTETA	Hexamethyl triethylene tetramine
HS-SPME	Headspace Solid Phase Microextraction
Log <i>P</i>	Octanol/water partition coefficient

MALDI-TOF MS	Matrix assisted laser desorption/ionization time-of-flight mass spectroscopy
MEHQ	4-Methoxyphenol
Me ₆ TREN	Tris-2-dimethyl aminoethyl amine
MMA	Methyl methacrylate
MI	Macroinitiator
NMP	Nitroxide Mediate radical Polymerization
NMR	Nuclear Magnetic Resonance
M_n	Number average molecular weight
M_w	Weight average molecular weight
PAA	Poly(acrylic acid)
PAMAM	Poly(amido amine)
PBMA	Poly(butyl methacrylate)
PCL	Poly(caprolactone)
PEG	Poly(ethylene glycol)
PEGMA	Poly(ethylene glycol) methyl ether methacrylate
PEO	Poly(ethylene oxide)
PGA	Poly(glycolic acid)
PLA	Poly(lactic acid)
PMDETA	Pentamethyl diethylene triamine
PP50	Ethoxylated pentaerythritol
PPO	Poly(propylene oxide)
PtBuA	Poly(<i>tert</i> -butyl acrylate)
PtBuMA	Poly(<i>tert</i> -butyl methacrylate)
P&T-HS	Through Purge and Trap
PVP	Poly(vinyl pyrrolidone)
RAFT	Reversible Addition Fragmentation Transfer
ROP	Ring-Opening Polymerization
SAXS	Small Angle X-ray Scattering
SFRP	Free Radical Polymerization
SHS	Static Headspace
Sn(Oct) ₂	Tin(II)-ethylhexanoate
S&T-HS	Static and Trapped Headspace
<i>t</i> -BOC	<i>Tert</i> -butyloxycarbonyl

<i>t</i> BuA	<i>Tert</i> -butyl acrylate
<i>t</i> BuMA	<i>Tert</i> -butyl methacrylate
TEM	Transmission Electronic Microscopy
TFA	Trifluoroacetic acid
T_g	Glass transition temperature
TGA	Thermogravimetry Analyser
T_m	Melting temperature
TMP	2-(Hydroxymethyl)-1,3-propanediol
TMSI	Trimethyl silyl iodine
VPO	Vapor pressure osmometry

Table of content

Chapter I. General introduction.....	5
Chapter II. State of the art on delivery systems: From classical polymers to dendritic structures.....	9
I. Encapsulation and release technologies	11
I.1. Traditional polymer architectures in delivery systems	11
I.1.1 Encapsulation in foods and cosmetics	12
(1) Encapsulation technologies.....	12
(2) Carrier materials.....	13
I.1.2 Delivery systems in pharmaceuticals and health care.....	13
I.2. More sophisticated architectures for the controlled release of guest molecules: block copolymer micelles.....	14
I.3. Release mechanisms of physically entrapped guest molecules from polymer carriers.....	15
I.3.1 Mechanisms of release from polymer carriers.....	15
I.3.2 Factors that govern the release of guest molecules from polymer carriers	16
(1) Influence of the polymer properties in a micellar structure.....	16
(2) Case of shell cross-linked micelles	17
(3) Importance of the polymer-guest affinity and of the guest properties.....	18
II. Dendritic macromolecules	18
II.1. What is a dendritic structure?	18
II.2. Synthesis of dendrimers and hyperbranched polymers.....	19
II.2.1 Dendrimer synthesis	19
II.2.2 Hyperbranched polymer synthesis.....	20
II.3. Degree of branching in hyperbranched polymers	23
II.4. Physico-chemical properties of dendritic macromolecules.....	25
III. Host-guest affinities in dendritic macromolecules	27
III.1. Presentation of the concept	27
III.2. Unimolecular systems.....	28
III.2.1 The dendritic box.....	29
III.2.2 Inverse unimolecular micelles	30
III.2.3 PEGylated dendrimers	30
III.2.4 pH-sensitive dendrimers	32
III.3. Complementary binding sites: “Dendritic receptors”	33
III.3.1 Interactions within the dendrimer core	33
III.3.2 Recognition within polymer branches	38
III.3.3 Use of surface functions for molecular recognition.....	39
IV. Conclusions	41

Chapter III. Polymer synthesis: generalities	43
I. Classification of polymerization techniques.....	44
II. Chain polymerization.....	46
II.1. Conventional chain polymerization	46
II.2. “Living” and “controlled” polymerization.....	47
II.3. Controlled radical polymerization (CRP)	49
II.3.1 Principle.....	49
II.3.2 Different types of CRP	49
II.3.3 Atom transfer radical polymerization (ATRP)	52
II.3.4 ATRP from multi-arm macroinitiators	55
III. Ring-opening polymerization (ROP).....	56
III.1. General considerations.....	56
III.2. Multi-arm macroinitiators	58
IV. Conclusion.....	59
Chapter IV. Experimental methods	61
I. Materials	62
II. Synthesis of the amphiphilic star-block copolymer.....	63
II.1. ROP of ϵ -caprolactone.....	63
II.2. Synthesis of a multifunctional macroinitiator for ATRP	66
II.3. Polymerization of <i>tert</i> -BuA by ATRP using H40-(PCL) _p -Br as the macroinitiator	69
II.4. Hydrolysis of <i>tert</i> -butyl groups.....	77
II.5. Deprotonation of the acidic functions of the star-block copolymer	81
III. Encapsulation of fragrance compounds.....	82
IV. Release of fragrance molecules	83
IV.1. Release of olfactory compounds monitored by TGA	83
IV.2. Release of olfactory molecules monitored by headspace analysis.....	83
IV.2.1 In a fine perfumery application.....	83
IV.2.2 In a fabric softener application	85
V. Instrumentation.....	86
V.1. Nuclear magnetic resonance (NMR)	86
V.2. Gel permeation chromatography (GPC)	86
V.3. Fourier transform infra red spectroscopy (FT-IR)	87
V.4. Differential scanning calorimetry (DSC).....	87
V.5. Thermogravimetric analysis (TGA).....	87
V.6. Dynamic light scattering (DLS).....	88
V.7. Transmission electron microscopy (TEM)	88
V.8. Atomic force microscopy (AFM)	88

Chapter V. Synthesis of amphiphilic star-block copolymers from Boltorn® hyperbranched polymer89

I. Boltorn® HBP: Background	90
I.1. Preparation of Boltorn® HBP.....	90
I.2. Characterization of hyperbranched polymers based on AB ₂ type monomers.....	92
II. Characterization of the HBP cores	93
II.1. GPC	93
II.2. NMR.....	95
III. Preparation of amphiphilic star-block copolymer based on HBP polyester.....	99
III.1. Introduction.....	99
III.2. The hydrophobic layer: ROP of ε-caprolactone.....	101
III.3. The hydrophilic shell	106
III.3.1 Macroinitiator synthesis.....	106
III.3.2 Preparation of pH-responsive star-block copolymers	111
(1) Optimization of ATRP with tert-butyl methacrylate (tBuMA)	111
(2) ATRP of tBuA for the synthesis and characterization of H30-(PCL) _p -(PtBuA) _q and H40-(PCL) _p -(PtBuA) _q	113
(3) Is the ATRP of tBuA well controlled?	118
(4) Hydrolysis of the tert-butyl groups	122
(5) Solution properties of the water soluble HBP-(PCL) _p -(PAA) _q	128
III.3.3 Preparation of cationic star-block copolymers	129
III.3.4 Preparation of non-ionic star-block copolymers.....	131
III.4. Preparation of amphiphilic star-block copolymer with a glassy core and a neutral outer shell: H40-(PBMA) _p -(PPEGMA) _q	132
IV. Conclusion.....	136

Chapter VI. Physical properties of the star-block copolymers in the bulk and in solution137

I. Thermal properties and morphologies of the polymers in the bulk	137
II. Characterization in solution.....	142
III. Conclusion.....	145

Chapter VII. Encapsulation of olfactory compounds in aqueous dispersions of star-block copolymer monitored by NMR spectroscopy147

I. Characteristics of polymers and fragrance compounds	148
II. NMR diffusion and relaxation studies.....	150
III. Quantification of fragrance molecule loadings in an aqueous dispersion of star-block copolymer	154
III.1. General results	154
III.2. Influence of the polymer architecture	157
III.2.1 Effect of the polymer block length	157
III.2.2 Effect of the HBP core functionality	158
III.2.3 Results for geraniol, decanal and Vertenex®	161
III.3. Influence of the log <i>P</i> of the fragrances	161
III.4. Influence of the solubility parameters.....	162
IV. Conclusions	166

Chapter VIII. Industrial application: controlled release of fragrance molecules in fine perfumery and in fabric softener applications167

I. Release monitored by thermogravimetric analysis (TGA).....	168
I.1. Fragrance behavior	169
I.2. Fragrance release in the presence of star-block copolymer	170
II. Release monitored by dynamic headspace analysis	174
II.1. What is headspace analysis?	174
II.2. A fine perfumery application.....	175
II.2.1 Behavior of the volatiles.....	176
II.2.2 Behavior of the volatiles in the presence of the star-block copolymer	178
II.3. A fabric softener application.....	182
II.4. Olfactory panel	185
III. Conclusions	186

Chapter IX. Conclusions and future work187

Chapter X. Appendix191

Chapter XI. References199

Chapter I. General introduction

The delivery of functional agents, molecules, ingredients, or compositions such as drugs, dyes, flavors, fragrances, pharmaceuticals and agrochemicals is an important issue in applied science. Without the stabilization of a concentrated, easily transportable and processible form of the functional agent, delivery becomes unreliable and the agent will only rarely exhibit its beneficial properties at a predetermined time and place. In the particular case of the fragrance industry, many perfumes are very volatile and after application are perceived over only a relatively short period of time. Due to the demand for improved performance and added value of consumer products, it is increasingly important to extend the perception of the fragrance compounds in bodycare and household applications, such as shampoos, fabric softeners or detergent powders. Effective encapsulation is therefore required in order to protect the fragrance compounds from degradation and to control their release and hence optimize their performance according to the requirements of the application. The importance of this issue is born out by an increase in industrial demand from 2,000 tons in 2000 to 10,000 tons in 2003 of encapsulated fragrances.^[1]

A particular group of encapsulation systems, micro- or nanocapsules, is based on particles that contain hydrophobic functional agents, including fragrances or flavors, but which are dispersible or soluble in an aqueous environment, such as the aqueous phase of an emulsion (for example a shampoo, lotion or shower-gel). The encapsulation technologies that have been developed to date are largely based on linear, branched or cross-linked natural or synthetic biodegradable polymers.^[2-7] Amphiphilic block copolymers are also often used for the encapsulation of hydrophobic molecules. Encapsulation in this case takes place after self-assembly of the amphiphilic block copolymers into micelles.^[8-13] However, such micelles do not constitute an ideal delivery system because release of the guest molecules is generally dependent on the dynamics of the micellar structure, which are in turn sensitive to the polymer concentration, temperature and pH.

A more versatile approach to the encapsulation and controlled release of guest molecules that has attracted considerable recent interest is the use of dendritic macromolecules.^[14-16] Given their inherently amphiphilic character, suitably functionalized dendrimers may be considered to constitute stable “unimolecular” micelles.^[12, 13, 17-24] Properties associated with dendritic macromolecules, such as regular shape, solubility, adaptable surface functionality and internal cavities make them adaptable hosts for the retention of small molecules. Moreover, tailoring of their numerous end groups offers considerable scope for fine-tuning of their solubility and host-guest affinity.^[21, 25-31] On the other hand, the loading capacity of dendrimers may be restricted, limiting the amount of guest molecules that can be delivered^[32] and their cost may be prohibitive in many applications. Our interest has therefore been directed toward the design of unimolecular micelles based on hyperbranched polymers (HBPs),^[33, 34] which have been largely studied in our laboratory,^[35-40] and whose synthesis is less complex and time consuming than that of perfect dendrimers but leads to comparable globular architectures and chain end densities.^[41-45] In order to increase the effective molecular sizes and hence the loading capacity of the resulting micelles, commercial hyperbranched polymers have been used as multifunctional initiators for the synthesis of high molar mass amphiphilic star-block copolymers which are composed of a lipophilic core designed to encapsulate guest molecules and a hydrophilic shell that provides water-solubility and prevents aggregation. Due to their covalent nature, the star-block

copolymer micelles do not suffer the disadvantages of their non-covalent analogues referred to above.

In what follows, we detail the synthesis of a new range of highly functional amphiphilic multi-arm star-block copolymers, which is based on commercial hyperbranched polyester polyols referred to here as H30 and H40 (these differ in the number of functional groups per molecule). HBP was first used as a macroinitiator for the ring-opening polymerization (ROP) of ϵ -caprolactone to form a polycaprolactone (PCL) layer. A second hydrophilic shell was subsequently synthesized by atom transfer radical polymerization (ATRP) of a *tert*-butyl acrylate monomer. The hydrolysis of *tert*-butyl groups of the HBP-(PCL)_p-(*t*BuA)_q provides a pH-responsive star-block copolymer with a poly(acrylic acid) (PAA) outer shell, HBP-(PCL)_p-(PAA)_q.^[46, 47] In order to investigate the effect of the number of arms, the block lengths, the presence of the hydrophobic layer and the influence of its chemical nature on the encapsulation of active molecules, a series of different structures has been prepared. These have also been compared with non-ionic H40-(PBMA)_p-(PPEGMA)_q star-block copolymers, prepared in parallel by G. Kreutzer et al. by consecutive ATRP of *n*-butyl methacrylate (BMA) and poly(ethylene glycol) methyl ether methacrylate (PEGMA).^[48]

The capacity of these core-shell structures to encapsulate fragrance molecules has been tested in an aqueous medium by studying the evolution of the diffusion coefficient of the fragrance compounds in water in the presence and absence of the star-block copolymers, and by determining the fragrance molecule loading in an aqueous dispersion of the polymer. Four fragrance molecules, representative of compounds frequently encountered in practice, were chosen to provide a range of polarity, chemical structure and function. Finally, the release of the fragrance molecules in the presence of the amphiphilic star-block copolymers was studied under conditions similar to those in real applications, namely a fine perfumery application and a fabric softener application. The encapsulation and release studies were carried out in collaboration with the “Analysis, Physical Chemistry and Human Bioresponses” department, Division Recherche et Développement at Firmenich SA (Geneva). The fast evaporation of fragrance molecule leads rapidly to ambient concentration of fragrance below the human olfactory threshold. The encapsulants are used to prolong the duration of human perception by slowing down the evaporation process as shown schematically in Figure I.1. This may be

assessed using analytical techniques such as headspace analysis, but, ultimately, human perception is subjective, and brief reference is therefore also made to the conclusions of an “olfactory panel”.

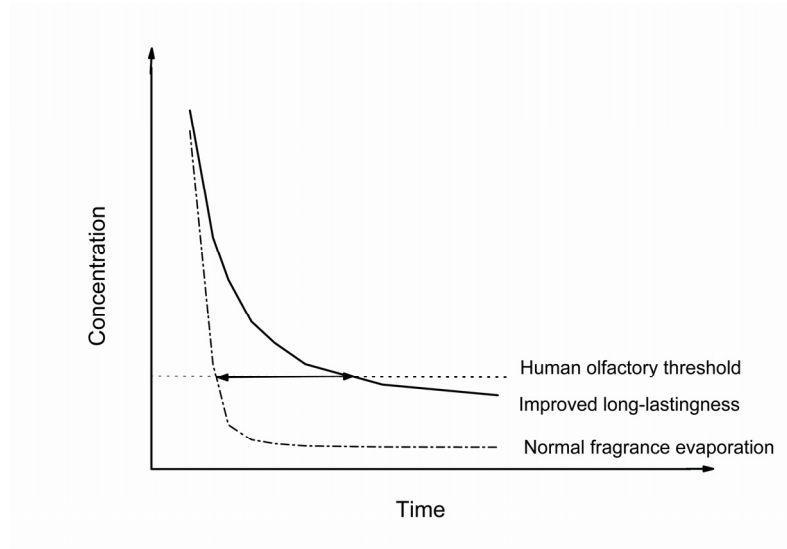


Figure I.1 Ambient concentration as a function of time of a fragrance molecule (-----) and of a fragrance molecule in the presence of an encapsulant (—)

Chapter II. State of the art on delivery systems: From classical polymers to dendritic structures

Delivery systems which include encapsulation and release technologies are currently of great interest in the field of perfumes, pharmaceuticals and foods industries, which explains their large development during the last years. In the field of controlled release systems, two main strategies have been adopted. In the first strategy, the polymer acts as *a carrier* for the active substance (guest) (Figure II.1, a) and the entrapment is based on non-specific or specific interactions. The release usually occurs by diffusion of the active substance or by degradation of the carrier by various mechanisms. The second strategy consists of covalently binding the active substance to the polymer, to give *polymer-“guest” conjugates*. Release then occurs on bond cleavage (Figure II.1, c and d). This chapter focuses on non-specific and specific interactions in *carrier* based systems which are the subject of this thesis, and *polymer-guest conjugates* (polymer prodrugs, etc) will not be discussed in detail, in spite of their considerable interest in a wider context.^[6, 7, 49, 50]

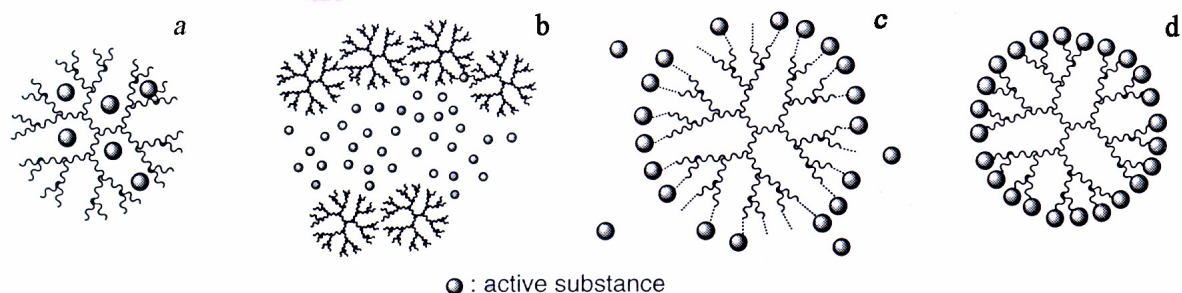


Figure II.1 Illustration of a carrier and a polymer-guest conjugate based on dendritic macromolecules.^[51] Physical entrapment: (a) encapsulation of guest molecules within the macromolecules or (b) macromolecular assembly. Polymer-guest conjugate: (c) labile bond and (d) covalent bond between the active substance and the polymer.

Until the development of dendritic structures (see section II)^[52, 53] in the 1980's, polymer science focused on the properties of linear (I), grafted (II and III) and network (IV) macromolecules (Figure II.2). Network polymers are also named cross-linked architectures. The encapsulation technologies frequently encountered until now essentially use linear and cross-linked polymers and depend on non-specific interactions between the carrier polymer and the guest molecule. These technologies are described in the first section of this chapter. The new polymer architectures recently developed as carrier molecules, such as micelles (obtained from block copolymers) and dendritic structures are then addressed. In the present work, the dendritic architecture is the basic building block. Details of the synthesis and properties of such macromolecules are therefore given in the second section of this chapter. Their advantages as host molecules, capable of interacting with guest molecules by non-specific and specific interactions are discussed in the final section

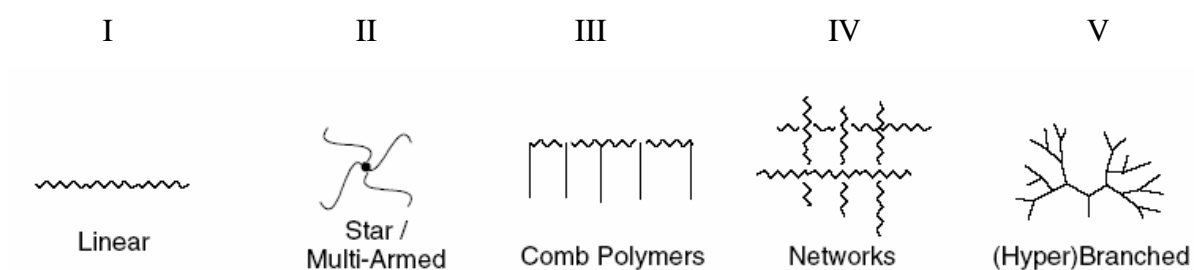


Figure II.2 Schematic of the four main type of polymer architecture. Linear (I), grafted (II and III), network (IV) and (hyper)branched (V) polymers.

I. Encapsulation and release technologies

In what follows traditional techniques are first described for the preparation of encapsulants based on linear polymers for perfumes, foods and pharmaceutic applications. Recent more sophisticated architectures, based on self assemblies of block copolymers that can directly incorporate guest molecules, are then discussed. The mechanisms of release of the guest molecules from the different capsule types are also described, as well as the effect of polymer properties on release.

I.1. Traditional polymer architectures in delivery systems

Controlled release systems have been initially developed in the food industry^[3, 54-56] in order to produce flavors in a dry form and to provide protection. Microencapsulation of flavors, fragrances and inks has also been widely described in the cosmetic and paper industries.^[2, 4, 57-59] Since 1950's delivery systems based on polymers have been implemented in pharmaceuticals and medicine.^[60-63] In recent years, increasingly sophisticated materials and techniques have been considered in these main field of applications, medicine^[64] cosmetics^[5] and food industries.^[5, 65]

The entities obtained after encapsulation of guest molecules by macromolecules are referred to as “microcapsules” or “microspheres”. Here, and in the rest of this manuscript, “microcapsule” refers to any particle in the size range of about 5 μm to 2000 μm that contains active agents. The prefix nano- is used to refer to any particle in the size range below 1 μm .

I.1.1 Encapsulation in foods and cosmetics

In the food industry, the protection of ingredients from the surrounding environment (water, acid, oxygen) and from other ingredients is of particular importance. However, in addition to protecting specific compounds, encapsulation methods have been developed to allow the controlled release of compounds or simply change the state of the ingredient from a liquid to a solid to permit its use in dry applications. Encapsulation can also be used to mask odors or tastes. In the cosmetics industry, encapsulation protects volatile components from the environment, improves long term stability and efficiency and sustains their release over long periods.

(1) Encapsulation technologies

Various techniques have been described in the literature, e.g. by Brannon-Peppas and Risch^[2, 66] and are similar in the food and cosmetic industries. They include atomization procedure (spray drying, chilling, cooling and fluidized bed coating), emulsion (simple or double), coacervation, extrusion, liposome entrapment and molecular inclusion.^[2-4, 66-68] Some of these are briefly described in Appendix 1. Liposome and molecular inclusion systems, even if they are not based on polymers assembly, are considered further here because they resemble the system considered in the present project in that the “host” pre-exists and is not produced by a particular technique, e.g. atomization or coacervation.

Liposomes,^[69] which are used in foods and cosmetics, are composed of natural phospholipids and sphingolipids. These amphiphilic macromolecules are self assembled in solution to form vesicles or membranes made up of one or two layers. Such structures are able to entrap hydrophobic or hydrophilic active molecules, and because they are lipophilic, they

penetrate the skin easily. Their size varies between 50 nm and a few microns. However, delivery is not controlled with these structures owing to their sensitivity toward temperature, salt concentration, extreme pH values and surfactants.^[59]

Molecular inclusion refers to the entrapment of the active molecules (fragrances, flavors or volatiles) by a pre-existing system analogous to a cage. Cyclodextrins are well known in this context. They are obtained by enzymatic degradation of starch and reassociation of the chain ends to form closed circular molecules with glucose monomers in the cavity and the hydroxyl functions at the periphery. Cyclodextrins thus combine a hydrophobic cavity with water solubility, making complexation with hydrophobic guest molecules possible.^[70-72] The use of cyclodextrins for the design of new architectures is currently under investigation,^[25, 67, 73-75] an example being the use of cyclodextrin as a hydrogel.^[76]

(2) *Carrier materials*

Microencapsulation in the food and cosmetic industries has been widely based on natural polymers. Carbohydrates such as starches (and modified starches), dextrans, maltodextrin, cyclodextrin, cellulose and gums are known for their exceptional capacity to encapsulate hydrophobic compounds^[77] and account for the majority of the food market. These are all hydrophilic amorphous substances capable of forming a glass on removal of water. Alginates, proteins, lipids (liposomes)^[69] and gelatin are also often used.^[2-5, 59, 68] Recently, Park and Arshady^[5] have published a compilation of patents on perfume microencapsulation, comprising a description of perfume materials and their properties also outlining the use of synthetic organic polymers in perfumes and cosmetics.^[5, 78]

I.1.2 Delivery systems in pharmaceuticals and health care

Pharmaceutical technologies, drug-delivery systems are chosen depending on how and where they will be degraded in human body. Some drugs need to be solubilized in the body before they can act on their target receptor. Other delivery systems consist of an implant of

the drug delivery system directly at the site. A drug that is to be released in the stomach will require controlled release very different from that of a drug that is to be released in the blood. For this reason delivery systems are classified as a function of the mechanisms of erosion of the drug. Biodegradable materials are preferable because the metabolism and excretion of the polymer results in its complete removal. Thus, the polymer materials most often employed in this field possess anhydride, ester or amide bonds, although nonbiodegradable backbones based on C-C bonds are also used in drug delivery.^[79]

The major families of natural and synthetic polymers (e.g. polyester: poly(lactic acid) (PLA), poly(glycolic acid) (PGA), poly(caprolactone) (PCL); polyanhydride; polyamide: poly(amino acid), poly(urethane); polysaccharides....) used in this field have been widely studied and reviewed^[79-81] with details being provided on formulation techniques and erosion mechanisms. Encapsulation technologies are similar to those employed in food and cosmetics applications. Oil in water emulsion or double emulsion, freeze drying, salting out and dialysis are used for the encapsulation of DNA (desoxyribo nucleique acid), calcein, coumarin and bovine serum albumin (BSA) for example.^[12, 82-85] Liposomes and biopolymers (chitin, cellulose, gelatine...) are also often used in drug delivery.^[80]

I.2. More sophisticated architectures for the controlled release of guest molecules: block copolymer micelles

The overview in section I.1 illustrates that the microencapsulation techniques developed to date are largely based on linear, branched or cross-linked natural or synthetic polymers, and need to be formulated to serve as carriers. Although physicochemical limitations are imposed by the use of natural polymers in pharmaceuticals, biopolymers remain strongly represented.

There has nevertheless been recent interest in the use of micelles as nanocarriers for hydrophobic drugs.^[8, 9, 12, 86, 87] Amphiphilic block copolymers with hydrophobic and hydrophilic blocks can self assemble under suitable conditions of pH, concentration, temperature and solvent. Thus, water-soluble polymeric micelles self-assemble by association

of the hydrophobic blocks to form an inner core, which is protected by hydrophilic segments. The driving force for micellization is hydrophobic interactions, but may involve additional forces, for example electrostatic interactions. PLA, PGA, poly(propylene oxide) (PPO), PCL are among the most frequent hydrophobic blocks and poly(acrylic acid) (PAA), poly(ethylene oxide) (PEO), poly(vinyl pyrrolidone) (PVP) are typically used as hydrophilic blocks.^[12] However, as is well known for liposomes, the instability of such assemblies to concentration, salt, pH, may cause problems in delivery systems. Recent research has shown that cross-linking of the external shell may improve stability.^[87] The structure of such an assembly is discussed in section I.3 in terms of release mechanisms.

I.3. Release mechanisms of physically entrapped guest molecules from polymer carriers

I.3.1 Mechanisms of release from polymer carriers

Depending on the technology used for encapsulation and the resulting guest molecule interactions, different release mechanisms may occur. As pointed out in section I.1.1(1), atomization procedure (spray drying, chilling, cooling and fluidized bed coating), emulsion (simple or double), coacervation, extrusion, liposome entrapment, molecular inclusion and self assembly of block copolymers are the usual technologies for the entrapment of drugs and volatiles in a polymer carrier. These encapsulation technologies generally involve release by the *solvent effect* and *diffusion*. Other release mechanisms include degradation and particle fracture.

Release by the *solvent effect* occurs on swelling of the particle by a solvent (generally water) followed by a sudden release of the active molecules due to bursting, or by continuous delivery, controlled by modification of the solvent, salt concentration or pH modification. In the case of micellar structures, release by the bursting effect is observed below the critical micellar concentration (cmc).

Release by *diffusion* is dependent on the rate at which the active molecules are able to pass through the particles. It is thus governed by the chemical and physical properties of the polymer and particles (pore size, matrix structure) and by the physicochemical properties of the guest molecules.^[79]

Release of the active substances by degradation may be induced by melting, hydrolysis (erosion) or enzymatic degradation of the matrix.^[79] Release by particle fracture may result from pressure, shear or differences in osmotic pressure or vapor pressure.

I.3.2 Factors that govern the release of guest molecules from polymer carriers

(1) Influence of the polymer properties in a micellar structure

It has been demonstrated, mainly on the basis of self-assembled amphiphilic block copolymer micelles, that various parameters influence the rate of diffusion of the active molecules. The thermal properties of polymers play an important role in the evaporation of volatiles.^[88] As reported by Stern,^[89] release from glassy polymers consists of diffusion through pores in the matrix, and depends on how the volatiles are introduced into the pores. Molecular motions are restricted and diffusion is slow in the glassy state, and loss of volatiles depends principally on the rate at which they migrate to the matrix surface (proportional to the molecular diffusion coefficient and the water concentration: at high relative humidity, the molecular mobility and diffusion coefficients increase, resulting in accelerated loss of volatiles^[90]), rather than the relative volatilities of the active molecules.^[91] Rubbery polymers generally have very short relaxation times and a greater free volume, so they respond relatively rapidly to variables such as temperature or moisture.

The crystalline properties of the matrix may also be important. Above T_g , macromolecular chains may have enough mobility to associate and form crystalline structures inducing a decrease in mobility and reducing the diffusion of active molecules. Moreover, crystallization limits the free volume between polymer chains, forcing the active molecules to

be released by expulsion.^[92] In the case of micellar structures, crystallization of the internal block stabilizes the structure and can cause a decrease in guest molecule mobility.^[12]

The polymer block length can also influence the rate of diffusion of the active molecules. An increase in the hydrophobic block length favors self-association of the copolymers and increases the size of the core, resulting in a longer diffusion path and a decrease in the release rate.^[93]

(2) *Case of shell cross-linked micelles*

Cross-linked micelles have been developed by Wooley and coworkers^[94] and subsequently by other groups.^[87, 95-98] The stability of micelles with cross-linked shells is enhanced, making them interesting for controlled release applications. Moreover, preparation of hollow nanosized particles (nanocages) is possible after removal of the core, as illustrated in Figure II.3.^[95, 98, 99] Nanocages are interesting for controlled release applications owing to their higher loading capacities, compared with the micellar precursors. Moreover, they may be suitable for hydrophilic guest molecules that cannot be encapsulated in a hydrophobic core. Their feasibility as delivery agents is currently under investigation and the first experiments suggest that the release rate of active molecules can be controlled by appropriate tailoring of the nanocages.^[95, 100, 101] As expected, active molecules present in the core-shell interface or in the shell diffuse faster than those located in the core.^[91]

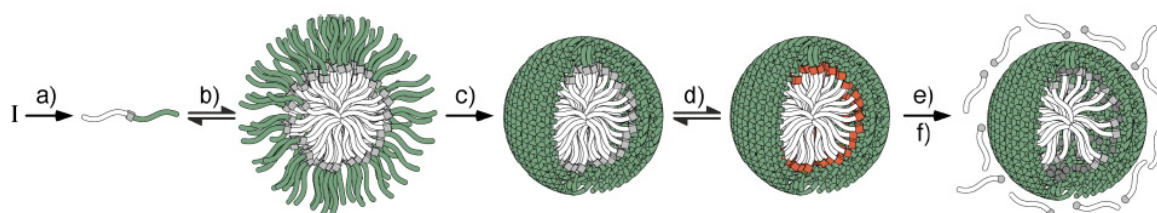


Figure II.3 Synthetic approach for the preparation of shell cross-linked nanocages. Preparation of the micelle (a, b), cross-linking (c), cleavage of the core-shell bonds (d) and solubilization of the hydrophobic core fragment in adequate solvent (e, f)^[101]

(3) *Importance of the polymer-guest affinity and of the guest properties*

The release of guest molecules is also governed by the polymer-guest molecule affinity and by the properties of the guest molecule. In general, the stronger the interaction, the slower the release. The physical state and molecular volume of the guest molecule also have an influence. The larger the molecular volume, the lower the diffusion coefficient and the diffusion rate. It has also been observed with certain drugs that the higher the loading, the lower the diffusion rate, owing to crystallization of the active molecules.^[93]

II. Dendritic macromolecules

Before discussing recent developments in host-guest systems based on dendritic macromolecules in section III, a presentation of the dendritic structures (synthesis and physico-chemical properties) is given which also serves to provide background for the synthesis and characterization work (Chapter V).

II.1. What is a dendritic structure?

Dendritic macromolecules are characterized by their globular structure which derives from a tree-like branched architecture. They are composed of a central core and of ramification points which correspond to monomer units. Because of their compact conformations they do not entangle in spite of their large molecular masses. The term “dendritic macromolecules”, includes dendrimers, dendrons, dendrigrafts and hyperbranched polymers (HBPs). It is usual to divide these into three subclasses according to the degree of structural perfection attained. Dendrimers and dendrons ((c) and (d)) are the most controlled structures, followed by dendrigrafts (b), which are semi-controlled, and hyperbranched polymers (a), which are poorly controlled (Figure II.4). In what follows, we focus essentially on dendrimers and hyperbranched macromolecules. In the present work, the term “dendritic macromolecules” is used to refer both to dendrimers and hyperbranched structures.

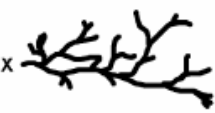
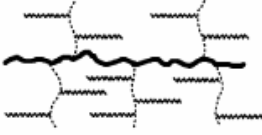


(a) Statistical Structure	(b) Semicontrolled Structure	(c) (d) Controlled Structures	
Random Hyperbranched	Dendrigrfts	Dendrons	Dendrimers
			
MW 1–100 kDa Mw/Mn = 2–10	MW 1–10 ⁴ kDa Mw/Mn = 1.1–1.5	MW 1–10 ³ kDa Mw/Mn = 1.0000–1.05	

Figure II.4 Tomalia's representation of the three subclasses of dendritic macromolecules^[102]

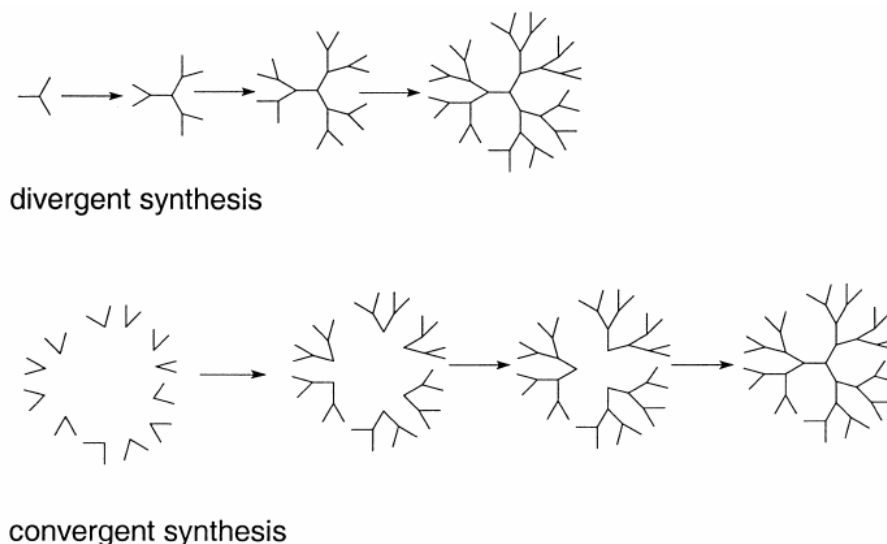
Dendrimers were envisaged for the first time by Flory in 1941.^[103] However the first reports of dendritic structures did not appear before 1978 with the work of Vögtle and coworkers.^[104] Since two decades, Newkome and Tomalia focused on the synthesis and chemical and physical properties of these particular architecture.^[52, 53] It is only in the past decade that researchers have begun to explore the potential of dendritic polymers in different fields of application, such as medicine, coatings, additives, nanotechnologies and supramolecular sciences, based on their rheological, conformational, electronic and magnetic properties.

II.2. Synthesis of dendrimers and hyperbranched polymers

II.2.1 Dendrimer synthesis

The first dendrimers were prepared by “divergent” synthesis during the 1980s,^[52, 53] in which the dendrimer built up from a polyfunctional core by successive addition of generations of branch units. This type of synthesis is a multi step process, requiring protection, deprotection and purification on addition of each generation. Another approach, called “convergent” synthesis, has lead to an increase in the range of dendrimers with controlled

structure and extreme purity. In convergent synthesis, (which was developed in the 1990s by Hawker and Fréchet^[105]) dendritic arms are first synthesized, then grafted to a core. A scheme of these two approaches is given in Scheme II.1.



Scheme II.1 Two approaches to dendrimer synthesis: “divergent” and “convergent” strategies^[106]

Since the development of convergent synthesis, the main innovations, adaptations and improvements have been aimed at decreasing the number of reaction steps and increasing the efficiency of the synthesis, e.g. the two stage convergent approach of Wooley et al.,^[107] the double exponential growth strategies of Moore and coworkers^[108] and the orthogonal monomer systems first described by Spindler and Fréchet^[109] but also demonstrated by Zeng and Zimmerman.^[110]

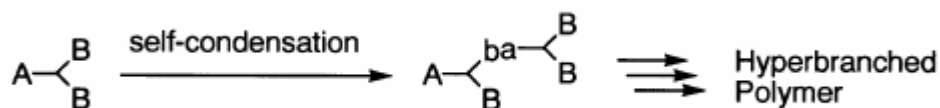
II.2.2 Hyperbranched polymer synthesis

The concept of hyperbranched polymer (HBP) synthesis first appeared in 1952, with the theoretical approach of Flory to the preparation of hyperbranched macromolecules from polyfunctional monomers in a statistical growth process.^[111] The preparation of well defined dendritic polymers is often time consuming and expensive. In the case of hyperbranched polymers, the time and the cost of the synthesis is typically reduced and “one pot” synthesis

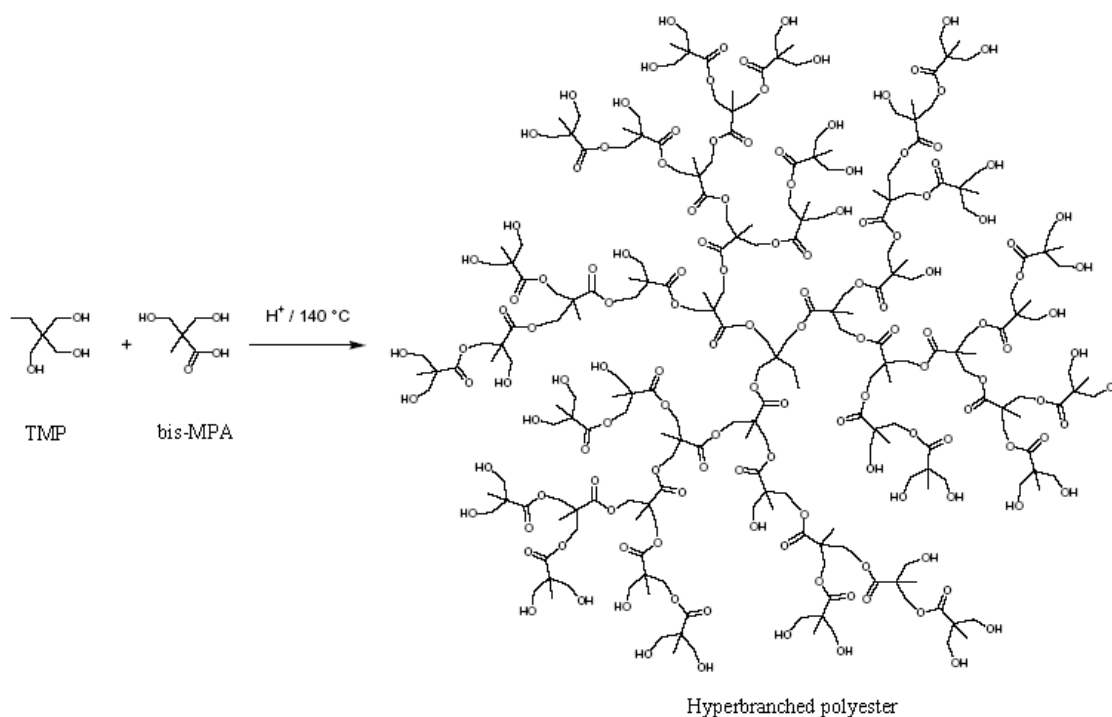
may be envisaged for large-scale production. Polydisperse highly branched dendritic molecules, with defects between segments, were first obtained in 1990 by Kim and Webster, who adopted the term “hyperbranched polymers”^[112] (HBPs). The synthesis and physico-chemical properties of hyperbranched polymers, which are intermediate between those of linear and dendritic polymers, have since been widely investigated.^[14, 15, 33, 34, 113-115]

There are now three major methods used for the preparation of hyperbranched polymers: step-growth polycondensation, self-condensing vinyl polymerization and multi-branch ring-opening polymerization. The HBP used in this project, has been prepared from the step-growth polycondensation procedure. This procedure is developed in what follows. The other two strategies are described in Appendix 2.

The step-growth strategy was initially used for the synthesis of a wide range of HBPs from AB_x monomers (Scheme II.2). AB_2 type monomers are often used as starting materials because of their relative ease of preparation. The synthesis of aliphatic hyperbranched polyesters has been studied extensively. A well known example is that of Malmström et al. (Scheme II.3), which makes use of 2-(hydroxymethyl)-1,3-propanediol (TMP) as a core and 2,2-bis(hydroxymethyl)propionic acid (*bis*-MPA) as the AB_2 monomer.^[41] The esterification was carried out in the bulk using an acid catalyst. The hyperbranched polyesters obtained possess high molecular weights ($M_w = 1880-10765 \text{ g mol}^{-1}$), high degrees of branching (96-83 %) and relatively low polydispersities ($M_w/M_n = 1.36-1.92$). In 1996, Malmström described the synthesis of hyperbranched polymers based on a *bis*-MPA monomer and different B_y functional polyol cores^[116] by polycondensation. This work was carried out in collaboration with Perstorp AB, a Swedish company. The importance of the presence of a core molecule for the polydispersity of the sample was demonstrated. The core molecule was shown to be crucial for the synthesis of hyperbranched polymers with structures comparable to those of dendrimers. Poly(phenylene), poly(amide), poly(carbonate), poly(urethane) and poly(ether) hyperbranched polymers have also been obtained by step-growth polycondensation.



Scheme II.2 Schematic of step-growth polycondensation of an AB_2 type monomer^[33]



Scheme II.3 Synthesis of hyperbranched aliphatic polyester from *bis*-MPA as the AB_2 monomer and TMP as the core molecule^[41]

Owing to the statistical nature of the synthesis, steric hindrance of the growing chains and the reactivity of functional groups, HBP structures are less well controlled than for perfect dendrimers and defects are present (linear units, Scheme II.4). Reactive groups are not located in regular positions. Thus the degree of branching of dendrimers and HBPs may be very different, resulting in differences in their physico-chemical properties.

II.3. Degree of branching in hyperbranched polymers

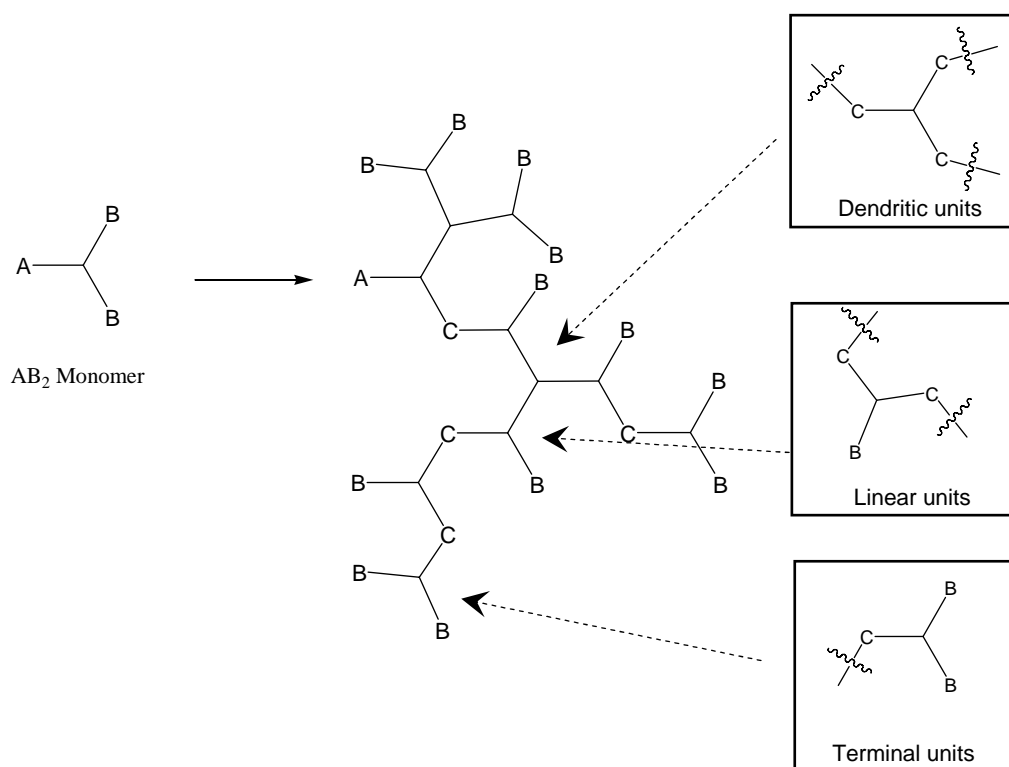
As shown in Scheme II.4, HBPs consist of dendritic units (D) (all the reactive groups of the AB_2 monomer have reacted), linear units (L) (one B group has not reacted) and terminal units (T) (the two B groups have not reacted). Linear units are generally considered to be defects. To compare the structure of HBPs with that of perfect dendrimers, Fréchet and coworkers introduced the “degree of branching” (DB) defined by comparing the sum of dendritic and terminal units to the total number of units in the macromolecule (Equation II.1).^[42]

$$DB = \frac{D+T}{D+T+L} \quad \text{Equation II.1}$$

In 1997, Frey and coworkers proposed another expression for the degree of branching, by considering the degree of polymerization (Equation II.2).^[117]

$$DB = \frac{D+T-N}{D+T+L-N} = \frac{2D}{2D+L} \quad \text{Equation II.2}$$

Here N is the number of molecules. Equations II.1 and II.2 give the same value of DB for hyperbranched polymers with high molecular weights, as N becomes negligible compared with the other quantities.



Scheme II.4 Representation of the three repeat units present in HBP architectures

The DB of a perfect dendrimer is hence 1, whereas for linear polymers DB is equal to 0. Frey suggested that DB for HBPs produced by a one pot synthesis of AB_2 monomers should be close to 0.5.^[117] One of the most important challenges in hyperbranched polymer synthesis is to produce HBPs with narrow molecular weight distributions and with DB close to 1 using a one pot polymerization of AB_x monomers. Frey and coworkers have described various attempts to increase the DB of HBPs.^[33, 118, 119] A limiting value of 0.66 was obtained using the technique of slow monomer addition at high degrees of conversion^[119] whereas Malmström et al. determined a value of 0.80 for hyperbranched polyester obtained by pseudo one pot synthesis.^[41]

II.4. Physico-chemical properties of dendritic macromolecules

Because of their compact globular shape, their high degrees of branching and large number of end groups, dendritic macromolecules show markedly different properties to their linear analogues. The high functionality of these macromolecules induces higher solubility in various solvents and the chemical reactivity offers the possibility of adapting their properties to different applications. For example, dendritic macromolecules with hydrophobic interiors can be made water soluble by introducing hydrophilic groups to their surface.^[112]

The viscosity of dendritic macromolecules in solution and in the melt is lower than for their linear analogs.^[120-123] Due to their globular shape, dendritic macromolecules have little or no entanglement. Fréchet^[123] studied the evolution of the intrinsic viscosity as a function of the molecular weight for linear polymers, dendrimers and HBPs. Figure II.5 shows the differences induced by variations in the backbone architecture. The bell-shaped curve obtained for dendrimers reflects the decrease in the viscosity of dendrimers at high generations due to their regular globular shape. For lower generations, dendrimers adopt a more extended structure. This curve illustrates that the Mark-Houwink-Sakurada equation (Equation II.3) is not obeyed with dendrimers.

$$[\eta] = K [M]^\alpha \qquad \text{Equation II.3}$$

The viscosity of HBPs, on the other hand, does not usually show a maximum. The Mark-Houwink-Sakurada relation is obeyed, even though the viscosity is lower than that of their linear analogs.^[120-122] For linear polymers α lies between 0.5 and 1, but is less than 0.5 for HBPs, again reflecting their globular shape. A factor that also influences the viscosity of hyperbranched macromolecules is the degree of branching.

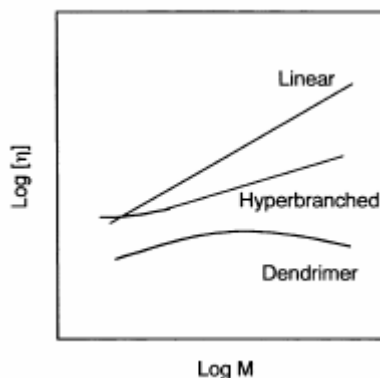


Figure II.5 Schematic of the evolution of the intrinsic viscosity $\log[\eta]$ as a function of the molecular weight of dendrimers and hyperbranched polymers and comparison with linear polymers^[33]

Thermal properties are also drastically different in dendritic macromolecules. The large number of end groups present in dendritic macromolecules decreases the glass transition (T_g) of dendrimers, but T_g increases with increased numbers of branched units and polarity of the end groups.^[124, 125] The impact of terminal groups (nature and length) on the thermal properties of HBPs has been studied by various authors.^[126-130] Malmström et al. studied in detail the behavior of hyperbranched polyesters based on *bis*-MPA and observed that short alkyl chain terminal groups decreased the T_g of the HBP from $T_g \approx 30$ °C to $T_g < 0$ °C, but that long alkyl chains induced crystallization.^[131] A few years later, they demonstrated that the degree of branching of hyperbranched polyethers influences their thermal properties. At high DB the polyether is amorphous with no entanglement ($T_g = 40$ °C) whereas a low DB results either in more entanglement or in a semi crystalline structure, (melting temperature (T_m) between 100 and 130 °C) increasing the viscosity.^[131]

III. Host-guest affinities in dendritic macromolecules

A presentation of the concept of unimolecular micelles based on dendritic macromolecules is given in the first part of section III. The entrapment of guest molecules in this tailorable architecture is described in the second part. Guest molecules may also bind to the dendrimer at complementary binding sites. This has been the subject of intense recent study and understanding the interaction mechanisms remains of great interest.^[25, 29, 30, 132-134] Thus, an overview of molecular recognition between dendrimers and guest molecules is given in the last part of this section. Because dendrimers show three different structural regions, a distinction is made between interactions that occur in the core, the branches and the dendrimer surface.

III.1. Presentation of the concept

The high functionality of the dendritic structure allows grafting of different molecules to its surface (Figure II.6). These sites may be used to graft active and/or target molecules for example. By recognition between the target molecule with its complementary molecule present at the site of action, the dendritic structure acts as a macromolecular vector and guest molecules can hence be delivered exactly where necessary. Instead of being grafted at the periphery, the active molecules may also be entrapped in the internal voids created by the branch units (Figure II.6).^[106, 114, 135, 136]

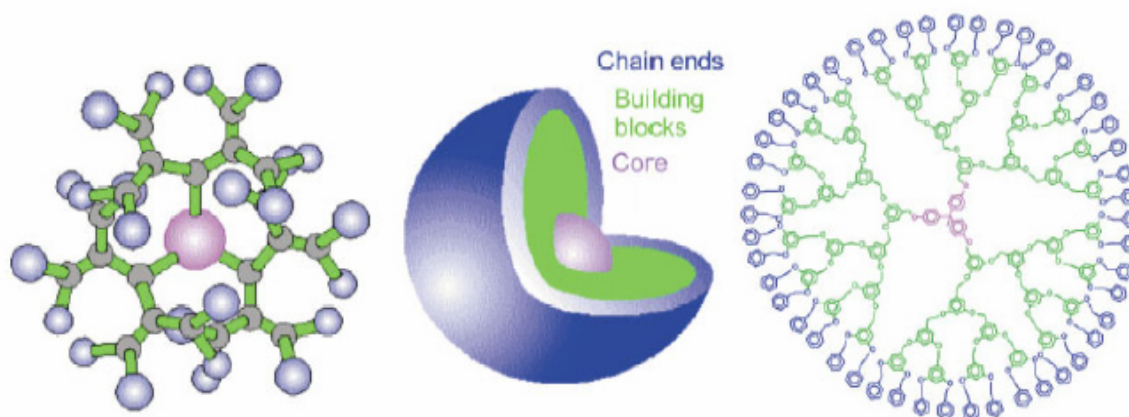


Figure II.6 Three representations of a dendrimer with the three main domains: the core, the branch units and the end groups^[137]

In 1982, Maciejewski first discussed the use of highly branched macromolecules as containers, underlining the challenges inherent in controlling host-guest interactions.^[138] Since then, the use of dendritic macromolecules for biological applications has developed considerably.^[17, 21, 25, 31, 34, 106, 132, 134-136, 139-144]

The analogy between dendritic macromolecules and micelles derives from the pioneering studies of Newkome et al.^[18] and Tomalia et al.^[145] Newkome et al. described the encapsulation of hydrophobic guests within the hydrophobic branches of a water soluble dendrimer. The polar functions present at the chain ends provide water-solubility.^[18] They introduced the term “unimolecular micelle,” which underlines the singularity of such covalently bound amphiphilic structures with the presence of branches and voids capable of guest inclusions. A few years later, Hawker et al. prepared a dendritic polyether capable of solubilizing polycyclic compounds in water as a result of π - π interactions, illustrating the relationship between encapsulation power and the electronic density.^[19] Unimolecular micelles were also investigated by Fréchet et al.,^[19, 146] using various guest molecules and dendrimer structures. The great advantage of these unimolecular micelles is the stability of the structure, regardless of concentration and temperature, unlike conventional micelles, which may become thermodynamically unstable. Moreover dendritic macromolecules have external functionalizable groups, which make them highly versatile.

III.2. Unimolecular systems

In the context of delivery systems, the aim of dendrimer functionalization is to improve the solubility of guest molecules in a given solvent, to prolong their effectiveness and protect them against the environment.^[19, 21, 31, 136, 142, 147, 148]

III.2.1 The dendritic box

The dendritic box is a selective delivery system based on a dense and rigid shell and a flexible core capable of entrapping molecules. The term “dendritic box” comes from the idea of physically “locked” guest molecules inside a dendritic container. The concept was developed by Jansen and Meijer, with the synthesis of a five generation poly(propylene imine) dendrimer as a core^[17, 25, 149, 150] and a *tert*-butyloxycarbonyl (*t*-BOC)-protected amino acid as an external shell (an amino acid which carboxylic groups are protected with *tert*-butyloxycarbonyl functions) (Figure II.7). They demonstrated that it is possible to entrap different guests in the internal cavities of the dendrimer during synthesis. It was observed that the number of guest molecules entrapped in the dendritic box is governed by the shape of the guest and the cavities. Up to ten small molecules (p-nitrophenol, $M_w = 139 \text{ g mol}^{-1}$) but only one large molecule (rose bengal, $M_w = 962 \text{ g mol}^{-1}$) could be entrapped by a single molecule. The dense surface shell prevents diffusion out of the dendrimers, even after prolonged heat or solvent extraction. Selective liberation of entrapped guest from dendritic box was also described. Small molecules could be released by hydrolysis of the *t*-BOC groups, but it was necessary to hydrolyze the amide functions of the outer shell to liberate larger molecules.

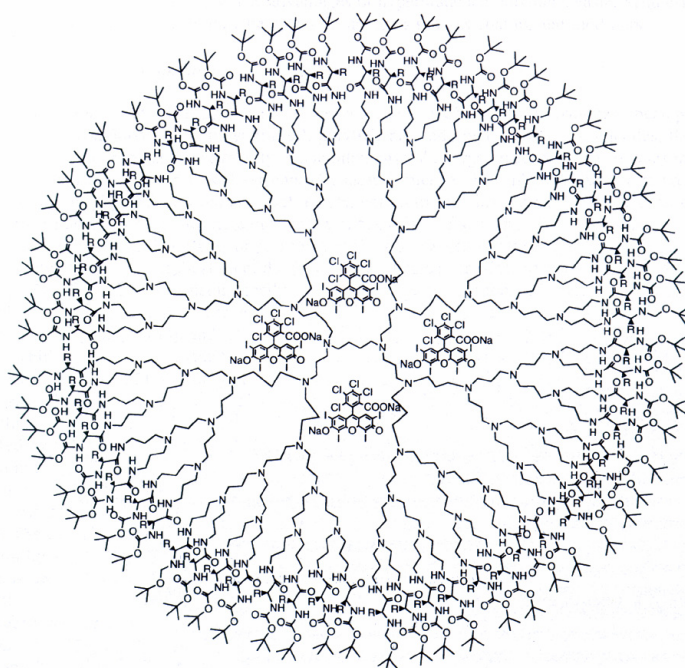


Figure II.7 Chemical structure of Meijer's dendritic box^[150]

III.2.2 Inverse unimolecular micelles

A few years after the introduction of the dendritic box, Meijer and coworkers reported an inverted unimolecular micelle, obtained by modifying the end groups of the poly(propylene imine) dendrimer with alkyl chains, thus creating a hydrophilic interior and a hydrophobic shell. These compounds are able to encapsulate molecules such as rose bengal in organic media.^[151] Based on this result, other inverted unimolecular micelles were investigated for the solubilization of fluorescent hydrophilic molecules in non polar media.^[152-154] Frey and coworkers described the preparation of a partially esterified hyperbranched polyglycerol by ring-opening multi-branching polymerization (ROMBP) of glycidol, followed by a partial esterification of the hydroxyl groups with fatty acid.^[155] It was shown that the encapsulation of hydrophilic molecules is dependent on the molecular weight of the hyperbranched polyglycerol, the number of remaining hydroxyl groups and the alkyl chain length. Release of the guest molecules is achieved by hydrolysis of the ester functions. By comparing linear and hyperbranched esterified polyglycerol they also provided evidence for the formation of hydrophilic compartments in amphiphilic hyperbranched core-shell molecules in apolar media, which does not occur with linear polymers. These cavities are favorable for the encapsulation of guest molecules.^[156]

Recently a novel biodegradable inverted unimolecular micelle composed of a poly(lactic acid) (PLA) shell and a hyperbranched polysaccharide core has been developed. This new architecture is also able to entrap hydrophilic molecules and to release them slowly from the core. The release rate can be accelerated by enzymatic cleavage of the PLA shell.^[157]

III.2.3 PEGylated dendrimers

When it is necessary to increase the water solubility of dendrimers, poly(ethylene glycol) (PEG) is typically grafted on the surface of dendrimer, providing a hydrophilic shell around a hydrophobic core.^[135, 158, 159] PEG is well known for its water solubility, its biocompatibility and its ability to modify the distribution of drugs, and is widely used in pharmaceutical applications.^[160-162] PEGylated dendrimers can act as unimolecular dendritic

micelles.^[20] Different research groups have shown that PEGylated dendrimers are able to entrap guest molecules in their hydrophobic cores and to increase the water solubility of hydrophobic pyrene,^[26, 163, 164] dyes^[165] or drugs.^[166, 167] Kojima et al. demonstrated with PEGylated poly(amido amine) that higher generation dendrimers can encapsulate drugs more efficiently. It was also demonstrated that the PEG chain length has an influence on the solubility and the stability of the hydrophobic molecules, and that longer chains induce better water solubility.^[163, 164, 167] A poly(propylene imine) modified with 3,4,5-tris(tetraethyleneoxy)benzoyl units was prepared by Baars et al. (Figure II.8). They demonstrated that in aqueous solution, dye molecules are preferentially localized in the dendrimer interior.^[165]

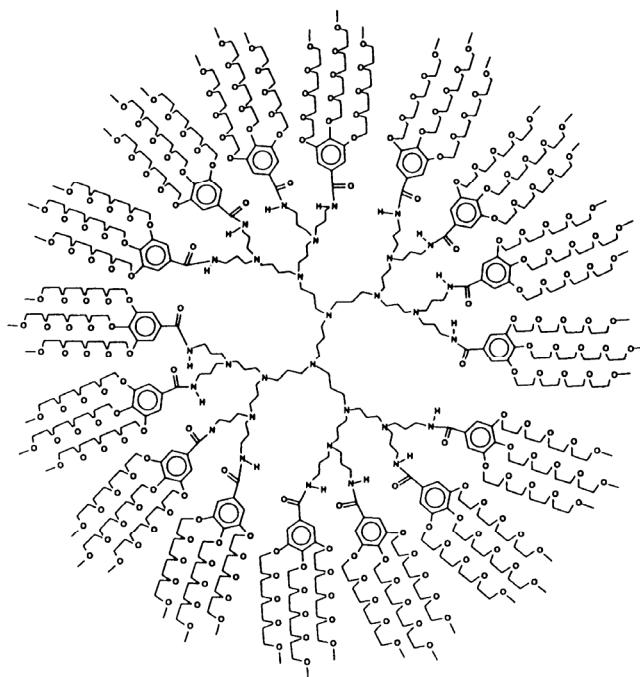


Figure II.8 Poly(propylene imine) dendrimer modified with 3,4,5-tris(tetraethyleneoxy)benzoyl units^[165]

III.2.4 pH-sensitive dendrimers

The entrapment of guest molecules in dendrimers may be a “physical” entrapment (see the dendritic box) or can be based on “specific” interaction (electrostatic, H-bonding, apolar interactions, ...). In what follows, examples are given which underline the effect of pH on the controlled release of the guest molecules.

With PAMAM dendrimer Tomalia and coworkers have demonstrated that specific interaction such as electrostatic attraction could be used to entrap deprotonated hydrophobic guest molecules in a protonated PAMAM dendrimer with the spin-lattice relaxation time of the guest molecule.^[168] They also underlined the influence of generation number and length of diamino alkyl core on the hydrophobicity of the PAMAM dendrimer and the entrapment of guest molecules.^[169] In biological applications they reported that protonated PAMAM dendrimers can interact with anionic guest molecules such as desoxyribo nucleic acid (DNA). This association is of interest for cellular biology, making it possible to transfer genetic material into cells.^[170] Thus dendrimers function as artificial gene-transfection reagents, similar to viruses and liposomes. Moreover, it has been observed that imperfect dendrimers are more efficient as gene-transfection vectors.^[170, 171]

Paleos et al. also demonstrated the promise of poly(propylene imine) dendrimer as a pH-sensitive controlled release system.^[172, 173] They reported the pH-controlled inclusion of pyrene in amine modified poly(propylene imine). At high pH, the dendrimer acts as an apolar hydrophobic internal host with deprotonated amine groups, whereas at low pH, the environment became polar enough to expulse pyrene owing to protonation of the internal amine. Inclusion has been demonstrated by NMR and fluorescence measurements.^[172]

III.3. Complementary binding sites: “Dendritic receptors”

In this section the capacity of such dendritic macromolecules to act as a “dendritic receptors” is illustrated by a number of examples. There has recently been particular interest in the development of dendritically buried recognition sites as mimics for biological systems, but this approach may find application in fields as diverse as molecular electronics, luminescent devices and energy transduction.^[29, 30, 174] Although complementary binding sites will not be considered explicitly in the remainder of this thesis, this section is included for completeness, since ultimately it would be of interest to apply similar principle to the systems developed here for the encapsulation of fragrance molecules.

III.3.1 Interactions within the dendrimer core

The most highly developed dendritic receptor is the dendropane macromolecule (Figure II.9) described by Diederich and coworkers in 1995. The cyclopane dendrimer contains one apolar binding site in the core which allow inclusion of aromatic guest molecules in water.^[175] The use of dendropane with large cavities enables entrapment of larger guest molecules such as steroids. The larger core implies less dense packing of the dendrimer branches, inducing faster host-guest exchange kinetics at the NMR time scale.^[176] The same group also used a poly(ether amide) synthesized by Newkome et al., to demonstrate that binding occurred with 1:1 host/guest stoichiometry. The perturbation of the nuclear magnetic resonances of the dendropane units validated the concept of molecular recognition by the dendritic core.^[177, 178]

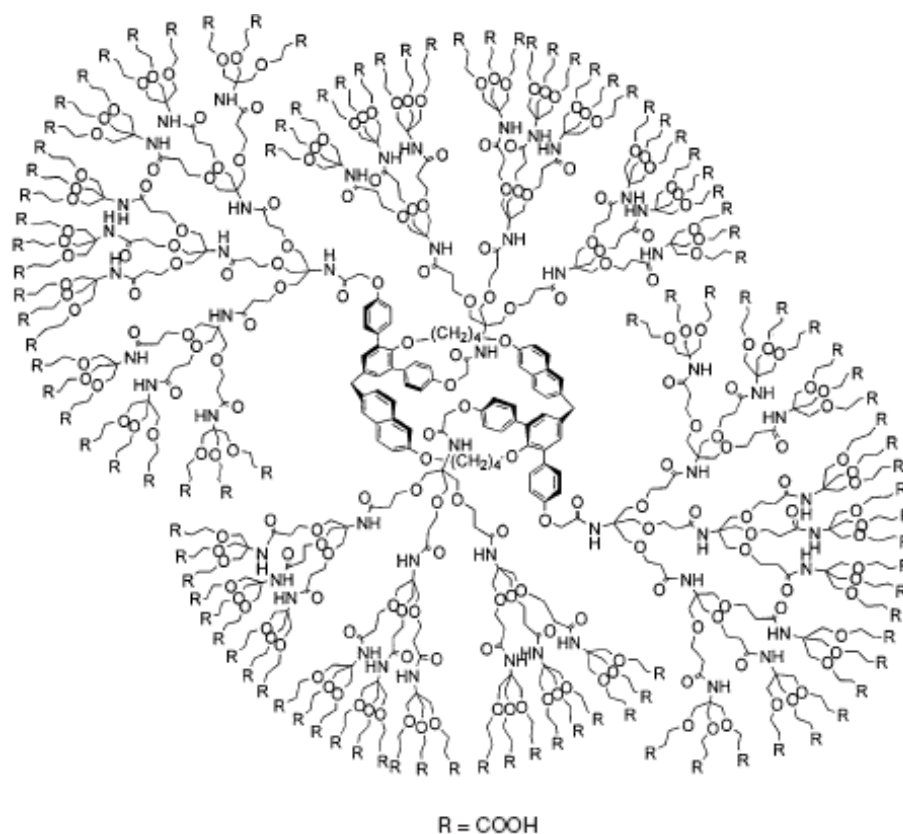


Figure II.9 Dendrophane with expanded cyclodextrin cavities for the entrapment of steroids^[29]

It is well known that β -cyclodextrin is able to entrap hydrophobic molecules (section I.1.1). Dendritic β -cyclodextrin (β -CD) was developed by Newkome et al. for the recognition of phenolphthalein (indicator) and adamantane. The absence of the coloration after introducing β -cyclodextrin into a basic aqueous solution illustrates the hydrophobic association between the phenolphthalein and β -cyclodextrin. They used adamantyl (known to bind very strongly to β -CD) to displace the phenolphthalein from the β -CD cavities to the aqueous solution. The color regeneration in the aqueous solution demonstrated the localization of phenolphthalein in the β -CD cavity and not in the dendrimer branches.^[179]

Because it is well known that ferrocene is another excellent guest molecule for β -CD, Kaifer and coworkers studied in detail ferrocene-based dendrimers as redox agents, using Newkome-type dendrimers with a single ferrocene unit at the focal point (Figure II.10). They

observed that the redox potential is significantly affected by the presence of the dendrimer and its complexation with β -CD.^[180, 181]

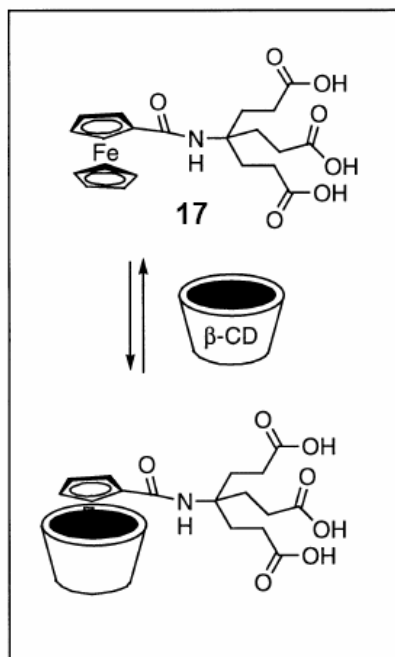


Figure II.10 Newkome-type dendrimer with a ferrocene unit and its complexation with β -cyclodextrin^[30]

The ability of modified Fréchet-type poly(aryl ether) dendrimers to bind C₆₀ fullerene was reported by Nierengarten et al.^[182] and Shinkai and coworkers^[183] They observed that the strength of binding increases with increases in the number of dendritic generations (Figure II.11).

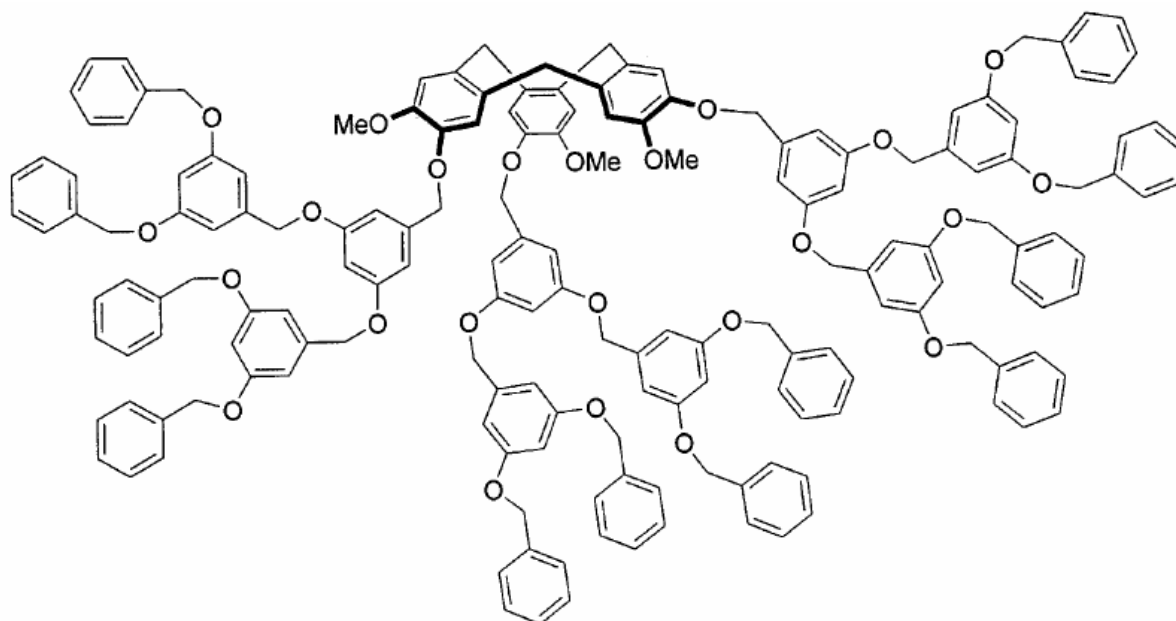


Figure II.11 Poly(aryl ether) modified for the recognition of C₆₀ fullerene^[29]

Hydrogen bonding is of primary importance in biology. The secondary structure of enzymes is based on these interactions and they also have a major role in catalysis and recognition. Newkome et al. reported H-bonding interactions with a dendritic receptor which contained four diamidopyridine units and barbituric acid as a guest molecule (Figure II.12). The solubility of barbituric acid was enhanced in an apolar solvent. An increase in the dendrimer size induced a decrease in barbituric acid association, probably because of increased self association and competing dendritic binding sites.^[184]

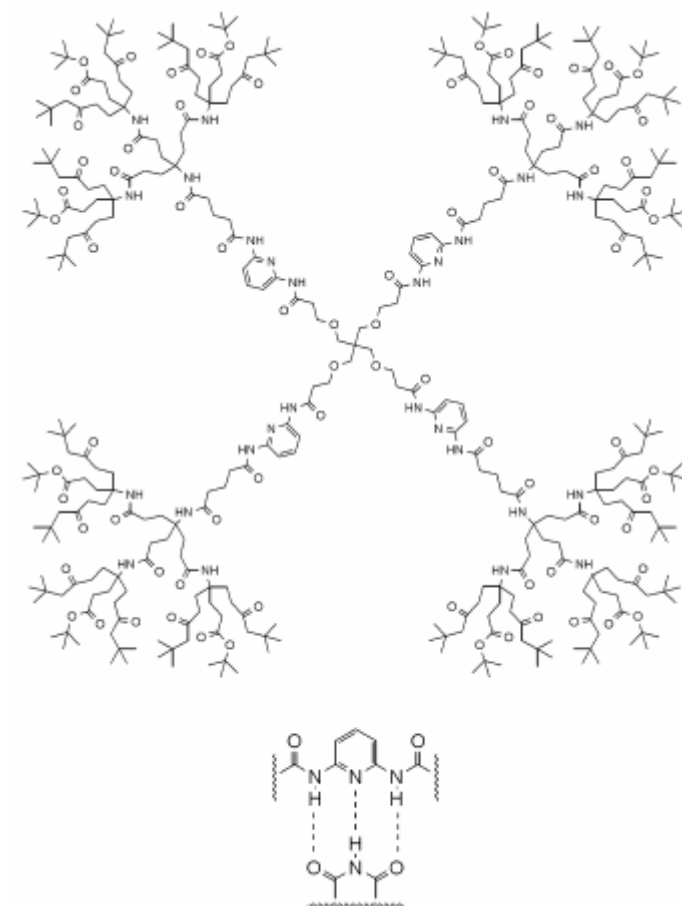


Figure II.12 Dendrimer receptor based on H-bonding association between diamidopyridine localized in the dendritic core and barbituric acid^[132]

Smith and Diederich reported chiral dendrimer receptors referred to as “dendroclefts”, based on H-bonding recognition of monosaccharides. The dendrimer branches altered the selectivity of this new receptor. They observed that the [G-0] core (without dendritic branching) showed enantioselectivity towards octyl α -D-glucoside over α -L-glucoside whereas the corresponding [G-1] and [G-2] dendrimers did not. Conversely, the [G-0] core exhibited little diastereoselectivity for octyl β -D-glucoside over octyl α -D-glucoside, whereas [G-1] and [G-2] dendrimers showed clear diastereoselectivity, which increased with generation number.^[185]

III.3.2 Recognition within polymer branches

Owing to the difficulty of synthesizing dendrimers with particular groups in their branches and to characterize recognition of guest molecules, few examples have so far been reported. Shinkai and coworkers^[186] described a dendrimer receptor with crown ether sites (Figure II.13). This receptor was developed for metal ion recognition and potassium extraction. They also observed that myoglobin is made soluble in organic solvents in the presence of the [G-1] receptor owing to interactions between the crown ether and protonated amines present at the myoglobin surface, but remains insoluble in the presence of higher generation dendrimers because of steric hindrance in the branches.

Sanders and coworkers^[187] reported similar cooperativity effects when binding rigid diamine guest molecules with branched metalloporphyrin, suggesting that such recognition can affect dendrimer properties.

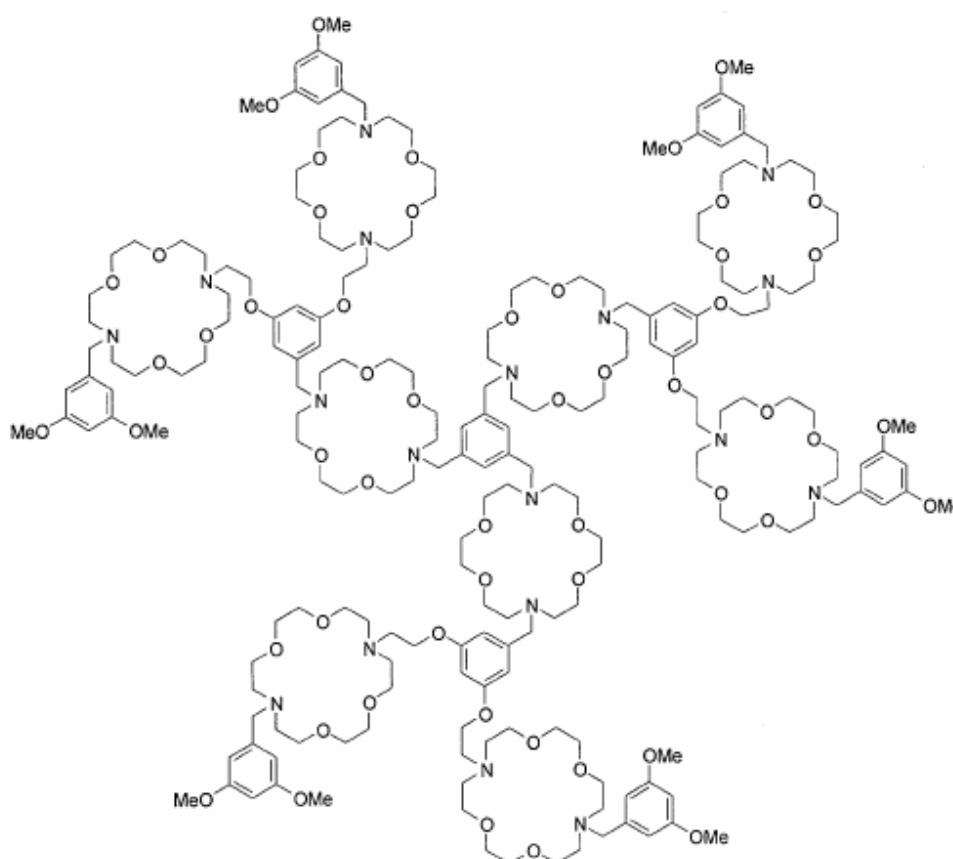


Figure II.13 Crown ether dendrimer for the recognition of metal ions^[29]

III.3.3 Use of surface functions for molecular recognition

The variety of functionality present at the dendrimer surface makes it particularly interesting for molecular recognition. Reinhoudt and coworkers^[188] modified poly(propylene imine) dendrimer surfaces with adamantyl group. Such dendrimers, which are insoluble in water, became water-soluble after complexation with β -CD. Kaifer and coworkers^[189] reported the functionalization of the poly(propylene imine) surface with ferrocene units. With both types of functionalization, the solubility decreases with increasing dendrimer generation since steric hindrance induces a decrease in complexation. On the other hand, by functionalizing peripheral end groups of the dendrimer with amido-ferrocene units, Astruc and coworkers produced a supramolecular redox sensor for the recognition of inorganic anions (Figure II.14). They also reported that interactions between dendrimers and anions are a function of the dendrimer generation number.^[190]

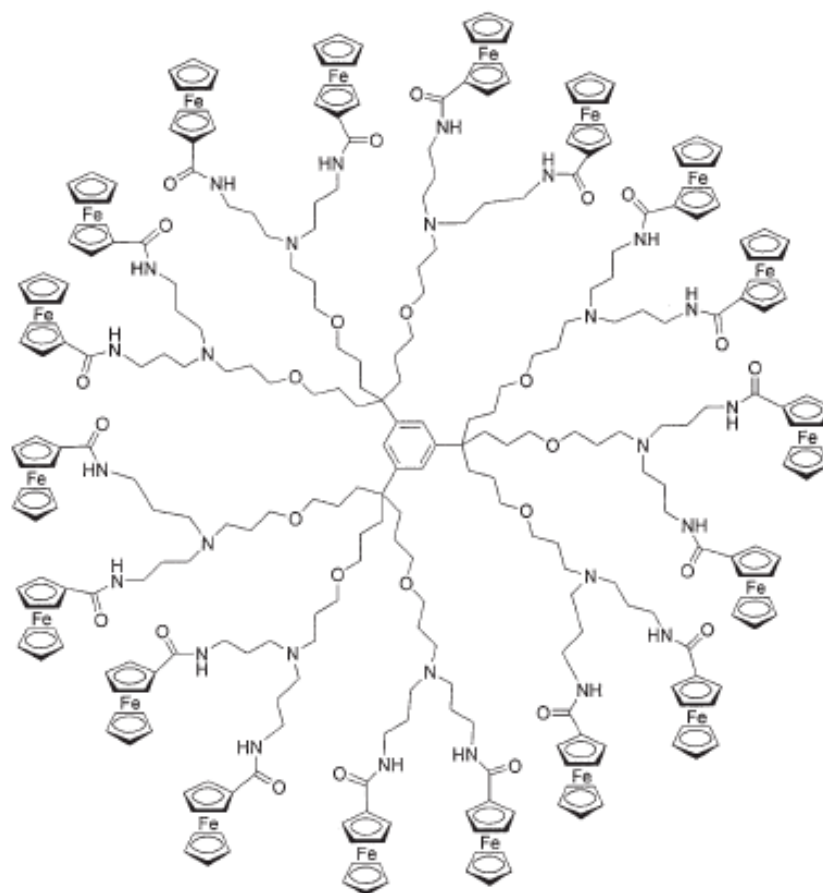


Figure II.14 Dendritic anion receptor with peripheral amido-ferrocene units^[29]

In the field of biological applications, e.g. cell recognition, cell adhesion or infections, proteins-carbohydrate interactions are predominant. Cell membranes are composed of glycoproteins and glycolipids and present α -sialinic acid groups at their surfaces. These α -sialinic acid groups bind viruses. With the use of multiple sialinic acid functions it is possible to enhance binding and thus to inhibit the interaction between viruses and the host cell. Thus, dendrimers with sialinic acid are of particular interest.^[191]

Dendritic receptors for monosaccharide guest molecules were developed by Shinkai et al.. They functionalized PAMAM dendrimer with boronic acid. In aqueous solution, boronic acid is able to form a cyclic boronate ester with the vicinal hydroxyl groups of the saccharides. The proximity of boronic acid groups localized at the dendritic surface increases cooperativity, enhancing the binding strength.^[192]

IV. Conclusions

In the field of cosmetics, food and pharmaceuticals, the main ways of obtaining capsules for the entrapment of guest molecules (for protection, prolonged delivery, ...) involve ad hoc processing routes and relatively simple macromolecules. A variety of functions is employed (ester, anhydride, acid...) and biodegradable natural polymers such as polysaccharides and phospholipids are well represented. More recently, most sophisticated architectures based on block copolymers have also been used. Their supramolecular association to form micelles and the concept of shell cross-linked micelles opens the door to a new approach in which the capsule is pre-formed and may directly accommodate guest molecules in its interior. In order to increase the stability of such structures, the idea of covalently bound macromolecular micelles has been introduced and the use of dendritic structures for this purpose has attracted particular attention, owing to their compact globular shape and high number of end groups. The use of dendritic macromolecules as delivery systems has been described in detail.

Relatively few results have been published on release kinetics, however whence our interest in investigating this aspect of our own system. Polymer property studies have nevertheless demonstrated an important link between the state of the polymer (T_g , T_m) and the release rate of the guest molecules. Moreover, the block lengths may also influence the mobility of the polymer and hence the release rate.

Finally, although not directly linked to the present project, which is focused on the non specific interactions between guest molecules and dendritic structures, the capacity of dendritic structures to create supramolecular assemblies for the recognition of specific guest molecules has also been discussed, since it illustrates well the vast potential of such macromolecules.

Chapter III. Polymer synthesis: generalities

The major part of this work has been the chemical modification of hyperbranched polymers for the synthesis of an amphiphilic unimolecular micelle. To achieve this we used ring-opening polymerization (ROP) and atom transfer radical polymerization (ATRP). In this chapter, some generalities are given on polymer synthesis and these two techniques in particular, as well as an overview of the previous use of ROP and ATRP with multi-arm macroinitiators.

I. Classification of polymerization techniques

Two main types of classification of polymer synthesis are currently employed and distinctions between them must be made carefully to avoid confusion. The first classification was proposed by Carothers in 1929^[193] and takes into consideration the **polymer structure**. *Condensation polymerization* is used to describe polymers obtained from polyfunctional monomers, with elimination of a small molecule. The polymer contains functional groups and its composition differs from that of the monomers. *Addition polymerization* is used to describe polymers that have repeat units that correspond to the monomer composition. No elimination of small molecules occurs. The second classification was proposed by Flory in 1953^[194] and is based on the **polymerization mechanism**. He distinguished between *step* and *chain polymerization*. In step polymerization, the reaction occurs between the functional groups of the monomer, producing dimers, trimers, tetramers and so on. This process is characterized by a gradual increase in molar masses with conversion. In chain polymerization, an initiator is used to produce an initiator species and the process is composed of three stages, initiation, propagation and termination. High molecular weights are obtained rapidly in this case. The two types of classification, together with their characteristics, are summarized in Table III.1.

Table III.1 Summary of the two main types of classification for polymers and polymerization processes

Based on polymer structure	Based on polymerization technique
<p style="text-align: center;">Condensation</p> <ul style="list-style-type: none"> • Requires polyfunctional monomers • Elimination of small molecules • Elemental composition of polymer differs from the monomers <p>e.g.: polyamide</p> $\text{H}_2\text{N}-\text{R}-\text{NH}_2 + \text{HOOC}-\text{R}'-\text{COOH} \longrightarrow \text{H}-\left(\text{NH}-\text{R}-\text{NHCO}-\text{R}'-\text{CO}\right)_n-\text{OH} + n\text{H}_2\text{O}$	<p style="text-align: center;">Step</p> <ul style="list-style-type: none"> • Reaction occurs between the different sized species present in the system • Monomer forms dimer, trimer, and so on • Molecular weight increases slowly with conversion • High molecular weight polymer is obtained at the end of the reaction • Long reaction times necessary to obtain high conversion and high molecular weights
<p style="text-align: center;">Addition</p> <ul style="list-style-type: none"> • No elimination of small molecules • Repeat units of the polymer have the same composition as the monomer <p>e.g.: polyethylene</p> $n \text{H}_2\text{C}=\text{CH}_2 \longrightarrow \left(\text{CH}_2-\text{CH}_2\right)_n^*$	<p style="text-align: center;">Chain</p> <ul style="list-style-type: none"> • Three major stages: Initiation, propagation, termination (transfer reaction) • Initiator may be a free radical, cation or anion • Monomer only reacts with the reactive center • High molecular weight polymer immediately • Chain growth is very rapid • Molecular weight of the polymer is substantially independent of monomer conversion

It is not possible simply to assimilate condensation and step polymerization, and addition and chain polymerization. Step polymerization not only covers polycondensation, but also polymerizations that do not induce elimination of small molecules. The ring-opening technique (which will be described in section III) illustrates that both structure and mechanism are usually needed to clearly classify a polymerization reaction. Indeed, ring-opening polymerization is structurally classified as condensation polymerization (functional groups in the polymer chain) but the mechanism corresponds to a chain polymerization, with initiation, propagation and termination stages.

II. Chain polymerization

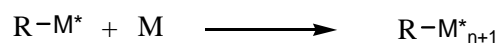
II.1. Conventional chain polymerization

The initiation stage of chain polymerization consists of the creation of reactive species (R^*) from an initiator (I). R^* may be a free radical, an anion or a cation. R^* adds to the monomer by cleaving the double bond, creating a new reactive center $R-M^*$ (Scheme III.1). Monomer molecules are successively added to the propagating reactive center. Termination occurs by destruction of the reactive center by recombination or dismutation (Scheme III.2).

Initiation



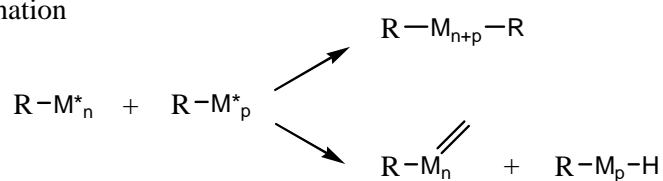
Propagation



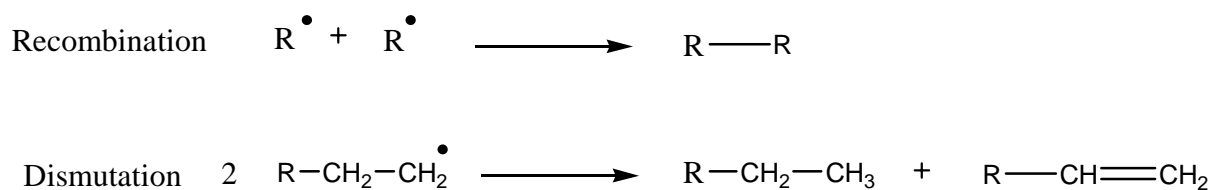
Transfer



Termination



Scheme III.1 Stages of chain polymerization



Scheme III.2 Termination mechanism in chain polymerization. Example of a radical polymerization

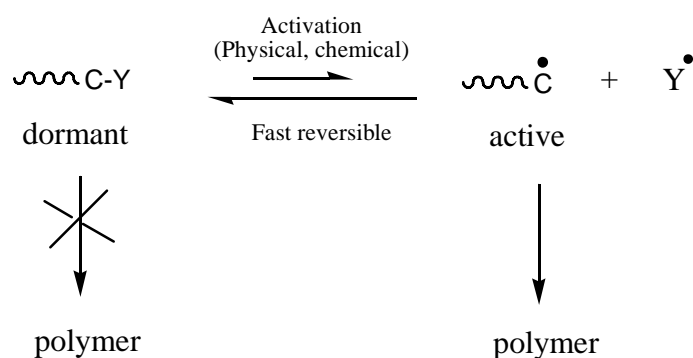
It has been observed in many polymerizations that the polymer molecular weight is lower than predicted. This phenomenon is due to premature termination of the growing chain by a transfer reaction. The monomer, initiator, solvent or polymer or a transfer agent may cause transfer reactions, which result in chain scission and hence a decrease in the molecular weight.

The differences between anionic, cationic and radical polymerization are linked to the types of reactive centers formed by the monomer. Odian has classified the different types of chain polymerization in terms of the initiation type.^[195] Most monomers undergo polymerization with a radical initiator but show high selectivity toward ionic initiators. The great advantage of radical polymerization is that vinylic monomers may be polymerized by this technique. Moreover, it is easier to implement than ionic polymerization. Radical polymerization is currently the most widely used process, representing more than 50 % of polymer production. Propagating radicals are insensitive toward impurities such as water or organic protic solvents so that the reaction may take place in mass, solvent, emulsion or suspension at temperatures between 40 and 150 °C. However it is better to avoid contamination by molecular oxygen which may induce transfer and inhibition of the reaction.

II.2. “Living” and “controlled” polymerization

In certain types of chain polymerization, neither transfer nor termination occur, resulting in a “living” polymer. Living polymerization was introduced in 1950 with the work of Szwarc,^[196] who determined optimum conditions for the controlled polymerization with

reactive anionic species. Initiation is rapid relative to the propagation stage. The concept of dormant states (inactivation of the polymer chain) was introduced to minimize bimolecular termination and prolong the lifetime of polymerization reaction initiated by radical species (Scheme III.3). In the mid-1990's, such "controlled" radical polymerization (CRP) was intensively studied because of its commercial potential for synthesis and the relative abundance of monomers that can undergo radical polymerization.



Scheme III.3 Principle of polymer chain inactivation in a CRP process

There has been considerable debate about the terminology for "living" and "controlled" radical polymerization. To simplify it is proposed in the present manuscript to use the same terminology as Fontanille and Gnanou.^[197] "Living" polymerization is used when neither termination nor transfer occur and when the initiation rate is variable, whereas "controlled" polymerization is used when termination and transfer are minimized and when the initiation stage is very fast in comparison with propagation stage. According to this terminology, a "living" polymerization is not always a "controlled" polymerization.

II.3. Controlled radical polymerization (CRP)

II.3.1 Principle

Controlled radical polymerization allows synthesis of polymers with well defined compositions offering substantial advantages for building nanostructures with a variety of architectures (block and graft copolymers, stars...)^[195] All the methods are based on the same strategy. For good control, a dynamic equilibrium has to be established between a small quantity of the active radical species and a large quantity of the covalent dormant species.^[198] Typically, large amounts of radical species are generated in a short time (each chain starts to propagate at the same time) but the instantaneous radical concentration remains as low as possible (radical concentration $\approx 10^{-8}$ to 10^{-9} mol L⁻¹). The frequent interconversion between the active and the dormant species not only decreases the probability of bimolecular radical termination, but also gives a uniform chain length. The rate of termination is directly proportional to the square of the radical concentration ($R_t = k_t [M^\bullet]^2$). A decrease in the radical concentration induces a significant decrease in termination.

A controlled radical polymerization fulfils the following conditions:

- Minimal termination
- Exchange between dormant and active species remains fast with respect to propagation, to maintain low polydispersity

It is then possible to control the molar mass of the polymer by adjusting the monomer versus the initiator ($[M]/[I]$) ratio. Polymer chains are in the dormant state at the end of the reaction and composition and topology are well defined.

II.3.2 Different types of CRP

Three methods of CRP have been established over the last decade. All are based on minimizing termination and transfer by the establishment of a dynamic equilibrium between a growth-active radical species and a dormant species as described above. Reversible

termination techniques such as stable free radical polymerization (SFRP) and atom transfer radical polymerization (ATRP), or reversible chain transfer processes such as reversible addition-fragmentation transfer (RAFT) have been developed. The dormant chain differs according to the specific method of radical polymerization.^[198]

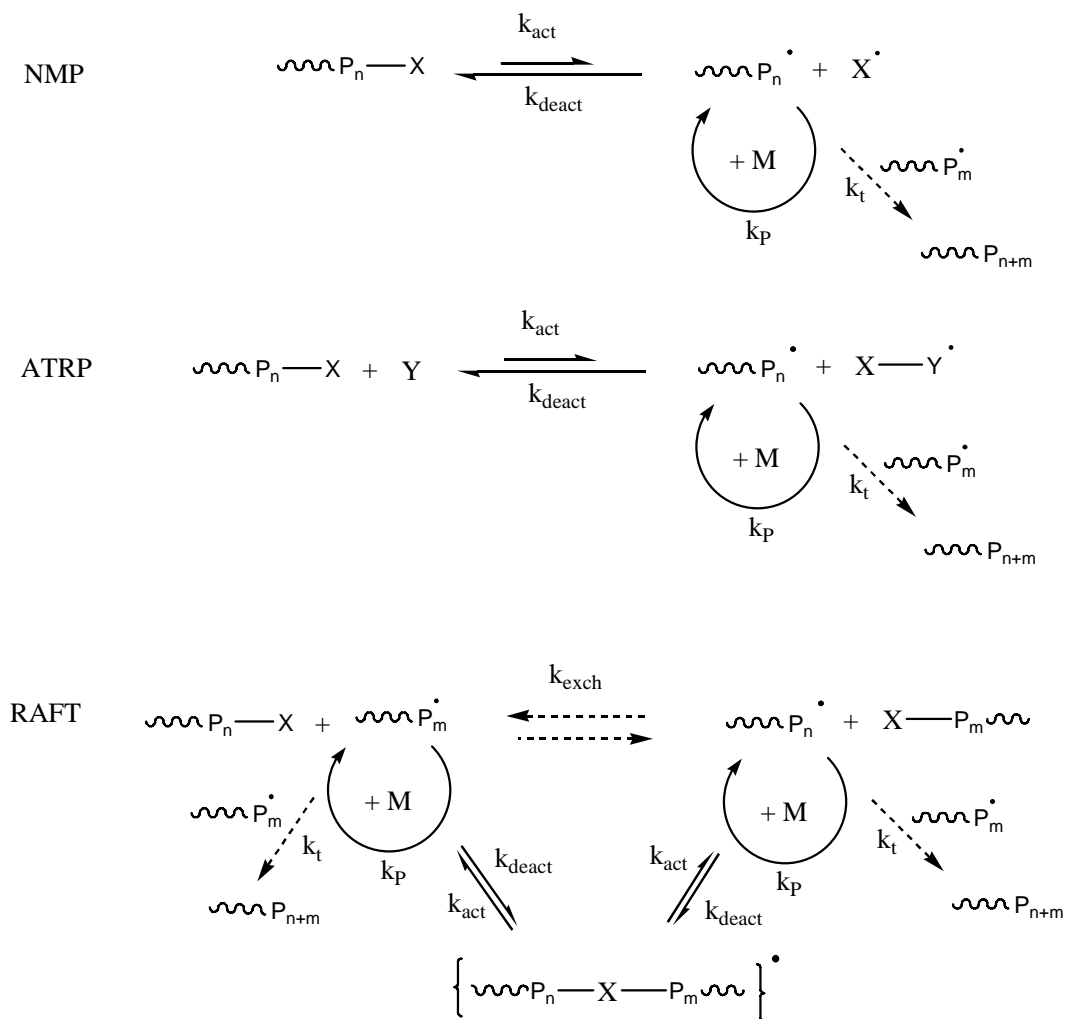
SFRP uses various mediating or persistent radicals such as nitroxide, triazolyl, trityl and dithiocarbamate. Due to the greater efficiency of nitroxides, SFRP has very often been called nitroxide mediated polymerization (NMP). Radical polymerization mediated by nitroxide was described for the first time by Solomon and Rizzardo in 1982.^[199] It has been used for the polymerization of styrene, acrylic (alkyl acrylate, acrylic acid), diene and acrylamide monomers.

ATRP was developed in the mid of 1990's by Sawamoto^[200] with the use of a ruthenium complex, and Matyjaszewski^[201] who proposed copper as the catalytic system. Details of the mechanisms, kinetics, effects of constituents (initiator, solvent, ligand, metal...) are reviewed elsewhere.^[202, 203] In the case of ATRP, the dormant species are alkyl halides, which undergo a reversible redox process catalyzed by the transition metal compound. The majority of the vinyl monomers have been polymerized by this method, with the exception of vinyl acetate, diene and acrylic acid.

RAFT, the most recent method of CRP, was developed by Rizzardo and coworkers.^[204] A chain transfer agent such as cumyldithiobenzoate reversibly transfers a labile end group (dithioester end group) to a propagating chain.

Scheme III.4 illustrates the three processes SFRP (NMP), ATRP and RAFT with the activation and deactivation stages. k_{act} corresponds to the rate constant from the dormant to the active species and k_{deact} to the rate constant from the active to the dormant species. k_p and k_t correspond respectively to the rate constants of propagation and termination. In NMP, the growing polymer chain (P_n^\bullet) is associated with nitroxide groups (X) to form an alkoxyamine dormant species. In the case of ATRP, a ligand (Y) is also present to complex the organometallic transfer agent (X). In RAFT polymerization, a dithioester (X) is introduced,

and is successively transferred from one growing chain ($-P_m^\bullet$) (to form a dormant chain ($X-P_m$)) to another ($-P_n^\bullet$) (to form another dormant chain ($X-P_n$)) with a k_{exch} rate constant.



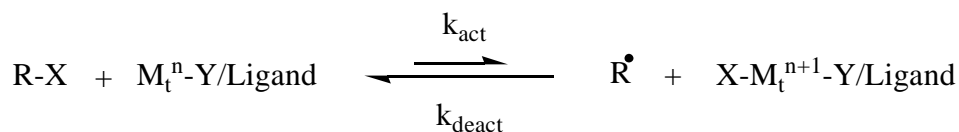
Scheme III.4 Three types of controlled radical polymerization

In the present work ATRP was used for the synthesis of the hydrophilic shell of the container. It is therefore proposed to describe the ATRP process in more detail. The emphasis will be on acrylate and methacrylate monomers.

II.3.3 Atom transfer radical polymerization (ATRP)

Many publications attest to the potential of ATRP for controlled radical polymerization and the generation of very well defined polymers. A wide range of monomer, transition metals and ligands have been used for this purpose.

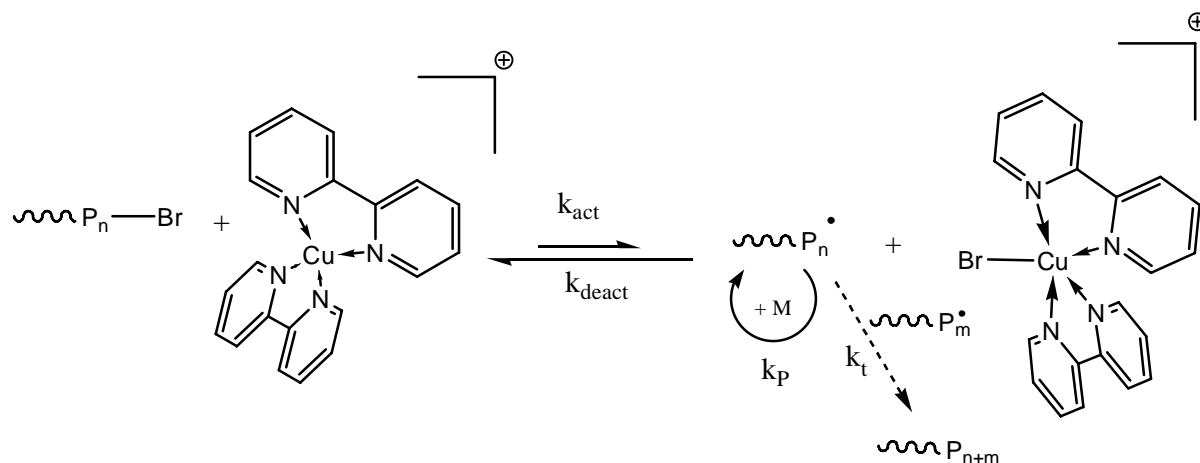
The name ATRP was proposed by Matyjaszewski and derives from the atom transfer step, which is responsible for the uniform growth of the polymer chain. This process originates from ATRA, which consists of the addition of alkyl halides and alkenes catalyzed by transition metal complexes.^[205] ATRP was developed by designing a suitable catalyst (transition metal and ligand), using an initiator with the appropriate structure and adjusting the polymerization conditions.^[201-203, 206-210] Active species are generated from the catalyst complex metal/ligand (Scheme III.5).



Scheme III.5 Activation of the ATRP from a metal/ligand complex with R-X: halogenated initiator, M_t^n : metal, Y: halogenated group, k_{act} : activation rate constant, k_{deact} : deactivation rate constant

The ligand is necessary to solubilize the metal and increase the metal oxidability. It has a donor character. These conditions allow control over the chain topology (star, branched), the composition (block, gradient, alternating, statistical) and the end functionality for a large range of monomers such as acrylate and methacrylate. With these monomers, copper works well as the metal catalyst. Ligands composed of multidentate nitrogen are very often used with copper. Bidentate (2,2'-bipyridyl and N-propyl-2-pyridylmethanimine) tridentate (pentamethyl diethylene triamine (PMDETA)) and tetradentate ligands (hexamethyl triethylene tetramine (HMTETA) and tris-2-dimethyl aminoethyl amine (Me_6TREN)) are found to be most effective owing to electronic and steric effects^[202, 206, 211] (chemical formula

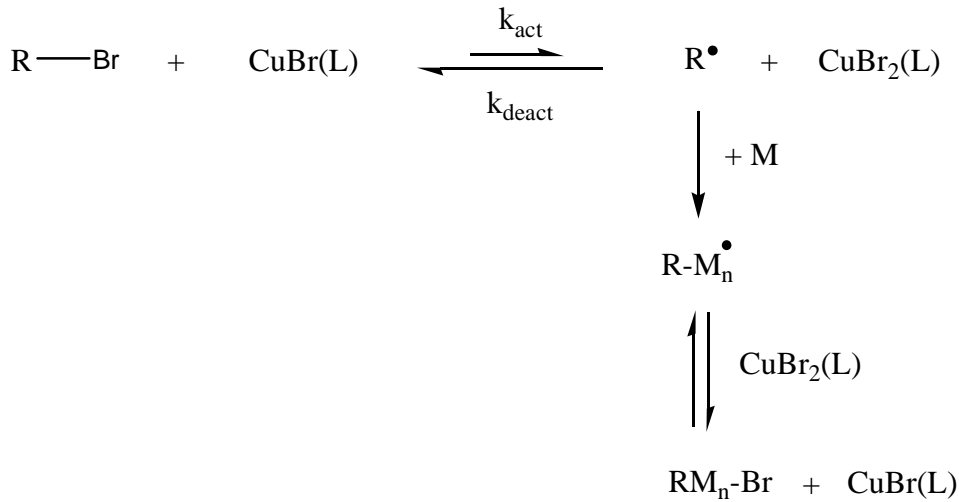
in appendix 3). Scheme III.6 gives an example of complexation between a metal (copper, Cu) and a ligand (2,2'-bipyridyl).



Scheme III.6 Representation of the complexation between metal (Cu) and ligand (2,2'-Bipyridyl) during ATRP polymerization

The initiator must also be well chosen for ATRP to be effective. For the synthesis of a well defined polymer, it is essential to prepare an initiator that can efficiently trigger the polymerization of the chosen monomer. It has been shown that alkyl halides containing activating substituents (such as carbonyl groups) at the α -carbon position can initiate the polymerization of *tert*-butyl acrylate^[212] and methyl methacrylate.^[213] A well defined polymer may be prepared by using a functional group that has a structure similar to that of the growing polymer chain end in its dormant form. The rate of the ATRP is then moderated and the polymerization better controlled. The choice of the monomer induces the chemical nature of the other components present in the reaction medium as well as the initiator.

First order kinetics have been verified in many ATRP conditions^[206, 214, 215] including multi-arm macroinitiators.^[216, 217] Scheme III.7 shows the propagation step of an ATRP polymerization.



Scheme III.7 Propagation step in ATRP polymerization

In ATRP polymerization, the initiation consists of the production of free radicals. The addition of one monomer to the radical follows with a rate constant K . The propagation consists of the growth of the propagating radical by the successive addition of a large number of monomer molecules. The propagation rate (R_p) is given in Equation III.1 by considering the propagation step shown in Scheme III.7 with the initiator $[I] = \text{R-Br}$, the initiation rate constant $K = k_{\text{act}}/k_{\text{deact}}$ (k_{act} , the rate constant for activation and k_{deact} , the rate constant for deactivation) and k_p , the rate constant for propagation.

$$R_p = Kk_p \frac{[M][I][\text{Cu}^+]}{[\text{Cu}^{2+}]} \quad \text{Equation III.1}$$

$$\text{with, } K = \frac{k_{\text{act}}}{k_{\text{deact}}} = \frac{[M^\bullet][\text{Cu}^{2+}]}{[I][\text{Cu}^+]} \quad \text{Equation III.2}$$

$$-\frac{dM}{dt} = r_p = Kk_p \frac{[M][I][\text{Cu}^+]}{[\text{Cu}^{2+}]} \quad \text{Equation III.3}$$

$$\text{Ln} \frac{[M_0]}{[M]} = Kk_p \frac{[I][\text{Cu}^+]}{[\text{Cu}^{2+}]} t \quad \text{Equation III.4}$$

Equation III.4 shows that by following the evolution of $Ln \frac{[M_0]}{[M]}$ as a function of the time it is possible to obtain to the rate constant of the reaction. Linearity of $Ln \frac{[M_0]}{[M]}$ over time confirms that the concentration of propagating radicals is constant throughout the polymerization.

II.3.4 ATRP from multi-arm macroinitiators

ATRP of multi-arm macroinitiators such as dendrimers and hyperbranched structures,^[218-223] calix[n]arenes with 4, 6, or 8 external functions,^[224-226] stars with 4 to 12 arms,^[227-230] or cyclodextrin with 21 branches^[231] has been investigated with styrene, acrylate and methacrylate as the monomer. Alkyl halides containing carbonyl groups, such as 2-bromoisobutyryl bromide, were used for the initiation of the polymerization of acrylate and methacrylate monomers. Polymerization was carried out with a catalyst complex containing copper bromide (CuBr) with different ligands such as dibromobis(triphenylphosphine)nickel (II) ($NiBr_2(PPh_3)_2$),^[218-220, 227] 2,2'-bipyridyl^[224, 225] or N-propyl-2-pyridylmethanimine.^[231, 232]

Haddleton et al. prepared glycopolymers using sugars as the macroinitiator. They polymerized hydrophobic (styrene and methyl methacrylate (MMA)) and hydrophilic 2-(N,N-dimethylamino)ethyl methacrylate (DMAEMA) and poly(ethylene glycol) methacrylate (PEGMA)) monomers by ATRP from glucose, galactose and maltose modified with 2-bromoisobutyryl bromide.^[233, 234] They demonstrated the possibility of synthesizing amphiphilic block copolymers from such carbohydrates.^[234] They also used polysaccharides, such as cyclodextrin with 21 arms, to initiate polymerization of hydrophilic monomers (PEGMA and DMAEMA).^[231] CuBr and N-propyl-2-pyridylmethanimine were used as the catalyst/ligand complex. They obtained hydrophilic star glycopolymers with good control over the molecular weight. Such structures, with the hydrophobic cavity present in the cyclodextrin, can be used as an inclusion complex for small organic molecules, as discussed in Chapter II.III.3.

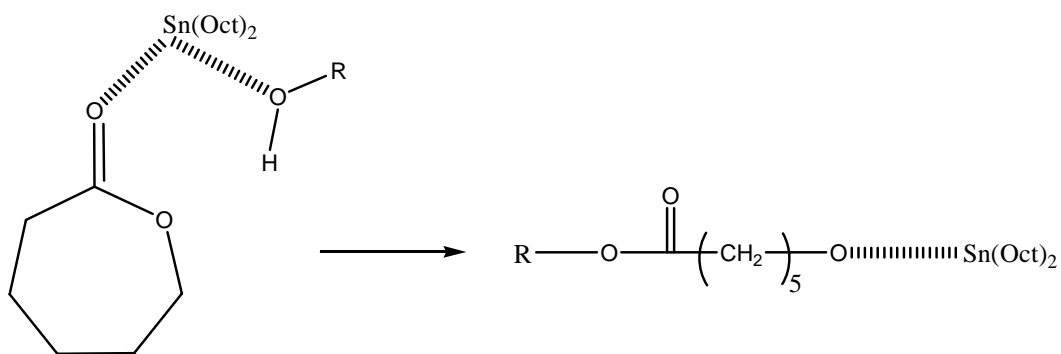
III. Ring-opening polymerization (ROP)

III.1. General considerations

Ring-opening polymerization is of importance for the polymerization of cyclic monomers. With regard to the process, ROP is a chain polymerization with a sequence of initiation, propagation and termination. Monomers are added to the growing chain after initiation by a cationic or anionic initiator, by a mechanism called the “insertion process”. This mechanism is different from anionic and cationic initiation. With regard to the kinetics, the propagation rate constants are closer to those of a step process than to those of a chain process with carbon-carbon double bond monomers. Thus the buildup of polymer molecular weight is slower for ROP than for chain polymerization of carbon-carbon double bond monomers. Many ROPs proceed as “living” polymerizations. The polymer molecular weight increases linearly with conversion and with the $[M]/[I]$ ratio, and narrow molecular weight distributions are obtained.^[195]

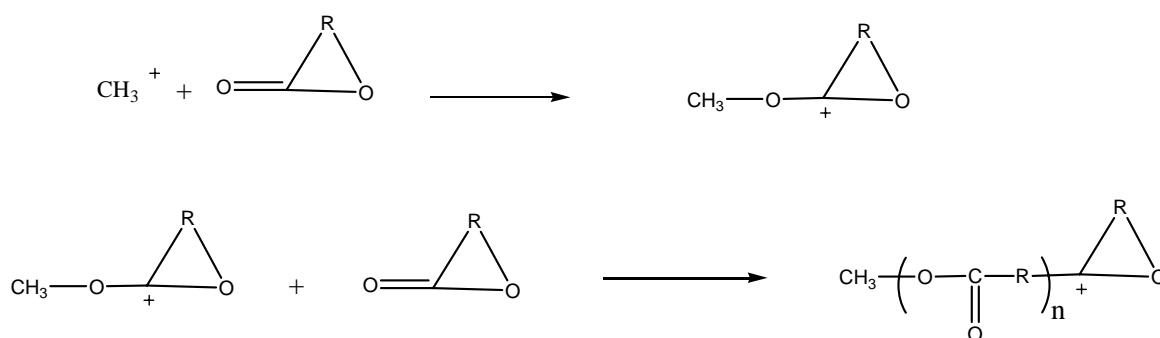
Here we are interested in the polymerization of a cyclic ester (lactone) by ROP. Polyesters are usually synthesized from polycondensation of a diol and a diacid. ROP is an alternative process for their synthesis and gives higher molar masses. Cyclic ether, lactam, nitrogen heterocycles, sulfur heterocycles and cycloalkenes are other monomers which may be polymerized by a ROP process. Their polymerization has been described in detail by Odian.^[195]

A variety of initiators have been used for the ROP of lactones. In the case of anionic ROP, anionic covalent initiators such as alkylmetal alkoxides and metal alkoxides, e.g. R_2AlOR' and $Al(OR_3)$, or metal carboxylates e.g. tin(II)-ethylhexanoate $[Sn(Oct)_2]$ may be used.^[235-237] For almost all lactones, the reaction proceeds by acyl-oxygen cleavage. With a coordination initiator, the metal coordinates with the oxygen of the carbonyl group of the monomer and oxygen of the propagating chain (Scheme III.8).



Scheme III.8 Insertion mechanism in ROP of ε-caprolactone initiated by an alcohol in the presence of a metal carboxylate [Sn(Oct)₂].

In the case of cationic ROP, a variety of cationic initiators are used which generate a tertiary oxonium ion-propagating species. Propagation follows with alkyl oxygen cleavage. An example of the initiation and propagation stages is given in Scheme III.9.



Scheme III.9 Mechanism of ROP of lactone initiated by methylene carbocation

Few details are given in the literature on the cationic ROP of lactone. The cationic route is limited by intramolecular transesterification (cyclisation) and other chain transfer reactions. Anionic polymerization is useful for the synthesis of high molecular weight poly(ester)s. Although transfer reactions (including transesterification) have also been observed in anionic polymerization, limiting the molecular weight and inducing relatively broad molecular weight distributions, it has been shown that transfer may be reduced by the use of less active initiators such as alkoxides of Al instead of Na, Mg and Zn.^[238] A wide

variety of catalysts have been tested.^[239, 240] Transesterification is dependent on the initiation rate, which is faster than propagation, and on the metal catalyst.^[238] It was observed that low temperature helps to avoid transesterification.^[240-242] Kricheldorf et al. described poly(lactide) polymerization with tin(II)-ethylhexanoate at $T < 120$ °C. Polymers with high molecular weight and low polydispersity were obtained.^[241]

ϵ -Caprolactone is usually synthesized by anionic ROP. The nucleophile may be water, acid, alcohol^[240, 242], amine^[243] or thiol. The nature of the catalyst^[240, 242, 244, 245] and the temperature influence the conversion and the control of the polymerization. One of the most widely used catalysts is tin(II)-ethylhexanoate [Sn(Oct)₂]. In the presence of this catalyst, it is possible to limit transesterification. The reaction rate is relatively high for reaction temperatures between 110 and 120° C.^[240, 241, 246, 247] The amount of catalyst is also important for controlled polymerization. When the amount of [Sn(Oct)₂] matches the number of initiator groups, two molar mass populations are formed, whereas when the quantity of catalyst is reduced, only one population is obtained. Thus, when less catalyst is used, the reaction time is longer, but transesterification is reduced (the number of active species decreases and the polymerization constant increases).^[236, 248-250] It has also been shown that it is not necessary to prolong the reaction time beyond 20 hours under these conditions.^[249]

III.2. Multi-arm macroinitiators

Hedrick et al. and Hult et al. have worked on the ROP of ϵ -caprolactone from multi-arm initiators. They considered stars, dendrimers and hyperbranched polymers.^[218, 248, 251, 252] Recently, other groups have reported ROP from stars with 4 to 12 arms^[228-230, 253] and hyperbranched polymers.^[222, 223] By transposition of the reaction conditions, polysaccharides have also been used as macroinitiators for ROP of lactide.^[249]

Hult et al. compared hyperbranched polymers and dendrimers.^[252, 254] They demonstrated that the polydispersity of the copolymer is higher with a hyperbranched molecule core than with a dendrimer due to the presence of significant number of monohydroxylated groups (linear units) in the HBP, which causes heterogeneity in the sample

and increased polydispersity. With the dendritic structure, on the other hand, initiation is limited to di-substituted groups (terminal units) leading to more uniform macromolecules.

Hedrick et al. studied another metal catalyst, tin(II) trifluoromethane sulfonate $[\text{Sn}(\text{OTf})_2]$, and compared it with tin(II)-ethylhexanoate $[\text{Sn}(\text{Oct})_2]$.^[240, 242] They showed that triflate-substituted catalysts $[\text{Sn}(\text{OTf})_2]$ were more active and allowed lower polymerization temperatures. The polymerization was better controlled and the polydispersity narrower, even for monoalcohols. According to this result, and to their previous work,^[251, 255] where they showed that ROP of lactone was well controlled by using $[\text{Sn}(\text{Oct})_2]$ with multi-arm branched macroinitiators, Hedrick et al. demonstrated that it was preferable to carry out the polymerization from monofunctional alcohols using $[\text{Sn}(\text{OTf})_2]$ and from multifunctional alcohols using $[\text{Sn}(\text{Oct})_2]$.^[256]

IV. Conclusion

This second literature chapter has described the theoretical background for the polymer synthesis and has particularly focused on ATRP and ROP procedures. Radical polymerization is widely used in polymer synthesis because of its easy implementation in comparison with ionic procedures. Since the introduction of dormant and active species during the 1990's there has been enormous interest in CRP processes and three main techniques of CRP have emerged NMP, ATRP and RAFT. The use of ATRP and ROP with multi-arm macroinitiators has also been widely investigated, providing a firm basis for their use in the present case of hyperbranched macroinitiators.

Chapter IV. Experimental methods

This chapter concerns the synthetic procedures used in this project. Two approaches were used for the design of the amphiphilic multi-arm star-block copolymers. The first strategy consisted of using Boltorn® H40 HBP (Perstorp, Sweden) (H40) as the initiator for the ring-opening polymerization of ϵ -caprolactone. Along with the H40 itself, the resulting poly(ϵ -caprolactone) (PCL) blocks provide the hydrophobic interior of the final multi-arm star-block copolymer (H40-(PCL)_p). In order to graft hydrophilic blocks to the precursor, functional groups serving as initiators for ATRP, such as 2-bromoisobutyryl bromide, were introduced to the ends of the PCL arms to give a H40-(PCL)_p-Br macroinitiator. Subsequent polymerization of *tert*-butyl acrylate (*tert*-BuA) monomer gave poly(*tert*-butyl acrylate) (PtBuA). The resulting H40-(PCL)_p-(PtBuA)_q star-block copolymer is not sufficiently hydrophilic to be dispersed in water. Removal of the *tert*-butyl ester protective groups was therefore used to convert the PtBuA to the corresponding poly(acrylic acid) (PAA), rendering the macromolecule water-soluble (H40-(PCL)_p-(PAA)_q).

I. Materials

H40 was obtained from Perstorp Chemicals and was washed in acetone and precipitated in diethyl ether before use. Tin(II) ethylhexanoate [Sn-(Oct)₂] (Aldrich) was used as received. ϵ -Caprolactone (99 % Aldrich) was dried over calcium hydride (CaH₂), distilled and stored under N₂ prior to use. Triethylamine (96 %, Aldrich) was distilled and stored under N₂ prior to use. 2-Bromoisobutyryl bromide (98 %, Aldrich), ethylene carbonate (98 % Aldrich), 2, 2'-bipyridyl (99 + % Acros), hexamethyl triethylene tetramine (HMTETA, Aldrich), pentamethyl diethylene triamine (PMDETA, Aldrich), trifluoroacetic acid (98 % Fluka) and CuBr (> 98 % Fluka) were used without further purification. N-Propyl-2-pyridylmethanimine was synthesized from *n*-propylamine and pyridine-2-carboxaldehyde according to literature.^[257] Triethylamine (Fluka) was distilled before use. *Tert*-butyl acrylate (*t*BuA) and *tert*-butyl methacrylate (*t*BuMA) (98 % Aldrich), 2-(*N,N*-dimethylamino)ethyl methacrylate (DMAEMA, 98 % Aldrich), diethylene glycol methyl ether methacrylate (DEGMA) and poly(ethylene glycol) methyl ether methacrylate (PEGMA $M_n \sim 475$ g/mol) were passed through a column of basic alumina to remove the stabilizer. *n*-Butyl methacrylate (BMA) was freshly distilled prior to use. Commercially available solvents were used without further purification. Reactions were carried out in standard glassware under inert atmosphere. Benzyl acetate, geraniol (trans-3,7-dimethyl-2,6-octadien-1-ol), decanal, Vertenex® (4-*tert*-butylcyclohexyl acetate, dorisyl), pipol ((*Z*)-3-hexenol), 3,5,5-trimethylhexanal, dimetol (2,6-dimethyl-2-heptanol), acetophenone, ethyl (*E*)-2,4-dimethyl-2-pentenoate jasmonitrile, benzylacetone (4-phenyl-2-butanone), 2-pentylcyclopentanol, 4-cyclohexyl-2-methyl-2-butanol, 10-undecenal, allyl 3-cyclohexylpropanoate were received from Firmenich SA.

II. Synthesis of the amphiphilic star-block copolymer

II.1. ROP of ϵ -caprolactone

Synthesis of H40-(PCL)₄₀

After precipitation from acetone into diethyl ether, H40 was dried under vacuum for 2 days. A 250 mL three-neck flask was charged with H40 (850.0 mg, 6.7 mmol of hydroxyl groups) under an inert atmosphere and placed in an oil bath at 107 °C in order to melt it and hence facilitate mixing with ϵ -caprolactone. ϵ -Caprolactone (22.8 g, 21.2 mL, 200.0 mmol) was slowly introduced and a catalytic amount ($[catalyst]/[macroinitiator] = 1/400$) of Sn-(Oct)₂ added. The polymerization reaction mixture was stirred for 14 h, diluted with THF, and precipitated into cold *n*-heptane to give 22.3 g (71.5 %) of a white crystalline powder.

The degree of polymerization DP_p , i.e. the average number of PCL repeat units of per arm, was determined from ¹H-NMR spectroscopy according to the following equation:

$$DP_p = \frac{I_{CH_2OCO}}{I_{CH_2OH}}$$

where I_{CH_2OH} is the integral of peak corresponding to the methyl groups adjacent to the chain ends and I_{CH_2OCO} is the integral of the peak corresponding to the methyl groups associated with the ester linkages. The average structure of the compound was in this case determined to be H40-(PCL)₄₀.

¹H NMR (400 MHz, CDCl₃): 4.05 (t, -(CO-CH₂-CH₂-CH₂-CH₂-CH₂-O)-, 80 H); 3.65 (t, -CO-CH₂-CH₂-CH₂-CH₂-CH₂-OH, 2 H); 2.31 (t, -(CO-CH₂-CH₂-CH₂-CH₂-O)-, 80 H); 1.70-1.60 (m, -(CO-CH₂-CH₂-CH₂-CH₂-O)-, 172.8 H); 1.45-1.32 (m, -(CO-CH₂-CH₂-CH₂-CH₂-O)- 84.8 H).

¹³C NMR (100.6 MHz, CDCl₃): 173.55 (s, -(CO-CH₂-CH₂-CH₂-CH₂-O)-); 64.16 (t, -(CO-CH₂-CH₂-CH₂-CH₂-O)-); 34.13 (t, -(CO-CH₂-CH₂-CH₂-CH₂-O)-); 28.37 (t, -(CO-CH₂-CH₂-CH₂-CH₂-O)-); 25.55 (t, -(CO-CH₂-CH₂-CH₂-CH₂-O)-); 24.59 (t, -(CO-CH₂-CH₂-CH₂-CH₂-O)-).

GPC (DMF): $M_n \sim 158900$ g/mol, $M_w/M_n = 2.07$.

Synthesis of H40-(PCL)₁₀

As described above with 2.0 g of Boltorn® H40 HBP and 17.4 mL of ϵ -caprolactone for 16 h to give 19.6 g (95%) of a white crystalline powder.

¹H-NMR (500 MHz, CDCl₃): 4.05 (t, 18 H); 3.65 (t, 1.69 H); 2.31 (t, 19.06 H); 1.70-1.60 (m, 40.6 H); 1.45-1.32 (m, 20 H).

¹³C-NMR (125.8 MHz, CDCl₃): 173.74(s); 64.15 (t); 34.13 (t); 28.36 (t); 25.54 (t) 24.59 (t).

IR: 3540 w, 3436 w, 2943 m, 2865 w, 1721 s, 1470 w, 1418 w, 1396 w, 1366 m, 1293 m, 1240 m, 1186 m, 1162 m, 1107 m, 1045 m, 961 m, 933 w, 840 w, 731 m, 706 w.

GPC (DMF): $M_n \sim 65380$ g/mol, $M_w/M_n = 2.03$.

A degree of polymerization $DP_p = 10$ corresponding to the number of repeated units of caprolactone per arm was determined, and the average structure of the compound was therefore assigned as H40-(PCL)₁₀.

Synthesis of H40-(PCL)₁₇

As described above with 2.50 g of Boltorn® H40 HBP and 43.2 mL of ϵ -caprolactone for 21 h to give 45.5 g (93%) of a white crystalline powder.

¹H-NMR (500 MHz, CDCl₃): 4.05 (t, 32 H); 3.65 (t, 1.88 H); 2.31 (t, 33 H); 1.70-1.60 (m, 66.2 H); 1.45-1.32 (m, 33 H).

¹³C-NMR (125.8 MHz, CDCl₃): 173.55 (s); 64.16 (t); 34.13 (t); 28.37 (t); 25.55 (t); 24.59 (t).

IR: 3534 w, 3443 w, 2940 m, 2863 m, 2643 w, 2319 w, 1720 s, 1470 m, 1416 m, 1396 m, 1364 m, 1292 m, 1237 s, 1167 s, 1107 s, 1064 m, 1045 s, 960 m, 933 m, 840 m, 731 m, 709 m.

GPC (DMF): $M_n \sim 89890$ g/mol, $M_w/M_n = 1.99$

A degree of polymerization $DP_p = 17$ corresponding to the number of repeated units of caprolactone per arm was determined, and the average structure of the compound was therefore assigned as H40-(PCL)₁₇.

Synthesis of H40-(PCL)₂₄

As described above with 0.30 g of Boltorn® H40 HBP and 5.79 mL of ϵ -caprolactone for 5.5 h to give 5.65 g (79%) of a white crystalline powder.

¹H-NMR (400 MHz, CDCl₃): 4.05 (t, 47.5 H); 3.65 (t, 1.96 H); 2.31 (t, 48 H); 1.70-1.60 (m, 101.7 H); 1.45-1.32 (m, 49.7 H).

¹³C-NMR (125.8 MHz, CDCl₃): 173.53 (s); 64.14 (t); 34.12 (t); 28.36 (t); 25.54 (t); 24.58 (t).

GPC (DMF): $M_n \sim 94300$ g/mol, $M_w/M_n = 2.46$

A degree of polymerization $DP_p = 24$ corresponding to the number of repeated units of caprolactone per arm was determined, and the average structure of the compound was therefore assigned as H40-(PCL)₂₄.

Synthesis of H40-(PCL)₅₀

As described above with 0.40 g of Boltorn® H40 HBP and 19.09 mL of ϵ -caprolactone for 14 h to give 19.8 g (94.6%) of a white crystalline powder.

¹H-NMR (400 MHz, CDCl₃): 4.05 (t, 100 H); 3.65 (t, 1.9 H); 2.31 (t, 100 H); 1.70-1.60 (m, 200.9 H); 1.45-1.32 (m, 101.8 H).

¹³C-NMR (100.6 MHz, CDCl₃): 173.53(s); 64.14 (t); 34.12 (t); 28.36 (t); 25.54 (t) 24.58 (t).

IR: 3440 w, 2944 m, 2867 w, 1722 s, 1471 m, 1417 m, 1396 w, 1364 m, 1293 m, 1238 m, 1166 m, 1107 m, 1065 m, 1047 m, 960 m, 933 w, 839 w, 773 w, 731 m, 709 w.

GPC (DMF): $M_n \sim 184640$ g/mol, $M_w/M_n = 2.57$.

A degree of polymerization $DP_p = 50$ corresponding to the number of repeated units of caprolactone per arm was determined, and the average structure of the compound was therefore assigned as H40-(PCL)₅₀.

Synthesis of H30-(PCL)₁₂

As described above with 0.17 g (1.56 mmol of hydroxyl groups) of Boltorn® H30 HBP and 2.0 mL of ϵ -caprolactone for 22 h to give 2.15 g (96.2%) of a white crystalline powder.

$^1\text{H-NMR}$ (400 MHz, CDCl_3): 4.05 (t, 22.7 H); 3.65 (t, 1.84 H); 2.31 (t, 24 H); 1.70-1.60 (m, 52.1 H); 1.45-1.32 (m, 25.17 H).

$^{13}\text{C-NMR}$ (100.6 MHz, CDCl_3): 172.96 (s); 63.58 (t); 33.56 (t); 27.8 (t); 24.97 (t) 24.02 (t)

GPC (DMF): $M_n \sim 41800$ g/mol, $M_w/M_n = 1.95$.

A degree of polymerization $DP_p = 12$ corresponding to the number of repeated units of caprolactone per arm was determined, and the average structure of the compound was therefore assigned as H30-(PCL)_{12} .

II.2. Synthesis of a multifunctional macroinitiator for ATRP

Functionalization of H40-(PCL)₄₀ to give H40-(PCL)₄₀-Br

H40-(PCL)_{40} (20.0 g, 4.3 mmol of hydroxyl functions) was dried under vacuum for 15 minutes. Dry THF (130.0 mL) was added, followed by 2-bromoisobutyryl bromide (9.8 g, 5.3 mL, 42.7 mmol), introduced dropwise from a syringe, and finally triethylamine (2.6 g, 3.6 mL, 25.6 mmol). The reaction was carried out at ambient temperature and terminated after 65 h. The reaction mixture was precipitated from THF into cold water and after drying under vacuum for 2 h, the polymer was again precipitated into cold water and then into *n*-heptane. After drying for one night under vacuum at 50 °C, 19.9 g (61.4 %) of $\text{H40-(PCL)}_{40}\text{-Br}$ was obtained as a white crystalline powder.

$^1\text{H NMR}$ (400 MHz, CDCl_3): 4.17 (t, $-(\text{CO-CH}_2\text{-CH}_2\text{-CH}_2\text{-CH}_2\text{-CH}_2\text{-O})\text{-CO-C}(\text{CH}_3)_2\text{-Br}$, 6.04 H); 4.05 (t, $-(\text{CO-CH}_2\text{-CH}_2\text{-CH}_2\text{-CH}_2\text{-CH}_2\text{-O})$, 80.23 H); 2.31 (t, $-(\text{CO-CH}_2\text{-CH}_2\text{-CH}_2\text{-CH}_2\text{-CH}_2\text{-O})$, 80 H); 1.93 (s, $-(\text{CO-CH}_2\text{-CH}_2\text{-CH}_2\text{-CH}_2\text{-CH}_2\text{-O})\text{-CO-C}(\text{CH}_3)_2\text{-Br}$, 6.68 H); 1.70-1.57 (m, $-(\text{CO-CH}_2\text{-CH}_2\text{-CH}_2\text{-CH}_2\text{-CH}_2\text{-O})$, 171.9 H); 1.43-1.38 (m, $-(\text{CO-CH}_2\text{-CH}_2\text{-CH}_2\text{-CH}_2\text{-CH}_2\text{-O})$, 88.0 H).

$^{13}\text{C NMR}$ (100.6 MHz, CDCl_3): 173.54 (s, $-(\text{CO-CH}_2\text{-CH}_2\text{-CH}_2\text{-CH}_2\text{-CH}_2\text{-O})$); 171.68 (s, $-(\text{CO-CH}_2\text{-CH}_2\text{-CH}_2\text{-CH}_2\text{-CH}_2\text{-O})\text{-CO-C}(\text{CH}_3)_2\text{-Br}$); 64.15 (t, $-(\text{CO-CH}_2\text{-CH}_2\text{-CH}_2\text{-CH}_2\text{-CH}_2\text{-O})$); 55.93 (s, $-(\text{CO-CH}_2\text{-CH}_2\text{-CH}_2\text{-CH}_2\text{-CH}_2\text{-O})\text{-CO-C}(\text{CH}_3)_2\text{-Br}$); 34.13 (t, $-(\text{CO-CH}_2\text{-CH}_2\text{-CH}_2\text{-CH}_2\text{-CH}_2\text{-O})$); 30.77 (q, $-(\text{CO-CH}_2\text{-CH}_2\text{-CH}_2\text{-CH}_2\text{-CH}_2\text{-O})\text{-CO-C}(\text{CH}_3)_2\text{-Br}$); 28.07 (t, -

(CO-CH₂-CH₂-CH₂-CH₂-O-); 25.54 (t, -(CO-CH₂-CH₂-CH₂-CH₂-O-); 24.59 (t, -(CO-CH₂-CH₂-CH₂-CH₂-O-).

GPC (DMF): $M_n \sim 177600$ g/mol, $M_w/M_n = 2.06$

Synthesis of H40-(PCL)₁₀-Br

As described above with 15 g of H40-(PCL)₁₀, 2.95 mL of 2-bromoisobutyryl bromide ($2.37 \cdot 10^{-2}$ mol) and 3.30 mL of triethylamine ($2.37 \cdot 10^{-2}$ mol) for 48 h to give 9.50 g (56.6 %) of H40-(PCL)₁₀-Br as a crystalline powder.

¹H-NMR (400 MHz, CDCl₃): 4.17 (t, 3.5 H); 4.05 (t, 18.7 H); 2.31 (t, 20 H); 1.93 (s, 5.2 H); 1.70-1.57 (m, 42.9 H); 1.43-1.33 (m, 22.1 H).

¹³C-NMR (100.6 MHz, CDCl₃): 173.53 (s); 64.14 (t); 55.93 (s); 34.12 (t); 30.77 (q); 28.36 (t); 28.07 (t); 25.54 (t); 24.59 (t).

IR: 2939 m, 2866 m, 2675 w, 2490 w, 1722 s, 1470 m, 1433 m, 1419 w, 1396 m, 1365 m, 1293 m, 1240 m, 1163 m, 1107 s, 1066 m, 1036 m, 961 m, 932 w, 840 w, 804 w, 731 m, 709 w.

GPC (DMF): $M_n \sim 54300$ g/mol, $M_w/M_n = 2.27$.

Synthesis of H40-(PCL)₁₇-Br

As described above with 43 g ($5.79 \cdot 10^{-4}$ mol) of H40-(PCL)₁₇, 5.2 mL of 2-bromoisobutyryl bromide ($4.17 \cdot 10^{-2}$ mol) and 5.8 mL of triethylamine ($4.17 \cdot 10^{-2}$ mol) for 65 h to give 43.3 g (93 %) of H40-(PCL)₁₇-Br as a white crystalline powder.

¹H-NMR (500 MHz, CDCl₃): 4.17 (t, 2.2 H); 4.05 (t, 32.7 H); 2.31 (t, 34 H); 1.93 (s, 4.39 H); 1.70-1.57 (m, 69.6 H); 1.43-1.33 (m, 34.9 H).

¹³C-NMR (125.8 MHz, CDCl₃): 173.54 (s); 171.68 (s); 64.15 (t); 55.93 (s); 34.13 (t); 30.77 (q); 28.07 (t); 25.54 (t); 24.59 (t).

IR: 3533 w, 3443 w, 2941 m, 2863 m, 2653 w, 2319 w, 1719 s, 1469 m, 1418 m, 1396 m, 1365 m, 1292 m, 1238 s, 1160 s, 1106 s, 1064 m, 1044 s, 960 m, 933 m, 840 m, 731 m, 709 m.

GPC (DMF): $M_n \sim 106000$ g/mol, $M_w/M_n = 1.79$.

Synthesis of H40-(PCL)₂₄-Br

As described above with 5 g ($4.76 \cdot 10^{-5}$ mol) of H40-(PCL)₂₄, 2.1 mL of 2-bromoisobutyryl bromide ($1.71 \cdot 10^{-2}$ mol) and 1.4 mL of triethylamine ($1.03 \cdot 10^{-2}$ mol) for 65 h to give 4.26 g (81 %) of H40-(PCL)₂₄-Br as a crystalline powder.

¹H-NMR (400 MHz, CDCl₃): 4.17 (t, 3.6 H); 4.05 (t, 46.7 H); 2.31 (t, 48 H); 1.93 (s, 6.1 H); 1.70-1.57 (m, 102.5 H); 1.43-1.33 (m, 52.3 H).

¹³C-NMR (100.6 MHz, CDCl₃): 172.94 (s); 65.21 (t); 63.56 (s); 33.55 (t); 30.21 (q); 27.8 (t); 24.97 (t); 24.02 (t).

GPC (DMF): $M_n \sim 111100$ g/mol, $M_w/M_n = 2.79$.

Synthesis of H40-(PCL)₅₀-Br

As described above with 15 g of H40-(PCL)₅₀, 3.13 mL of 2-bromoisobutyryl bromide ($2.53 \cdot 10^{-2}$ mol) and 2.10 mL of triethylamine ($1.51 \cdot 10^{-2}$ mol) for 63 h to give 14.10 g (93.4 %) of H40-(PCL)₅₀-Br as a crystalline powder.

¹H-NMR (400 MHz, CDCl₃): 4.17 (t, 3 H); 4.05 (t, 100.3 H); 2.31 (t, 100 H); 1.93 (s, 4.9 H); 1.70-1.57 (m, 213.7 H); 1.43-1.33 (m, 106.9 H).

¹³C-NMR (100.6 MHz, CDCl₃): 173.51 (s); 64.13 (t); 55.93 (s); 34.12 (t); 30.77 (q); 28.36 (t); 28.07 (t); 25.54 (t); 24.58 (t).

IR: 2943 m, 2866 w, 1721 m, 1470 w, 1418 w, 1396 w, 1364 m, 1293 m, 1238 m, 1164 m, 1107 s, 1062 m, 1045 m, 960 m, 933 w, 840 w, 772 w, 731 m, 706 w.

GPC (DMF): $M_n \sim 125700$ g/mol, $M_w/M_n = 2.38$.

Synthesis of H30-(PCL)₁₂-Br

As described above with 1.65 g of H30-(PCL)₁₂, 1.63 mL of 2-bromoisobutyryl bromide ($1.31 \cdot 10^{-2}$ mol) and 1.10 mL of triethylamine ($7.9 \cdot 10^{-3}$ mol) for 65 h to give 1.26 g (68.4 %) of H30-(PCL)₁₂-Br as a crystalline powder.

¹H-NMR (400 MHz, CDCl₃): 4.17 (t, 2.9 H); 4.05 (t, 22.9 H); 2.31 (t, 24 H); 1.93 (s, 4.3 H); 1.70-1.57 (m, 52.1 H); 1.43-1.33 (m, 26 H).

^{13}C -NMR (125.7 MHz, CDCl_3): 173.56 (s); 64.16 (t); 34.13 (t); 30.78 (q); 28.36 (t); 25.54 (t); 24.59 (t).

GPC (DMF): $M_n \sim 42170$ g/mol, $M_w/M_n = 2.13$.

Synthesis of H40-Br

A solution of vacuum-dried Boltorn® H40 (2.80 g, corresponding to 25.0 mmol of hydroxyl groups) in dry THF (80.0 mL) was added to a solution of 4-(dimethylamino)pyridine (4.79 g, 39.3 mmol) and triethylamine (2.53 g, 3.48 mL, 25.0 mmol) in dry THF (20 mL) under an inert atmosphere. Then, 2-bromoisobutyryl bromide (17.24 g, 9.27 mL, 75.0 mmol) was added dropwise at room temperature. After 48 h, precipitated salts were filtered off and the solvent partially evaporated. The residual solution was precipitated into methanol. The precipitate was dried under vacuum to give 3.55 g (54 %) of a pure product.

^1H -NMR (400 MHz, CDCl_3): 4.40-4.10 (m, 3.86 H); 1.85 (s, 6 H); 1.35-1.05 (m, 3.03 H).

^{13}C -NMR (100.6 MHz, CDCl_3): 171.6 (s); 171.4 (s); 170.8 (s); 66.0 (m); 55.4 (s); 46.7 (s); 30.6 (q); 17.8 (q).

GPC (DMF): $M_n \sim 12300$ g/mol, $M_w/M_n = 1.72$

II.3. Polymerization of *tert*-BuA by ATRP using H40-(PCL)_p-Br as the macroinitiator

Synthesis of H40-(PCL)₄₀-(PtBuA)₁₀₀

A three-necked flask was charged with the multifunctional macroinitiator (H40-(PCL)₄₀-Br) (10.0 g, 2.1 mmol of initiator functional groups), ethylene carbonate (5.0 g, 10% wt. monomer) and 2,2'-bipyridyl (718.4 mg, 4.6 mmol) and the contents dried under vacuum for 1 h 30. *Tert*-BuA (44.2 g, 50.0 mL, 345.0 mmol) was added after purification (to remove any inhibitor) and the resulting mixture was subjected to three freeze-vacuum-thaw cycles. Addition of CuBr (329.9 mg, 2.3 mmol) was followed by one further freeze-vacuum-thaw cycle. The flask was then placed in a thermostatically controlled oil bath at 90 °C. After 20 h, the reaction was terminated by placing the flask in an ice bath. After stirring, the polymer was diluted in THF and the contents were passed through a column of neutral alumina to remove

copper salts. The THF was evaporated and the polymer precipitated in a mixture of methanol/water (90/10 v/v), filtered and dried under vacuum for several hours.

A degree of polymerization $DP_q = 100$, i.e. the average number of *tert*-BuA repeat units per arm was determined from $^1\text{H-NMR}$ spectroscopy according to the following equation:

$$DP_q = \frac{I_{(m,br;1.60-1.28\text{ ppm})} - I_{CH_2(PCL)}}{9 \frac{I_{CH_2(PCL)}}{2DP_p}}$$

where $I_{(m,br;1.60-1.28\text{ ppm})} - I_{CH_2(PCL)}$ is given by the integral of the peak corresponding to the *tert*-butyl groups of *tert*-BuA and $I_{CH_2(PCL)}$ is the integral of the peak corresponding to the PCL methyl groups at 4.06 ppm. The average structure of the compound was therefore designated H40-(PCL)₄₀-(*Pt*BuA)₁₀₀.

$^1\text{H NMR}$ (400 MHz, CDCl_3): 3.99 (t, $-(\text{CO}-\text{CH}_2-\text{CH}_2-\text{CH}_2-\text{CH}_2-\underline{\text{CH}_2}-\text{O})-\text{CO}-\text{C}(\text{CH}_3)_2(\text{CH}_2-\text{CH}(\text{COO}-\text{C}(\text{CH}_3)_3)-$, 78 H); 2.24 (t, $-(\text{CO}-\underline{\text{CH}_2}-\text{CH}_2-\text{CH}_2-\text{CH}_2-\text{CH}_2-\text{O})-\text{CO}-\text{C}(\text{CH}_3)_2(\text{CH}_2-\text{CH}(\text{COO}-\text{C}(\text{CH}_3)_3)$, 78 H); 2.34-2.01 (m, br., $-(\text{CO}-\text{CH}_2-\text{CH}_2-\text{CH}_2-\text{CH}_2-\text{CH}_2-\text{O})-\text{CO}-\text{C}(\text{CH}_3)_2(\text{CH}_2-\underline{\text{CH}}(\text{COO}-\text{C}(\text{CH}_3)_3)-$, 159.1 H); 1.87-1.65 (m, $-(\text{CO}-\text{CH}_2-\text{CH}_2-\text{CH}_2-\text{CH}_2-\text{CH}_2-\text{O})-\text{CO}-\text{C}(\underline{\text{CH}_3})_2(\text{CH}_2-\text{CH}(\text{COO}-\text{C}(\text{CH}_3)_3)-$ + $-(\text{CO}-\text{CH}_2-\text{CH}_2-\text{CH}_2-\text{CH}_2-\text{CH}_2-\text{O})-\text{CO}-\text{C}(\text{CH}_3)_2(\underline{\text{CH}_2}-\text{CH}(\text{COO}-\text{C}(\text{CH}_3)_3)-$, 51.9 H); 1.64-1.52 (m, $-(\text{CO}-\text{CH}_2-\underline{\text{CH}_2}-\text{CH}_2-\underline{\text{CH}_2}-\text{CH}_2-\text{O})-\text{CO}-\text{C}(\text{CH}_3)_2(\text{CH}_2-\text{CH}(\text{COO}-\text{C}(\text{CH}_3)_3)-$ + $-(\text{CO}-\text{CH}_2-\text{CH}_2-\text{CH}_2-\text{CH}_2-\text{CH}_2-\text{O})-\text{CO}-\text{C}(\text{CH}_3)_2(\underline{\text{CH}_2}-\text{CH}(\text{COO}-\text{C}(\text{CH}_3)_3)-$, 166.9 H); 1.51-1.10 (m, $-(\text{CO}-\text{CH}_2-\text{CH}_2-\text{CH}_2-\text{CH}_2-\text{CH}_2-\text{O})-\text{CO}-\text{C}(\text{CH}_3)_2(\text{CH}_2-\text{CH}(\text{COO}-\text{C}(\underline{\text{CH}_3})_3)-$ + (t, $-(\text{CO}-\text{CH}_2-\text{CH}_2-\underline{\text{CH}_2}-\text{CH}_2-\text{CH}_2-\text{O})-\text{CO}-\text{C}(\text{CH}_3)_2(\text{CH}_2-\text{CH}(\text{COO}-\text{C}(\text{CH}_3)_3)-$; 950.9 H).

$^{13}\text{C NMR}$ (100.6 MHz, CDCl_3): 174.45 (s, $-(\text{CO}-\text{CH}_2-\text{CH}_2-\text{CH}_2-\text{CH}_2-\text{CH}_2-\text{O})-\text{CO}-\text{C}(\text{CH}_3)_2(\text{CH}_2-\text{CH}(\underline{\text{COO}}-\text{C}(\text{CH}_3)_3)-$); 173.82 (s, $-(\underline{\text{CO}}-\text{CH}_2-\text{CH}_2-\text{CH}_2-\text{CH}_2-\text{CH}_2-\text{O})-\underline{\text{CO}}-\text{C}(\text{CH}_3)_2(\text{CH}_2-\text{CH}(\text{COO}-\text{C}(\text{CH}_3)_3)-$); 80.60 (s, $-(\text{CO}-\text{CH}_2-\text{CH}_2-\text{CH}_2-\text{CH}_2-\text{CH}_2-\text{O})-\text{CO}-\text{C}(\text{CH}_3)_2(\text{CH}_2-\text{CH}(\text{COO}-\underline{\text{C}}(\text{CH}_3)_3)-$); 64.43 (t, $-(\text{CO}-\text{CH}_2-\text{CH}_2-\text{CH}_2-\text{CH}_2-\underline{\text{CH}_2}-\text{O})-\text{CO}-\text{C}(\text{CH}_3)_2(\text{CH}_2-\text{CH}(\text{COO}-\text{C}(\text{CH}_3)_3)-$); 42.67 & 42.18 (d, $-(\text{CO}-\text{CH}_2-\text{CH}_2-\text{CH}_2-\text{CH}_2-\text{CH}_2-\text{O})-\text{CO}-\text{C}(\text{CH}_3)_2(\text{CH}_2-\underline{\text{CH}}(\text{COO}-\text{C}(\text{CH}_3)_3)-$); 34.40 (t, $-(\text{CO}-\underline{\text{CH}_2}-\text{CH}_2-\text{CH}_2-\text{CH}_2-\text{CH}_2-\text{O})-\text{CO}-$

$C(CH_3)_2(CH_2-CH(COO-C(CH_3)_3-))$;	28.64	(t,	$-(CO-CH_2-CH_2-CH_2-\underline{C}H_2-CH_2-O)-CO-$
$C(CH_3)_2(CH_2-CH(COO-C(CH_3)_3-))$;	28.39	(q,	$-(CO-CH_2-CH_2-CH_2-CH_2-CH_2-O)-CO-$
$C(CH_3)_2(CH_2-CH(COO-C(\underline{C}H_3)_3-))$;	25.82	(t,	$-(CO-CH_2-\underline{C}H_2-CH_2-CH_2-CH_2-O)-CO-$
$C(CH_3)_2(CH_2-CH(COO-C(CH_3)_3-))$;	24.87	(t,	$-(CO-CH_2-CH_2-\underline{C}H_2-CH_2-CH_2-O)-CO-$
$C(CH_3)_2(CH_2-CH(COO-C(CH_3)_3-))$.			

GPC (DMF): $M_n \sim 452350$ g/mol, $M_w/M_n = 2.33$.

Synthesis of H40-(PCL)₁₀-(PtBuA)₆₈

As described above with 1 g of H40-(PCL)₁₀-Br, 1.3 g of ethylene carbonate, 222 mg ($1.41 \cdot 10^{-3}$ mol) of 2,2'-bipyridyl, 10.3 mL of *t*BuA ($7.08 \cdot 10^{-2}$ mol) and 101.6 mg ($7.08 \cdot 10^{-4}$ mol) of CuBr for 21 h at 90 °C to give 4.38 g of pure product.

¹H-NMR (400 MHz, CDCl₃): 4.04 (t, 20 H); 2.28 (t, 20 H); 2.44-2.02 (m, 68.9 H); 1.93-1.73 (m, 15.8 H) 1.73-1.57 (m, 45.2 H); 1.56-1.28 (m, 612.2 H).

¹³C-NMR (100.8 MHz, CDCl₃): 173.62 (s) and 173.42 (s); 172.96 (s); 79.75 (s); 63.58 (t); 41.83 and 41.4 (d); 33.55 (t); 27.8 (q); 27.54 (t); 24.97 (t); 24.01 (t).

IR: 2977 m, 2933 m, 2871 m, 1788 w, 1722 s, 1474 m, 1450 m, 1392 m, 1366 s, 1253 s, 1141 s, 1035 m, 960 m, 908 m, 844 s, 751 m.

GPC (DMF): $M_n \sim 488520$ g/mol, $M_w/M_n = 2.44$.

A degree of polymerisation $DP_q = 68$ corresponding to the number of repeated units of *t*BuA per arm was determined, and the average structure of the compound was therefore assigned as H40-(PCL)₁₀-(PtBuA)₆₈.

Synthesis of H40-(PCL)₁₀-(PtBuA)₇₀

As described above with 1 g of H40-(PCL)₁₀-Br, 2.05 g of ethylene carbonate, 222 mg ($1.41 \cdot 10^{-3}$ mol) of 2,2'-bipyridyl, 20.6 mL of *t*BuA ($1.41 \cdot 10^{-1}$ mol) and 101.6 mg ($7.08 \cdot 10^{-4}$ mol) of CuBr for 21 h at 90 °C to give 4.28 g of pure product.

¹H-NMR (500 MHz, CDCl₃): 4.06 (t, 20 H); 2.30 (t, 20 H); 2.39-2.06 (m, 78.5 H); 1.94-1.71 (m, 17.8 H) 1.70-1.57 (m, 46.5 H); 1.57-1.28 (m, 742.4 H).

¹³C-NMR (125.8 MHz, CDCl₃): 174.19 (s); 173.53 (s); 80.34 (s); 64.14 (t); 42.39 and 41.9 (d); 34.13 (t); 28.37 (q); 28.09 (t); 25.54 (t); 24.59 (t).

IR: 2977 m, 2933 m, 2871 m, 1788 w, 1722 s, 1474 m, 1450 m, 1392 m, 1366 s, 1253 s, 1141 s, 1035 m, 960 m, 908 m, 844 s, 751 m.

GPC (DMF): $M_n \sim 459740$ g/mol, $M_w/M_n = 1.84$.

A degree of polymerisation $DP_q = 70$ corresponding to the number of repeated units of *t*BuA per arm was determined, and the average structure of the compound was therefore assigned as H40-(PCL)₁₀-(*Pt*BuA)₇₀.

Synthesis of H40-(PCL)₁₀-(PtBuA)₁₁₅

As described above with 1 g of H40-(PCL)₁₀-Br, 2.05 g of ethylene carbonate, 222 mg ($1.41 \cdot 10^{-3}$ mol) of 2,2'-bipyridyl, 20.6 mL of *t*BuA ($1.41 \cdot 10^{-1}$ mol) and 101.6 mg ($7.08 \cdot 10^{-4}$ mol) of CuBr for 48 h at 90 °C to give 6.35 g of pure product.

¹H-NMR (500 MHz, CDCl₃): 4.06 (t, 20 H); 2.30 (t, 20 H); 2.39-2.06 (m, 128.4 H); 1.94-1.71 (m, 49.5 H) 1.70-1.57 (m, 66.8 H); 1.57-1.28 (m, 1239 H).

¹³C-NMR (125.8 MHz, CDCl₃): 174.19 (s); 173.53 (s); 80.33 (s); 67.98 (t); 64.14 (t) 42.38 and 41.9 (d); 34.13 (t); 28.37 (t); 28.03 (q); 25.55 (t); 24.59 (t).

IR: 2977 m, 2933 m, 2869 m, 1790 w, 1722 s, 1478 m, 1449 m, 1392 m, 1366 s, 1253 s, 1141 s, 1036 m, 1036 m, 906 m, 844 s, 751 m.

GPC (DMF): $M_n \sim 549000$ g/mol, $M_w/M_n = 2.06$.

A degree of polymerisation $DP_q = 115$ corresponding to the number of repeated units of *t*BuA per arm was determined, and the average structure of the compound was therefore assigned as H40-(PCL)₁₀-(*Pt*BuA)₁₁₅.

Synthesis of H40-(PCL)₁₇-(PtBuA)₁₈

As described above with 0.5 g ($6.25 \cdot 10^{-6}$ mol) of H40-(PCL)₁₇-Br, 288 mg of ethylene carbonate, 70.27 mg ($4.5 \cdot 10^{-4}$ mol) of 2,2'-bipyridyl, 3.27 mL of *t*BuA (2.88 g, $2.25 \cdot 10^{-2}$ mol) and 32.3 mg ($2.25 \cdot 10^{-4}$ mol) of CuBr for 17 h at 100 °C to give 812.5 g of pure product.

¹H-NMR (500 MHz, CDCl₃): 4.06 (t, 34 H); 2.31 (t, 34 H); 2.36-2.15 (m, br., 60.1 H); 1.71-1.60 (m, 69.8 H); 1.59-1.28 (m, 245 H).

¹³C-NMR (125.8 MHz, CDCl₃): 174.20 and 173.97 (s); 173.54 (s); 80.34 (s); 64.15 (t); 42.37 and 41.9 (d); 34.13 (t); 30.33 (q); 28.03 (q); 28.37 (t); 25.55 (t); 24.59 (t).

IR: 2974 m, 2932 m, 2866 m, 1790 w, 1721 s, 1477 m, 1448 m, 1391 m, 1365 s, 1252 s, 1141 s, 1037 m, 961 m, 910 m, 844 s, 750 m.

GPC (DMF): $M_n \sim 205000$ g/mol, $M_w/M_n = 1.80$.

A degree of polymerisation $DP_q = 18$ corresponding to the number of repeated units of *t*BuA per arm was determined from $^1\text{H-NMR}$ spectroscopy according to the following equation:

The average structure of the compound was therefore assigned as $\text{H40-(PCL)}_{17}\text{-(PtBuA)}_{18}$.

Synthesis of H40-(PCL)₁₇-(PtBuA)₅₀

As described above with 7 g ($8.76 \cdot 10^{-5}$ mol) of $\text{H40-(PCL)}_{17}\text{-Br}$, 4.04 g of ethylene carbonate, 984.80 mg ($6.31 \cdot 10^{-3}$ mol) of 2,2'-bipyridyl, 45.76 mL of *t*BuA (40.41 g, 0.31 mol) and 452 mg ($3.15 \cdot 10^{-3}$ mol) of CuBr for 17 h at 100 °C to give 17.48 g of pure product. The degree of conversion was determined by NMR and confirmed with GPC.

$^1\text{H-NMR}$ (500 MHz, CDCl_3): 4.06 (t, 34 H); 2.31 (t, 38 H); 2.36-2.28 (m, br., 80.1 H); 1.71-1.60 (m, 79 H); 1.59-1.28 (m, 585 H).

$^{13}\text{C-NMR}$ (125.8 MHz, CDCl_3): 174.20 and 173.97 (s); 173.54 (s); 80.34 (s); 64.15 (t); 42.37 and 41.9 (d); 34.13 (t); 30.33 (q); 28.03 (q); 28.37 (t); 25.55 (t); 24.59 (t).

IR: 2974 m, 2932 m, 2866 m, 1790 w, 1721 s, 1477 m, 1448 m, 1391 m, 1365 s, 1252 s, 1141 s, 1037 m, 961 m, 910 m, 844 s, 750 m.

GPC (DMF): $M_n \sim 274930$ g/mol, $M_w/M_n = 1.95$.

A degree of polymerisation $DP_q = 50$ corresponding to the number of repeated units of *t*BuA per arm was determined from $^1\text{H-NMR}$ spectroscopy according to the following equation:

The average structure of the compound was therefore assigned as $\text{H40-(PCL)}_{17}\text{-(PtBuA)}_{50}$.

Synthesis of H40-(PCL)₂₄-(PtBuA)₈₂

As described above with 2 g of $\text{H40-(PCL)}_{24}\text{-Br}$, 1.11 g of ethylene carbonate, 226.1 mg ($1.30 \cdot 10^{-3}$ mol) of 2,2'-bipyridyl, 12.6 mL of *t*BuA ($8.47 \cdot 10^{-2}$ mol) and 103.8 mg ($6.51 \cdot 10^{-4}$ mol) of CuBr for 6 h at 90 °C to give 6.33 g of pure product.

$^1\text{H-NMR}$ (400 MHz, CDCl_3): 4.05 (t, 48 H); 2.29 (t, 48 H); 2.38-2.10 (m, 114.7 H); 1.89-1.73 (m, 26 H) 1.71-1.58 (m, 115 H); 1.58-1.30 (m, 767.3 H).

^{13}C -NMR (100.6 MHz, CDCl_3): 173.62 and 173.38 (s); 172.94 (s); 79.8 (s); 63.58 (t); 41.81 and 41.4 (d); 33.56 (t); 27.8 (q); 27.53 (q); 27.45 (t); 24.97 (t); 24.04 (t).

GPC (DMF): $M_n \sim 357700$ g/mol, $M_w/M_n = 3.17$.

A degree of polymerisation $DP_q = 82$ corresponding to the number of repeated units of *t*BuA per arm was determined, and the average structure of the compound was therefore assigned as $\text{H40-(PCL)}_{24}\text{-(PtBuA)}_{82}$.

Synthesis of H40-(PCL)₅₀-(PtBuA)₄₄

As described above with 2 g of $\text{H40-(PCL)}_{50}\text{-Br}$, 972 mg of ethylene carbonate, 104.6 mg ($6.7 \cdot 10^{-4}$ mol) of 2,2'-bipyridyl, 9.72 mL of *t*BuA ($6.69 \cdot 10^{-2}$ mol) and 48 mg ($3.3 \cdot 10^{-4}$ mol) of CuBr for 7 h 20 at 90 °C to give 3.36 g of pure product.

^1H -NMR (500 MHz, CDCl_3): 4.06 (t, 100 H); 2.30 (t, 100 H); 2.40-2.14 (m, 130 H); 1.75-1.60 (m, 203.3 H); 1.59-1.28 (m, 511.6 H).

^{13}C -NMR (125.8 MHz, CDCl_3): 174.20 and 173.97 (s); 173.53 (s); 80.34 (s); 64.15 (t); 42.37 and 41.9 (d); 34.13 (t); 28.37 (t); 28.03 (q); 25.55 (t); 24.59 (t).

IR: 2937 m, 2867 m, 1721 s, 1458 m, 1419 m; 1392 m, 1365 s, 1293 m, 1239 s, 1145 s, 1108 m, 1065 m; 1045 m, 961 m, 935 m, 844 s, 732 m.

GPC (DMF): $M_n \sim 376280$ g/mol, $M_w/M_n = 2.27$.

A degree of polymerisation $DP_q = 44$ corresponding to the number of repeated units of *t*BuA per arm was determined, and the average structure of the compound was therefore assigned as $\text{H40-(PCL)}_{50}\text{-(PtBuA)}_{44}$.

Synthesis of H40-(PCL)₅₀-(PtBuA)₅₄

As described above with 2 g of $\text{H40-(PCL)}_{50}\text{-Br}$, 972 mg of ethylene carbonate, 104.6 mg ($6.7 \cdot 10^{-4}$ mol) of 2,2'-bipyridyl, 9.72 mL of *t*BuA ($6.69 \cdot 10^{-2}$ mol) and 48 mg ($3.3 \cdot 10^{-4}$ mol) of CuBr for 20 h at 90 °C to give 3.31 g of pure product.

^1H -NMR (500 MHz, CDCl_3): 4.06 (t, 100 H); 2.30 (t, 100 H); 2.40-2.14 (m, 136.6 H); 1.75-1.60 (m, 209.1 H); 1.59-1.28 (m, 532.8 H).

^{13}C -NMR (125.8 MHz, CDCl_3): 174.20 and 173.97 (s); 173.53 (s); 80.34 (s); 64.15 (t); 42.37 and 41.9 (d); 34.13 (t); 28.37 (t); 28.03 (q); 25.55 (t); 24.59 (t).

IR: 2937 m, 2867 m, 1721 s, 1458 m, 1419 m; 1392 m, 1365 s, 1293 m, 1239 s, 1145 s, 1108 m, 1065 m; 1045 m, 961 m, 935 m, 844 s, 732 m.

GPC (DMF): $M_n \sim 376280$ g/mol, $M_w/M_n = 2.27$.

A degree of polymerisation $DP_q = 54$ corresponding to the number of repeated units of *t*BuA per arm was determined, and the average structure of the compound was therefore assigned as H40-(PCL)₅₀-(*Pt*BuA)₅₄.

Synthesis of H40-(PCL)₅₀-(*Pt*BuA)₅₆

As described above with 2 g of H40-(PCL)₅₀-Br, 972 mg of ethylene carbonate, 104.6 mg ($6.7 \cdot 10^{-4}$ mol) of 2,2'-bipyridyl, 9.72 mL of *t*BuA ($6.69 \cdot 10^{-2}$ mol) and 48 mg ($3.3 \cdot 10^{-4}$ mol) of CuBr for 14 h 30 at 90 °C to give 3.55 g of pure product.

¹H-NMR (500 MHz, CDCl₃): 4.06 (t, 100 H); 2.30 (t, 100 H); 2.40-2.14 (m, 160 H); 1.75-1.60 (m, 211.4 H); 1.59-1.28 (m, 622.3 H).

¹³C-NMR (125.8 MHz, CDCl₃): 174.20 and 173.97 (s); 173.53 (s); 80.34 (s); 64.15 (t); 42.37 and 41.9 (d); 34.13 (t); 28.37 (t); 28.03 (q); 25.55 (t); 24.59 (t).

IR: 2937 m, 2867 m, 1721 s, 1458 m, 1419 m; 1392 m, 1365 s, 1293 m, 1239 s, 1145 s, 1108 m, 1065 m; 1045 m, 961 m, 935 m, 844 s, 732 m.

GPC (DMF): $M_n \sim 536860$ g/mol, $M_w/M_n = 2.19$.

A degree of polymerisation $DP_q = 56$ corresponding to the number of repeated units of *t*BuA per arm was determined, and the average structure of the compound was therefore assigned as H40-(PCL)₅₀-(*Pt*BuA)₅₆.

Synthesis of H40-(PCL)₅₀-(*Pt*BuA)₆₄

As described above with 1.5 g of H40-(PCL)₅₀-Br, 805 mg of ethylene carbonate, 78.47 mg ($5.0 \cdot 10^{-4}$ mol) of 2,2'-bipyridyl, 9.12 mL of *t*BuA ($6.28 \cdot 10^{-2}$ mol) and 36.04 mg ($2.5 \cdot 10^{-4}$ mol) of CuBr for 48 h at 90 °C to give 5.86 g of pure product.

¹H-NMR (400 MHz, CDCl₃): 4.04 (t, 100 H); 2.36-2.09 (m, 159.3 H); 2.29 (t, 100 H); 1.94-1.56 (m, 334.9 H); 1.48-1.28 (m, 657.5 H).

¹³C-NMR (100.6 MHz, CDCl₃): 174.20 and 173.97 (s); 173.53 (s); 80.34 (s); 64.15 (t); 42.37 and 41.9 (d); 34.13 (t); 28.37 (t); 28.03 (q); 25.55 (t); 24.59 (t).

IR: 2976 m, 2934 m, 2867 m, 1722 s, 1455 m, 1419 m, 1392 m, 1366 s, 1293 m, 1240 s, 1144 s, 1108 m, 1045 m, 961 m, 935 m, 845 s, 733 m.

GPC (DMF): $M_n \sim 732760$ g/mol, $M_w/M_n = 3.37$.

A degree of polymerisation $DP_q = 64$ corresponding to the number of repeated units of *t*BuA per arm was determined, and the average structure of the compound was therefore assigned as H40-(PCL)₅₀-(PtBuA)₆₄.

Synthesis of H30-(PCL)₁₂-(PtBuA)₆₀

As described above with 1 g of H30-(PCL)₁₂-Br, 693 mg of ethylene carbonate, 211.1 mg ($1.35 \cdot 10^{-3}$ mol) of 2,2'-bipyridyl, 7.85 mL of *t*BuA ($5.41 \cdot 10^{-2}$ mol) and 96.9 mg ($6.76 \cdot 10^{-4}$ mol) of CuBr for 6 h at 90 °C to give 3.88 g of pure product.

¹H-NMR (400 MHz, CDCl₃): 4.04 (t, 24 H); 2.29 (t, 24 H); 2.36-2.10 (m, 73.5 H); 1.91-1.70 (m, 33.6 H) 1.69-1.58 (m, 57.8 H); 1.57-1.27 (m, 581.1 H).

¹³C-NMR (100.6 MHz, CDCl₃): 174.19 and 173.95 (s); 173.54 (s); 80.33 (s); 64.14 (t); 42.36 and 41.89 (d); 34.12 (t); 28.36 (t); 28.09 (q); 25.53 (t); 24.58 (t).

GPC (DMF): $M_n \sim 204000$ g/mol, $M_w/M_n = 2.40$.

A degree of polymerisation $DP_q = 60$ corresponding to the number of repeated units of *t*BuA per arm was determined, and the average structure of the compound was therefore assigned as H30-(PCL)₁₂-(PtBuA)₆₀.

Synthesis of H40-(PtBuA)₃₆

As described above with 0.2 g of H40-Br, 640 mg of ethylene carbonate, 195 mg ($1.25 \cdot 10^{-3}$ mol) of 2,2'-bipyridyl, 7.26 mL of *t*BuA ($5.0 \cdot 10^{-2}$ mol) and 89.5 mg ($6.24 \cdot 10^{-4}$ mol) of CuBr for 5 h 30 at 90 °C to give 1.82 g of pure product.

¹H-NMR (400 MHz, CDCl₃): 2.37-2.08 (m, 26.8 H); 1.91-1.68 (m, 6.64 H) 1.62-1.49 (m, 25.7 H); 1.48-1.19 (m, 324 H).

¹³C-NMR (100.6 MHz, CDCl₃): 173.62 (s); 79.77 (s); 27.53 (q)

GPC (DMF): $M_n \sim 199500$ g/mol, $M_w/M_n = 2.06$.

A degree of polymerization $DP_q = 36$ corresponding to the number of repeated units of *t*BuA per arm was determined by taking into account the difference of the molar masses (measured with GPC) before and after the polymerization. The value was confirmed with the integration values determined by NMR. The average structure of the compound was therefore assigned as H40-(*Pt*BuA)₃₆.

II.4. Hydrolysis of *tert*-butyl groups

Preparation of H40-(PCL)₄₀-(PAA)₁₀₀

The multifunctional star polymer H40-(PCL)₄₀-(*Pt*BuA)₁₀₀ (26.9 g, 4.26 mmol of *tert*-BuA) was dissolved in dichloromethane (330 mL). Trifluoroacetic acid (120 mL, 1.70 mol) was added to the flask. The solution was stirred for 2.5 at room temperature and the solvent then removed using a rotary evaporator. The product was redissolved in THF and precipitated in *n*-heptane. The resulting product was finally dried 3 days under vacuum at 50 °C to give 18.54 g of H40-(PCL)₄₀-(PAA)₁₀₀ as a white powder.

¹H NMR (400 MHz, DMSO-d₆): 12.23 (s, br., -(CO-CH₂-CH₂-CH₂-CH₂-O)-CO-C(CH₃)₂(CH₂-CH(COOH))) 42.8 H); 3.97 (t, -(CO-CH₂-CH₂-CH₂-CH₂-O)-CO-C(CH₃)₂(CH₂-CH(COOH)), 80 H); 2.34-2.05 (m, -(CO-CH₂-CH₂-CH₂-CH₂-O)-CO-C(CH₃)₂(CH₂-CH(COOH)), + -(CO-CH₂-CH₂-CH₂-CH₂-O)-CO-C(CH₃)₂(CH₂-CH(COOH)), 145.9 H); 1.86-1.41 (m., -(CO-CH₂-CH₂-CH₂-CH₂-O)-CO-C(CH₃)₂(CH₂-CH(COOH)) + -(CO-CH₂-CH₂-CH₂-CH₂-O)-CO-C(CH₃)₂(CH₂-CH(COOH)), 268.6 H); 1.40-1.33 (m, -(CO-CH₂-CH₂-CH₂-CH₂-O)-CO-C(CH₃)₂(CH₂-CH(COO-C(CH₃)₃), 47.7 H), 1.33-1.18 -(CO-CH₂-CH₂-CH₂-CH₂-O)-CO-C(CH₃)₂(CH₂-CH(COOH)), 89.9 H).

¹³C NMR (100.6 MHz, DMSO-d₆): 175.69 and 175.53 (s, -(CO-CH₂-CH₂-CH₂-CH₂-O)-CO-C(CH₃)₂(CH₂-CH(COOH))); 172.58 (s, -(CO-CH₂-CH₂-CH₂-CH₂-O)-CO-C(CH₃)₂(CH₂-CH(COOH))); 63.29 (t, -(CO-CH₂-CH₂-CH₂-CH₂-O)-CO-C(CH₃)₂(CH₂-CH(COOH))); 41.13-40.72 (d, br., -(CO-CH₂-CH₂-CH₂-CH₂-O)-CO-C(CH₃)₂(CH₂-CH(COOH))); 36.50-34.00 (t, br., -(CO-CH₂-CH₂-CH₂-CH₂-O)-CO-C(CH₃)₂(CH₂-CH(COOH))); 33.13 (t, -(CO-CH₂-CH₂-CH₂-CH₂-O)-CO-C(CH₃)₂(CH₂-CH(COOH))); 27.60 (t, -(CO-CH₂-CH₂-CH₂-CH₂-O)-CO-C(CH₃)₂(CH₂-CH(COOH))); 24.68 (t, -(CO-CH₂-CH₂-CH₂-CH₂-O)-CO-C(CH₃)₂(CH₂-CH(COOH))); 27.35 (q, -(CO-CH₂-CH₂-CH₂-

CH₂-CH₂-O)-CO-C(CH₃)₂(CH₂-CH(COO(CH₃)₃))); 23.68 (t, -(CO-CH₂-CH₂-CH₂-CH₂-CH₂-O)-CO-C(CH₃)₂(CH₂-CH(COOH)))).

Synthesis of H40-(PCL)₁₀-(PAA)₆₈

As described above with 3.18 g ($8.8 \cdot 10^{-6}$ mol) of H40-(PCL)₁₀-(PtBuA)₆₈ in 36.5 mL of dichloromethane and 16.5 mL ($2.22 \cdot 10^{-1}$ mol) of trifluoroacetic acid to give a product redissolved in ethanol (30 mL), precipitated into 300 mL of ether and dried under vacuum for 3 d. 1.67 g of purified H40-(PCL)₁₀-(PAA)₆₈ was obtained.

¹H NMR (400 MHz, DMSO-d₆): 12.23 (s, br., 28.9 H); 3.97 (s, br., 20 H); 2.34-2.05 (m, 70.9 H); 1.86-1.41 (m., 124.7 H); 1.40-1.33 (m, 16.84 H), 1.33-1.18(m, 29.5 H).

¹³C NMR (100.6 MHz, DMSO-d₆): 175.91 and 175.61 (s); 172.55 (s); 64.97 (t); 41.24-40.92 (d, br.); 36.15-34.95 (t, br.); 33.37 (t); 27.84 (t); 24.92 (t); 24.11 (t).

Synthesis of H40-(PCL)₁₀-(PAA)₇₀

As described above with 3.22 g ($8 \cdot 10^{-6}$ mol) of H40-(PCL)₁₀-(PtBuA)₇₀ in 36.5 mL of dichloromethane and 16.5 mL ($2.22 \cdot 10^{-1}$ mol) of trifluoroacetic acid to give a product redissolved in ethanol (30 mL), precipitated into 300 mL of ether and dried under vacuum for 3 d. 1.75 g of purified H40-(PCL)₁₀-(PAA)₇₀ was obtained.

¹H NMR (400 MHz, DMSO-d₆): 12.23 (s, br., 34 H); 3.97 (s, br., 20 H); 2.34-2.05 (m, 63.2 H); 1.86-1.41 (m., 111.42 H); 1.40-1.33 (m, 14.6 H), 1.33-1.18 (m, 25 H).

¹³C-NMR (100.6 MHz, DMSO-d₆): 175.75 (s); 64.95 (t); 41.44-40.94 (d, br.); 33.37 (t); 27.82 (t); 24.92 (t.); 24.11 (t).

IR: 3100 w, 2935 s, 2590 w, 1701 s, 1452 m, 1415 m, 1360 m, 1237 s. 1161 s, 1107 m, 1064 w, 910 w, 798 s.

Synthesis of H40-(PCL)₁₀-(PAA)₁₁₅

As described above with 4.56 g ($7.9 \cdot 10^{-6}$ mol) of H40-(PCL)₁₀-(PtBuA)₁₁₅ in 52 mL of dichloromethane and 24.3 mL ($3.27 \cdot 10^{-1}$ mol) of trifluoroacetic acid for 2 h 15 to give a product redissolved in ethanol (30 mL), precipitated into 300 mL of ether and dried under vacuum for 2 d. 2.28 g of purified H40-(PCL)₁₀-(PAA)₁₁₅ was obtained.

¹H NMR (400 MHz, DMSO-d₆): 12.23 (s, br.); 3.97 (s, br., 20 H); 2.34-2.05 (m, 123.8 H); 1.86-1.41 (m., 208.4 H); 1.40-1.33 (m, 40.8 H), 1.33-1.18 (m, 30 H).

^{13}C NMR (100.6 MHz, DMSO- d_6): 175.79 and 175.64 (s); 172.66 (s); 64.82 (t); 40.84-40.33 (d, br.); 36.05-34.93 (t, br.); 33.26 (t); 27.70 (t); 27.46 (q); 24.79 (t); 23.98 (t).

IR: 3077 m, 2935 s, 2595 w, 1703 s, 1454 m, 1415 m, 1360 m, 1238 s, 1163 s, 1108 m, 1058 w, 910 w, 799 s.

Synthesis of H40-(PCL)₁₇-(PAA)₅₀

As described above with 10 g ($3.25 \cdot 10^{-5}$ mol) of H40-(PCL)₁₇-(PtBuA)₅₀ in 100 mL of dichloromethane and 43 mL ($5.85 \cdot 10^{-1}$ mol) of trifluoroacetic acid to give a product redissolved in THF (60 mL), precipitated into 650 mL heptane and dried under vacuum for 3 d. 4.98 g of purified H40-(PCL)₁₇-Y-(PAA)₅₀ was obtained.

^1H NMR (500 MHz, DMSO- d_6): 12.23 (s, br.); 3.99 (t, 34 H); 2.32-2.14 (m, 123.8 H); 1.85-1.42 (m., 348.8 H); 1.42-1.38 (m, 15 H), 1.38-1.22 (m, 36 H).

^{13}C -NMR (125.8 MHz, DMSO- d_6): 175.78 (s); 175.61 (s); 172.67 (s); 63.39 (t); 41.70-40.50 (d, br.); 36.50-34.00 (t, br.); 33.27 (t); 27.69 (t); 23.98 (t).

IR: 3033 m, 2932 s, 2871 m, 2658 m, 2557 m, 1694 s, 1450 s, 1412 s, 1358 m, 1231 s, 1157 s, 1105 m, 961 m, 910 m, 844 s, 750 m.

Synthesis of H40-(PCL)₂₄-(PAA)₈₂

As described above with 4 g ($8.40 \cdot 10^{-6}$ mol) of H40-(PCL)₂₄-(PtBuA)₈₂ in 90 mL of dichloromethane and 30.7 mL ($4.13 \cdot 10^{-1}$ mol) of trifluoroacetic acid for 2 h 45 to give a product redissolved in THF, precipitated into heptane and dried under vacuum overnight. 2.59 g of H40-(PCL)₂₄-(PAA)₈₂ brown powder was obtained.

^1H NMR (400 MHz, DMSO- d_6): 12.23 (s, br., 33.7 H); 3.97 (t, 48 H); 2.34-2.05 (m, 94.8 H); 1.86-1.41 (m., 167.4 H); 1.40-1.33 (m, 24.4 H), 1.33-1.18(m, 53.4 H).

^{13}C -NMR (100.6 MHz, DMSO- d_6): 175.77 (s); 175.61 (s); 172.70 (s); 63.40 (t); 40.82 (d, br.); 35.94-34.77 (t, br.); 33.40 (t); 27.69 (t); 27.46 (q); 24.86 (t); 24.08 (t).

Synthesis of H40-(PCL)₅₀-(PAA)₅₄

As described above with 0.79 g ($1.82 \cdot 10^{-6}$ mol) of H40-(PCL)₅₀-(PtBuA)₅₄ in 11.5 mL of dichloromethane and 1.95 mL ($2.63 \cdot 10^{-2}$ mol) of trifluoroacetic acid for 1 h to give a product redissolved in ethanol (20 mL), precipitated into 200 mL of ether and dried under vacuum

overnight. 333.5 mg of H40-(PCL)₅₀-(PAA)₅₄ white powder of the partially hydrolyzed product (to at least 27%) was obtained.

¹H NMR (400 MHz, DMSO-d₆): 12.23 (s, br.); 3.97 (s, br., 100 H); 2.34-2.05 (m, 134.8 H); 1.86-1.41 (m., 232.6 H); 1.40-1.33 (m, 110.4 H), 1.33-1.18 (m, 115.4 H).

Synthesis of H40-(PCL)₅₀-(PAA)₅₆

As described above with 0.50 g ($1.46 \cdot 10^{-6}$ mol) of H40-(PCL)₅₀-(PtBuA)₅₆ in 7.5 mL of dichloromethane and 0.87 mL ($1.17 \cdot 10^{-2}$ mol) of trifluoroacetic acid for 1 h to give a product redissolved in ethanol, precipitated into ether and dried under vacuum overnight. H40-(PCL)₅₀-(PAA)₅₆ was obtained as a white powder of the partially hydrolyzed product.

¹H NMR (400 MHz, DMSO-d₆): 12.23 (s, br.); 3.97 (s, br., 100 H); 2.34-2.05 (m, 146 H); 1.86-1.41 (m., 245 H); 1.40-1.33 (m, 205 H), 1.33-1.18 (m, 130 H).

Synthesis of H40-(PCL)₅₀-(PAA)₆₄

As described above with 1.5 g ($2.95 \cdot 10^{-6}$ mol) of H40-(PCL)₅₀-(PtBuA)₆₄ in 20 mL of dichloromethane and 4.7 mL ($6.38 \cdot 10^{-2}$ mol) of trifluoroacetic acid for 2 h 15 to give a product redissolved in ethanol (15 mL), precipitated into ether and dried under vacuum overnight. H40-(PCL)₅₀-(PAA)₆₄ was obtained as a white powder of the partially hydrolyzed product.

¹H NMR (400 MHz, DMSO-d₆): 12.23 (s, br., 31.3 H); 3.97 (s, br., 100 H); 2.34-2.05 (m, 141.3 H); 1.86-1.41 (m., 243.7 H); 1.40-1.33 (m, 74.5 H), 1.33-1.18 (m, 111 H).

Synthesis of H30-(PCL)₁₂-(PAA)₆₀

As described above with 3 g ($9.7 \cdot 10^{-6}$ mol) of H30-(PCL)₁₂-(PtBuA)₆₀ in 50 mL of dichloromethane and 17.2 mL ($2.3 \cdot 10^{-1}$ mol) of trifluoroacetic acid for 2 h 40 to give a product redissolved in THF, precipitated into heptane and dried under vacuum overnight. 1.73 g of H30-(PCL)₁₂-(PAA)₆₀ was weighed.

¹H NMR (400 MHz, DMSO-d₆): 12.23 (s, br., 29.9 H); 3.97 (t, 24 H); 2.34-2.05 (m, 65.6 H); 1.86-1.41 (m., 120.3 H); 1.40-1.33 (m, 32.4 H), 1.33-1.18 (m, 36.4 H).

¹³C NMR (100.6 MHz, DMSO-d₆): 175.76 and 175.61 (s); 172.67 (s); 63.39 (s); 40.74-40.33 (d, br.); 33.26 (t); 27.69 (t); 27.46 (q); 24.78 (t); 23.98 (t).

Synthesis of H40-(PAA)₃₆

As described above with 1.6 g ($9.18 \cdot 10^{-6}$ mol) of H40-(PtBuA)₃₆ in 50 mL of dichloromethane and 14.7 mL ($1.98 \cdot 10^{-1}$ mol) of trifluoroacetic acid for 2 h 30 to give a product redissolved in THF, precipitated into heptane and dried under vacuum overnight. 797.8 mg of H40-(PAA)₃₆ as a pinky powder was weighed.

¹H NMR (400 MHz, DMSO-d₆): 12.23 (s, br., 8.9 H); 2.4-2.02 (m, 66.5 H); 1.93-1.41 (m., 108 H); 1.41-1.26 (m, 41 H).

¹³C NMR (100.6 MHz, DMSO-d₆): 175.76 and 175.61 (s); 41.17-40.80 (d, br.); 36.4 and 34.69 (t, br.); 27.44 (q)

II.5. Deprotonation of the acidic functions of the star-block copolymer***Deprotonation of H40-(PCL)₂₄-(PAA)₈₂***

1.913 g of H40-(PCL)₂₄-(PAA)₈₂ was dissolved in water. The appropriate quantity of NaHCO₃ (0.3 g mol^{-1}) was added until the pH reaches the value of 8. After lyophilization of the aqueous solution, 6.793 g of a salt H40-(PCL)₂₄-(PAA)₈₂ was obtained as a water soluble powder.

Deprotonation of H40-(PCL)₄₀-(PAA)₁₀₀

As described above with 2.5 g of H40-(PCL)₄₀-(PAA)₁₀₀ dissolved in water, NaHCO₃ (0.3 g mol^{-1}) was added. After mixing, a pH of 8.3 was measured. Lyophilization provided 2.787 g of H40-(PCL)₄₀-(PAA)₁₀₀ as a water soluble powder.

Deprotonation of H30-(PCL)₁₂-(PAA)₆₀

As described above with 1.647 g of H30-(PCL)₁₂-(PAA)₆₀ dissolved in water, NaHCO₃ (0.3 g mol^{-1}) was added. After mixing, a pH of 8 was measured. Lyophilization provided 1.7 g of H30-(PCL)₁₂-(PAA)₆₀ as a water soluble powder.

Deprotonation of H40-(PAA)₃₆

As described above with 609.1 mg of H40-(PAA)₃₆ dissolved in water, NaHCO₃ (0.3 g mol⁻¹) was added. After mixing, a pH of 8 was measured. Lyophilization provided 793 mg of H40-(PAA)₃₆ as a water soluble powder.

III. Encapsulation of fragrance compounds

Procedure for encapsulation monitored by ¹H NMR

Star-block copolymers HBP-(PCL)_p-(PAA)_q and H40-(PBMA)_p-(PPEGMA)_q^[48] (~10/20/30/40 mg) were precisely weighed and dissolved in 1.4 g of D₂O (pure D₂O was used as a blank sample). After one night the polymer had dispersed and ~50 mg of a olfactory molecule (benzyl acetate, (*E*)-3,7-dimethyl-2,6-octadien-1-ol (geraniol), 4-*tert*-butyl-1-cyclohexyl acetate (Vertenex®) or decanal) were respectively added to the solutions. After shaking for one day, the samples were centrifuged. Aliquots of the water phase were weighed into NMR tubes, and an exact amount of DMSO was added to the samples as a reference for quantification. NMR spectra were recorded using the following acquisition conditions: preacquisition delay 20 s, acquisition time 5 s, number of data points 64 k, 64 scans. When processing the spectra, a line broadening of 0.1 Hz and a zero filling of 1024 k was used. Spectra were manually integrated, without additional baseline correction. The following signals were used for the quantification of the various fragrance molecules that served as examples of hydrophobic guests: benzyl acetate, C₆H₅-CH₂-O(CO)-CH₃, s, δ = 7.41 to 7.12 ppm, depending on the concentration of polymer; geraniol C=CH-CH₂-OH, t, δ = 4.10 ppm; Vertenex® -C(CH₃)₃, δ = 0.82 ppm, decanal, -CH₂-CHO, pert t, δ = 2.1 ppm in water, 2.31 ppm in polymer solutions. All signals were well separated from the polymer signals except for H40-(PBMA)_p-(PPEGMA)_q/Vertenex®, which limited the accuracy of the corresponding measurements.

IV. Release of fragrance molecules

IV.1. Release of olfactory compounds monitored by TGA

40 mg (2 % (w/w)) of either one of the amphiphilic star-block copolymers H40-(PCL)₁₀-(PAA)₇₀ or H40-(PBMA)₃₇-(PPEGMA)₃₉ were solubilized in 1.70 g (85 % (w/w)) of ethanol. After stirring, 160 mg (8 % (w/w)) of pure water were added and 100 mg (5 % (w/w)) of either one of the following fragrance molecules: Vertenex®, benzyl acetate, geraniol or decanal. This sample was kept under agitation at room temperature for at least 2 d. In a similar way, a reference sample was prepared using the Boltorn® H40. A volume of 10 µL of the sample prepared above was placed in an aluminium oxide crucible and analyzed with a Thermogravimetric Analyzer (Mettler Toledo TGA/SDTA 851e) under a constant flow of nitrogen gas (20 mL/min). The evaporation of the pure fragrance molecule in this composition was measured by using the following method which consists of heating the sample from 25 to 50 °C at 5 °C/min followed by an isotherm at 50 °C during 115 minutes, then heating from 50 °C to 130 °C at 4 °C/min and finally an isotherm at 130 °C during 15 minutes. The analyses were repeated twice and compared to those of the pure fragrance molecules as well as to the Boltorn® H40 reference.

IV.2. Release of olfactory molecules monitored by headspace analysis

IV.2.1 In a fine perfumery application

A model perfume was obtained by mixing equimolecular quantities (0.2 mol) of 15 fragrance compounds with different chemical functionalities (aldehydes, ketones, alcohols, nitriles and esters). The following compounds were weighed in: (*Z*)-3-hexenol (pipol, 2.00 g), 3,5,5-trimethylhexanal (2.84 g), 2,6-dimethyl-2-heptanol (dimetol, 2.88 g), acetophenone (2.40 g), ethyl (*E*)-2,4-dimethyl-2-pentenoate (3.12 g), benzyl acetate (3.00 g), jasmonitrile (3.06 g), decanal (3.12g), 4-phenyl-2-butanone (benzylacetone, 2.96 g), 2-

pentylcyclopentanol (3.12 g), geraniol (3.08 g), 4-cyclohexyl-2-methyl-2-butanol (3.40 g), 10-undecenal (3.36 g), Vertenex® (3.96 g), allyl 3-cyclohexylpropanoate (3.92 g).

Amphiphilic star-block copolymer H40-(PCL)₁₀-(PAA)₇₀ 40 mg (2% (w/w)) was solubilized in 1.70 g (85 % (w/w)) of ethanol. After stirring, 160 mg of water were added and 100 mg (5 % (w/w)) of the model perfume described above. The sample was kept under agitation at room temperature for at least 3 days. A total of 2 µL of the sample was then placed in a headspace sampling cell (160 mL) thermostatted at 25 °C and exposed to a constant air flow of 200 mL/min, respectively. The air was filtered through active charcoal and aspirated through a saturated solution of NaCl. The volatiles were continuously adsorbed onto 100 mg Tenax® TA cartridges, which were changed after t = 3.5, 4.5, 6, 8, 10, 13, 16, 20, 30, 45, and 60 min. The cartridges were desorbed thermally in a Perkin Elmer TurboMatrix ATD desorber and the volatiles analyzed with a Carlo Erba MFC 500 gas chromatograph equipped with a FID detector. The analyses were carried out using a J&W Scientific DB capillary column (30 m x 0.45 mm i.d., film thickness 0.42 µm) from 70 °C to 130 °C (at 3 °C/min) then to 260 °C at 35 °C/min. The injection temperature was 240 °C and the detector temperature was 260 °C. Headspace concentrations (in ng/L) were obtained by external standard calibration of the corresponding fragrance molecules using six different concentrations in ethanol. 0.2 µL of each calibration solution was injected onto Tenax® TA cartridges, which were desorbed under the same conditions as previously. The results are the average of two measurements.

The above experiment was repeated using 100 mg (5 % (w/w)) of the model perfume described above solubilized in 1.70 g (85 % (w/w)) of ethanol and 200 mg of water without the amphiphilic star-block copolymer. The sample was kept under agitation at room temperature for 3 days. 2 µL of the sample was placed in the headspace sampling cell as a reference, in order to compare the long-lastingness of the fragrance compound evaporation in the presence or absence of the amphiphilic star-block copolymer.

IV.2.2 In a fabric softener application

The use of the amphiphilic star-block copolymers has been investigated for the controlled release of fragrance compounds in a fabric softener application. A fabric softener base with the following composition has been prepared:

Stepantex [®] VK90 or VHR90 (origin: Stepan)	16.5 % by weight
Calcium chloride	0.2 % by weight
Water	83.3 % by weight

A solution of equimolar amounts (0.45 mmol) of 4-phenyl-2-butanone (benzylacetone, 63.8 mg), allyl 3-cyclohexylpropanoate (86 mg), 4-cyclohexyl-2-methyl-2-butanol (78.7 mg) and benzyl acetate (69.3 mg) in 10 mL of ethanol was prepared. 3.30 mL of this solution were added to 40 mg ($1.33 \cdot 10^{-4}$ mmol) of amphiphilic star-block copolymer H40-(PCL)₁₀-(PAA)₇₀ and stirred for one day. A total of 1.80 g of the fabric softener base described above was weighed into two small vials. 1 mL of the solution containing the fragrance molecules and the polymer was then added to one of the vials, and 1 mL of the solution containing the fragrance molecules but no polymer was added to the other. Both vials were closed and left under agitation at room temperature for 4 days. The samples were then dispersed in a beaker with 600 mL of demineralized cold tap water. One cotton towel (EMPA cotton test cloth Nr. 221, origin: Eidgenössische Materialprüfanstalt (EMPA), pre-washed with an unperfumed detergent powder and cut to ca. 12 x 12 cm sheets) was added to each beaker and agitated manually for 3 min, left standing for 2 min, then wrung out by hand and weighed to check for a constant quantity of residual water. The two towels (one with the amphiphilic star-block copolymer and one without) were analyzed immediately after treatment with the softener. For the measurements, one towel was put into an headspace sampling cell (160 mL) thermostatted at 25 °C and exposed to a constant air flow of 200 mL/min, respectively. The air was filtered through activated carbon and aspirated through a saturated solution of NaCl. The headspace system was equilibrated for 75 min, and the volatiles then adsorbed for 5 min on a clean Tenax[®] cartridge. Sampling was repeated 7 times every 50 min. The cartridges were desorbed on a Perkin Elmer TurboMatrix ATD desorber as described above.

The above experiment was repeated using the amphiphilic star-block copolymer H40-(PBMA)₃₇-(PPEGMA)₃₉ instead of H40-(PCL)₁₀-(PAA)₇₀. The headspace system was equilibrated for 15 min, and the volatiles were adsorbed for 5 min. Sampling was repeated again 7 times every 50 min.

V. Instrumentation

V.1. Nuclear magnetic resonance (NMR)

Nuclear magnetic resonance (NMR) spectra of the polymers were recorded on Bruker Avance 400 and AV 500 spectrometers operating at 400 or 500 MHz for ¹H and 100.6 or 125.8 MHz for ¹³C NMR spectra. CDCl₃, DMSO-d₆ and D₂O were used as the solvents, and tetramethyl silane (TMS) was used for calibration. Quantitative ¹³C NMR spectra for the characterization of the H40 were obtained at 300 K using inverse-gated decoupling with a relaxation delay of 30 s. The proportions of the different structural units were determined by integration of the corresponding peaks in the quaternary carbon region (42-54 ppm).

Quantitative ¹H NMR spectra for the encapsulation measurements were recorded under the following conditions: PULPROG (pulse program): zg; TD (time domain data points): 64k; AQ (acquisition time): 5 sec; D1 (delay time): 20 sec; SW (sweep width): 13 ppm. 64 scans were recorded. All integrations were made relative to DMSO, which was added as an internal reference.

V.2. Gel permeation chromatography (GPC)

GPC in DMF was performed on a Waters Alliance GPCV 2000 equipped with refractive index, differential viscosimeter and light scattering detection. Separation was carried out with two consecutive TSK-Gel Alpha 3,000 + 4,000 or 4,000 + 5,000 columns (hydrophilic PMMA-type stationary phase), and eluted at 60 °C with DMF containing 1 g/L

of LiBr at a flow rate of 0.6 mL/min. The polymer concentration was 4 mg/mL. Molar masses were determined using the universal calibration method with narrow polydispersity poly(methyl methacrylate) PMMA standards and Empower Pro multi-detection GPC software (Ver 5.00).

GPC measurements in water were performed on a Waters 150cv instrument (modified for refractive index measurement and differential viscosimeter) equipped with two consecutive Shodex OH-Pak SB-804 + SB 805 columns, and eluted at 25 °C with water containing 0.1 M of NaHCO₃ at a flow rate of 0.5 mL/min. The polymer concentration was 4 mg/mL.

V.3. Fourier transform infra red spectroscopy (FT-IR)

Fourier transform infra-red (FTIR) spectroscopy was carried out using a Perkin Elmer Spectrum One FT-IR spectrometer.

V.4. Differential scanning calorimetry (DSC)

Differential scanning calorimetry (DSC) data were obtained using a TA Instruments DSC Q100. Around 10 mg of the specimens were heated from -120 °C to 120 °C (or 200 °C, depending on the polymer) at 10 °C/min and then cooling from 120 °C (or 200 °C) to -120 °C at 10 °C/min. Before each scan, the temperature was maintained at -120 °C and 120 °C (or 200 °C) for 1 min. The cycle was repeated and T_g and T_m values determined from the second cycle.

V.5. Thermogravimetric analysis (TGA)

The TGA (Mettler-Toledo) is a very sensitive microbalance (accuracy: 1 µg) equipped with an accurate oven with an internal volume of 35 mL. The loss of weight due to evaporation is recorded as a function of time. The evaporation of the pure fragrance molecule

in the composition was measured by heating the sample from 25 to 50 °C at 5 °C/min to rapidly evaporate ethanol. Then the sample is weighed at 50 °C over 115 minutes to follow the evaporation of the fragrances. Finally the sample is heated from 50 °C to 130 °C at 4 °C/min and maintained at 130 °C for 15 minutes to remove all the fragrance compounds from the polymer.

V.6. Dynamic light scattering (DLS)

The sizes of the amphiphilic star-block copolymers or aggregates in water have been measured by dynamic light scattering (DLS) using a Malvern Zetasizer Nanoseries. The light source diffuses at 365 nm. Autocorrelation functions for each sample at a concentration of 0.34 mg mL⁻¹ were collected three times at 25° C. The data were fitted using a cumulant method to derive apparent hydrodynamic radii.

V.7. Transmission electron microscopy (TEM)

Continuous films were cast onto freshly cleaved mica, floated onto distilled water and picked up with 400 mesh copper grids covered with a thin film of carbon. The specimens were then exposed to RuO₄ vapor for a few minutes in order to provide contrast. All TEM observations were carried out using a Philips EM430 TEM at 300 kV in bright field mode.

V.8. Atomic force microscopy (AFM)

Observations were made on specimens cast from dilute solutions (typically between 2 and 100 mg L⁻¹) in chloroform or THF onto freshly cleaved mica. The images were obtained using a Veeco Multimode AFM, with an ultrasharp silicon tip operated in intermittent contact mode in air at room temperature and the drive amplitude was varied systematically.

Chapter V. Synthesis of amphiphilic star-block copolymers from Boltorn® hyperbranched polymer

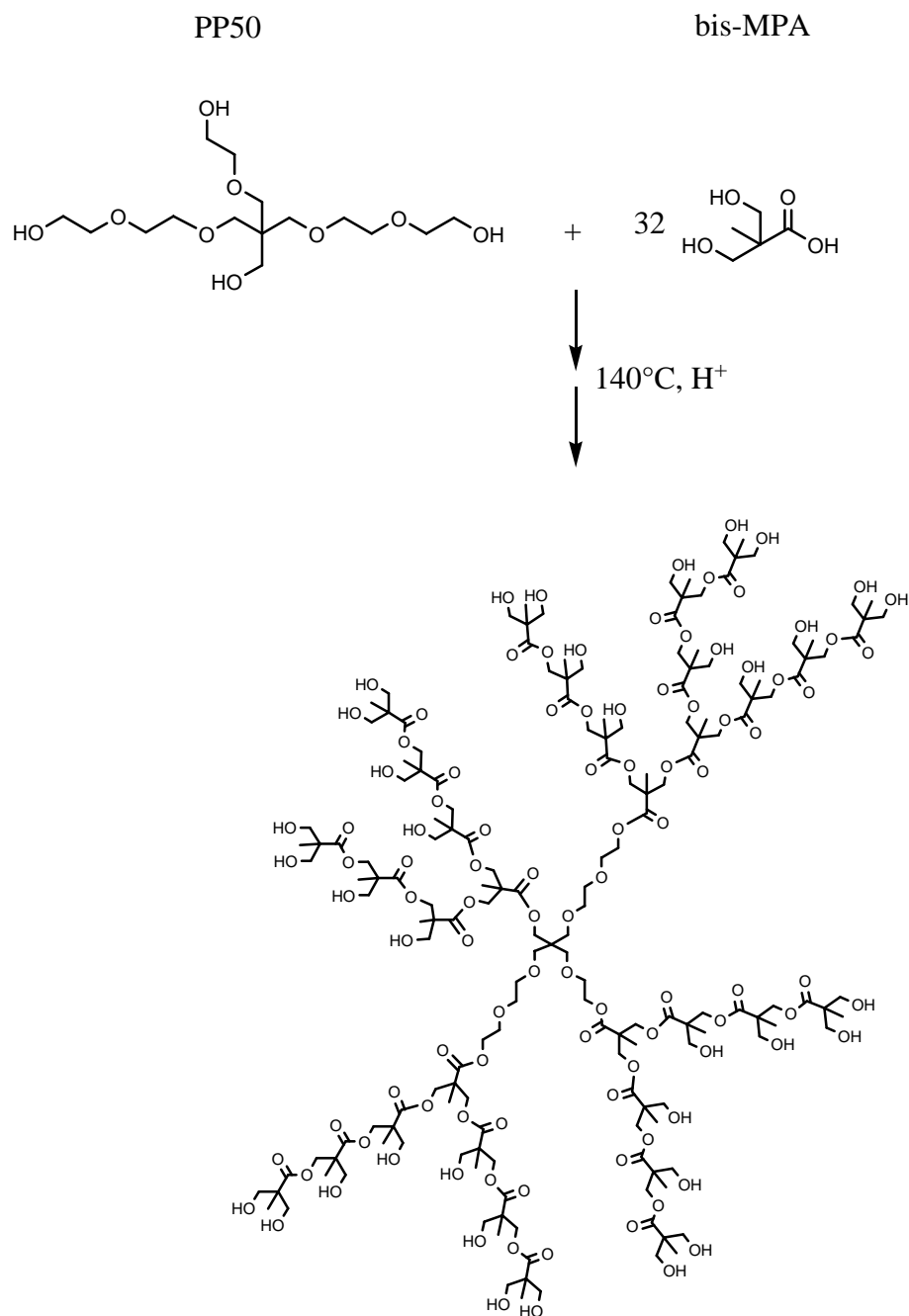
Thanks to their straightforward, relatively low cost synthesis, hyperbranched polymers are more promising candidates for many industrial applications than dendrimers. Although their synthesis produces ill-defined microstructures with irregular branches, the large number of end groups and the globular architecture are maintained. They also show similar properties to dendrimers, including lower viscosity than their linear analogues, tailored solubility, thermal properties and chemical reactivity.

The HBP cores (Boltorn®) used in the present work have been commercialized by Perstorp (Sweden). A brief description of their synthesis and characterization is given in section I. The degree of polymerization and the number of hydroxyl groups per molecule have been estimated in the present work using gel permeation chromatography (GPC) and nuclear magnetic resonance (NMR) as described in section II. Finally, section III details the chemical modification of the hydroxyl groups present at the surface of the HBP and the subsequent preparation of the star-block copolymers.

I. Boltorn® HBP: Background

I.1. Preparation of Boltorn® HBP

The family of hyperbranched aliphatic polyesters considered here was first investigated by Malmström et al.^[41] This work resulted in a commercially available HBP polyol named Boltorn® HBP. Three generations of this HBP are marketed under the tradenames H40, H30 and H20, which differ in size and consequently in the number of hydroxyl groups per molecule. The corresponding perfect dendrimer analogues contain 64, 32 and 16 hydroxyl groups per molecule respectively according to the Perstorp data sheets.^[258] Boltorn® HBP is prepared from 2,2-bis (hydroxymethyl)propionic acid (*bis*-MPA) and a tetrafunctional ethoxylated pentaerythritol core (PP50) according to the procedure of Malmström et al.^[41, 259] The synthesis with PP50 as the core molecule is given in Scheme V.1.



Scheme V.1 Pseudo-one-step synthesis of the hydroxyl-functional hyperbranched polyester H40

I.2. Characterization of hyperbranched polymers based on AB₂ type monomers

GPC and NMR are the most widely used techniques in the literature for the characterization of hyperbranched polymers.^[41, 260-263] Frey and coworkers investigated HBPs based on an AB₂ type monomer with a TMP core.^[260] The molar masses they obtained from NMR and VPO (vapor pressure osmometry) let them to conclude that cyclization occurred during the reaction. The differences between the molar masses obtained by NMR and VPO and by GPC carried out in DMF at 45 °C with poly(propylene oxide) as the standard, also suggested that GPC overestimated the molar mass. However, the values obtained were very different from those determined by Hult and coworkers for an HBP with a TMP core.^[261]

Zagar and Zigon^[263] have also characterized a fourth generation Boltorn® HBP (H40) by ¹H and ¹³C NMR and they found that the number of dendritic units and the degree of branching were very low in comparison with the expected values from random polymerization ($DB = 0.40$). They explained this difference on the basis of their NMR investigations. They showed that deactivation of carboxylic groups occurs, resulting in self-condensation of *bis*-MPA. This reaction explains the presence of macromolecules with no PP50 core, which reduces the number average molecular weight (M_n) with respect to the value determined by GPC using dimethyl acetamide with LiBr (0.7 %) as the eluant.

The hydroxyl number for three generations Boltorn® HBP (H20, H30 and H40) have also been determined by titration experiments after acetylation in an excess of acetic anhydride with pyridine as the solvent. Unreacted acetic anhydride has been hydrolyzed with water and the acetic acid formed titrated with NaOH (1 M). The hydroxyl number have been calculated from the difference between the sample and a control. Results obtained by Garámszegi et al.^[43] for H20, H30 and H40 are listed in Table V.1. Their results were in the expected range and in good agreement with the values of 430 to 470 mg OH/g of HBP provided by Perstorp.^[258]

Table V.1 End group titration of the HBP

	H20	H30	H40
mg OH/g	498.64	477.28	472.31
mmol OH/g	8.87	8.51	8.42
M_n HBP [g mol ⁻¹]	1 320	2 900	4 40
N_{OH}/HBP^a	11.7	24.7	37.2

^a Number of hydroxyl group per HBP molecule from titration

These examples illustrate the difficulties inherent in determining the molar mass and hence the absolute number of hydroxyl groups per molecule and point also to inconsistencies between the work of different authors.

II. Characterization of the HBP cores

Three generations of HBP were investigated. However, the emphasis here will be on H40, which was the largest one and hence showed the highest functionality.

II.1. GPC

Zagar and Zigon^[263] and Garámszegi et al.^[43] demonstrated that the absolute molecular weight of HBPs is accessible with GPC combined with universal calibration under appropriate conditions (polymer/solvent/stationary phase). We therefore first used GPC under the same conditions as Garámszegi et al., taking care to avoid secondary separation mechanisms such as adsorption, thermodynamic partition, phase separation and ionic effects.

Because of the large number of polar hydroxyl end groups, Boltorn® HBP has a strong tendency to associate by intermolecular interactions and hydrogen bonding (e.g. between the hydroxyl and carbonyl groups).^[263, 264] To disrupt these interactions, the HBP was dissolved in dimethyl formamide (DMF) with 1 g L⁻¹ of LiBr.^[43] As found previously by

Rodlert et al.,^[39] the resulting chromatograms were monomodal. Results for all three generations are given in Table V.2. The polydispersities (M_w/M_n) were relatively high in each case owing to the synthetic procedure.

The degree of polymerization was determined according to the following equation, from which the number of hydroxyl groups may also be inferred: $N_{OH} = DP_n + 4$

$$DP_n = \frac{M_{n_{exp}} - M_{core}}{M_{BMPA}}$$

$M_{n_{exp}}$: average number molecular weight measured with GPC

M_{core} : theoretical molecular weight (molar mass) of the PP50 core ($M = 356 \text{ g mol}^{-1}$).

M_{BMPA} : molar mass of the repeat unit (*bis*-MPA) ($M = 116 \text{ g mol}^{-1}$).

Table V.2 GPC data for three generations of HBP after purification

	M_n [g mol^{-1}] ^a	M_w [g mol^{-1}] ^b	M_w/M_n ^c	DP_n	$N_{OH}(\text{theo})$ ^d	$N_{OH}(\text{GPC})$ ^e
H20	1 320	4 740	3.59	8	16	12
H30	2 900	8 170	2.82	22	32	26
H40	4 100	11 700	2.86	32	64	36

^a average number molecular weight determined by GPC

^b average weight molecular weight determined by GPC

^c molecular weight distribution

^d theoretical number of hydroxyl groups per HBP (based on the stoichiometry)

^e calculated number of hydroxyl groups per HBP

II.2. NMR

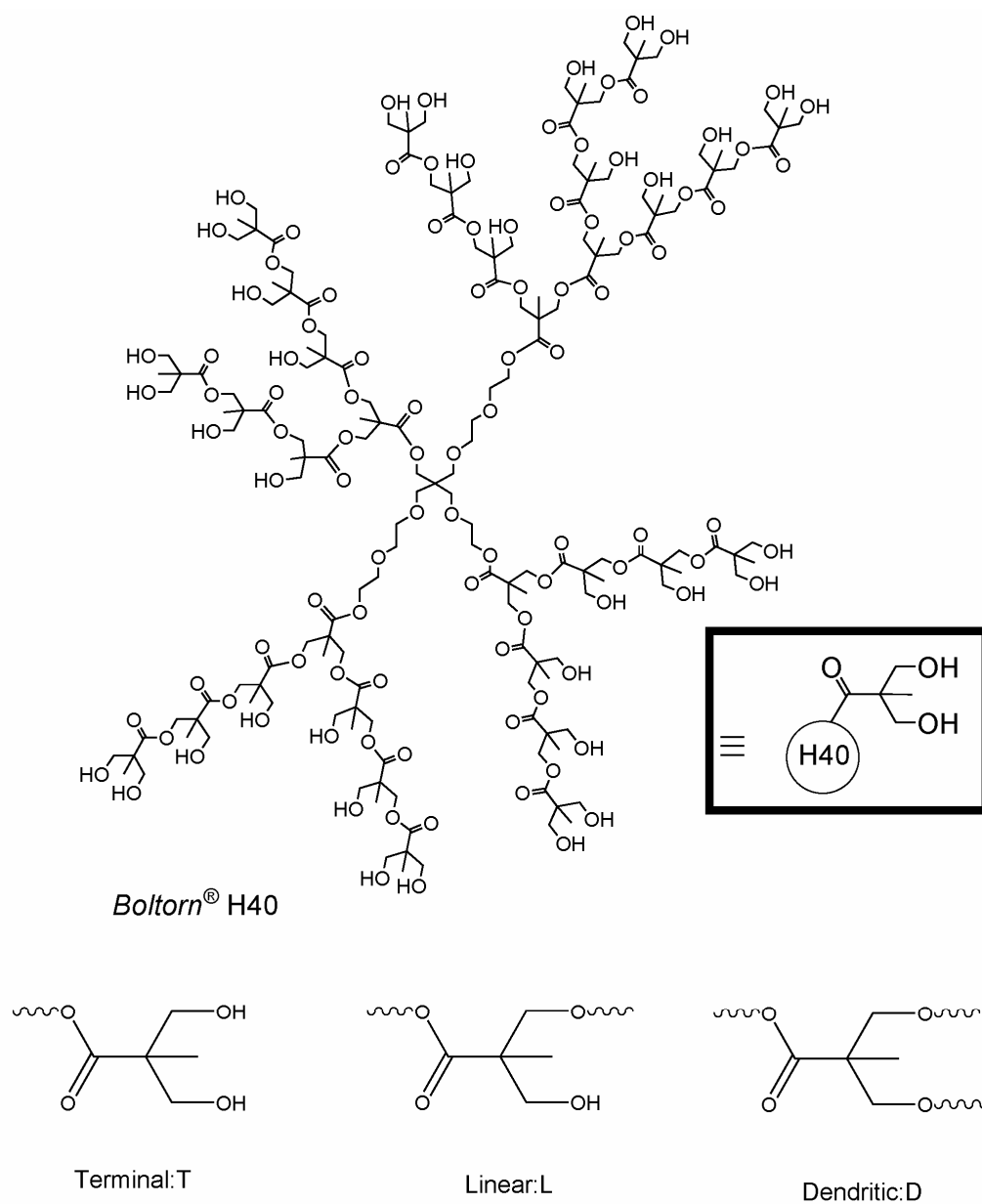


Figure V.1 Average structure of Boltorn® HBP H40 along with the three repeat units present in the structure.

HBP H40 has been studied by quantitative NMR spectroscopy. The proportion of the three main types of repeat unit (terminal (T), linear (L) and dendritic (D)) present in Boltorn® HBP as defined in Figure V.1 can be calculated from ^1H NMR spectroscopy in DMSO by integrating the corresponding methyl peaks at 1.11, 1.16 and 1.26 ppm (peaks e, f, g respectively in Figure.V.2), values of 25, 56 and 19 % (Figure.V.3) were obtained for T, L and D respectively. The number of linear units was hence inferred to be significantly greater than the number of dendritic and terminal units.

From Figure.V.2 the integrations of the protons corresponding to the methyl, the methylene and the hydroxyl groups of the HBP were used for the determination of the number of protons in the H40 molecule assuming a DP_n of 32 (from GPC in DMF). The three repeat units L, T, and D present in the H40 molecule (Figure V.1) have been considered. The linear repeat unit is composed of 1 $-\text{CH}_2\text{OH}$, 1 $-\text{CH}_2\text{OR}$ and 1 $-\text{OH}$ groups which corresponds to 2 H, 2 H and 1 H respectively. The terminal repeat unit is composed of 2 $-\text{CH}_2\text{OH}$ and 2 $-\text{OH}$ groups which corresponds to 4 H, 2 H respectively. The dendritic repeat unit is composed of 2 $-\text{CH}_2\text{OR}$ groups which corresponds to 4 H. The PP50 core molecule is composed of 14 $-\text{CH}_2\text{O}$ groups which corresponds to 28 H. Moreover each repeat unit contains a $-\text{CH}_3$ group so the total number of $-\text{CH}_3$ groups (each of which contributes 3 H) is equal to DP_n . The results are summarized in Table V.3. Considering the methyl and methylene groups intensities, results obtained from GPC and NMR are in good agreement. In the case of OH group intensities, a poorer agreement is determined (24 H from NMR instead of 36 H from GPC). This may be attributed to H-bonding^[263] (broad peaks and lower accuracy). Thus, in this work, the number of OH groups per HBP molecule were determined by considering the methyl and the methylene intensities instead of only considering the OH groups intensities and a value of 36 hydroxyl functions are considering from NMR measurements.

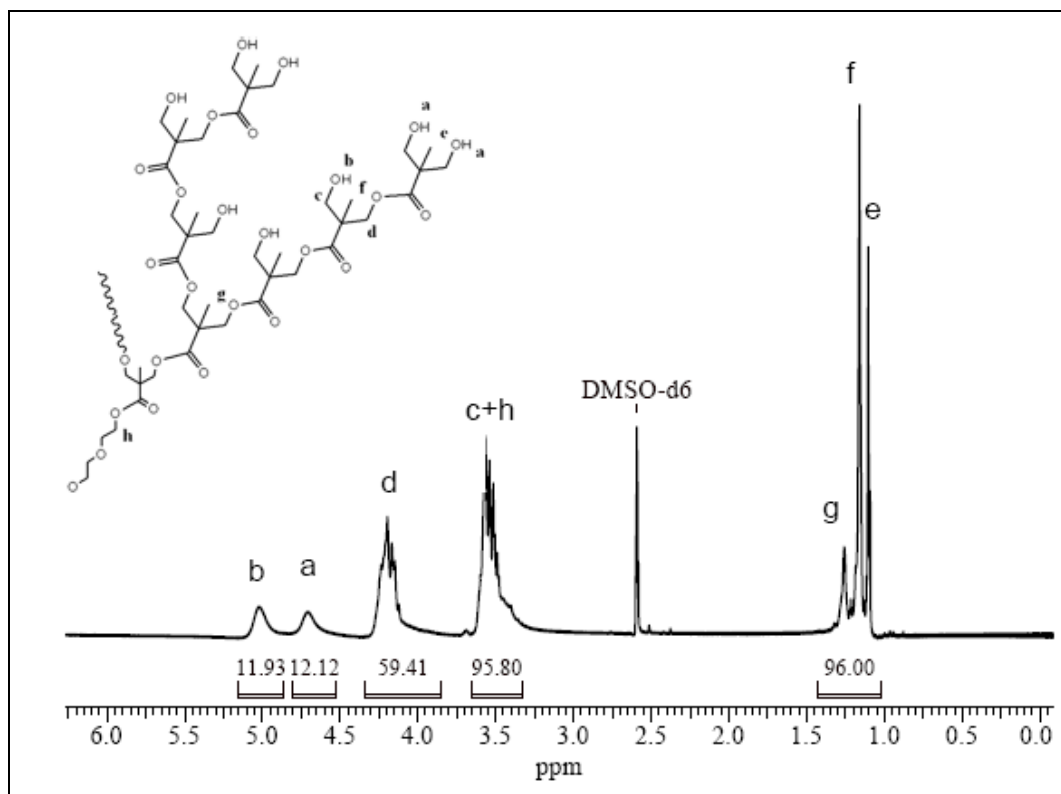


Figure.V.2 ^1H NMR spectrum of H40 in DMSO

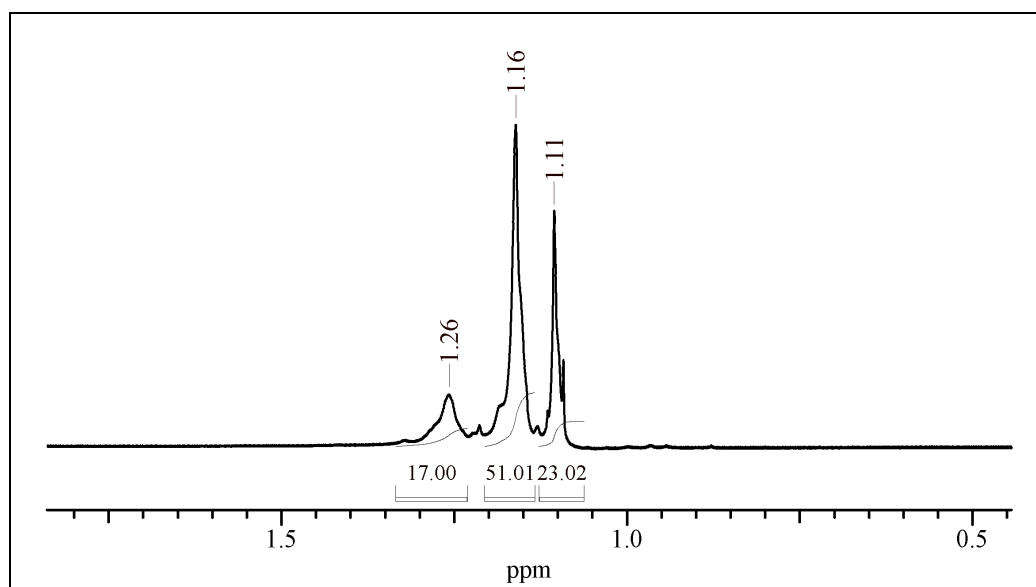


Figure.V.3 Enlarged ^1H NMR spectrum of the H40 in DMSO. Region of the methylene groups.

Table V.3 Comparison of the numbers of protons expected for H40 for $DP_n = 32$ (GPC) and those determined by ^1H NMR in DMSO

Corresponding peaks	Theoretical number of proton	Calculated number of proton from GPC with $DP_n = 32$	Experimental number of proton from NMR
CH_3 (e, f, g)	$DP_n \times 3\text{H}$	96	96
CH_2OH (c, h)	$4\text{H} \cdot DP_n \% \text{T} = 32$ $2\text{H} \cdot DP_n \% \text{L} = 35.8$ From PP50 core \approx 28H	95.8	95.8
CH_2OR (d)	$2\text{H} \cdot DP_n \% \text{L} = 35.8$ $4\text{H} \cdot DP_n \% \text{D} = 24.3$	60.1	59.4
OH (a, b)	$DP_n + 4\text{H}$	36	24.0

Table V.4 summarizes the experimental values for N_{OH} obtained with GPC and NMR for three generations of Boltorn® HBP. The titration experiments on H20, H30 and H40 were carried out by Garámszegi et al.^[43] on the same series of H20, H30 and H40 as analyzed here by GPC and NMR. The results are also given in Table V.4 and are consistent in the case of H40. In the case of H20 and H30, the good correlation between the GPC and titration results is assumed to validate the GPC results, although NMR results were not available in this case. An average of 26 OH groups per Boltorn® H30 and of 36 OH groups per Boltorn® H40 molecule was therefore assumed for the remainder of this study.

Table V.4 Comparison of the number of hydroxyl groups determined for Boltorn HBP using three techniques

	H20	H30	H40
GPC	12.3	26	36
NMR	-	-	36
Titration	11.7	24.7	37.2

III. Preparation of amphiphilic star-block copolymer based on HBP polyester

III.1. Introduction

This section describes the preparation of an amphiphilic star-block copolymer comprising a hydrophobic and a hydrophilic block. The hydrophobic block has the purpose of encapsulating, absorbing or associating hydrophobic volatiles. The hydrophilic block provides the necessary polarity for solubilizing the star-block copolymer in an aqueous medium.

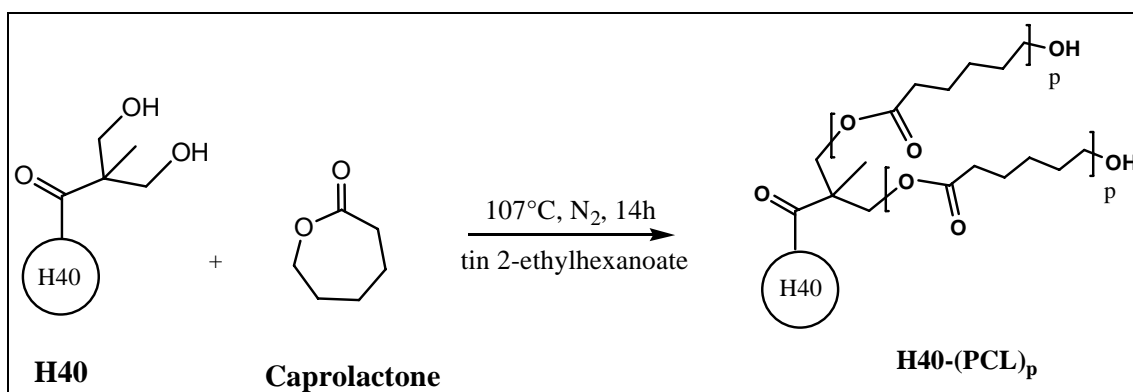
In the fragrance industry, the products (shampoos, lotion, cream,...) are manufactured from a base composed essentially of water, surfactant (which stabilize the composition and improve the deposition of the perfume), and small amount of perfume. As a function of the application, the surfactants used are cationic, anionic or non-ionic. For example, in shampoos, lotions and softeners^[1, 265-267] cationic surfactants are introduced whereas anionic surfactants are used in detergents, and non-ionic surfactants are used in creams and makeup. In order to introduce the new amphiphilic star-block copolymers into one of the numerous compositions and to study their effect on deposition, cationic, anionic and non-ionic star-block copolymers were all initially considered and different (meth)acrylate monomers were therefore investigated for ATRP.

Due to the globular architecture of the HBP core which induces steric hindrance at the periphery, and the presence of internal hydroxyl groups (presence of linear units), the hydroxyl functions that serve for the modification of the HBP properties are less accessible than in linear polymers, precluding the “grafting onto” technique which consists of the addition of a pre-existing polymer to the HBP core. Thus, the “grafting from” technique was envisaged for the preparation of star-block copolymers, i.e. the use of the hydroxyl functions present at the surface of the HBP, which is considered to be a macroinitiator. ROP and ATRP are convenient methods for the synthesis of a well-defined polymer as it was discussed in the literature review (Chapter III). The possibility of propagating each arm simultaneously is highly advantageous as are the wide range of monomers that can be polymerized by ATRP and the low number of side reactions.

Then the preparation of the hydrophobic internal layer by ROP of ϵ -caprolactone from HBP (H30 and H40) to give a HBP-(PCL)_p is described in section III.2. The synthesis of the outer hydrophilic shell is considered in section III.3, starting with the esterification of the –OH groups present at the surface of the HBP-(PCL)_p by 2-bromoisobutyryl bromide to give an HBP-(PCL)_p-Br macroinitiator for ATRP (section III.3.1). The preparation of pH-responsive star-block copolymer is then described in section III.3.2. After preliminary experiments with *tert*-butyl methacrylate, used of *tert*-butyl acrylate monomer, to give HBP-(PCL)_p-(*t*BuA)_q was found to give better results. Hydrolysis of the *tert*-butyl group provides a poly(acrylic acid) (PAA) outer shell HBP-(PCL)_p-(PAA)_q. Water soluble star-block copolymers without the internal hydrophobic core (H40-(PAA)_q) were also prepared in order to study the importance of the hydrophobic layer for encapsulation of volatiles (Chapter VII). Similar conditions were tested for the optimization of cationic (section III.3.3) and non-ionic star-block copolymers (section III.3.4). Finally, non-ionic star-block copolymers, based on H40 macroinitiator and prepared by G. Kreutzer from the Polymer Laboratory of the EPFL, are also briefly described in section III.4 since they will be referred to in the following chapters.^[48]

III.2. The hydrophobic layer: ROP of ϵ -caprolactone

The peripheral hydroxyl groups of H30 or H40 were used to initiate the ROP of ϵ -caprolactone. The number of OH groups per HBP molecule controls the graft density, while the ϵ -caprolactone concentration and reaction time determine the graft length.

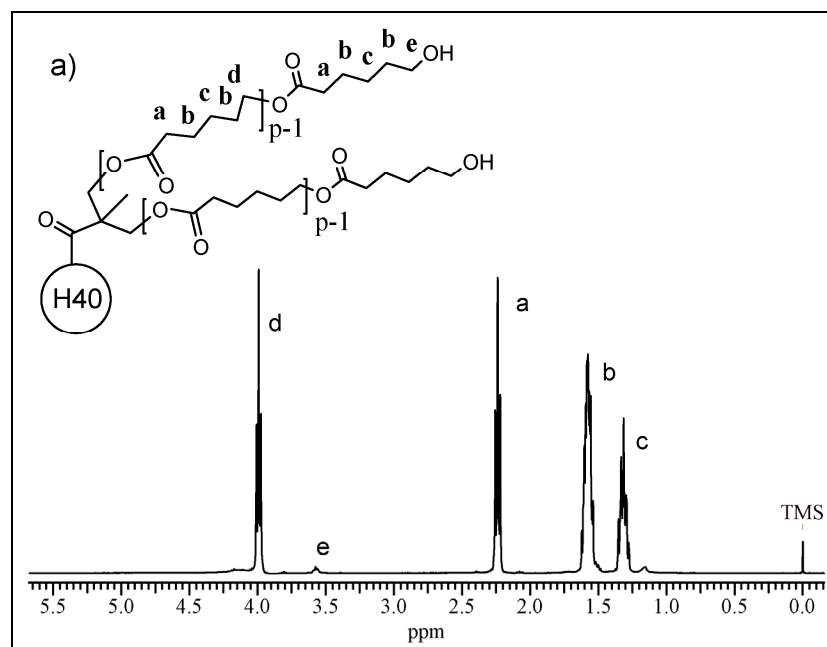


Scheme V.2 Synthesis of H40-(PCL)_p

The reaction proceeded in the bulk at 107 °C under an inert atmosphere, as shown in Scheme V.2, and according to procedure described in the experimental section (Chapter IV.II.1). By varying the ratio of the initiating species (H30 and H40) to the ϵ -caprolactone, a series of six copolymers was synthesized and characterized with ¹H and ¹³C NMR in CDCl₃ and GPC in DMF. Table V.5 details the $[M]/[I]$ ratio, molar mass and other parameters determined from ¹H NMR and GPC. A representative ¹H NMR spectrum of H40-(PCL)₂₄ is shown in Figure V.4. The degree of polymerization (DP_n) was calculated from the triplet at 3.65 ppm (e), which corresponds to the methylene group adjacent to the hydroxyl at the chain end, and the triplet at 4.05 ppm (d), which corresponds to the methylene group adjacent to the ester linkage.^[254] The average number molar masses of the series HBP-(PCL)_p from NMR and GPC analysis are compared in Figure V.5. A representative GPC curve of H40-(PCL)₂₄ in DMF is given in Figure V.6.

Table V.5 $[M]/[I]$ ratio and characterization of the star-block copolymer synthesized from ROP of ϵ -caprolactone

	$[M]/[I]$	DP_n/arm Stoichiometry	DP_p/arm^a	M_n [g mol ⁻¹] ^a	M_n [g mol ⁻¹] ^b	M_w/M_n^b	α^b
H30	-	-	-	2 908	2 900	2.82	0.22
H40	-	-	-	4 070	4 100	2.86	0.27
H30-(PCL) ₁₂	300	11.5	12	38 470	41 800	1.95	0.07
H40-(PCL) ₁₀	360	10	10	45 140	65 380	2.03	0.07
H40-(PCL) ₁₇	720	20	17	73 870	89 890	1.99	0.07
H40-(PCL) ₂₄	792	22	24	104 650	94 300	2.46	0.001
H40-(PCL) ₄₀	1080	30	40	168 260	158 900	2.07	0.08
H40-(PCL) ₅₀	1980	55	50	209 300	184 640	2.57	-

^a ¹H NMR in CDCl₃^b GPC in DMF**Figure V.4** ¹H NMR of the H40-(PCL)₂₄ star-block copolymer

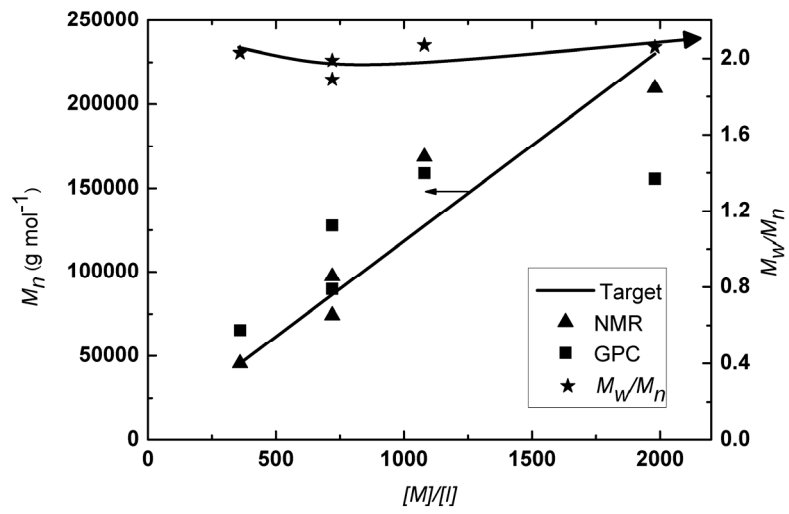


Figure V.5 Dependence of M_n and polydispersity on the $[M]/[I]$ ratio for H40-(PCL) $_p$; comparison between NMR and GPC results and the target M_n

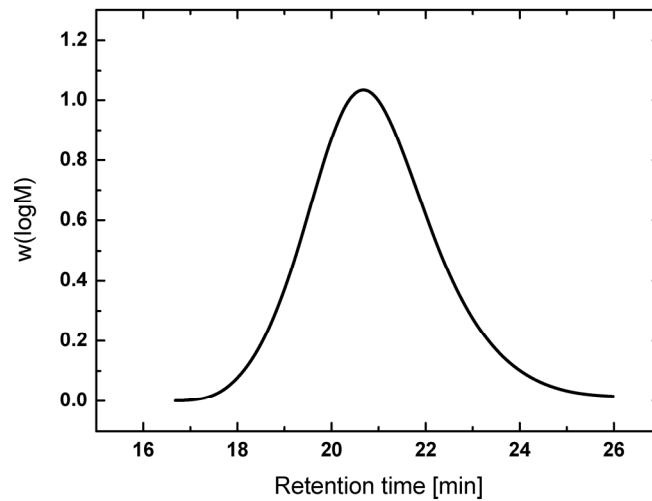


Figure V.6 GPC chromatogram of H40-(PCL) $_{24}$ in DMF

The signal from the H40 core was not visible in any of the ^1H spectra because of the large excess of PCL. The GPC curves for the H30-(PCL)_p and H40-(PCL)_p were monomodal and the molar mass distribution decreased with the polymerization of the ϵ -caprolactone in comparison with H30 and H40 precursor (Table V.5). This is thought to be due to the fractionation during the precipitation. Figure V.5 compares the behaviour of the molar mass determined by NMR and GPC and the target values, i.e. the molar mass expected from the $[M]/[I]$ ratio from Table V.5. As seen from Figure V.5, M_n generally increased linearly with increasing target M_n ($[M]/[I]$ ratio). Values from NMR were in good agreement with target M_n whereas GPC values for high molar masses polymers were in less good agreement, especially for H40-(PCL)₅₀, for which the Mark-Houwink Sakurada coefficient (α) was not calculable (see Equation II.3). More generally, the Mark-Houwink Sakurada coefficient decreased to close to zero (Table V.5) as the length of the (PCL) arms increased. This suggested the polymers to behave as compact spheres. Frey et al.^[119, 268, 269] also observed a difference between molar masses determined with NMR and GPC in the case of modified hyperbranched polymers. They attributed the molar mass differences between the two techniques to the compact spherical structure of the HBP.

It has been widely reported^[41, 218, 248, 251, 252, 254] that the quaternary carbon region of the ^{13}C NMR spectrum gives information on the substitution of the hydroxyl group of the multi-arm initiator. The quaternary carbon resonances appear at 46.14 ppm when both hydroxyl groups react, at 48.14 ppm if one hydroxyl group remains and at 50.15 ppm when both hydroxyl did not react, as shown in Figure V.7. Hedrick and coworkers and Hult and coworkers^[252, 254, 255] thus showed from analysis of the quaternary carbon region of ^{13}C NMR spectrum that terminal repeat units are more reactive than the linear repeat units and they attributed this observation to steric hindrance and H-binding. In the present case, analysis of the ^{13}C NMR spectrum from 46 to 51 ppm, in the region of the quaternary carbon of the H40, showed all the hydroxyl functions (linear and terminal units) to have reacted (Figure V.8) (spectrum quality can be improve by increasing the number of scan). This indicated homogeneous multi-arm star polymers to have been obtained.

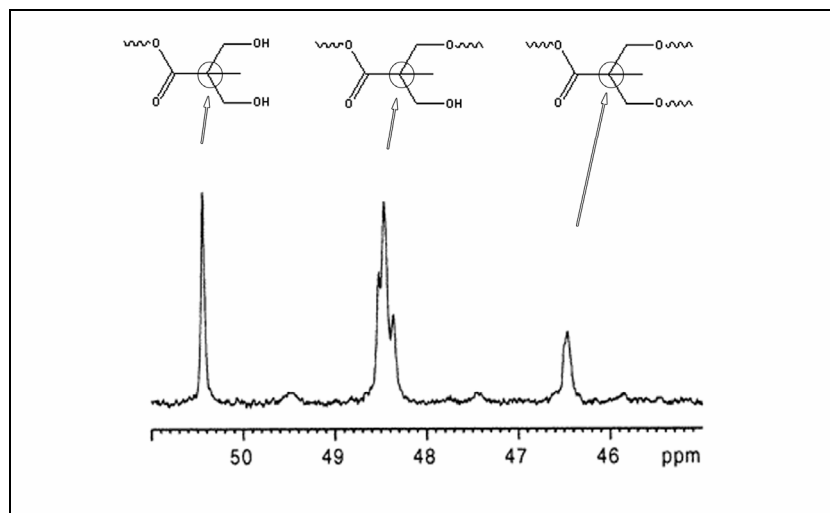


Figure V.7 ^{13}C NMR (DMSO): Quaternary carbon region for poly (*bis*-MPA) samples^[262]

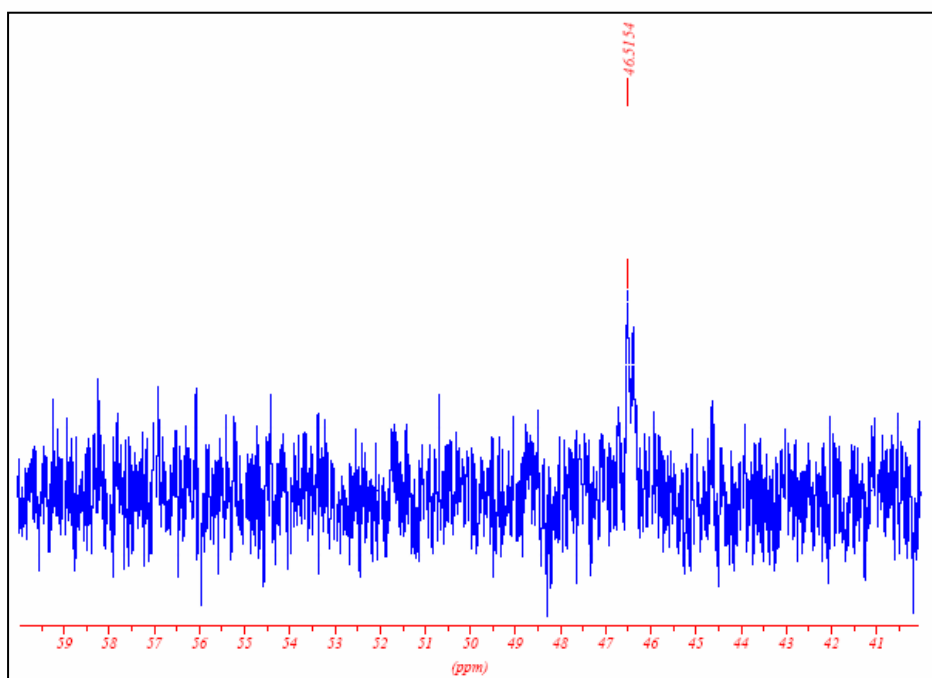
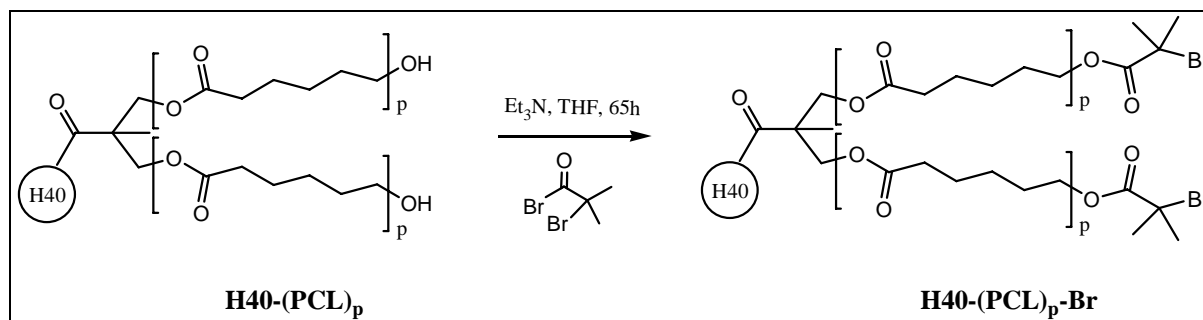


Figure V.8 Enlarged ^{13}C NMR spectrum in CDCl_3 for H40-(PCL)_{10}

III.3. The hydrophilic shell

III.3.1 Macroinitiator synthesis

For the synthesis of a well defined star-block copolymer by ATRP, it is essential to prepare an initiator that can efficiently trigger the polymerization of the chosen monomer. It has been shown that alkyl halides containing activating substituents (such as carbonyl groups) at the α -carbon position can initiate the polymerization of *tert*-butyl acrylate^[212] and methyl methacrylate.^[213] A well defined polymer may be prepared by using a functional group that has a structure similar to that of the growing polymer chain end in its dormant form. In the present case, the H40-(PCL)_p and H30-(PCL)_p star-blocks were dissolved in THF and modified with 2-bromoisobutyryl bromide in the presence of triethylamine (Scheme V.3).^[216, 270] The efficiency of this alkyl halide initiator for the ATRP of acrylate has been demonstrated, although 2-bromobutyryl bromide or 2-bromopropionyl bromide may also represent viable alternatives in our case.



Scheme V.3 Synthesis of the hyperbranched macroinitiator: H40-(PCL)_p-Br

Following this procedure a series of six macroinitiators was prepared according to Table V.6 and characterized with NMR in CDCl_3 (^1H and ^{13}C) and GPC in DMF. Excesses of 2-bromoisobutyl bromide and triethylamine were used. The synthesis of H40-Br, for the initiation of ATRP directly on the H40 core has been prepared with 4-(dimethylamino)pyridine and triethylamine as described in the experimental section (Chapter IV.II.2).

Table V.6 Conditions for the different macroinitiator syntheses

	Origin	n_{eq}/OH [bromide]	n_{eq}/OH [NEt ₃]	Time [h]	Yield [%]
H30-(PCL) ₁₂ -Br	H30-(PCL) ₁₂	10	6	65	68.4
H40-(PCL) ₁₀ -Br	H40-(PCL) ₁₀	2	2	48	56.6
H40-(PCL) ₁₇ -Br	H40-(PCL) ₁₇	2	2	65	93.6
H40-(PCL) ₂₄ -Br	H40-(PCL) ₂₄	10	6	65	81.0
H40-(PCL) ₄₀ -Br	H40-(PCL) ₄₀	10	6	65	61.4
H40-(PCL) ₅₀ -Br	H40-(PCL) ₅₀	10	6	63	93.4

The degree of functionalization was determined by ^1H NMR. Figure V.9 shows the ^1H NMR spectrum in CDCl_3 for the macroinitiator H40-(PCL)₂₄-Br. In comparison with the spectrum of H40-(PCL)₂₄ (Figure V.4) the shift associated with the methyl group adjacent to the hydroxyl (e) from 3.65 to 4.26 ppm and the disappearance of the peak at 3.65 ppm indicated the reaction to be complete. The additional peak (f) at 1.93 ppm in the ^1H NMR spectrum and an absorption peak at 30.21 ppm in the ^{13}C NMR spectrum (Figure V.10) were attributed to the methyl groups of the 2-bromoisobutyl bromide. Table V.7 and Figure V.9 showed the complete conversion of the $-\text{OH}$ groups of the PCL, with an integral of 5.6 H (instead of 6) being obtained for the methyl groups of the 2-bromoisobutyl bromide.

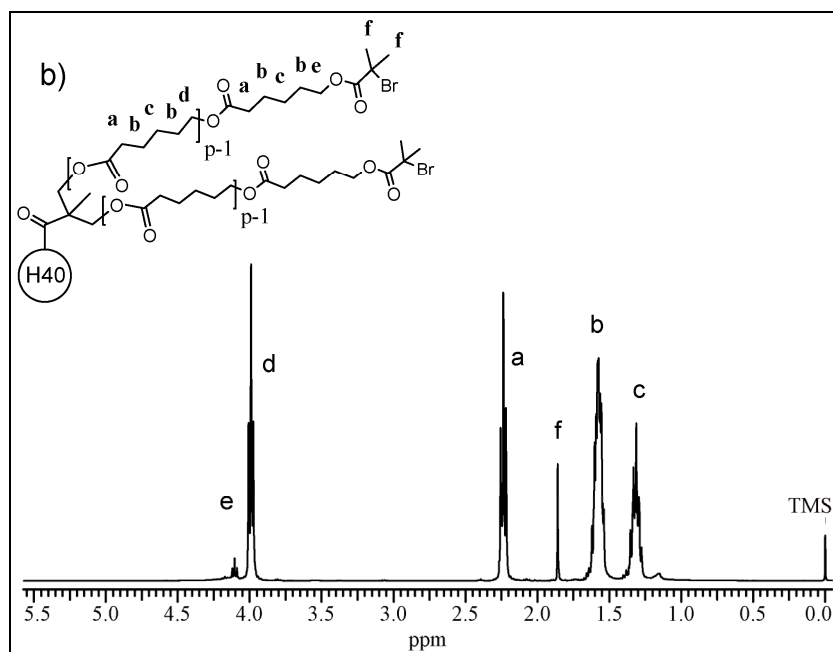


Figure V.9 ^1H NMR of the macroinitiator H40-(PCL) $_{24}$ -Br

Table V.7 Comparison between the expected number of protons per arm (for $DP_p = 24$) and the ^1H NMR peak integrals.

peak	(ppm)	Integral measured by NMR	Expected number of protons/arm
c	[1.23 .. 1.44]	48.42	$24 \times 2\text{H}$ 48
b	[1.47 .. 1.68]	94.90	$24 \times 4\text{H}$ 96
f	[1.82 .. 1.90]	5.64	$2 \times 3\text{H}$ 6
a	[2.14 .. 2.33]	44.43	$24 \times 2\text{H}$ 48
d+e	[3.90 .. 4.17]	48.00	$23 \times 2\text{H} + 2\text{H}$ 48

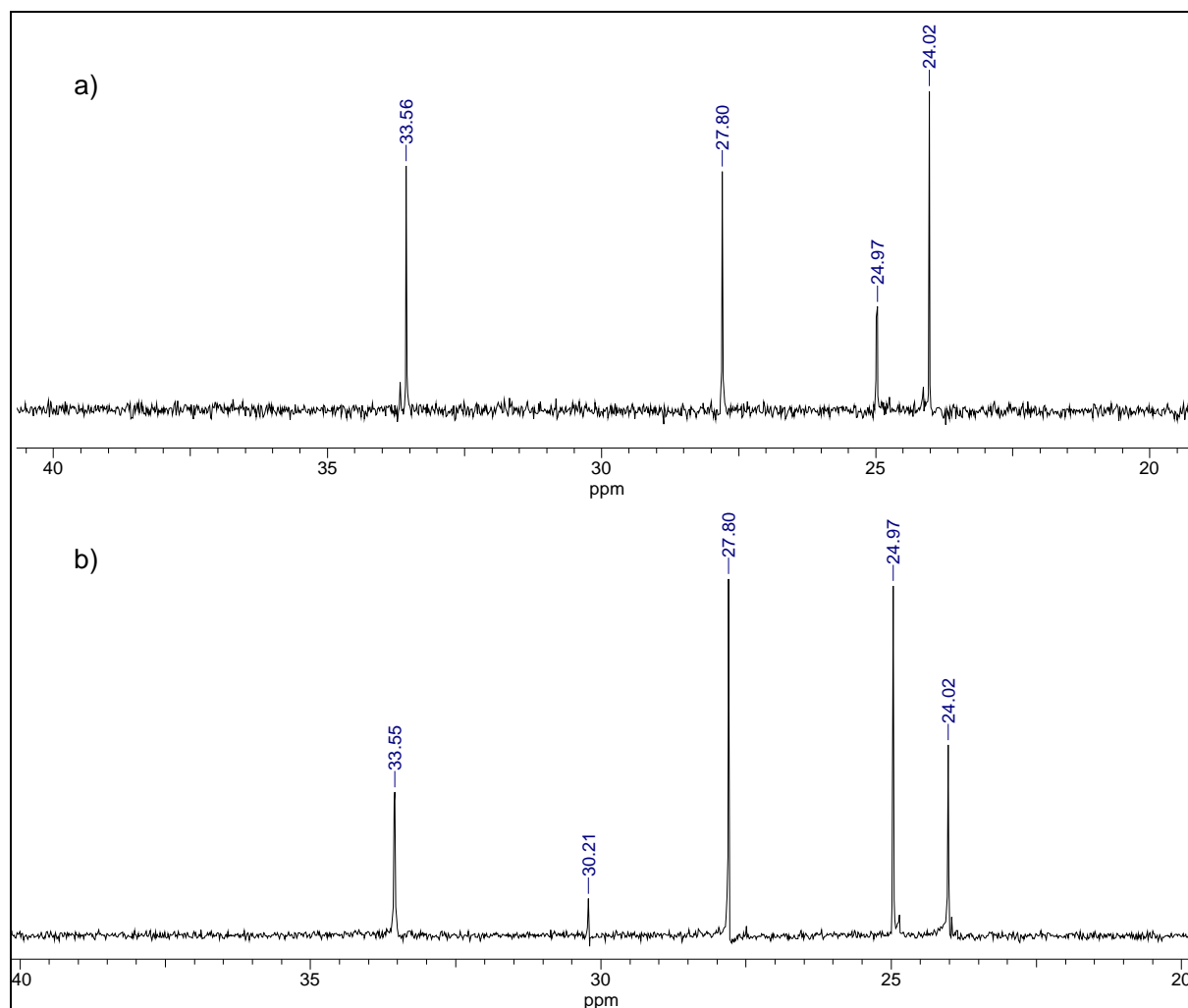


Figure V.10 Enlarged ^{13}C NMR spectrum (between 20 and 40 ppm) for (a) H40-(PCL)_p and (b) H40-(PCL)_p-Br star-block copolymer

Molar masses were calculated from NMR measurements assuming complete conversion of the $-\text{OH}$ groups of the PCL and from GPC in DMF. The values given in Table V.8 are in good agreement. The exception in the case of H40-(PCL)₅₀-Br where the M_n measured by GPC is lower than the NMR calculation (but of a similar order of magnitude) is attributed to uncertainties inherent in the GPC technique due to the particular polymer architectures. Figure V.11 shows GPC traces for H40-(PCL)₂₄ and H40-(PCL)₂₄-Br and illustrates the small difference between the precursor and the bromide macroinitiator. The completion of the reaction has been shown by NMR however it would have been possible to use MALDI-TOF MS measurements (although this technique is not easily adapted to block

copolymer and to high M_w/M_n values) to investigate further the evolution of the molar masses.^[271, 272]

Table V.8 Characterization of H40-(PCL)_p-Br macroinitiator with GPC in DMF. Comparison with the expected values determined from NMR for complete conversion

Sample name	M_n [g mol ⁻¹]	M_n [g mol ⁻¹]	M_w/M_n
	NMR	GPC	
H30-(PCL) ₁₂ -Br	42 340	42 170	2.13
H40-Br	9 460	12 300	1.72
H40-(PCL) ₁₀ -Br	50 500	54 300	2.27
H40-(PCL) ₁₇ -Br	79 230	106 000	1.79
H40-(PCL) ₂₄ -Br	110 000	111 100	2.79
H40-(PCL) ₄₀ -Br	173 600	177 600	2.06
H40-(PCL) ₅₀ -Br	214 660	178 900	2.65

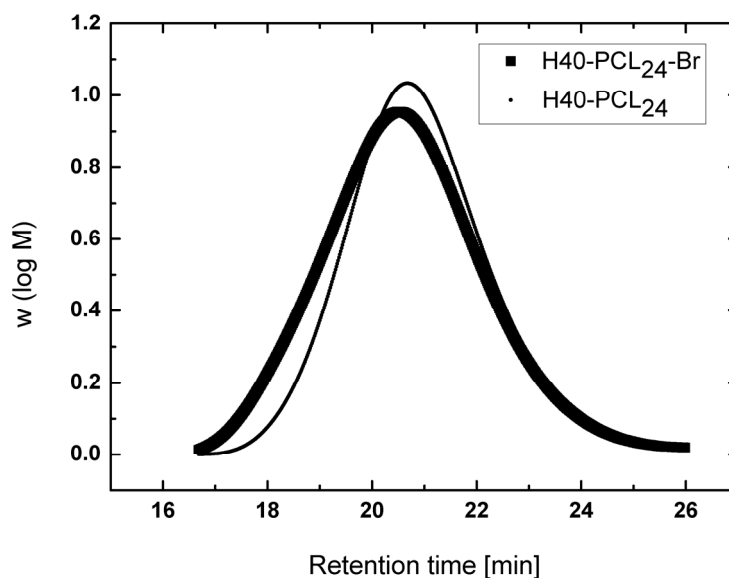


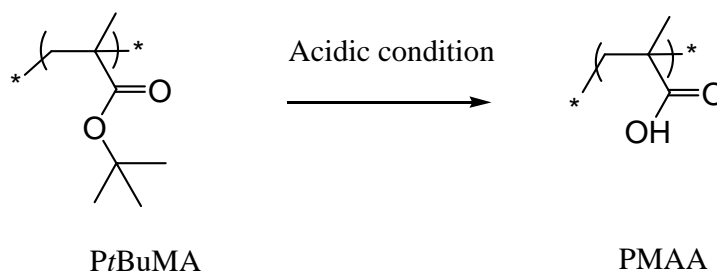
Figure V.11 GPC trace of H40-(PCL)₂₄-Br and the precursor H40-(PCL)₂₄ in DMF

III.3.2 Preparation of pH-responsive star-block copolymers

Because of the interactions between the ionic monomers and the catalyst/ligand complex the preparation of ionic polymers by ATRP was carried out in two steps.^[202] The method was to polymerize a monomer containing neutral hydrophobic groups, which could then be functionalized to provide ionic water soluble polymers.

In order to prepare pH-responsive capsules with free carboxylic acid functions, (meth)acrylate monomer with *tert*-butyl groups such as *tert*-butyl methacrylate (*t*BuMA) or *tert*-butyl acrylate (*t*BuA) were considered. The free carboxylic acid were obtained after hydrolysis of the *tert*-butyl groups (Scheme V.4). Hence as a function of the pH, the -COOH groups may be deprotonated providing an anionic capsule.^[273] In the case of poly(acrylic acid), the pK_a is around 5.^[274]

75

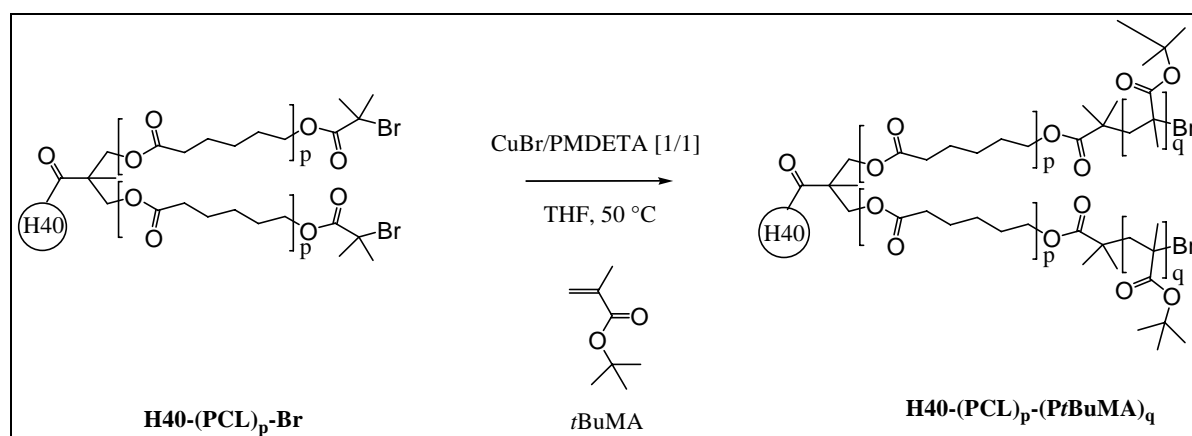


Scheme V.4 Strategy for obtaining a pH-responsive polymer based on *tert*-butyl methacrylate

(1) *Optimization of ATRP with tert-butyl methacrylate (tBuMA)*

Following the literature,^[275] the ATRP of *t*BuMA was carried out with CuBr and PMDETA as catalyst and ligand respectively. The choice of the solvent was first investigated and reaction in THF at 50 °C gave better conversion (30.4 %) than in anisol at 90 °C (22.5 %) or in ethyl acetate at 50 °C (0 %). The concentration of the solvent [*S*] as a function of the monomer [*M*] proportion was then studied and it was shown that [*M*]/[*S*] of 30/70 gave better

conversion (41 %) than $[M]/[S] = 50/50$, where gelation appeared immediately after the introduction of the monomer. The optimum conditions for the ATRP of *t*BuMA in the presence of PMDETA are given in Scheme V.5. Even if gelation did not appear immediately when $[M]/[S] = 30/70$ was used, it remained a problem during the purification of the product and GPC (Figure V.12) confirmed the presence of star-star coupling during ATRP under these conditions.



Scheme V.5 Procedure followed for the ATRP of *t*BuMA

As discussed in the literature, a potential problem with the synthesis of star polymers using multifunctional initiators is star-star coupling, depending on the catalyst/ligand complex and the monomer to be polymerized.^[216, 221, 225, 231] The proportion of termination by radical coupling can be reduced by using more dilute solutions or limiting monomer conversions.^[225] However, star-star coupling could also be alleviated by using the appropriate alkyl halide initiator and catalyst/ligand complex. Under appropriate conditions control is satisfactory and many different star-block copolymers have been successfully prepared.^[276] With the polymerization of styrene and *t*BuA initiated by calixarene containing 8 branches, Angot et al. demonstrated that it is possible to avoid star-star coupling in ATRP.^[224] In the present case, to avoid star-star coupling, polymerization of *t*BuA with **H40-(PCL)_p-Br** as the macroinitiator using CuBr and bipyridyl as catalyst and ligand respectively was considered. Under these conditions no gelation appeared during the reaction and the purification of the product was

simplified. GPC traces of $\text{H40-(PCL)}_{17}\text{-(PtBuA)}_q$ in DMF confirmed the absence of star-star coupling (Figure V.12).

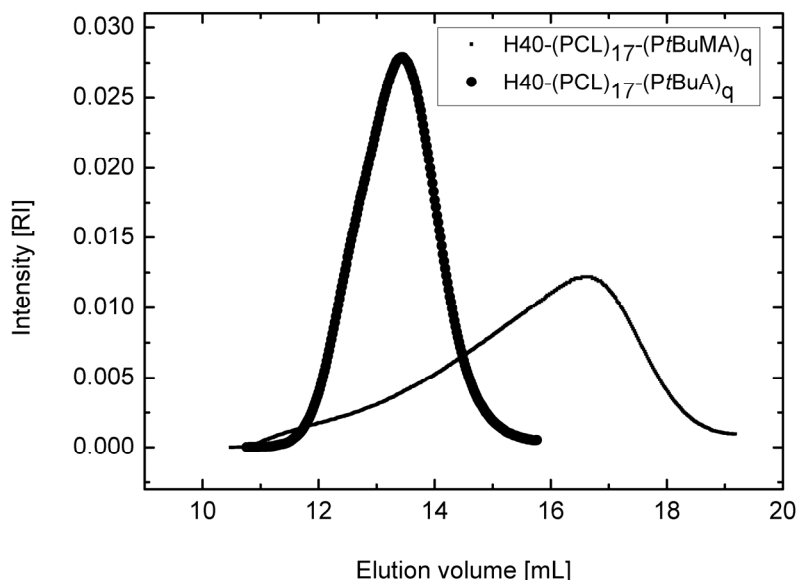


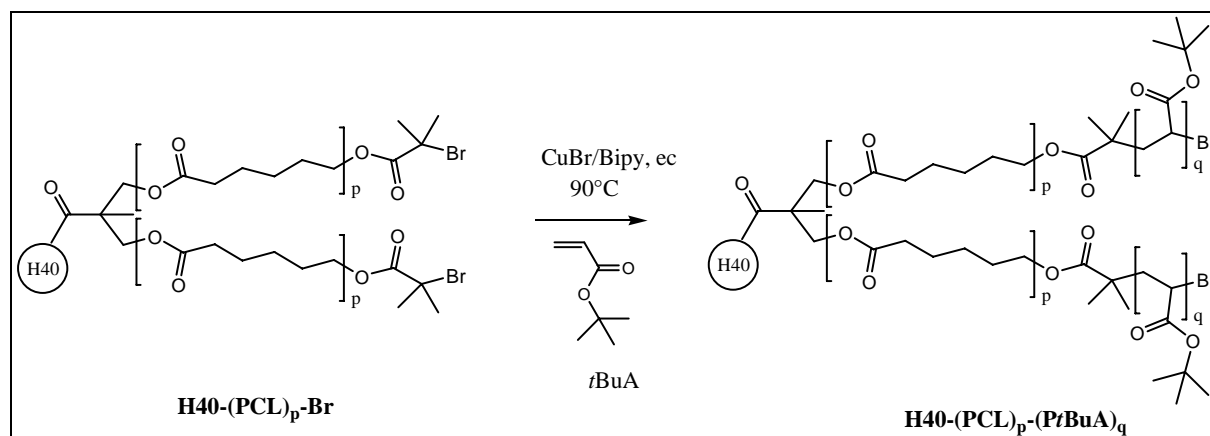
Figure V.12 GPC traces in DMF after the ATRP of *t*BuMA and *t*BuA initiated with $\text{H40-(PCL)}_{17}\text{-Br}$

(2) *ATRP of tBuA for the synthesis and characterization of $\text{H30-(PCL)}_p\text{-(PtBuA)}_q$ and $\text{H40-(PCL)}_p\text{-(PtBuA)}_q$*

Due to the absence of a radical stabilizer in the acrylate monomers the polymerization of acrylate is better controlled than that of methacrylate. Moreover acrylates are more water soluble. A further advantage of the resulting capsules is the possibility of varying the surface charge by varying the pH.^[273]

According to the literature, the polymerization of *t*BuA from a multi-arm macroinitiator may be carried out in the bulk with copper bromide and 2,2'-bipyridyl with the optimum proportions of macroinitiator (MI), catalyst and ligand (L) of $[\text{MI}]/[\text{Cu}]/[\text{L}] = 1/1/2$ ^[224] or PMDETA as ligand.^[212, 277] In the present work $\text{H40-(PCL)}_p\text{-(PtBuA)}_q$ was

prepared by ATRP of *t*BuA in the bulk at 90 °C, with CuBr/2,2'-bipyridyl as the catalyst (Scheme V.6) in the proportions [MI]/[Cu]/[L] = 1/1/2, and in the presence of ethylene carbonate (ec). Ethylene carbonate is used to increase the homogeneity of the copper salt and was introduced as a function of the monomer weight (10 % w/w monomer).^[278] ¹H and ¹³C NMR were carried out in CDCl₃ and GPC in DMF to characterize the product and to follow the ATRP.



Scheme V.6 ATRP of *t*BuA initiated by H40-(PCL)_p-Br macroinitiator

A representative ¹H NMR spectrum is given in Figure V.13. All the peaks of the PCL were clearly visible as well as the additional peak associated with the *Pt*BuA blocks. The degree of polymerization of the *Pt*BuA (DP_q) was calculated from ¹H NMR spectroscopy from the multiplets between 1.58 and 1.30 ppm (c + i), and the triplet at 4.06 ppm which corresponds to the ester methylene group of the PCL (d). The multiplets between 1.58 and 1.30 ppm correspond to the methylene group in the middle of the PCL chain (c) and to the *tert*-butyl groups of the *Pt*BuA block (i). The degree of polymerization of the *Pt*BuA (DP_q) could also have been calculated by taking into account the multiplet between 2.2 and 2.5 ppm (a + h), and the triplet at 4.06 ppm (d). The multiplets (a + h) correspond to the methylene group of the PCL chain (a) and to the -CH groups of the *Pt*BuA block (h). The appearance of *tert*-butyl groups between 1.58 and 1.30 ppm was easily detectable in the ¹H NMR spectrum.

The PCL blocks of the $\text{H40-(PCL)}_p\text{-(PtBuA)}_q$ were detectable by ^{13}C NMR with the presence of the methylene peaks at 24.55, 25.50, 28.33, 34.08 and 64.11 ppm and the carbonyl at 173.50 ppm. The peaks attributed to the PtBuA blocks (174.14, 80.29, 42.28, 41.87 and 28.08 ppm) were also visible. As a representative example, the ^{13}C NMR spectrum of $\text{H40-(PCL)}_{40}\text{-(PtBuA)}_{100}$ is given in Figure V.14.

Figure V.15 shows GPC curves for the star-block copolymers $\text{H40-(PCL)}_{40}\text{-(PtBuA)}_{100}$ along with that of the macroinitiator $\text{H40-(PCL)}_{40}\text{-Br}$ and of the H40-(PCL)_{40} . The shift towards the high molar masses for the star-block copolymer indicated that the reaction proceeds. These results confirmed the bromo ester to be an efficient initiator for the ATRP of *t*BuA in the presence of ethylene carbonate and $\text{CuBr}/2,2'$ -bipyridyl.

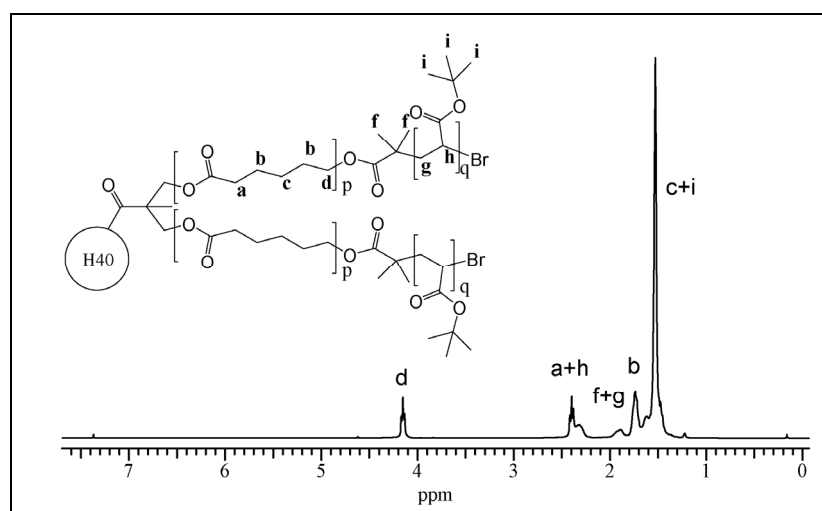


Figure V.13 ^1H NMR spectrum of $\text{H40-(PCL)}_{40}\text{-(PtBuA)}_{100}$ in CDCl_3

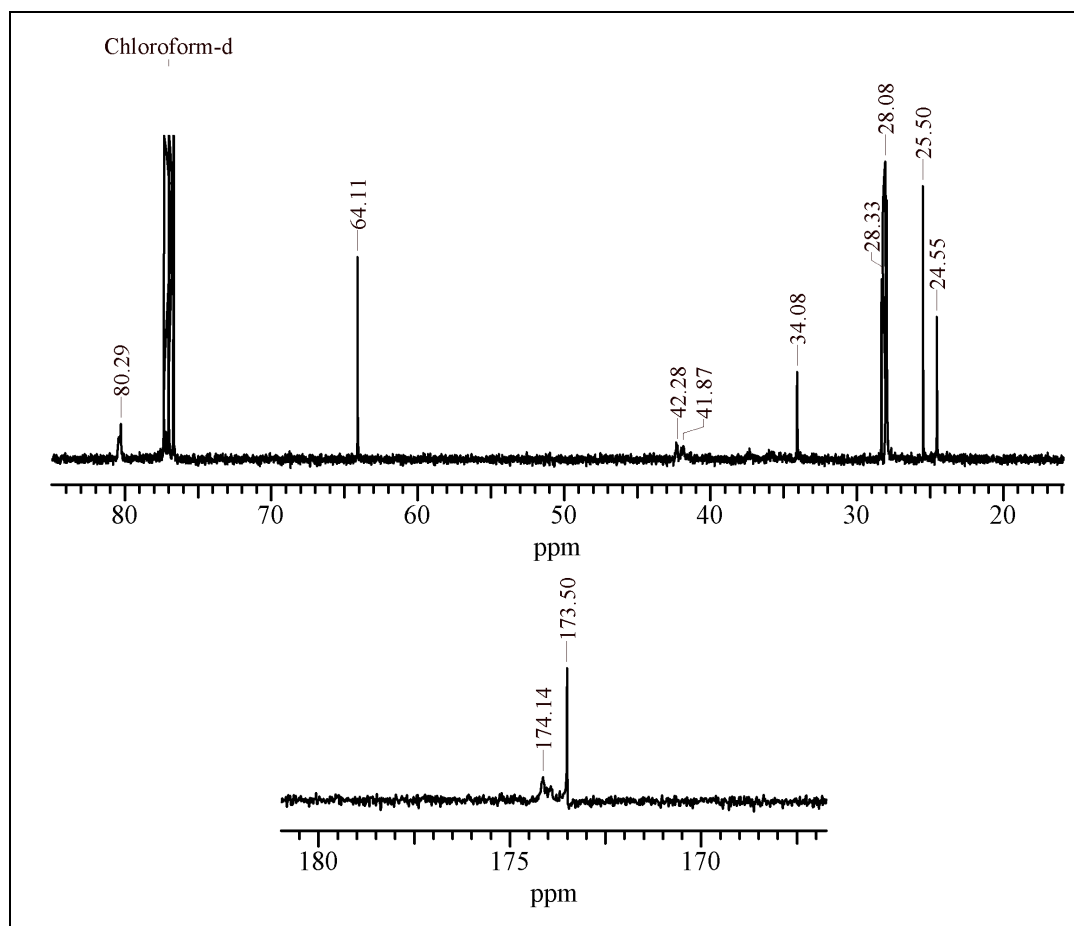


Figure V.14 ^{13}C NMR spectrum of $\text{H40-(PCL)}_{40}\text{-(PtBuA)}_{100}$ in CDCl_3

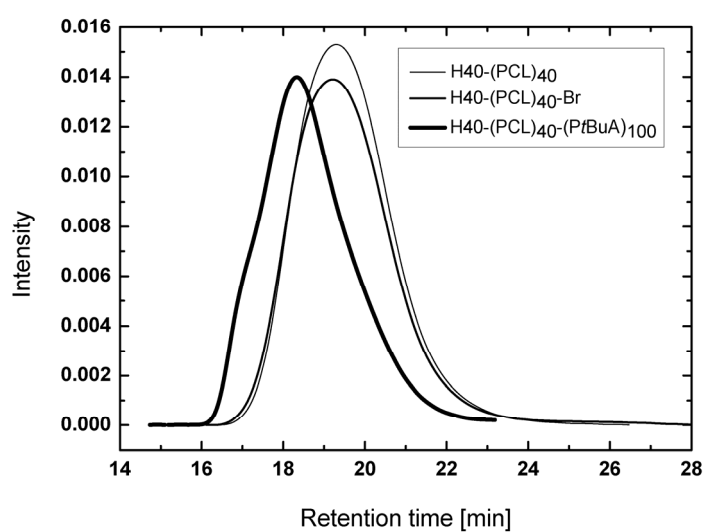


Figure V.15 GPC in DMF of H40-(PCL)_{40} , $\text{H40-(PCL)}_{40}\text{-Br}$ and $\text{H40-(PCL)}_{40}\text{-(PtBuA)}_{100}$

By varying the monomer concentration or the reaction time, a series of star-block copolymers with different polymer lengths and two generations HBP (H30 or H40) were synthesized and characterized with ^1H and ^{13}C NMR in CDCl_3 and GPC in DMF. Data corresponding to the star-block copolymers prepared are summarized in Table V.9. The nomenclature refers to the degree of polymerization determined by NMR as described above.

Table V.9 ATRP conditions and analytical results for the polymerization of *t*BuA initiated by different multi-arm star-block copolymers

Sample Entry	Macroinitiator	MI weight [g]	$[\text{MI}]/[\text{CuBr}]/[\text{L}]/[\text{M}]$ molar ratio	Reaction time [h]	M_n^a [g mol $^{-1}$]	M_n^b [g mol $^{-1}$]	M_w/M_n
H30-(PCL) $_{12}$ -(PtBuA) $_{60}$	H30-PCL $_{12}$ -Br	1	1/1/2/80	6.0	240 380	204 000	2.40
H40-(PtBuA) $_{36}$	H40-Br	0.2	1/1/2/88	5.5	174 270	199 490	2.06
H40-(PCL) $_{10}$ -(PtBuA) $_{68}$		1	1/1/2/100	21.5	361 310	488 520	2.44
H40-(PCL) $_{10}$ -(PtBuA) $_{70}$	H40-PCL $_{10}$ -Br	1	1/1/2/200	-	370 460	459 740	1.84
H40-(PCL) $_{10}$ -(PtBuA) $_{115}$		1	1/1/2/200	21.0	576 200	549 000	2.06
H40-(PCL) $_{17}$ -(PtBuA) $_{18}$		0.5	1/1/2/100	17.0	161 140	205 000	1.80
H40-(PCL) $_{17}$ -(PtBuA) $_{20}$	H40-PCL $_{17}$ -Br	7	1/1/2/100	17.0	170 590	262 675	3.43
H40-(PCL) $_{17}$ -(PtBuA) $_{50}$		2	1/1/2/130	6.0	307 750	274 930	1.95
H40-(PCL) $_{24}$ -(PtBuA) $_{82}$	H40-PCL $_{24}$ -Br	10	1/1/2/160	20.0	484 800	357 700	3.17
H40-(PCL) $_{40}$ -(PtBuA) $_{100}$	H40-PCL $_{40}$ -Br	2	1/1/2/200	7.3	630 740	452 350	2.33
H40-(PCL) $_{50}$ -(PtBuA) $_{44}$		2	1/1/2/200	7.3	315 160	396 600	2.23
H40-(PCL) $_{50}$ -(PtBuA) $_{54}$	H40-PCL $_{50}$ -Br	2	1/1/2/200	14.5	461 470	376 280	2.27
H40-(PCL) $_{50}$ -(PtBuA) $_{56}$		2	1/1/2/200	20.0	470 610	536 860	2.19
H40-(PCL) $_{50}$ -(PtBuA) $_{64}$		1.5	1/1/2/250	48.0	507 190	732 760	3.37

MI: macroinitiator, CuBr, L: ligand, M: monomer

^a measurement by ^1H NMR in CDCl_3

^b measurement by GPC in DMF

The results in Table V.9 illustrate the importance of the amount of macroinitiator introduced at the beginning of the reaction on the conversion. As often observed in organic chemistry, the reaction becomes significantly faster at a large scale. When 0.5 g of H40-(PCL)₁₇-Br macroinitiator were introduced during 17 h with $[MI]/[CuBr]/[L]/[M] = 1/1/2/100$ ratio, a degree of polymerization (DP_n) of 18 was determined from ¹H NMR whereas under the same reaction conditions, 7 g of the same macroinitiator gave a $DP_n = 50$.

The higher the molar mass of the macroinitiator, the slower the polymerization rate. When H40-(PCL)₁₀-Br is used, a degree of polymerization of 115 is obtained providing a H40-(PCL)₁₀-(PtBuA)₁₁₅ whereas DP_n is only 56 when initiating from H40-(PCL)₅₀-Br providing a H40-(PCL)₅₀-(PtBuA)₅₆ after 20 h. This is thought to be due to increased steric hindrance.

Molar masses determined by NMR in CDCl₃ and measured with GPC in DMF are in good agreement for the majority of the star-block copolymers synthesized with GPC molar masses often slightly higher than NMR values. When the difference between NMR and GPC is high, the polydispersity is also high (> 3), which may lead to errors in the M_n determination. Surprisingly, the molar mass obtained from GPC for H40-(PCL)₅₀-(PtBuA)₄₄ was somewhat higher than that for H40-(PCL)₅₀-(PtBuA)₅₄. However, given that the expected molar masses were relatively close this may be attributed to experimental scatter in the GPC measurements. The polydispersities (> 2) were larger than expected for polymers prepared via ATRP, owing to the heterogeneity of the macroinitiator, which have polydispersities between 1.72 and 2.79.

(3) *Is the ATRP of tBuA well controlled?*

A kinetic study of the ATRP of tBuA with H40-(PCL)₁₀-Br as the macroinitiator, CuBr as the catalyst and 2,2'-bipyridyl as the ligand, was carried out as follows. Aliquots of the reaction medium were taken at different time intervals and analyzed by ¹H NMR in CDCl₃ and GPC in DMF. The conversion was determined by comparing the intensity of the monomer protons between 5.5 and 6.3 ppm and the methylene groups of the PCL at around 4.02 ppm (peak (d) in Figure V.16).

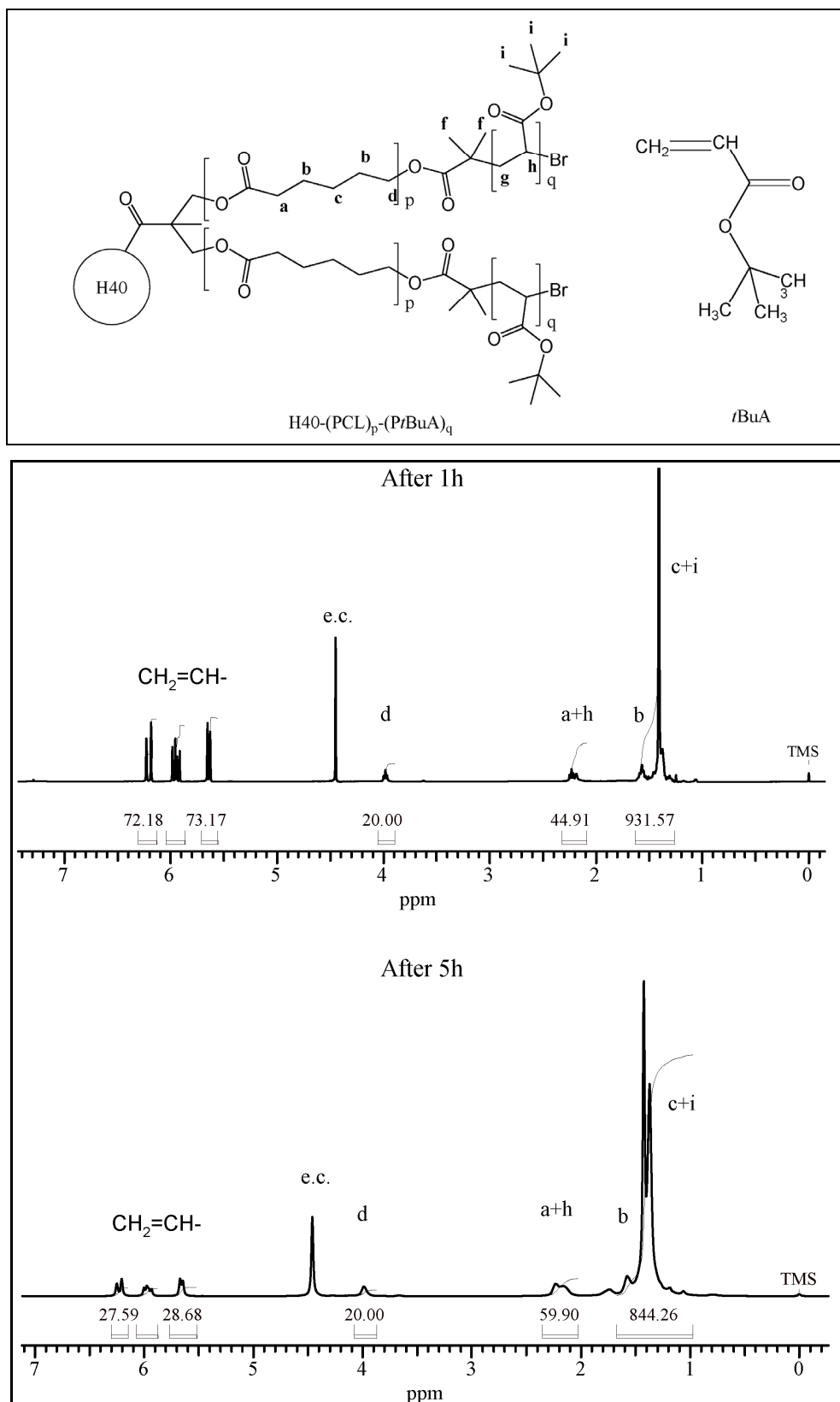


Figure V.16 $^1\text{H NMR}$ spectra of the aliquots of ATRP of $t\text{-BuA}$ initiated by $\text{H40-(PCL)}_{10}\text{-Br}$ after 1h and 5h reaction.

Figure V.16 shows the decrease in the monomer concentration. After 1 h reaction the peak integration of the proton at around 5.5 ppm was 73.17 whereas after 5 h it decreased to 28.68. Moreover the increase of the peak surface from 44.91 to 59.90 of the peak at 2.3 ppm, which corresponds to the methylene groups of the PCL (a) and of the *Pt*BuA (h), also indicates polymerization. The integration measured for (c + i) peak after 1 h and 5 h conversion, which corresponds to the *tert*-butyl groups and to the methylene groups of the PCL blocks, remains constant (931.57 compared with 844.26), since the protons associated with the *tert*-butyl groups are present in the monomer and in the polymer.

The dependence of $[M]/[I]$ ratio on time has been considered for the ATRP of *t*BuA under the conditions referred to above (in section (2)). In Figure V.17 the evolution of the molar mass of the sample (followed by the decrease in the initial monomer concentration $[M_0]/[M]$ as a function of time), determined from GPC in DMF, as a function of the reaction time has been given for monomer/initiator ratios of 100 and of 200 ($[M]/[I] = 100$ and $[M]/[I] = 200$). The results showed that the concentration of the propagating radicals was constant throughout the polymerization, and that $[M]/[I]$ significantly influenced the conversion and the rate of the reaction. The reaction was slower with a high monomer concentration ($[M]/[I] = 200$) and faster with a high initiator concentration ($[M]/[I] = 100$), as required by Equation II.6. Well controlled behaviour was maintained, as confirmed by the monomodal GPC curve obtained for H40-(PCL)₁₀-(PAA)₇₀ (results not shown), even above 80 % conversion. The low rate measured for $[M]/[I] = 200$ due to the dilution of the medium was consistent with results obtained previously with an octafunctional initiator.^[224]

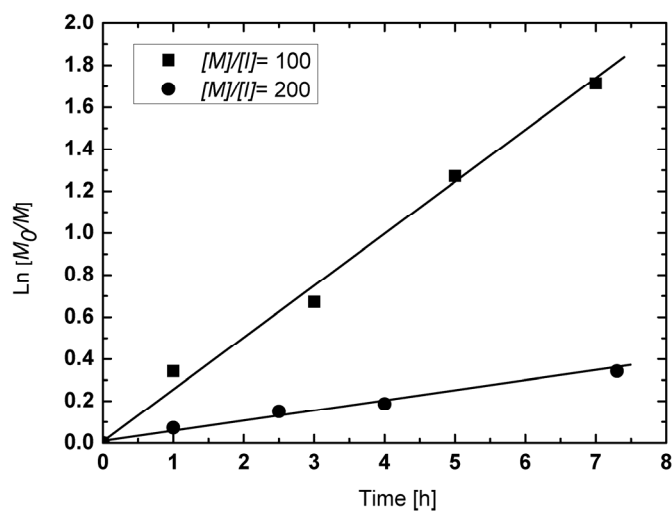


Figure V.17 Plots of $\ln([M_0]/[M])$ versus time during ATRP of *t*BuA at 90 °C initiated with H40-(PCL)₁₀-Br for two $[M]/[I]$ molar ratios.

Figure V.18 shows the GPC traces, after purification, obtained in DMF at different times during the preparation of a star-block copolymer H40-(PCL)₁₇-(P*t*BuA)_q in the presence of ethylene carbonate and CuBr/2,2'-bipyridyl. The chromatograms showed no star-star coupling in spite of the large number of arms, reflecting the lower reactivity of the acrylate compared with that of methacrylates^[224] and the importance of the choice of catalyst/ligand complex.

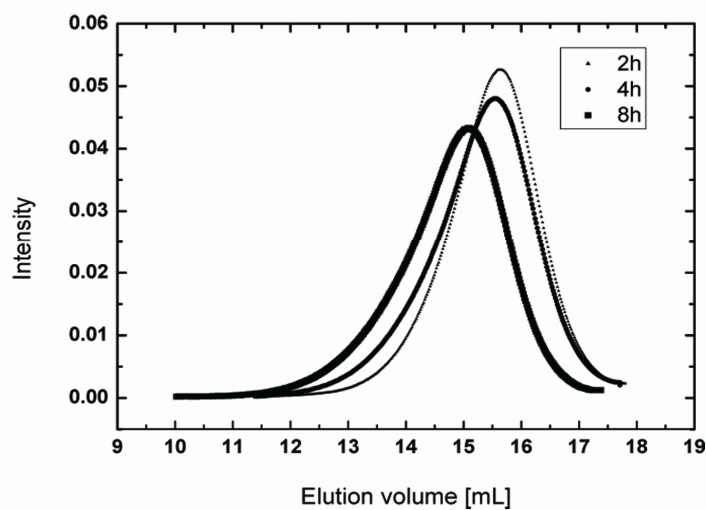
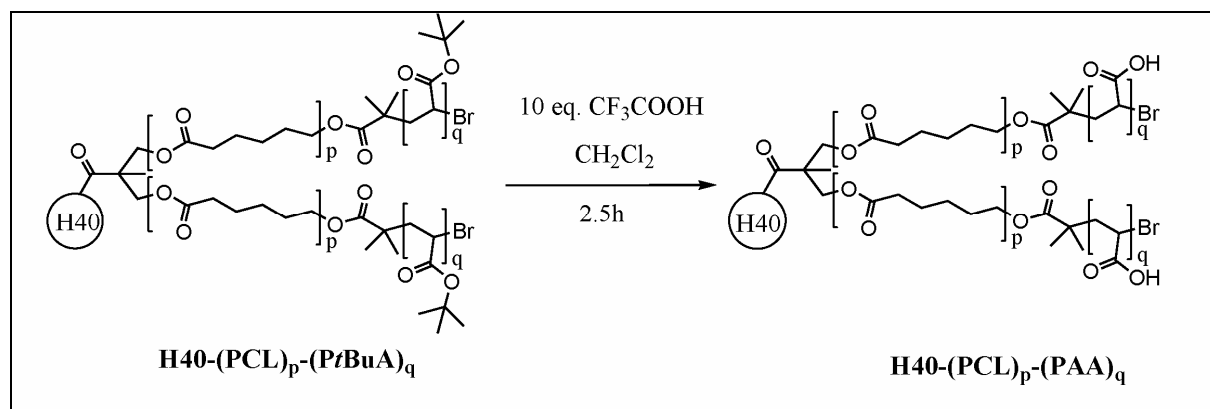


Figure V.18 GPC in DMF of ATRP of tBuA initiated with H40-(PCL)₁₇-Br

(4) Hydrolysis of the *tert*-butyl groups

The final step in obtaining amphiphilic multi-arm star-block copolymers (H40-(PCL)_p-(PAA)_q) is hydrolysis of the *tert*-butyl groups of the H40-(PCL)_p-(*Pt*BuA)_q under acidic conditions. Different routes may be followed.^[99, 212, 216, 227, 279] For example, the hydrolysis of *tert*-butyl groups from a linear PCL-*b*-*Pt*BuA block copolymer by using trimethyl silyl iodine (TMSI) followed by reaction with HCl aq. has been reported.^[99] However, with high concentrations of TMSI, due to the large quantity of *tert*-butyl groups, it is observed that the PCL blocks are partially hydrolyzed. For this reason trifluoroacetic acid (TFA) has been chosen in the present work.



Scheme V.7 Hydrolysis of *tert*-butyl groups of the $\text{H40-(PCL)}_p\text{-(PtBuA)}_q$ with TFA

The reaction was carried out by dissolving the polymer in dichloromethane in the presence of trifluoroacetic acid at room temperature. A first optimization was carried out on $\text{H40-(PCL)}_{17}\text{-(PtBuA)}_{50}$ star-block copolymer by varying the acidic concentration and the time of the reaction as described in Table V.10. Full conversion was obtained after 120 minutes when the polymer was dissolved in dichloromethane at 6 wt% in the presence of 10 equivalents of trifluoroacetic acid per *tert*-butyl group. According to these results, each star-block copolymer prepared previously was dissolved in dichloromethane at 6 wt% and the *tert*-butyl groups were hydrolyzed under the conditions summarized in Table V.11.

Table V.10 Optimization of the hydrolysis of the *tert*-butyl groups of $\text{H40-(PCL)}_{17}\text{-(PtBuA)}_{50}$ by TFA

Concentration [wt.%]	Molar ratio <i>t</i> BuA/TFA	Reaction time [min]	Conversion [%]
10	1/1	30	0
10	1/10	30	66
10	1/10	35	66
10	1/10	45	74
10	1/10	60	85
6	1/10	120	100

Table V.11 Hydrolysis of the *tert*-butyl groups of the H40-(PCL)_p-(PtBuA)_q

Initial star-block copolymer	Molar ratio <i>t</i> BuA/TFA	Reaction time [h]	Conversion [%]
H40-(PtBuA) ₃₆	1/15	2.5	90
H30-(PCL) ₁₂ -(PtBuA) ₆₀	1/15	2.66	95
H40-(PCL) ₁₀ -(PtBuA) ₆₈	1/10	2.25	100
H40-(PCL) ₁₀ -(PtBuA) ₇₀	1/10	2.00	100
H40-(PCL) ₁₀ -(PtBuA) ₁₁₅	1/10	2.25	84
H40-(PCL) ₁₇ -(PtBuA) ₅₀	1/10	2.00	52
H40-(PCL) ₂₄ -(PtBuA) ₈₂	1/15	2.66	90
H40-(PCL) ₄₀ -(PtBuA) ₁₀₀	1/10	2.50	90
H40-(PCL) ₄₀ -(PtBuA) ₁₀₀	1/15	2.50	100
H40-(PCL) ₅₀ -(PtBuA) ₅₄	1/10	1.00	77
H40-(PCL) ₅₀ -(PtBuA) ₅₆	1/10	1.00	59
H40-(PCL) ₅₀ -(PtBuA) ₆₄	1/10	2.25	87

¹H NMR spectroscopy in DMSO was used to characterize the product and the reaction (Figure V.19). The appearance of the carboxylic acid function was demonstrated by the formation of a broad peak at 12 ppm. The conversion was determined from the multiplet between 1.80 and 1.22 ppm (b+c+f+g), and the triplet at 3.99 ppm which corresponds to the methylene group of the PCL (d).

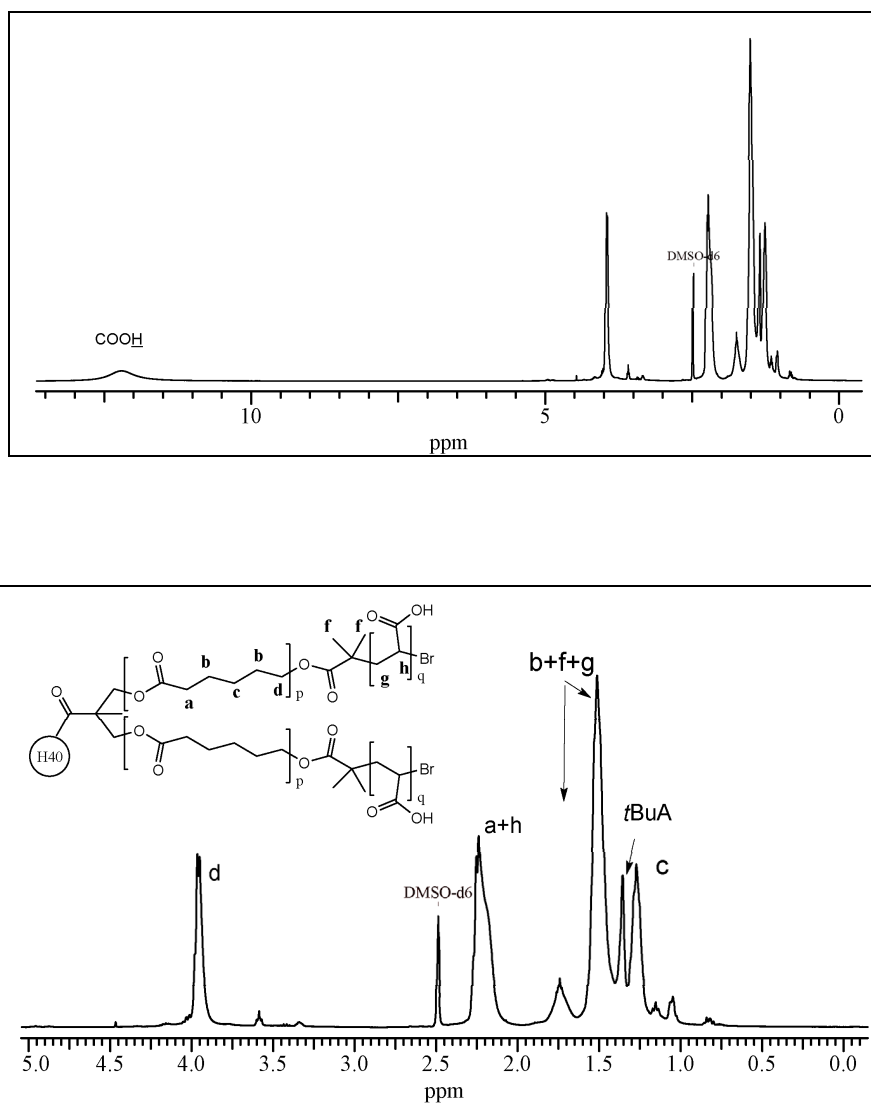


Figure V.19 ^1H NMR spectrum in DMSO of H40-(PCL) $_{40}$ -(PAA) $_{100}$ (top) and enlarged spectrum (bottom)

^{13}C NMR spectroscopy in DMSO showed the presence of the PCL block (24.08 ppm, 24.89 ppm, 27.81 ppm, 33.37 ppm, 63.50 ppm and 175.73 ppm) and of the PAA block (40.84 ppm, 41.33 ppm and 172.78 ppm) (Figure V.20). The presence of the carbonyl of the acidic function (172.78 ppm) and the disappearance of the peak at 80.29 ppm (which was attributed to the quaternary carbon of the *tert*-butyl groups) illustrated the success of the reaction. As was also seen in ^1H spectrum, the ^{13}C spectrum showed a peak at 27.56 ppm which corresponds to residual *tert*-butyl groups. However, although the presence of *tert*-butyl groups was

detectable, their amount decreased drastically in comparison with the precursor H40-(PCL)₄₀-(*t*BuA)₁₀₀ (peak at 28.08 in Figure V.14). The shift of the peaks between the two figures is due to the different solvents (CDCl₃ in Figure V.14 and DMSO in Figure V.20). 100 *tert*-butyl groups were measured per arm of hyperbranched polymer with ¹H NMR spectrum in Figure V.13 and only 5 *tert*-butyl remained after hydrolysis with TFA. For this reason it was assumed that the reaction was essentially completed, giving an amphiphilic star block copolymer H40-(PCL)₄₀-(PAA)₁₀₀.

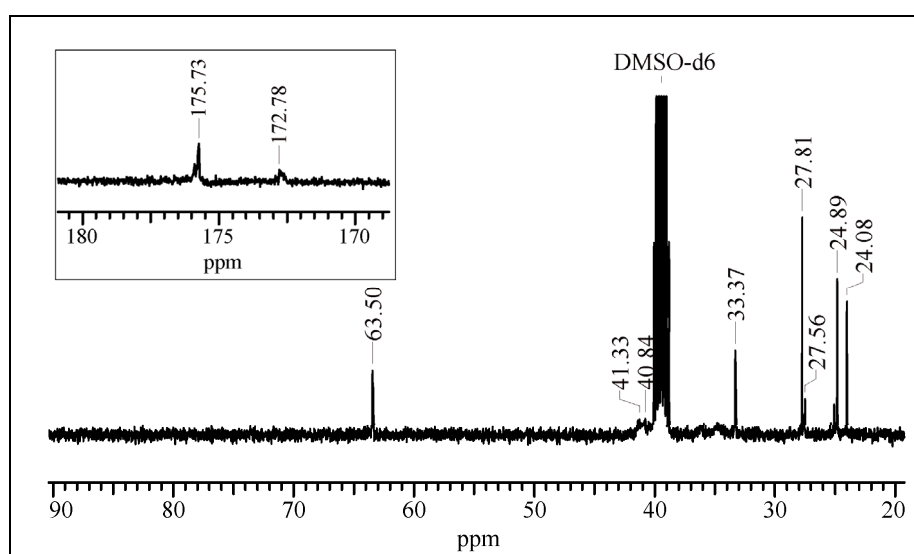


Figure V.20 ¹³C NMR spectrum of H40-(PCL)₄₀-(PAA)₁₀₀

The enlarged ¹³C NMR spectrum of H40-(PCL)₁₀-(*t*BuA)₆₈ (Figure V.21 (a)) compared with the one of H40-(PCL)₁₀-(PAA)₆₈ (Figure V.21 (b)) indicated the conversion to be 100 % with the total disappearance of peaks corresponding to the *tert*-butyl groups at 27.5 ppm and without any degradation of PCL. As it is shown in Figure V.20, the integrity of the PCL block was also maintained in H40-(PCL)₄₀-(PAA)₁₀₀ even though TFA was introduced in a large excess. This has been confirmed by GPC measurements with H40-(PCL)₂₄ block copolymer. H40-Br and H40-(PCL)₂₄ were solubilized in CH₂Cl₂ in the presence of TFA for 2 h 15. After removal of the solvent the product has been precipitated in THF and the molar mass of the polymer determined by GPC in DMF. The M_n were compared with those of the

H40-Br and H40-(PCL)₂₄ determined by GPC before treatment (Table V.12 and Figure V.22). No degradation was observed. The difference in the molar mass observed between H40-(PCL)₂₄ before and after 2.5 h with TFA are not significant and again arise from experimental scatter inherent to the technique.

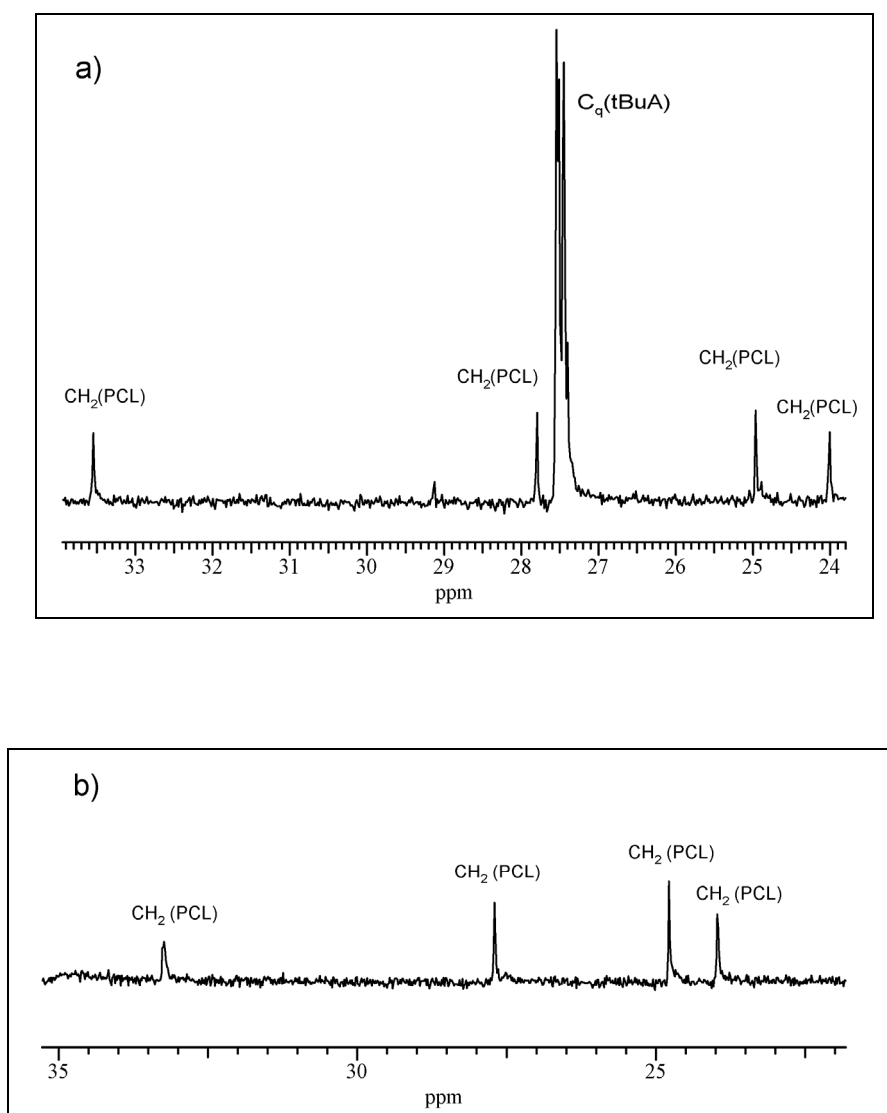
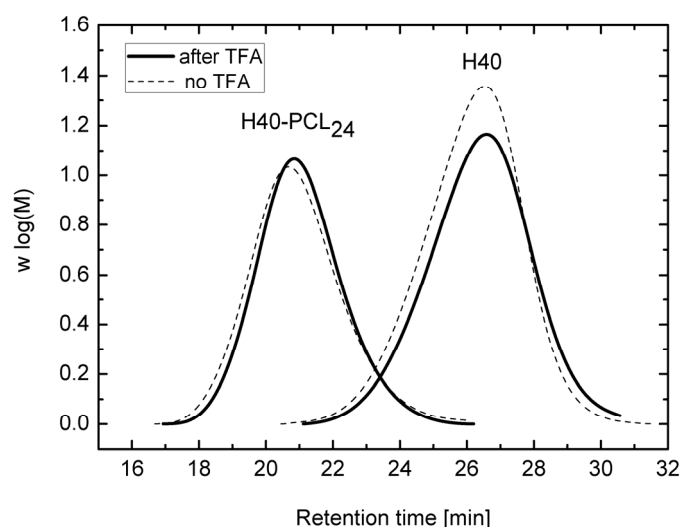


Figure V.21 Enlarged ¹³C NMR spectra in CDCl₃ of H40-(PCL)₁₀-(PtBuA)₆₈ (a) and H40-(PCL)₁₀-(PAA)₆₈ (b) (region corresponding to 22-35 ppm)

Table V.12 Comparison between molar masses determined by GPC in DMF before and after TFA treatment

M_n [g mol ⁻¹]	No TFA	TFA
H40-Br	12 300	13 400
H40-(PCL)₂₄	94 300	114 300

**Figure V.22 GPC traces of H40 and H40-(PCL)₂₄ without (---) and after (—) treatment by TFA**

(5) *Solution properties of the water soluble HBP-(PCL)_p-(PAA)_q*

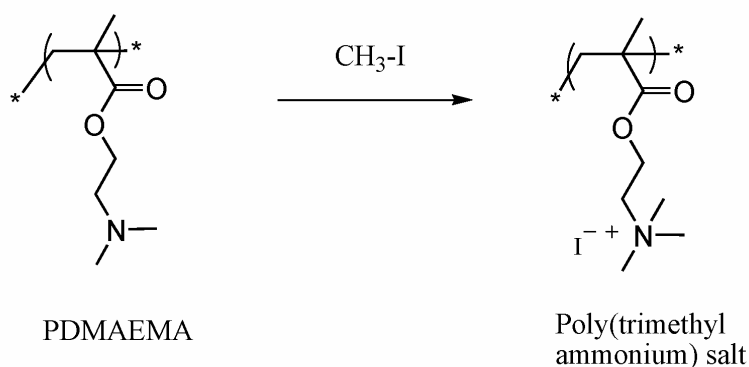
The solubility of the amphiphilic star-block copolymer H40-(PCL)_p-(PAA)_q contrasted with that of the star-block copolymer H40-(PCL)_p-(PtBuA)_q. Whatever the polyelectrolyte block length, milky dispersions were obtained in water at pH = 2.5 instead of clear solutions. However, deprotonation of the carboxylic acid with sodium hydrogenocarbonate (0.1 g mol⁻¹) (pH between 7 and 8) allowed good solubilization of the polyelectrolyte in aqueous solution (except in the case of H40-(PCL)₁₇-(PAA)₅₀ and H40-(PCL)₅₀-(PAA)_q). This observation is in agreement with the literature where it is demonstrated that the solution properties of branched PAA are influenced by the branched architecture, the molecular weights, the number of non

polar segment at the vicinity of the carboxylic acids and by the pH. A high *DB* branched PAA is soluble in CH_2Cl_2 , acetone and dioxane and is only soluble in water at $\text{pH} > 10$.^[280] As observed with branched PAA polymers,^[280, 281] high degrees of dissociation are required for water solubility in the present case.

The poor water solubility of $\text{H40-(PCL)}_{17}\text{-(PAA)}_{50}$ and of $\text{H40-(PCL)}_{50}\text{-(PAA)}_q$ is thought to be due to the high DP_n of PCL block relative to the DP_n of the PAA block. Thus, $\text{H40-(PCL)}_{17}\text{-(PAA)}_{50}$ and the series $\text{H40-(PCL)}_{50}\text{-(PAA)}_q$ will not be considered as encapsulant for volatiles in water solution in the remainder of the work.

III.3.3 Preparation of cationic star-block copolymers

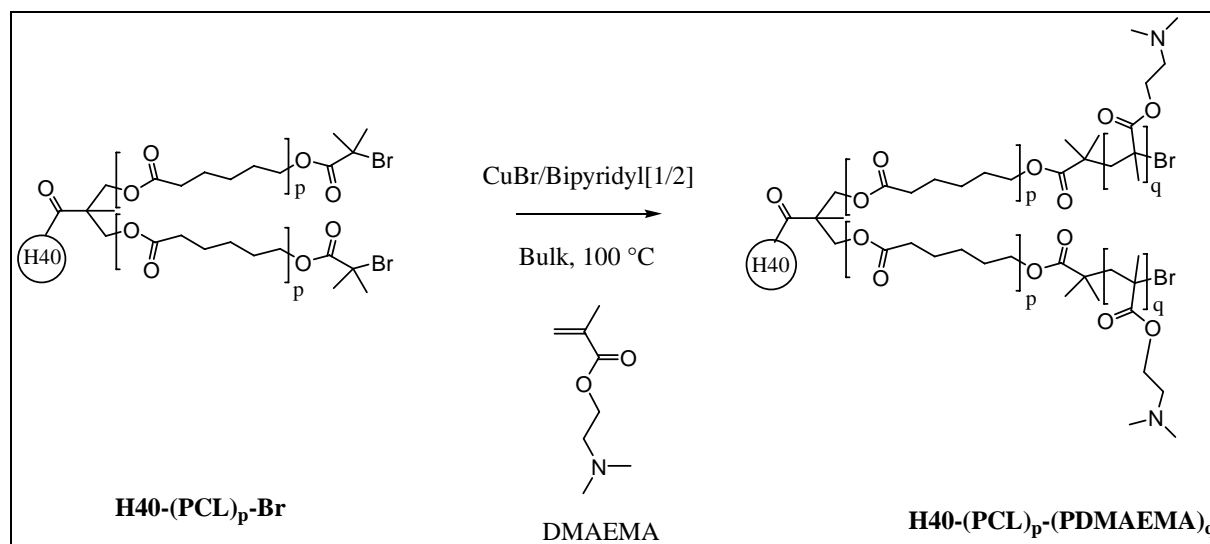
For the synthesis of a cationic polymer, 2-(*N,N*-dimethylamino)ethyl methacrylate (DMAEMA) was considered for ATRP. The methylation of the amine functions leads to a polymer containing quaternary ammonium (Scheme V.8).^[282, 283]



Scheme V.8 Strategy for obtaining a cationic polymer

Following the literature, the ATRP of DMAEMA was carried out in the bulk at 25 °C with CuBr and HMTETA as the ligand.^[212] Under such conditions, gelation was observed after 2 h 20 and the reproducibility was poor. For these reasons, the conditions of the ATRP of *t*BuA were transposed to DMAEMA and the reaction with CuBr and bipyridyl was carried

out in the bulk at 100 °C (Scheme V.9). After 21 h, 50 % conversion was reached as determined with ^1H NMR. However, the reaction was not reproducible.



Scheme V.9 Procedure of the ATRP of DMAEMA with H40-(PCL)₁₇-Br as macroinitiator

N-Propyl-2-pyridylmethanimine^[231], tris-2-dimethyl aminoethyl amine (Me₆TREN)^[211, 284] and HMTETA^[285, 286] could also have been used for the ATRP of DMAEMA since it has been shown that rates of polymerization are faster with HMTETA and Me₆TREN than with bipyridyl for a monofunctional initiator. This has not so far been attempted with the multifunctional initiator HBP-(PCL)_p-Br. However it should be kept in mind that Me₆TREN induces fast reactions and it has been shown with star macroinitiators that too fast a reaction induces bimodal GPC traces.^[216] Finally the use of other ligands for the preparation of H40-(PCL)_p-(PDMAEMA)_q might be considered based on the preliminary results obtained here.

III.3.4 Preparation of non-ionic star-block copolymers

The chemical structures of the monomers used for the preparation of non-ionic water soluble capsules are given in Figure V.23 with DEGMA (diethylene glycol methacrylate) and PEGMA (poly(ethylene glycol) methyl ether methacrylate).

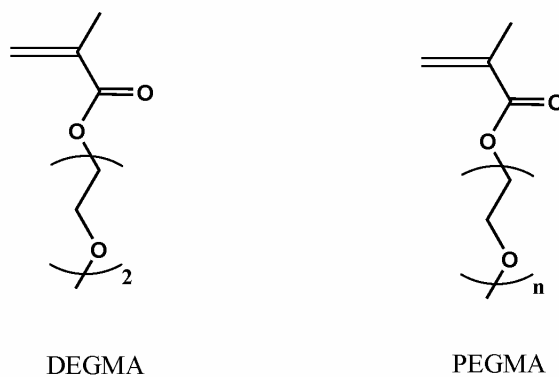
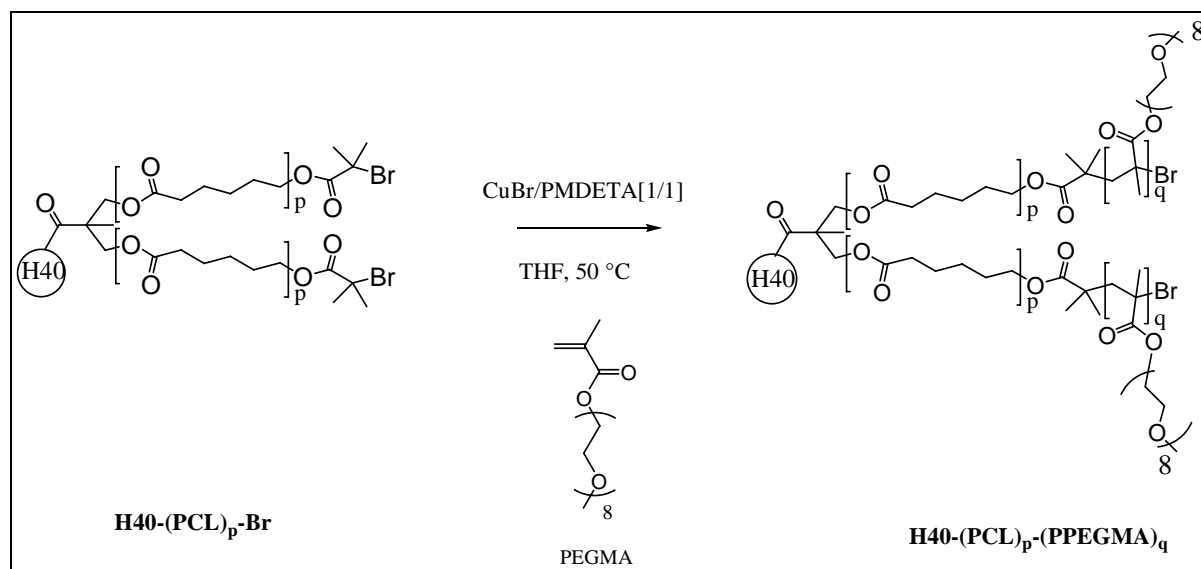


Figure V.23 Chemical structure of non-ionic monomers

ATRP of DEGMA, with CuBr and PMDETA as the catalyst and ligand respectively, was investigated in THF at 50 °C and with $[M]/[S]$ of 30/70 as determined for the ATRP of *t*BuMA. Similar problems were encountered i.e. star-star coupling and gelation. ATRP of PEGMA ($M_n = 450 \text{ g mol}^{-1}$) has been investigated with CuBr and PMDETA in THF with $[M]/[S]$ of 50/50 (Scheme V.10). Because of the low conversion obtained for the ATRP of PEGMA with $[M]/[S]$ of 30/70, a molar ratio of 50/50 has been used. Under these conditions there was no gelation, but the conversion remained relatively low, presumably due to the size of the monomer.



Scheme V.10 Procedure of the ATRP of PEGMA with $\text{H40-(PCL)}_{17}\text{-Br}$ macroinitiator^[48]

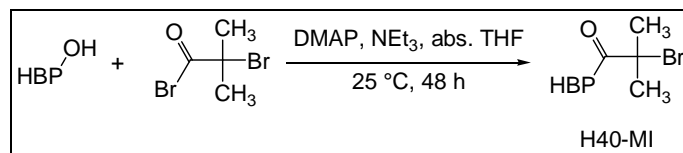
Finally, the conditions found for the ATRP of *t*BuA were transposed to the ATRP of PEGMA. Thus the reaction was carried out in the presence of CuBr and bipyridyl in toluene at $75\text{ }^\circ\text{C}$ for 4 h 45 and with $[M]/[S] = 60/40$. The reaction gave a $\text{H40-(PCL)}_{17}\text{-(PPEGMA)}_6$ with only 6 % conversion and it was not possible under these conditions to significantly increase the conversion by varying the time or the monomer concentration. According to the literature,^[231] a possible solution might be to use N-propyl-2-pyridylmethanimine as the ligand instead of bipyridyl. This has been investigated by G. Kreutzer et al. and is briefly described in section III.4.^[48]

III.4. Preparation of amphiphilic star-block copolymer with a glassy core and a neutral outer shell: $\text{H40-(PBMA)}_p\text{-(PPEGMA)}_q$

After functionalization with 2-bromoisobutyryl bromide, HBP Boltorn® H40 was used as a macroinitiator for consecutive ATRP of n-butyl methacrylate (BMA) and poly-(ethylene glycol) methyl ether methacrylate (PEGMA) to give $\text{H40-(PBMA)}_p\text{-(PPEGMA)}_q$. H40-(PPEGMA)_{50} was also prepared according to the same procedure, resulting in a star-

block copolymer without the internal hydrophobic layer. Procedures are given in Appendix 4 and in the literature.^[48]

The synthesis of the star-block copolymer began with the modification of the hyperbranched polyester Boltorn® H40 with 2-bromoisobutyryl bromide (Scheme V.11). ¹H-NMR was used to demonstrate the complete conversion of the hydroxyl groups (disappearance of the $-\text{CH}_2\text{OH}$ multiplet, which is found at 3.35-3.60 ppm for the H40 precursor, and appearance of a new signal due to the $-\text{CH}_3$ groups of the isobutyryl moiety at 1.89 ppm) (Figure V.24). GPC analysis of the H40 and H40-MI revealed an increase in M_n from 3 600 g mol⁻¹ to 12 300 g mol⁻¹, which was consistent with complete substitution of all hydroxyl functions of H40. The macroinitiator H40-Br can act as an initiator for ATRP.



Scheme V.11 Synthesis of the H40-Br macroinitiator^[48]

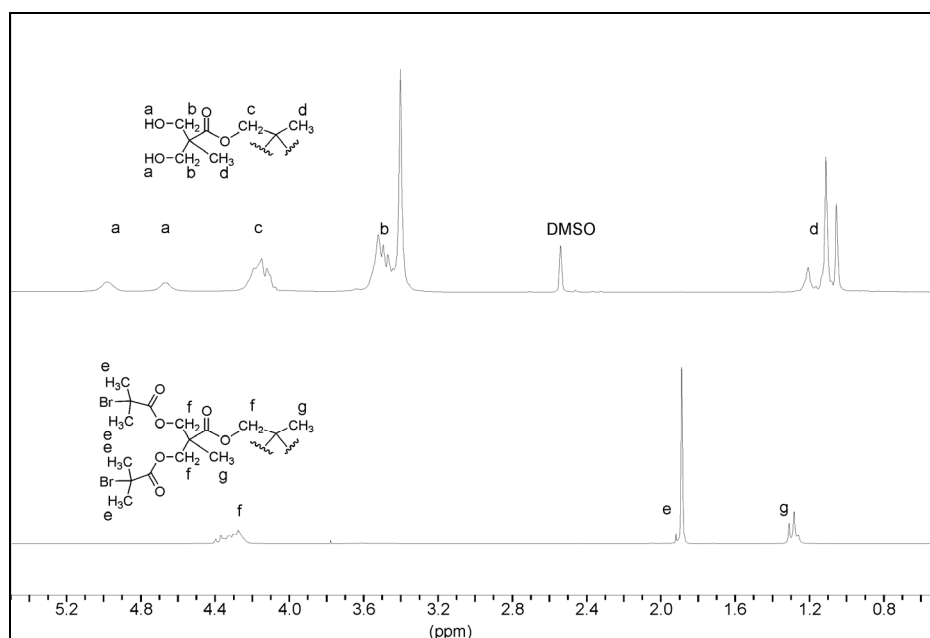
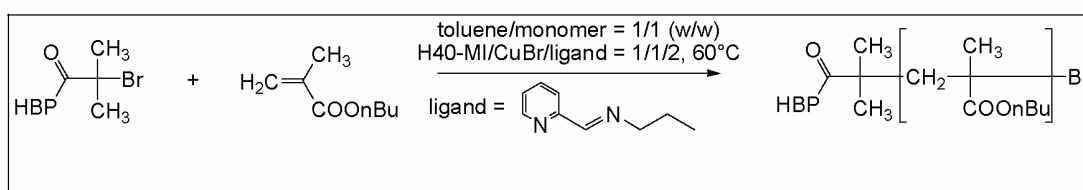


Figure V.24 ¹H NMR spectrum of the precursor (H40) in DMSO and of the macroinitiator H40-Br in CDCl_3 ^[48]

Well-defined poly(*n*-butyl methacrylate) star polymers (H40-(PBMA)_p) were prepared in toluene using CuBr/*N*-propyl-2-pyridylmethanimine as the catalyst and H40-Br as the macroinitiator (Scheme V.12). GPC chromatograms of samples taken during the course of the polymerization were monomodal and did not indicate star-star coupling. Monomer conversion was monitored with ¹H-NMR spectroscopy. Kreutzer et al. confirmed the controlled nature of the ATRP process by plotting $\ln([M]_0/[M])$ versus time and M_n and M_w/M_n versus monomer conversion. Table V.13 provides a summary of the reaction conditions, monomer conversion and GPC results for a H40-(PBMA)₃₇ multi-arm star polymer.



Scheme V.12 ATRP of BMA initiated by H40-Br macroinitiator to give H40-(PBMA)_p^[48]

Table V.13 ATRP conditions and analytical results for the polymerization of BMA initiated by H40-Br^[48]

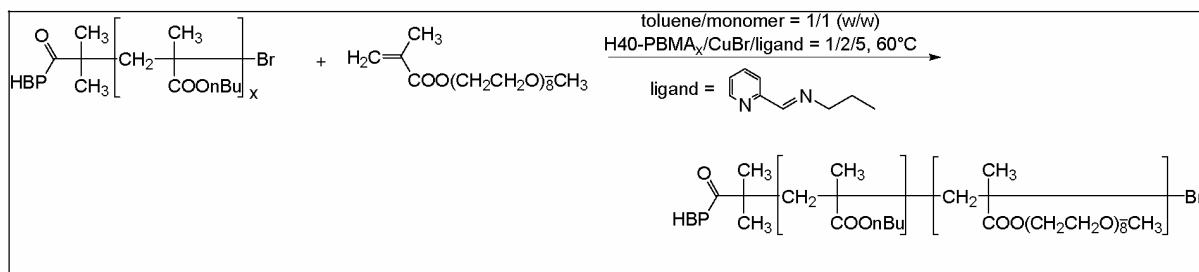
Polymer	Molar ratio of H40-Br/CuBr/ligand/BMA	BMA conversion ^a [%]	M_n^b [g mol ⁻¹]	M_w/M_n^b	DP_n^b
H40-(PBMA) ₃₇	1/1/2/100	11.9	182 000	1.69	37

^a Determined with ¹H-NMR spectroscopy.

^b Number-average molecular weight (M_n), polydispersity (M_w/M_n), and number-average degree of polymerization per arm (DP_n).

Kreutzer et al. prepared amphiphilic multi-arm star-block copolymers via ATRP of PEGMA using H40-(PBMA)₃₇ as the macroinitiator (Scheme V.13). The reaction was carried out in toluene at 60 °C for 5 h using CuBr/*N*-propyl-2-pyridylmethanimine as the catalyst. Star-block copolymers with PBMA and different PPEGMA block lengths were obtained. Polymerization conditions for each of these experiments together with GPC data of the

resulting polymers are given in Table V.14. H40-PPEGMA₅₀ is a reference sample that was prepared by polymerization of PEGMA using H40-Br as the macroinitiator.



Scheme V.13 ATRP of PEGMA initiated by H40-(PBMA)_p-Br macroinitiator to give H40-(PBMA)_p-(PPEGMA)_q^[48]

Table V.14 ATRP of PEGMA with H40-(PBMA)₃₇-Br^[48]

Polymer	Molar ratio of H40-PBMA/ CuBr/ligand/PEGMA	PEGMA conversion ^a [%]	M_n^b [g mol ⁻¹]	M_w/M_n^b	DP_n^b
H40-(PBMA) ₃₇ -(PPEGMA) ₃₉	1/2/4/100	18.9	782 000	2.04	39
H40-(PBMA) ₃₇ -(PPEGMA) ₁₉	1/2/4/500	6.5	476 000	1.81	19
H40-(PPEGMA) ₅₀	1/2/4/250	-	780 000	1.82	50

^a Determined with ¹H-NMR spectroscopy.

^b Number-average molecular weight (M_n), polydispersity (M_w/M_n), and number-average degree of polymerization per arm (DP_n).

¹H-NMR analysis was used to demonstrate that ATRP was well controlled. The absence of star-star coupling during the ATRP of BMA and PEGMA was verified by GPC. To prevent crosslinking between the PPEGMA blocks^[287] of H40-(PBMA)_p-(PPEGMA)_q, 0.1 wt % 2,6-di-tert-butyl-4-methylphenol (BHT) and 4-methoxyphenol (MEHQ) was added directly after workup. GPC analysis of star-block copolymers stored in bulk at 2 °C did not show any changes in molecular weight and polydispersity, even after 4 months.

IV. Conclusion

The particular architecture of HBPs leads to difficulties with characterization. To be consistent here, the HBPs were first investigated by GPC and NMR and these techniques were used subsequently to validate each stage of the synthesis. Given the results from GPC, NMR and titration, 36 hydroxyl groups per H40 molecule and 26 per H30 molecule were assumed throughout.

A series of star-block copolymers containing a hydrophobic PCL block and a hydrophilic PAA block were prepared from the HBP by the combination of ROP and ATRP to give pH-responsive copolymers. These block copolymers were characterized at each stage of the synthesis using ^1H and ^{13}C NMR in CDCl_3 or DMSO, GPC in DMF and IR spectroscopy. Good control of the ROP and ATRP was demonstrated for the *t*BuA monomer. In order to develop cationic and non-ionic star-block copolymer to extend their use in various perfume compositions, other monomers were considered for ATRP such as DMAEMA, DEGMA and PEGMA. The expected star-block copolymers were not obtained with DMAEMA and DEGMA under conditions similar to those used for *t*BuA. However optimum conditions were obtained with PEGMA by modifying the ligand.

GPC measurements on the $\text{HBP}-(\text{PCL})_p-(\text{PAA})_q$ star-block copolymers in water, using a Shodex column did not provide valid molar masses owing to the charges present on the star-block copolymers. To avoid interactions with the column an alternative might be considered e.g. use of an improved column. In this work, the carboxylic acid of the outer shell of the star-block copolymers $\text{HBP}-(\text{PCL})_p-(\text{PAA})_q$ has been deprotonated improving the solubility in aqueous media and the molar masses were determined by ^1H NMR.

Chapter VI. Physical properties of the star-block copolymers in the bulk and in solution

In order to determine the structure-property relationships of the star-block copolymers and to gain a better understanding of their interactions with fragrance molecules inside the nanocapsules, the thermal properties and morphology have been investigated in the bulk and in solution.

I. Thermal properties and morphologies of the polymers in the bulk

The thermal properties of the H40-(PCL)_p, H40-(PCL)_p-(P*t*BuA)_q and the analogous water soluble H40-(PCL)_p-(PAA)_q were investigated by DSC. Glass transition, T_g , and melting temperatures, T_m , were measured and compared with those of a linear (PCL)₃₀. The results are summarized in Table VI.1. Values obtained for H40-(PBMA)₃₇-(PPEGMA)₃₉ and H40-(PPEGMA)₅₀ are also given.^[48]

The T_g of the H40-(PCL)_p star polymers decreased strongly with respect to that of H40, and continued to decrease as DP_p increased, so that for large DP_p , T_g was generally comparable with that of the linear (PCL)₃₀. This suggested a positive contribution to T_g from hydrogen bonding at the chain ends.^[127] Melting behavior was also observed for H40-(PCL)_p, with T_m showing a marked increase as DP_p increased and increasingly sharp melting peaks (Figure VI.1). Indeed, T_m of H40-(PCL)₅₀ exceeded that of (PCL)₃₀, as expected on the basis of previous observations.^[288] These have indicated a strong correlation between the equilibrium melting point of H40-(PCL)_p, obtained from extrapolating experimental data, and that of linear (PCL)_p analogues, both of which increase with DP_p , albeit with slightly higher values being deduced for H40-(PCL)_p for a given DP_p . This may be explained in terms of the reduced conformational entropy of the star polymers.^[288] On the other hand, the increased constraints on the chain conformations lead to reduced degrees of crystallinity, particularly for the shortest block lengths. Under the crystallization conditions corresponding to the present DSC experiments the star polymers showed spherulitic textures similar to those observed in linear PCL (Figure VI.2 (a)), which implies the presence of chain folded lamellae, at least for the largest DP_p . This observation has been confirmed by TEM (Figure VI.3 (a and b)).

Table VI.1 Thermal properties for different amphiphilic star-block copolymers H40-(PCL)_p-(PAA)_q, the analogous non water soluble H40-(PCL)_p-(PtBuA)_q and star H40-(PCL)_p

Name	M_n [g mol ⁻¹]	T_{g1} [°C]	T_{g2} [°C]	T_m [°C]	ΔH_m [J/g]
H40	4 100 ^a	29.9	-	-	-
(PCL) ₃₀	3 300 ^a	-61.3	-	51.7	82.3
H40-(PCL) ₁₀	65 380 ^a	-57.6	-	41.1	62.3
H40-(PCL) ₁₇	89 890 ^a	-59.2	-	49.1	71.2
H40-(PCL) ₄₀	158 900 ^a	-61.8	-	52.8	62.1
H40-(PCL) ₅₀	184 640 ^a	-62.2	-	54.1	65.7
H30-(PCL) ₁₂ -(PtBuA) ₆₀	204 000 ^a	-76.2	25.2	-	-
H40-(PtBuA) ₃₆	199 490 ^a	-	45.1	-	-
H40-(PCL) ₁₀ -(PtBuA) ₆₈	488 520 ^a	-70.4	25.9	-	-
H40-(PCL) ₁₀ -(PtBuA) ₇₀	459 740 ^a	-69.6	27.4	-	-
H40-(PCL) ₁₀ -(PtBuA) ₁₁₅	549 000 ^a	-69.8	29.8	-	-
H40-(PCL) ₁₇ -(PtBuA) ₁₈	205 000 ^a	-57.7	21.1	-	-
H40-(PCL) ₁₇ -(PtBuA) ₅₀	274 930 ^a	-60.6	27.7	-	-
H40-(PCL) ₂₄ -(PtBuA) ₈₂	357 700 ^a	-58.3	25.2	-	-
H40-(PCL) ₄₀ -(PtBuA) ₁₀₀	452 300 ^a	-64.3	32.4	-	-
H40-(PCL) ₅₀ -(PtBuA) ₄₄	396 600 ^a	-60.5	-	48.0	21.9
H40-(PCL) ₅₀ -(PtBuA) ₅₄	376 280 ^a	-68.0	-	42.7	20.1
H40-(PCL) ₅₀ -(PtBuA) ₅₆	536 860 ^a	-64.0	-	45.9	21.4
H40-(PCL) ₅₀ -(PtBuA) ₆₄	732 761 ^a	-63.8	-	45.2	21.0
H30-(PCL) ₁₂ -(PAA) ₆₀	151 460 ^b	-48.7	98.2	-	-
H40-(PAA) ₃₆	100 400 ^b	-	99.3	-	-
H40-(PCL) ₁₀ -(PAA) ₇₀	226 800 ^b	-65.4	116	-	-
H40-(PCL) ₁₀ -(PAA) ₁₁₅	340 200 ^b	-69.7	117.6	-	-
H40-(PCL) ₂₄ -(PAA) ₈₂	307 400 ^b	-71.2	81.9	25.1	7.42
H40-(PCL) ₄₀ -(PAA) ₁₀₀	425 500 ^b	-67.3	116.9	30.0	10.3
H40-(PBMA) ₃₇ -(PPEGMA) ₃₉	782 000 ^a	-64.1	12.2	-	-
H40-(PPEGMA) ₅₀	780 000 ^a	-64.9	-	-	-

^a GPC in DMF^b ¹H NMR in DMSO

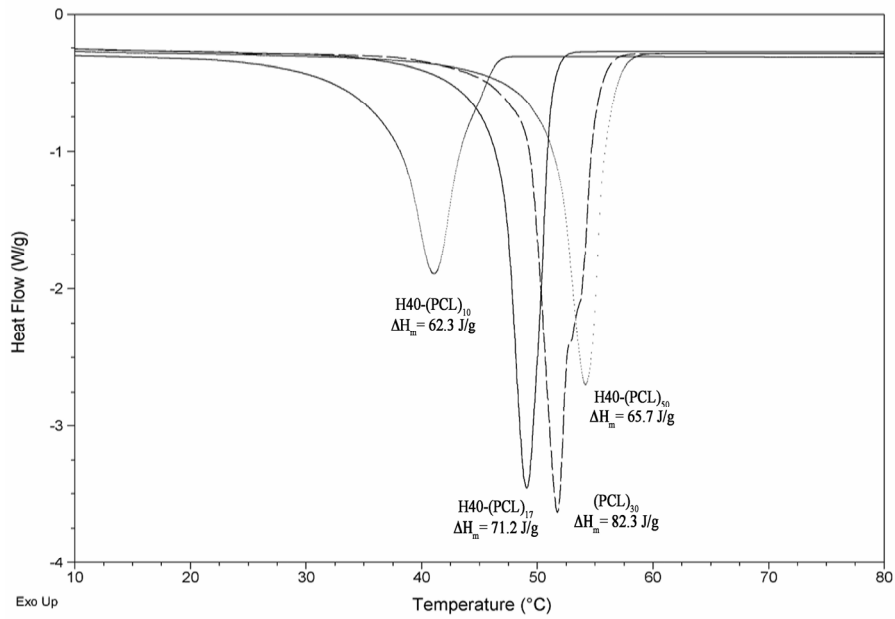


Figure VI.1 Melting behavior of H40-(PCL)_p for different p compared with that of (PCL)₃₀

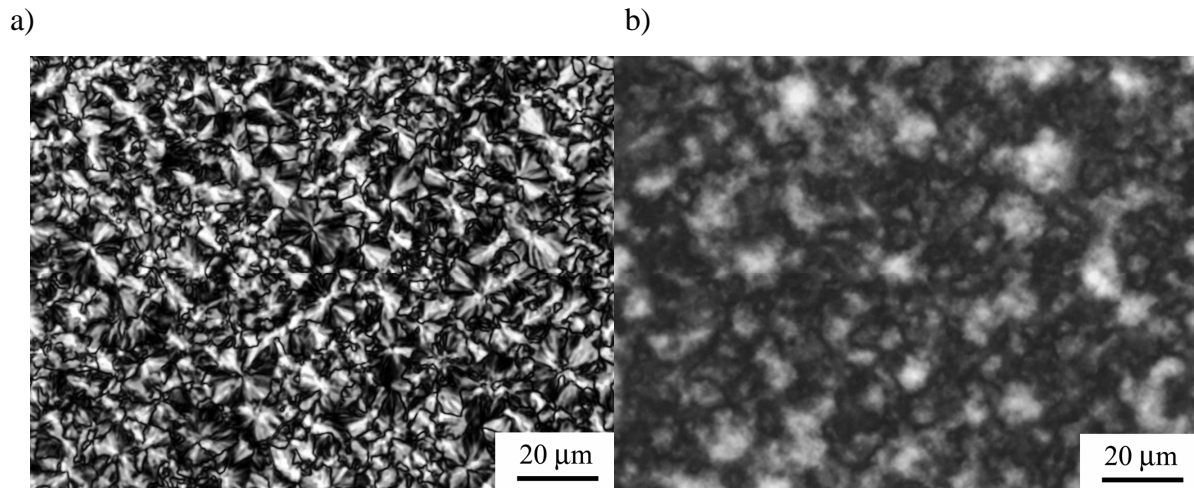


Figure VI.2 Optical micrographs taken under crossed-polarizers of films of (a) H40-(PCL)₅₀ and (b) H40-(PCL)₅₀-(PtBuA)₆₄ cooled from the melt at 10 °C/min.

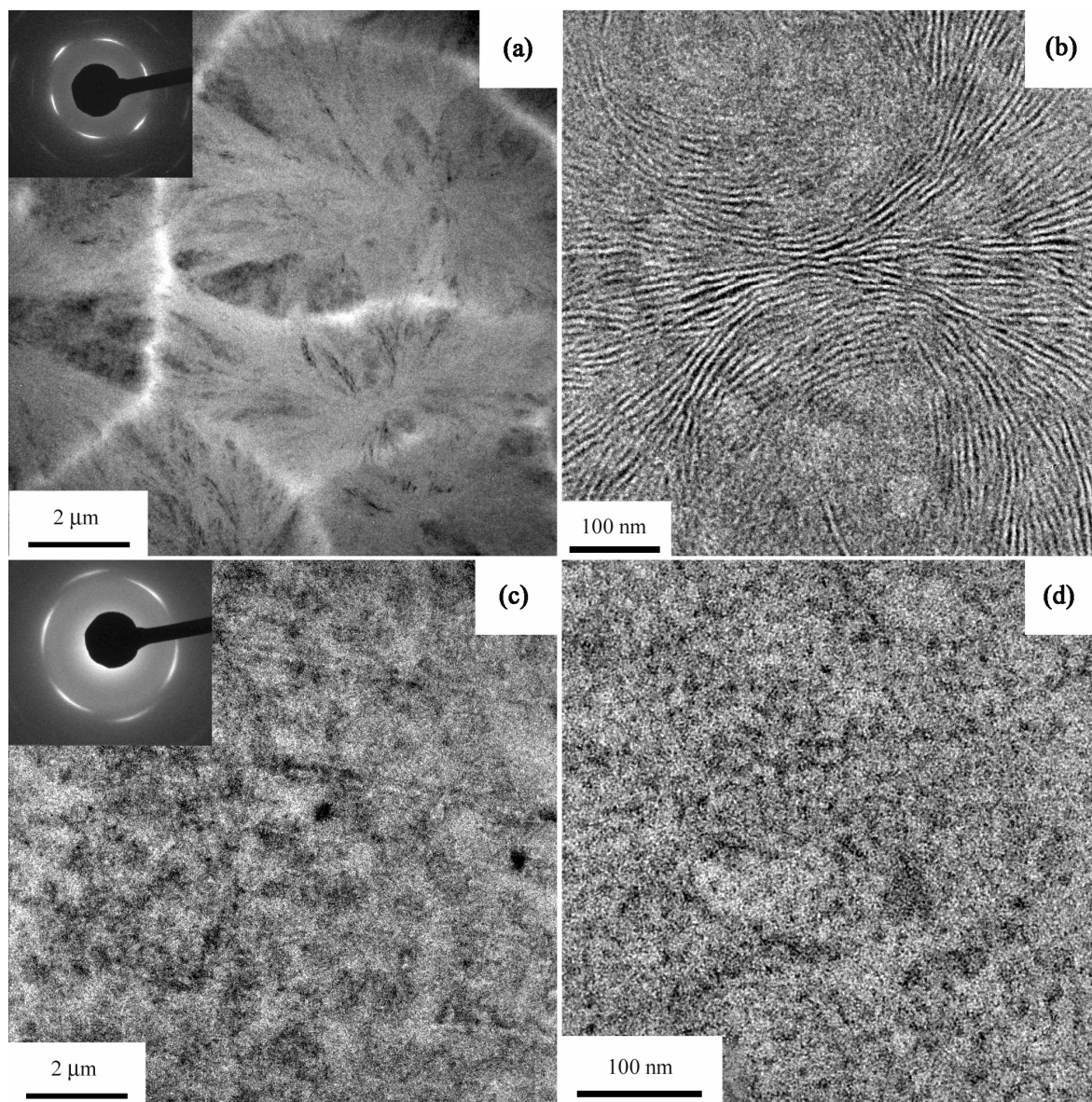


Figure VI.3 TEM micrographs of thin films of H40-(PCL)₅₀ ((a) and (b)) and H40-(PCL)₅₀-(PtBuA)₅₄ ((c) and (d))

The thermal properties of the star-block copolymers were found to depend on the lengths of both blocks. A phase-separated morphology was clearly present in at least some of the copolymers as indicated by the observation of two T_g s. The transitions at about -60 °C were assumed to be characteristic of the PCL block and the transitions at between 11 and 30 °C, were attributed to the PtBuA. In the case of H40-(PCL)₅₀-(PtBuA)_q, the apparent absence of a T_g associated with the PtBuA blocks was thought to be due to the relatively high

proportion of PCL and the limited sensitivity of the apparatus. T_m and ΔH_m were only measurable for the PCL blocks in H40-(PCL)₅₀-(PtBuA)_q, for which T_m was somewhat lower than in H40-(PCL)₅₀, particularly for the longer PtBuA blocks. Thus, although these polymers were still able to form quasi spherulitic textures, the presence of the PtBuA blocks placed significant kinetic or thermodynamic restrictions on crystallization. This is well reflected by the optical (Figure VI.2 (b)) and TEM micrographs (Figure VI.3 (c) and (d)).

Two T_g s were again observed after the hydrolysis of the *tert*-butyl groups, as well as melting peak in the case of H40-(PCL)₄₀-(PAA)₁₀₀. The higher T_g at about 117 °C was consistent with previous observations of the T_g in PAA rich domains of a linear block PAA-graft-PE copolymer.^[289] $T_m = 30$ °C, and $\Delta H_m = 10.3$ J/g was measured for the PCL layers in H40-(PCL)₄₀-(PAA)₁₀₀. Thus, the amphiphilic H40-(PCL)_p-(PAA)_q star-block copolymers again showed phase-separated morphologies, as also demonstrated for H40-(PBMA)₃₇-(PPEGMA)₃₉.^[48] Moreover, the disappearance of the T_g corresponding to PtBuA ($T_g \approx 30$ °C) provided a further indication of efficient conversion to acrylic acid functionality.

II. Characterization in solution

Dynamic light scattering (DLS) has been used to determine the size of the star-block copolymers in water. The solutions were diluted to 0.34 mg mL⁻¹. The results presented correspond to an average of three consecutive measurements at room temperature. Figure VI.4 shows the percentage by volume (left) and by number (right) of the particle sizes obtained for H30-(PCL)₁₂-(PAA)₆₀.

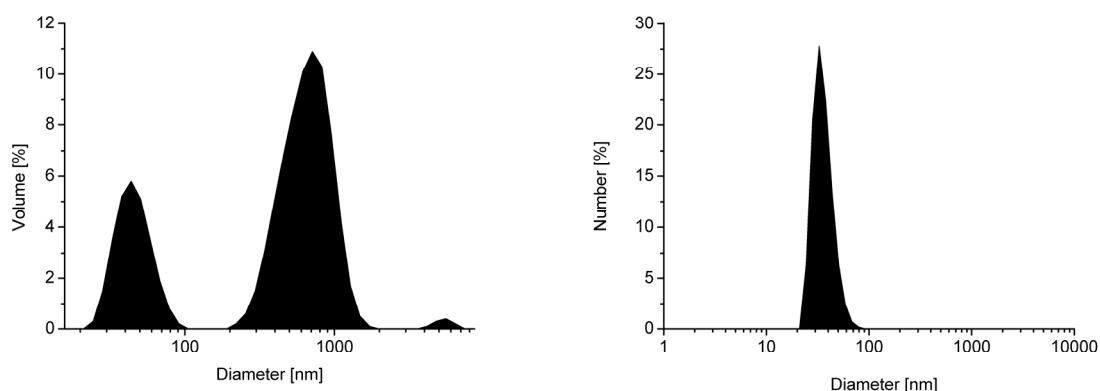


Figure VI.4 Hydrodynamic diameter distribution by volume (left) and by number (right) for H30-(PCL)₁₂-(PAA)₆₀ in aqueous solution

The volume distribution for H30-(PCL)₁₂-(PAA)₆₀ shows that the sample was composed of three populations of particles. Two populations correspond to relatively large particles (diameters around 700 and 5000 nm). However the sample was essentially composed of small particles (diameter around 40 nm) as reflected by the number distribution (more than 99 % of the particles have a diameter of around 40 nm). The same trend was observed for H40-(PAA)₃₆ and H40-(PCL)₂₄-(PAA)₈₂ with three different populations evident in the volume distribution. In the case of H40-(PCL)₄₀-(PAA)₁₀₀ only two populations were observed.

The data for the star-block copolymers are summarized in Table VI.2, along with the number average molar masses. The diameters of the star-block copolymers HBP-(PCL)_p-(PAA)_q and H40-(PBMA)_p-(PPEGMA)_q were very different relative to their molar masses. When PPEGMA was used as the hydrophilic layer, the diameter of the particles was reduced, although the molar masses were high. These differences may suggest aggregation of the molecules in the case of HBP-(PCL)_p-(PAA)_q. Diameters of 75 to 100 nm have been observed by AFM images (Figure VI.5) for H40-(PCL)₄₀-(PtBuA)₁₀₀ cast from dilute solution. Phase images (Figure VI.5) indicated differences in rigidity consistent with a phase separated core-shell structure. This was confirmed by the AFM image in Figure VI.6 in which individual arms of the star-block copolymer are visible.

Table VI.2 Diameter of the star-block copolymer in aqueous solution from number distribution DLS measurement

Copolymer	M_n (g mol ⁻¹)	Diameter (nm) (number average)
H30-(PCL) ₁₂ -(PAA) ₆₀	151 460 ^a	42.8
H40-(PCL) ₂₄ -(PAA) ₈₂	307 400 ^a	59.2
H40-(PCL) ₄₀ -(PAA) ₁₀₀	425 540 ^a	128.7
H40-(PPEGMA) ₅₀	780 000 ^b	24.2
H40-(PBMA) ₃₇ -(PPEGMA) ₃₉	782 000 ^b	26.6

^a M_n based on NMR conversion

^b GPC

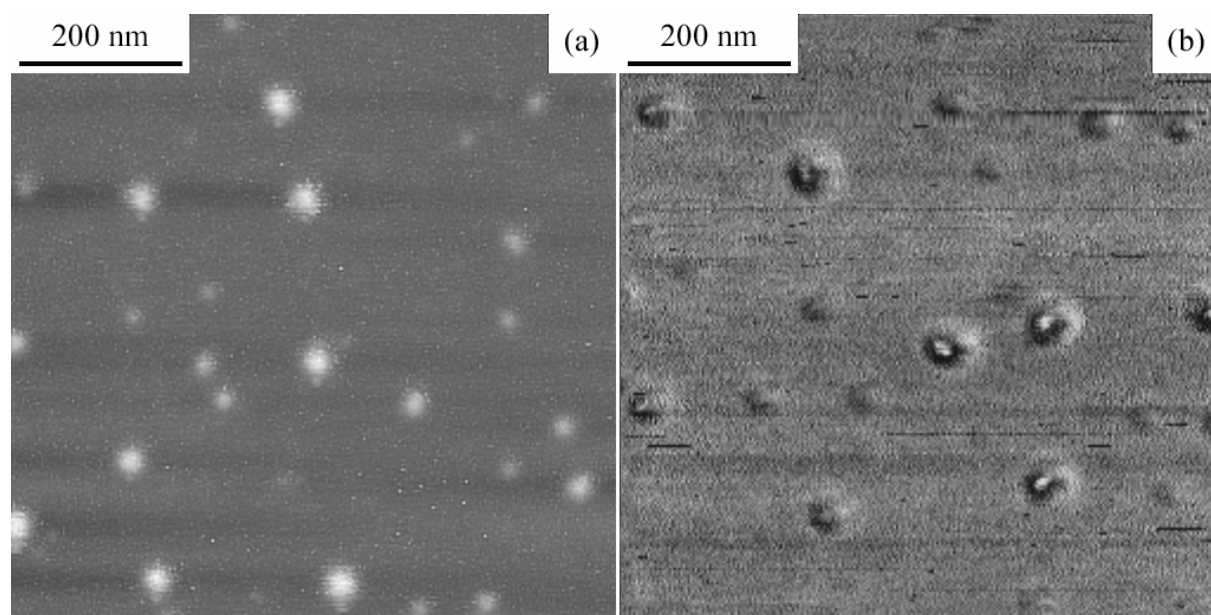


Figure VI.5 AFM intermittent contact mode images from H40-(PCL)₄₀-(PtBuA)₁₀₀ cast from dilute solution onto mica: (a) height image; (b) phase image

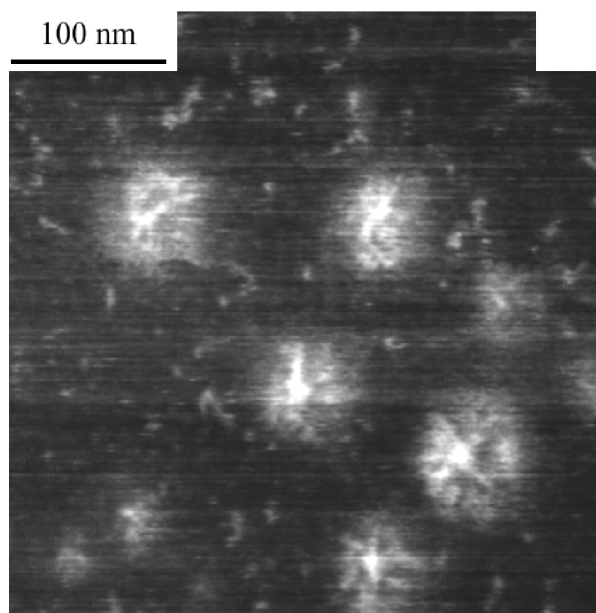


Figure VI.6 AFM intermittent contact mode height image from H40-(PCL)₄₀-(PtBuA)₁₀₀ cast from dilute solution onto mica

III. Conclusion

A phase separated structure has been observed in the amphiphilic star-block copolymers prepared as described in Chapter V.III consistent with the core-shell architecture. In the case of H40-(PCL)₅₀-(PAA)_q, the observation of a melting point, associated with the PCL block, and the absence of the T_{g2} of the PtBuA block, which was attributed to high proportion of PCL relative to the PtBuA, also reflected the poor water solubility of this series (Chapter V.III.3.2(5)).

Particle diameters of up to 100 nm were measured in dilute aqueous solution by DLS, and similar particle sizes were seen in AFM images of H40-(PCL)₄₀-(PtBuA)₁₀₀ cast from an organic solvent. The individual arms are also visible in certain AFM images.

Chapter VII. Encapsulation of olfactory compounds in aqueous dispersions of star-block copolymer monitored by NMR spectroscopy

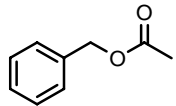
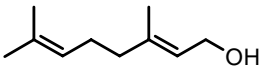
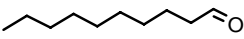
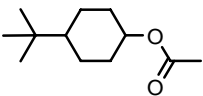
Fragrances and flavors are complex mixtures of molecules with specific physicochemical properties. They are typically volatile, hydrophobic and some of them are unstable. Their lifetime is limited due to their rapid evaporation and instability, which result in loss of freshness during storage and use. Thus, they need to be stabilized by modifying their environment. Specific delivery systems that protect volatiles during storage and control their release during and after use, allow one to maintain freshness over relatively long periods.^[59]

To demonstrate their capacity to entrap small hydrophobic molecules in aqueous media, selected multi-arm star-block copolymers synthesized in Chapter V.III were exposed to an excess of fragrance compound. The subsequent behavior has been studied by ^1H NMR spectroscopy in D_2O . In this chapter, after presenting the fragrance molecules and the selected water soluble star-block copolymers, the results of NMR diffusion and relaxometry measurements, carried out at Firmenich SA, are described. The encapsulation of the fragrance molecules in aqueous dispersions of the star-block copolymers and the parameters that influence the fragrance molecule loadings in the star-block copolymer are then discussed.

I. Characteristics of polymers and fragrance compounds

The four olfactory compounds investigated provide a range of polarity, chemical structure and function, vapor pressure, and solubility parameters. They were also chosen to be representative of compounds frequently encountered in practical applications. The hydrophobicity of an olfactory compound is characterized by $\log P$ (the octanol-water partition coefficient).^[290-292] This is a frequently used parameter in organic synthetic chemistry. However, the practical applications of $\log P$ are much broader. $\log P$ is commonly used in cosmetics to classify fragrances as a function of their water affinity and in drug design, where it is related to drug absorption, bioavailability, metabolism, and toxicity.^[293] Table VII.1 summarize the characteristics of the four olfactory compounds: benzyl acetate, (*E*)-3,7-dimethyl-2,6-octadienol (geraniol), decanal and 4-*tert*-butyl-1-cyclohexyl acetate (Vertenex®). $\log P$ were calculated by J.-Y. de Saint Laumer (Firmenich SA) using the EPIwin v 3.10 program (US Environmental Protection Agency, 2000).

Table VII.1 Chemical structure and properties of four olfactory compounds

	Chemical structure	Molar mass [g mol ⁻¹]	LogP ^a	Vapor pressure ^a [Pa]	Volatility ^a [μg L ⁻¹]
Benzyl acetate		150.2	1.96	24.9	500
Geraniol		154.2	3.47	2.1	93
Decanal		156.3	3.76	31.3	528
Vertenex®		198.2	4.42	9.1	189.3

^a Values calculated using the EPIwin v 3.10 program (US Environmental Protection Agency, 2000)150

The ^1H NMR measurements for determining the fragrance loadings of the copolymers were carried out using water soluble star-block copolymers that differ in the length of their hydrophobic blocks ($\text{H40-(PCL)}_{10}\text{-(PAA)}_{115}$, $\text{H40-(PCL)}_{24}\text{-(PAA)}_{82}$ and $\text{H40-(PCL)}_{40}\text{-(PAA)}_{100}$), in the functionality of the HBP core (H30 (26 arms) or H40 (36 arms)) and in the chemical nature of the blocks ($\text{H40-(PCL)}_p\text{-(PAA)}_q$ and $\text{H40-(PBMA)}_p\text{-(PPEGMA)}_q$) as shown in Figure VII.1.

It is expected that the presence of the hydrophobic layer should facilitate the incorporation of hydrophobic guest molecules and therefore have an influence on the concentration of volatiles present in the capsule. Hence, encapsulation was also investigated with H40-(PAA)_{36} and H40-(PPEGMA)_{50} , which did not include a hydrophobic layer.

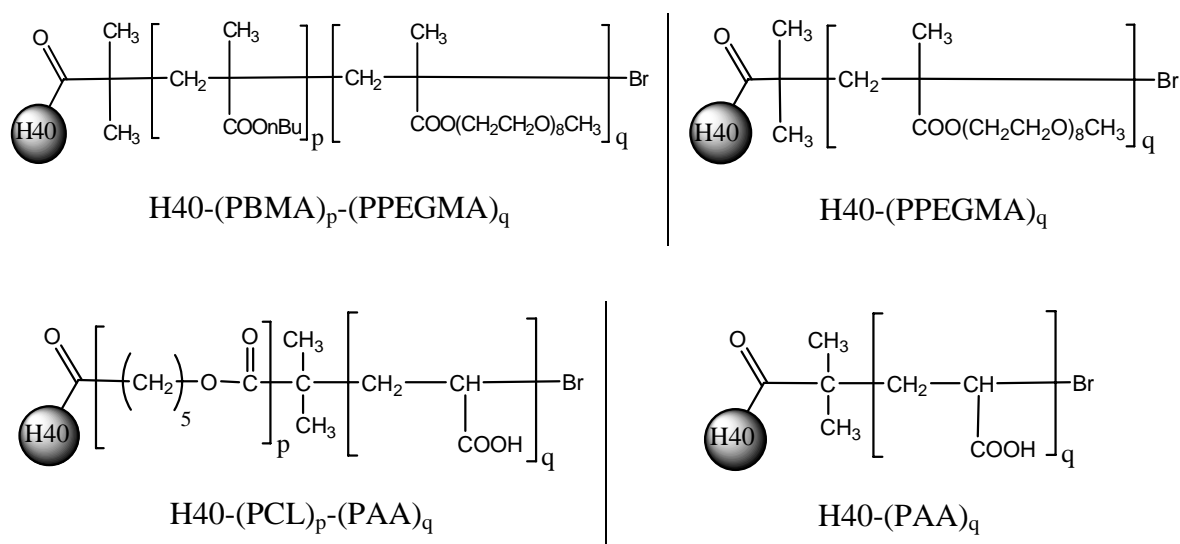


Figure VII.1 Structure of the two types of polymers used for the encapsulation of fragrance molecules, with and without the hydrophobic internal layer

II. NMR diffusion and relaxation studies

The diffusion and relaxation studies described here only involved the H40-(PBMA)₃₇-(PPEGMA)₃₉ amphiphilic star-block copolymer and were carried out by W. Fieber and H. Sommer (Firmenich SA).^[47, 294] However, they are expected to provide general insight into the encapsulation behavior of such systems.

The mobility of a molecule in solution is defined by its diffusion coefficient, which is inversely proportional to the size of the molecule and hence to its molecular mass. Due to the large difference in mass between fragrance molecules and the star-block copolymers, the diffusion coefficient of a fragrance molecule in pure water is different from that of a molecule entrapped in a copolymer. This technique therefore gives information on the partition of the fragrance compounds in the solution. Relaxation time measurements may also be carried out to investigate the dynamics of the star-block copolymer, the localization of the guest and the dynamics of the polymer/fragrance molecule system. The relaxation time T_1 corresponds to the reorientation of large molecules. T_2 (restricted motion) provides information on the internal motion of the individual blocks of the star-block copolymer.

The mobility of the hydrophilic shell in water has been studied by Fieber et al. by following the evolution of the relaxation times of the methyl groups of the hydrophilic block as a function of their position in the polymer chain in a 1 wt% solution of H40-(PBMA)_p-(PPEGMA)_q in D₂O. A significant decrease in the relaxation times from the external end group of the PPEGMA chain to the polymer backbone is observed, as shown in Figure VII.2. Moreover, the presence of a phase separated structure in water with a dense internal core and a highly mobile hydrophilic shell has also been confirmed by such relaxation studies. PBMA block is not observed in D₂O, on the other hand, when the measurement is carried out in CDCl₃, PBMA peaks are detected.

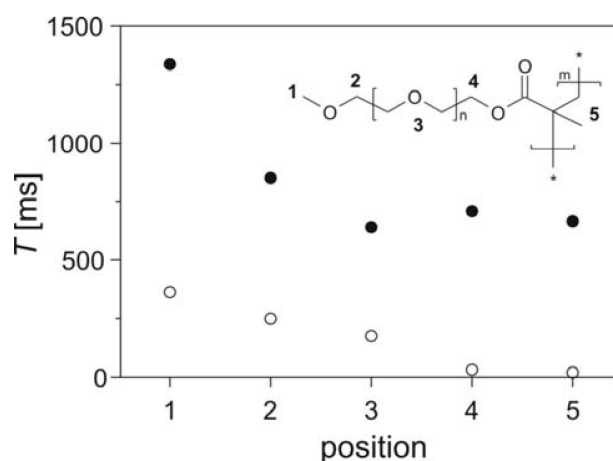


Figure VII.2 Longitudinal T_1 (full circle) and transverse T_2 (open circle) proton relaxation times as a function of position in the PEGMA unit of H40-(PBMA)_p-(PPEGMA)_q^[294]

The diffusion coefficients for the four fragrance molecules presented in Table VII.2 were determined in pure water by mixing 1 μL of fragrance with 700 μL D₂O. Further dilutions were necessary for Vertenex® and decanal. The samples containing polymer were prepared by saturating a solution of the polymer in D₂O with the fragrance molecules and then removing the excess of fragrance molecules. The polymer concentration was 10.7 mg mL⁻¹ in D₂O. Details on the procedure and the NMR apparatus are given in literature.^[294]

All the fragrance molecules showed a high diffusion coefficient in D₂O (around $6 \times 10^{-10} \text{ m}^2 \text{ s}^{-1}$) reflecting their unrestricted motion (Table VII.2). However, when the olfactory molecules were added to the polymer in aqueous solution, their diffusion rates decreased dramatically indicating a decrease in their mobility. Indeed, the diffusion coefficients of the fragrance molecules were generally close to those of the star-block copolymer (around $1 \times 10^{-12} \text{ m}^2 \text{ s}^{-1}$), which is an indication that the olfactory molecules are encapsulated in the polymer and travel at the speed of the macromolecule. This was particularly true for fragrance molecules with high $\log P$ as shown in Figure VII.3, where the evolution of the diffusion coefficients of the fragrance compounds, in the absence and the presence of star-block copolymers, is given as a function of their $\log P$. Similar measurements in the presence of H40-(PPEGMA)₅₀ (which does not contain the hydrophobic layer) indicated the diffusion coefficient values to decrease relatively little, suggesting that the fragrance molecules are localized in the internal core of the star-block copolymers. The encapsulation of the fragrance molecules in the polymer has also been demonstrated from the evolution of the relaxation times of the fragrance molecules in water. The decrease in T_1 and T_2 of the fragrances in the presence of H40-(PBMA)_p-(PPEGMA)_q compared with the values obtained in the absence of the polymer indicated a decrease in the fragrance mobility.^[294] (The $\log P$ of the fragrance molecules used by Fieber et al. were determined by high performance liquid chromatography (HPLC) and are therefore slightly different from those calculated using the EPIwin v 3.10 program).

Table VII.2 Diffusion coefficients for the fragrance compounds and H40-(PBMA)₃₇-(PPEGMA)₃₉ in D₂O at 25 °C^[294]

Fragrance molecules	LogP^a	D^{fragrance} (D₂O) [m² s⁻¹]	D^{fragrance} (with star block copolymer) [m² s⁻¹]	D^{copolymer} (with fragrance) [m² s⁻¹]
Benzyl acetate	2.04	7.33×10^{-10}	3.09×10^{-10}	1.03×10^{-11}
Geraniol	2.97	5.98×10^{-10}	1.74×10^{-10}	1.13×10^{-11}
Decanal	4.00	5.49×10^{-10}	2.03×10^{-11}	9.66×10^{-12}
Vertenex [®]	4.47	5.59×10^{-10}	2.47×10^{-11}	9.50×10^{-12}

^a values determined by HPLC

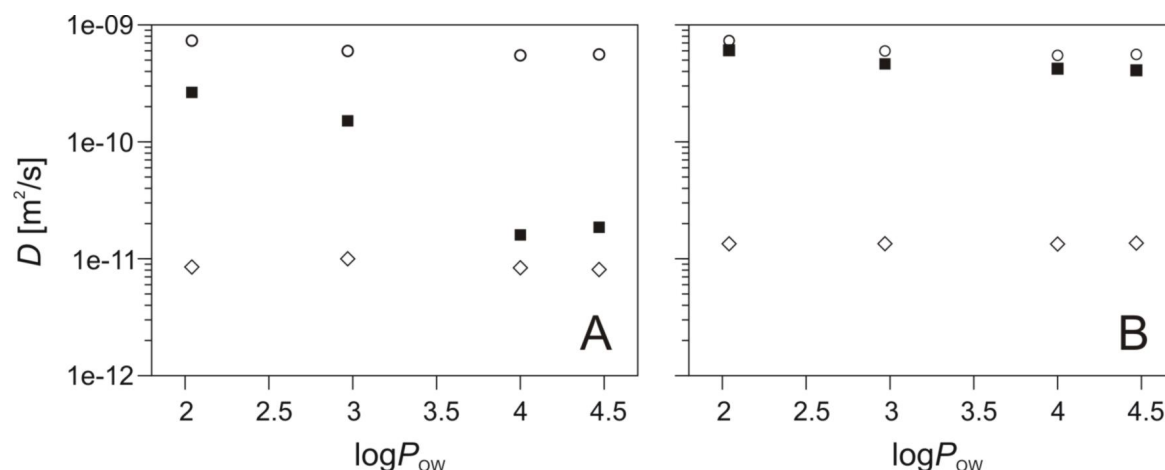


Figure VII.3 Encapsulation of different fragrance molecules in a water dispersion of H40-(PBMA)₃₇-(PPEGMA)₃₉ (A) and H40-(PPEGMA)₅₀ (B). Diffusion coefficients are given for the fragrance molecules in the free form (open circles) and encapsulated form (filled squares), and for the polymer molecules (open diamonds)^[294]

To obtain a better understanding of the chemical equilibrium of star-block copolymer and fragrance molecules, a titration measurement was carried out by increasing the amount of benzyl acetate introduced into the star-block copolymer until saturation was attained. An increase in the amount of benzyl acetate in H40-(PBMA)₃₇-(PPEGMA)₃₉ in water resulted in a decrease in the diffusion coefficient of the benzyl acetate, illustrating that the encapsulation process represents an equilibrium between the free forms (of fragrance molecule and polymer) and the fragrance molecule/polymer complex. This equilibrium is shifted towards the complex form as the fragrance molecule concentration increases. The evolution of the relaxation times of benzyl acetate as a function of its concentration has been studied under the same conditions. T_1 and T_2 increase as the concentration of benzyl acetate increases. This may indicate that the benzyl acetate is first localized in the hydrophobic part of the nanocapsule where slow and restricted motions are observed (low T_1 and T_2) but, as more benzyl acetate is introduced, the nanocapsules fill up, so that benzyl acetate is also present in the outer shell (increased T_1 and T_2).

III. Quantification of fragrance molecule loadings in an aqueous dispersion of star-block copolymer

Diffusion and relaxation measurements do not give direct information on the capacity of the star-block copolymer to entrap the fragrance molecules, i.e. the fragrance loading. This question is addressed in the present section.

III.1. General results

The encapsulation experiments were carried out by saturating a solution of the polymer in D₂O with the fragrance molecules. After removal of the excess, the total amount of fragrance in the D₂O phase was determined by ¹H-NMR spectroscopy. Figure VII.4 to Figure VII.6 compare the uptake of benzyl acetate, geraniol, decanal and Vertenex® by H40-(PCL)₂₄-(PAA)₈₂, H40-(PCL)₄₀-(PAA)₁₀₀ and H40-(PBMA)₃₇-(PPEGMA)₃₉ respectively. There was a strong linear correlation between the amount of polymer and the maximum amount of benzyl acetate, geraniol, decanal and Vertenex® that could be maintained in aqueous solution, suggesting encapsulation and dispersion of volatile hydrophobic molecules in water to have been achieved. Similar experiments were carried out with benzyl acetate and Vertenex® in the presence of aqueous solutions of H30-(PCL)₁₂-(PAA)₆₀ and with benzyl acetate in the presence of H40-(PCL)₁₀-(PAA)₁₁₅. The results confirmed the dispersion of volatiles in D₂O in each case. The experiments were also repeated with the four olfactory compounds in the presence of H40-(PAA)₃₆ and with benzyl acetate in the presence of H40-(PPEGMA)₅₀ to study the effect of the hydrophobic core.

For each polymer/fragrance system, the fragrance loading was determined by dividing the fragrance concentration by the corresponding polymer concentration and its mean value therefore corresponds to the slope of the linear regression line for the data in Figure VII.4 to Figure VII.6 and for H40-(PCL)₁₀-(PAA)₁₁₅ and H30-(PCL)₁₂-(PAA)₆₀. Table VII.3 summarizes the loadings (in %) for the four fragrance molecules in an aqueous dispersion of one of the star-block copolymers studied.

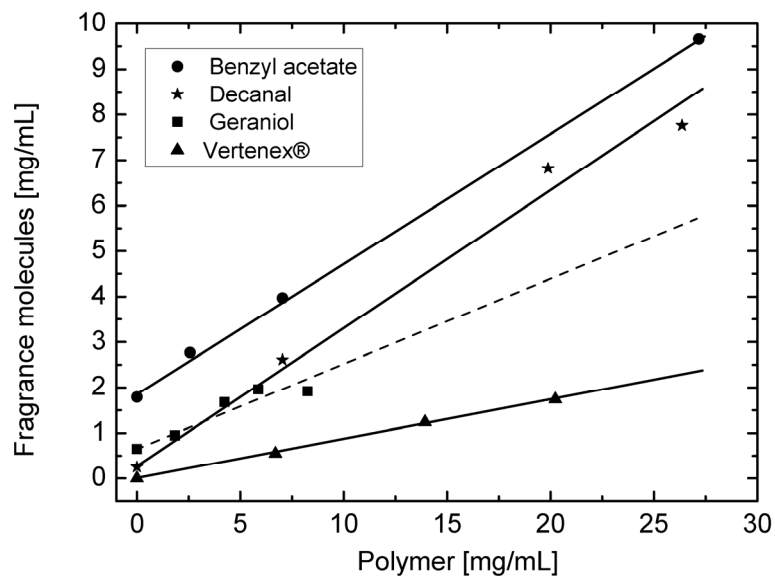


Figure VII.4 Amounts of different fragrance molecules dispersed in D₂O as a function of H40-(PCL)₂₄-(PAA)₈₂ concentration

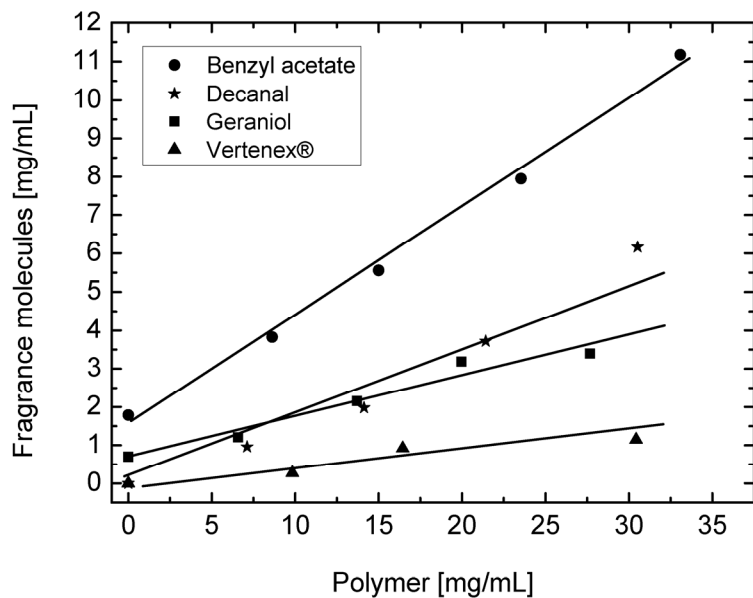


Figure VII.5 Amounts of different fragrance molecules dispersed in D₂O as a function of H40-(PCL)₄₀-(PAA)₁₀₀ concentration

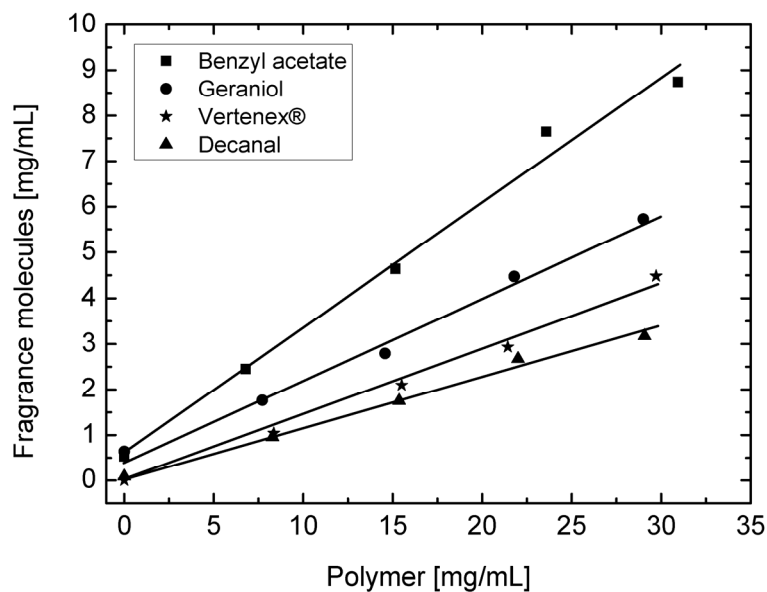


Figure VII.6 Amounts of different fragrance molecules dispersed in D₂O as a function of H40-(PBMA)₃₇-(PPEGMA)₃₉ concentration

Table VII.3 Mean ratio of fragrance to polymer concentration (effective loading) for the different fragrance molecules in aqueous solutions of the copolymer

	Load of volatiles quantified by ¹ H NMR [%]			
	Benzyl acetate	Geraniol	Decanal	Vertenex®
H30-(PCL) ₁₂ -(PAA) ₆₀	16.0	-	-	4.9
H40-(PAA) ₃₆	2.0	0.5	0	0.5
H40-(PCL) ₁₀ -(PAA) ₁₁₅	9.2	-	-	-
H40-(PCL) ₂₄ -(PAA) ₈₂	23.3	19.7	28.6	8.7
H40-(PCL) ₄₀ -(PAA) ₁₀₀	27.1	10.7	20.1	4.0
H40-(PPEGMA) ₅₀	3.9	-	-	-
H40-(PBMA) ₃₇ -(PPEGMA) ₃₉	25.2	24.4	12.4	17.7

(-) not measured

The effective loadings obtained in H40-(PCL)_p-(PAA)_q, were at least 8.7 wt % (Vertenex® in H40-(PCL)₂₄-(PAA)₈₂), which was significantly higher than the loadings of 2 wt % measured for H40-(PAA)₃₆ (Table VII.3). A similar trend was observed with benzyl acetate measured in the presence of H40-(PBMA)₃₇-(PPEGMA)₃₉ and H40-(PPEGMA)₅₀, again illustrating the importance of the core-shell architecture for the encapsulation of guest molecules and, the entrapment of volatiles in the hydrophobic core of the star-block copolymers, as also indicated by the diffusion and relaxation studies (section II).^[294]

III.2. Influence of the polymer architecture

Structural parameters of the “host”, such as the block length, degree of branching and the rigidity of the blocks may be crucial for encapsulation. External factors such as the solvent type and pH, also influence the conformational behavior of the carrier.^[15] The role of the polymer block length and the core functionality have therefore been investigated for benzyl acetate and HBP-(PCL)_p-(PAA)_q star-block copolymers. The number of arms per molecule was varied by using HBPs with different functionalities (H40 and H30).

III.2.1 Effect of the polymer block length

The benzyl acetate loading was determined by ¹H NMR spectroscopy for H40-(PCL)₁₀-(PAA)₁₁₅, H40-(PCL)₂₄-(PAA)₈₂, H40-(PCL)₄₀-(PAA)₁₀₀ and H40-(PAA)₃₆ copolymers, by saturating a solution of each polymer in D₂O with benzyl acetate as described previously (in section III.1). Figure VII.7 shows the amount of benzyl acetate as a function of the polymer concentration for each copolymer.

The loading increased as the PCL block length increased and approached zero (load of only 2.0 % in the case of H40-(PAA)₃₆) in the absence of PCL block. The mean benzyl acetate loading for each polymer is given in Table VII.3.

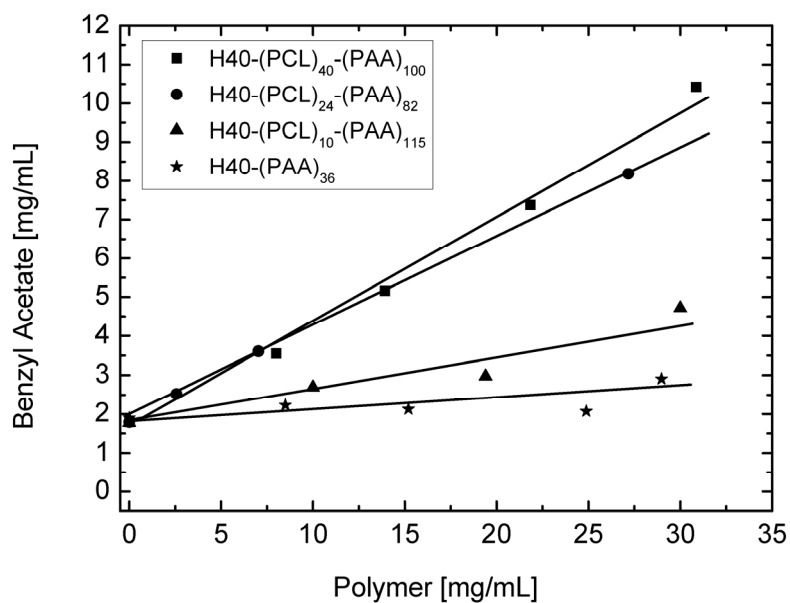


Figure VII.7 Benzyl acetate concentration as a function of the star-block copolymer concentration for **H40-(PCL)₁₀-(PAA)₁₁₅**, **H40-(PCL)₂₄-(PAA)₈₂**, **H40-(PCL)₄₀-(PAA)₁₀₀** and **H40-(PAA)₃₆**

III.2.2 Effect of the HBP core functionality

The effect of the HBP core functionality was investigated by comparing the benzyl acetate loading determined in an aqueous dispersion of H30-(PCL)₁₂-(PAA)₆₀ with that in H40-(PCL)₁₀-(PAA)₁₁₅ (Table VII.3 and Figure VII.8).

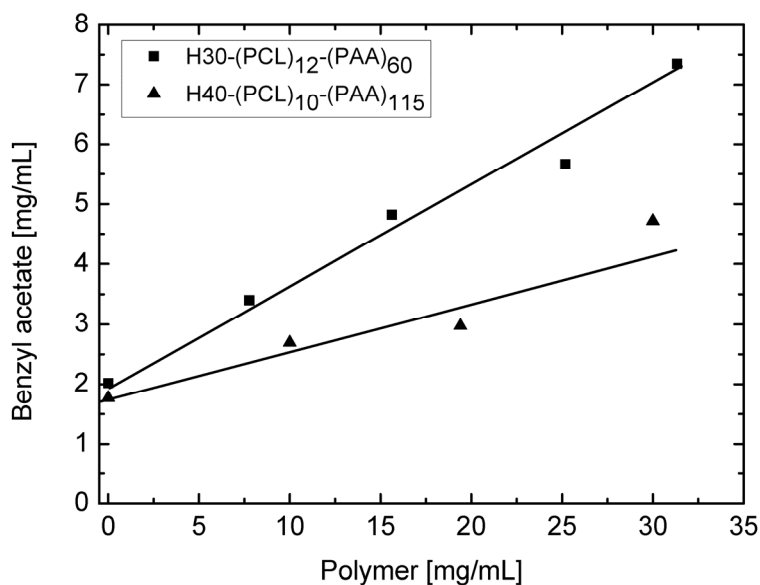


Figure VII.8 Amounts of benzyl acetate as a function of the polymer concentration for two different core functionalities

In spite of the lower core functionality, the loading of benzyl acetate in H30-(PCL)₁₂-(PAA)₆₀ was higher than in H40-(PCL)₁₀-(PAA)₁₁₅. To gain a better understanding of the influence of the core on the entrapment of benzyl acetate another representation of the results is given in Figure VII.9, taking into account both the functionality of the core (number of arms per HBP molecule) and the length of the PCL blocks. The weight percentage of hydrophobic block was calculated by dividing the molar mass of the hydrophobic layer by the molar mass of the amphiphilic star-block copolymer (Table VII.4). The weight percentage of the hydrophobic block for H30-(PCL)₁₂-(PAA)₆₀ was 27.8 % which is considerably higher than 14.9 %, determined for H40-(PCL)₁₀-(PAA)₁₁₅. Hence, the high loadings in H30-(PCL)₁₂-(PAA)₆₀ may be attributed to the greater proportion of the hydrophobic blocks than in H40-(PCL)₁₀-(PAA)₁₁₅. The linearity of the data in Figure VII.9 suggests this to be a general trend.

Table VII.4 Molar masses and percentage of hydrophobic block (by weight) for H40-(PCL)_p-(PAA)_q and H40-(PBMA)_p-(PPEGMA)_q amphiphilic star-block copolymers

	M_n [g mol ⁻¹] hydrophobic block	M_n [g mol ⁻¹] hydrophobic and hydrophilic block	wt % of the hydrophobic layer
H30-(PCL) ₁₂ -(PAA) ₆₀	42 160 ^a	151 460 ^a	27.8
H40-(PAA) ₃₆	-	100 400 ^a	-
H40-(PCL) ₁₀ -(PAA) ₁₁₅	50 800 ^a	340 200 ^a	14.9
H40-(PCL) ₂₄ -(PAA) ₈₂	108 300 ^a	307 400 ^a	35.2
H40-(PCL) ₄₀ -(PAA) ₁₀₀	173 900 ^a	425 500 ^a	40.8
H40-(PBMA) ₃₇ -(PPEGMA) ₃₉	182 000 ^b	782 000 ^b	23.3
H40-(PPEGMA) ₅₀	-	780 000 ^b	-

^a ¹H NMR

^b GPC in DMF

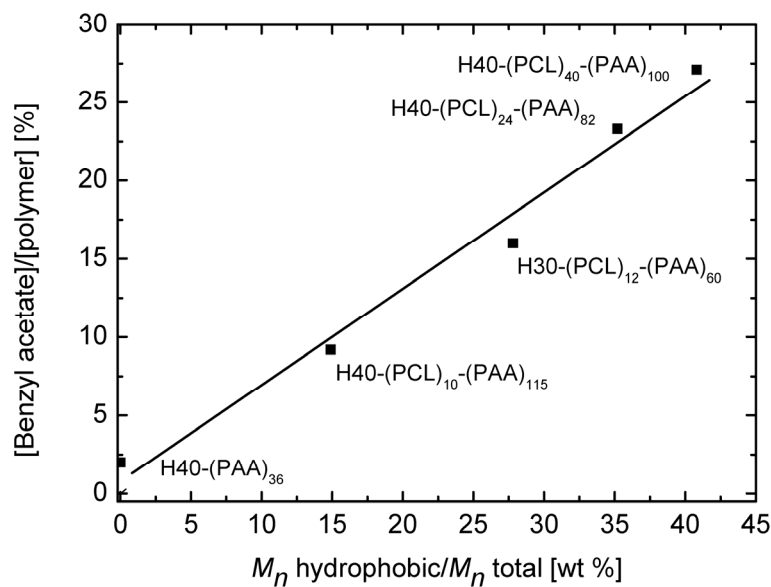


Figure VII.9 Benzyl acetate loading (in %) as a function of the proportion of hydrophobic blocks in the star-block copolymers (in wt %)

III.2.3 Results for geraniol, decanal and Vertenex®

The loadings of geraniol, decanal and Vertenex® were higher in the presence of a star-block copolymer with a shorter PCL block (i.e. H40-(PCL)₂₄-(PAA)₈₂) than for a longer PCL block (Table VII.3) so that the trend observed for benzyl acetate was not apparently a general one. More systematic tests would be needed to investigate this point.

III.3. Influence of the log*P* of the fragrances

In this section an attempt is made to correlate the loading of the fragrance compounds with log*P* as was done in the NMR diffusion study (section II).

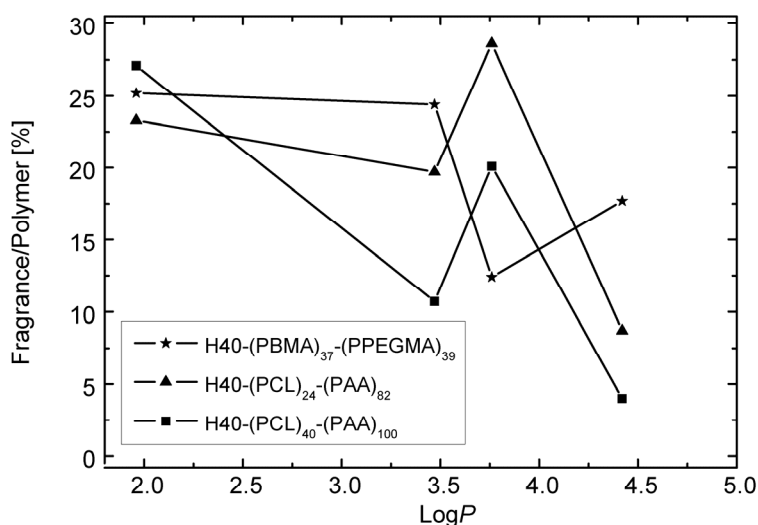


Figure VII.10 Loadings of the four fragrance compounds for each polymer (mean ratio of fragrance to polymer concentration in %) as a function of the log*P* values for each fragrance compound (see Table VII.1) for three star-block copolymers (H40-(PBMA)₃₇-(PPEGMA)₃₉ (star); H40-(PCL)₂₄-(PAA)₈₂ (triangle) and H40-(PCL)₄₀-(PAA)₁₀₀ (square))

Figure VII.10 shows the fragrance loading, calculated by dividing the concentration of the fragrance molecule by the concentration of the polymer, for the four fragrance molecules in the presence of each of the three star-block copolymers (H40-(PCL)₂₄-(PAA)₈₂, H40-(PCL)₄₀-(PAA)₁₀₀ and H40-(PBMA)₃₇-(PPEGMA)₃₉) as a function of $\log P$ of the fragrance compounds (Table VII.1). If only benzyl acetate, geraniol and Vertenex® are considered, the fragrance loading in the star-block copolymer appears to decrease with increasing $\log P$. The more hydrophobic the volatile (higher $\log P$), the lower the loading in the polymer. This effect was observed for the three star-block copolymers. However, in the case of decanal, the loading in H40-(PCL)_p-(PAA)_q was relatively high, in spite of its high $\log P$. Hence, there is a globally negative correlation between the loading of fragrances and $\log P$ for the molecules chosen, but also a significant deviation from this trend (decanal). However, a further important factor is the solubility of the volatiles in the polymer. This is discussed in the last part of this section.

III.4. Influence of the solubility parameters

A way of assessing the solubility of the guest molecules in the polymer core is to use the solubility parameter approach. The Flory-Huggins interaction parameter^[111] (χ_{12}) between the polymer (1) and the fragrance compound (2) is a measure of the interaction between the polymer and the volatiles and may be expressed as

$$\chi_{12} \equiv V_m \frac{(\delta_1 - \delta_2)^2}{RT}$$

where δ_1 and δ_2 are the Hildebrand solubility parameters for the polymer and the volatile respectively and V_m is the molar volume of a polymer “segment”. The one parameter approach is generally inadequate, so δ is often separated into hydrogen (δ_h), polar (δ_p) and dispersive (δ_d) contributions. δ_h , δ_p and δ_d , which are called the Hansen parameters, are used to assess miscibility using $(\delta_{h1} - \delta_{h2})^2 + (\delta_{p1} - \delta_{p2})^2 + (\delta_{d1} - \delta_{d2})^2$ rather than $(\delta_1 - \delta_2)^2$ as a

criterion.^[295] In either case, good solubility is implied for small χ_{12} , i.e. matching values of the δ .

In the literature^[295], tables have been established allowing δ to be estimated from “group contributions” corresponding to each chemical function. The values of the Hansen parameters for the fragrance molecules and the polymers hydrophobic blocks have been determined using these tables and are summarized in Table VII.5. For the determination of the solubility parameter of the polymers only the hydrophobic block have been considered since it has already been demonstrated by NMR spectroscopy (in section II and III) that the hydrophilic outer shell does not contribute to the encapsulation of the fragrances. The difference between the solubility parameters of the hydrophobic block and of the fragrance molecules were determined for each polymer/fragrance system and are summarized in Table VII.6. These values are compared with the loadings (in %) determined by NMR in Table VII.7, the loadings being plotted as a function of the solubility parameter difference for each polymer/fragrance system in Figure VII.11.

Table VII.5 Hildebrand solubility parameter calculated by the Hansen parameters approach for the four fragrance molecules and the two different hydrophobic polymer blocks PCL and PBMA

	δ_d [J ^{1/2} cm ^{-3/2}]	δ_p [J ^{1/2} cm ^{-3/2}]	δ_h [J ^{1/2} cm ^{-3/2}]	$\delta = (\delta_d^2 + \delta_p^2 + \delta_h^2)^{1/2}$ [J ^{1/2} cm ^{-3/2}]
Benzyl acetate	18.96	3.79	7.27	20.66
Geraniol	15.84	2.81	10.60	19.26
Decanal	16.52	4.33	4.94	17.78
Vertenex®	24.32	3.29	6.86	25.48
PCL block	17.66	4.97	8.43	20.19
PBMA block	21.70	3.76	7.33	23.21

Table VII.6 Solubility parameter differences between the volatiles and the hydrophobic blocks (PCL or PBMA)

	PCL block $[(\delta_{h1}-\delta_{h2})^2+(\delta_{p1}-\delta_{p2})^2+(\delta_{d1}-\delta_{d2})^2]^{1/2}$ [J ^{1/2} cm ^{-3/2}]	PBMA block $[(\delta_{h1}-\delta_{h2})^2+(\delta_{p1}-\delta_{p2})^2+(\delta_{d1}-\delta_{d2})^2]^{1/2}$ [J ^{1/2} cm ^{-3/2}]
Benzyl acetate	2.10	2.74
Geraniol	3.56	6.78
Decanal	3.72	5.73
Vertenex®	7.04	2.7

Table VII.7 Solubility parameter difference for the fragrance loadings/star-block copolymers systems and the associated fragranal loadings for H40-(PCL)₄₀-(PAA)₁₀₀ and H40-(PBMA)₃₇-(PPEGMA)₃₉

	H40-(PCL)₄₀-(PAA)₁₀₀		H40-(PBMA)₃₇-(PPEGMA)₃₉	
	Fragrance loading [%]	Solubility parameter difference	Fragrance loading [%]	Solubility parameter difference
Benzyl acetate	27.1	2.10	25.2	2.74
Geraniol	10.7	3.56	24.4	6.78
Decanal	20.1	3.72	12.4	5.73
Vertenex®	4.0	7.04	17.7	2.7

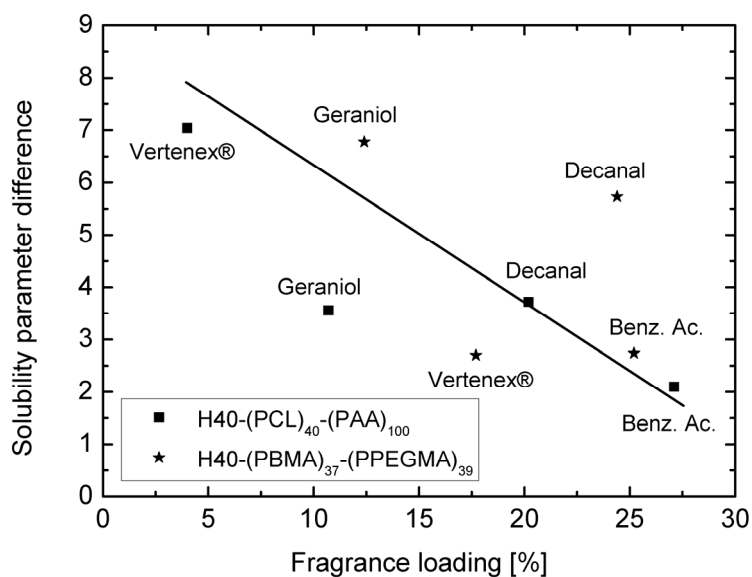


Figure VII.11 Solubility parameter difference as a function of the fragrance loadings. The solubility parameter differences were calculated with the three parameter approach

There is an apparent global correlation between the loadings of volatiles in the polymer and the solubility parameter differences. The correlation is more pronounced if decanal in H40-(PBMA)₃₇-(PPEGMA)₃₉ is not considered. The fragrance molecule loadings in the star-block copolymer increase with decreasing solubility parameter differences between the polymer and the volatile. This result suggests that the encapsulation of fragrance molecules in the amphiphilic star-block copolymer is strongly influenced by the solubility of the fragrance molecule in the hydrophobic part of the polymer. Moreover, the significant differences in the solubility parameters of the different blocks (PBMA or PCL) illustrate the importance of the choice of the chemical groups of the internal core for the fragrance loadings. However, this approach does not appear to be valid for decanal in H40-(PBMA)₃₇-(PPEGMA)₃₉ reflecting either the need to consider other parameters (such as the polymer water solubility, the expansion coefficient of such polymer in water, or steric hindrance) or the inadequacy of the solubility parameter to describe the host-guest affinity.

IV. Conclusions

The ability of the star-block copolymers to encapsulate fragrance molecules has been demonstrated by NMR spectroscopy. The encapsulation process in water reflects a dynamic equilibrium between the free and encapsulated forms which is shifted towards the encapsulated form as the fragrance molecule concentration increases. The core-shell architecture with its phase separated morphology has been confirmed by NMR and the crucial role played by the hydrophobic internal core of the polymer has been demonstrated by diffusion and quantification experiments.

The decrease in the diffusion coefficients of the fragrance molecules in the presence of the star-block copolymers is most marked at high $\log P$. This reflects an increased affinity of the volatiles with the hydrophobic core of the polymers with respect to the surrounding aqueous medium. However, the loading capacity of the polymers is also dependent on the solubility of the volatiles in the hydrophobic core of the polymers. The solubility parameter approach may be used to predict the host/guest affinity, and is shown here to account at least in part for the observed loadings, and may hence be considered a useful tool in the design of systems with affinities for specific fragrance molecules. However, in such systems, other parameters, such as the volatility of the fragrance molecules, the polymer water solubility or the temperature, which are correlated between each other, may still need to be considered to find a trend between the fragrance loadings and the star-block copolymer properties.

Chapter VIII. Industrial application: controlled release of fragrance molecules in fine perfumery and in fabric softener applications

As pointed out in Chapter II.I.3, little data is available on the release of low molar mass active organic compounds from polymers. It is nevertheless clear that for the controlled release of fragrance molecules, drugs, and other active molecules from unimolecular micelles, diffusion is a primary consideration.^[26, 151, 155, 165] However, many other parameters must be taken into account, such as the volatility and the solubility parameter of the perfume, for example. Moreover, in a final product, other compounds are present such as surfactants. In a softener, for example, 15 % cationic surfactant, 1 % perfume and 1 % of the polymer encapsulant are present in the aqueous phase (83 %). Under these conditions, it is necessary to take into account perfume diffusion from the encapsulant to the surfactant micelles. This illustrates the numerous parameters that must be taken into account in release studies for real applications. However the aim here was to investigate the capacity of the new amphiphilic star-block copolymers to prolong perception of the fragrance molecules. The pH-dependence property of H40-(PCL)_p-(PAA)_q is of particular interest in application such as the softener application where an increase of pH from acidic to neutral conditions is observed. At the beginning, pH in the softener base is between 3 and 5 whereas at the end, pH increased with

the immersion of the sample in pure water. The behavior of such pH-responsive polymer in this application is of interest. These pH-responsive nanocapsules have also been tested in fine perfumery compositions, which is not of direct practical interest due to the irritant character of ionic molecules for skin. However, comparison with the results obtained with the non-ionic capsules (H40-(PBMA)_p-(PPEGMA)_q) was of interest.

In what follows, the release of fragrance molecules from HBP-(PCL)_p-(PAA)_q and H40-(PBMA)_p-(PPEGMA)_q is described. Release rates were investigated by thermogravimetric analysis (TGA) and headspace analysis. In TGA measurements the weight loss of perfume dissolved in ethanol is monitored as a function of time. In headspace analysis, the evaporation of fragrance molecules under a constant air flow with humidity control is measured for compositions representative of a fine perfumery and a softener application. A reference sample containing the precursor hyperbranched polymer H40 has been used as a control in each case. Headspace analysis^[296] is often used in the fragrance industry because of the speed of analysis and the possibility of studying conditions that mimic exactly the application conditions.

I. Release monitored by thermogravimetric analysis (TGA)

The amphiphilic star-block copolymer H40-(PCL)₁₀-(PAA)₇₀ and H40-(PBMA)₃₇-(PPEGMA)₃₉ (2 % (w/w)) and one of a range of fragrance compounds (benzyl acetate, geraniol, decanal or Vertenex[®]) (5 % (w/w)) were mixed in ethanol/water solution (85/8 % (w/w)). 10 μL of the solution were placed in an aluminium oxide crucible and the evaporation of the fragrance molecules was followed by measuring the weight loss of the sample as a function of time. The evaporation of the fragrance molecule was measured by heating the sample from 25 to 50 °C at 5 °C/min in order to evaporate the ethanol relatively rapidly. The sample was then held at 50 °C for 115 minutes. It was finally heated from 50 to 130 °C at 4 °C/min and held at 130 °C for 15 minutes to remove any remaining fragrance molecules from the polymer.

I.1. Fragrance behavior

The first tests were carried out by mixing the fragrance molecules alone (5 % (w/w)) in ethanol/water (85/10 % (w/w)). The evaporation (weight in % relative to the initial weight at the beginning of the experiment as a function of time in min) for each fragrance molecule is given in Figure VIII.1. The evaporation of very volatile compounds (i.e. benzyl acetate ($500 \mu\text{g L}^{-1}$) and decanal ($528 \mu\text{g L}^{-1}$)) was relatively fast, the fragrance compound evaporating completely after 20 minutes. In the case of Vertenex[®] (volatility of $200 \mu\text{g L}^{-1}$) the slope of the curve was reduced complete evaporation taking 50 minutes. The complete evaporation of the least volatile compound, geraniol ($93 \mu\text{g L}^{-1}$), could only be achieved by increasing the oven temperature to $130 \text{ }^\circ\text{C}$. As expected, therefore, the thermograms (weight loss of fragrance molecule (%) as a function of time) were directly correlated with the volatility of the fragrance molecules.

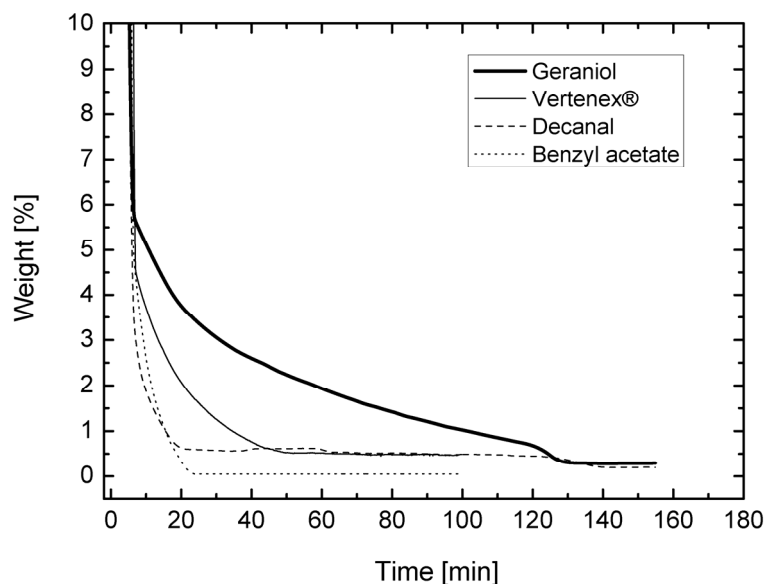


Figure VIII.1 Evaporation of the fragrance compounds in an ethanol/water mixture, without any polymer

I.2. Fragrance release in the presence of star-block copolymer

The evaporation of the fragrance compound in the presence of H40 or one of the amphiphilic star-block copolymers H40-(PBMA)₃₇-(PPEGMA)₃₉ or H40-(PCL)₁₀-(PAA)₇₀ was investigated. Figure VIII.2 gives a representative example of the evaporation of benzyl acetate alone and in the presence of H40, H40-(PCL)₁₀-(PAA)₇₀ and H40-(PBMA)₃₇-(PPEGMA)₃₉. The evaporation of benzyl acetate was in all cases significantly slowed down by the presence of the amphiphilic star-block copolymers. The effect was more pronounced than for H40 reference. Similar trends were also observed for geraniol, decanal and Vertenex® (Figure VIII.3). This underlines the importance of the hydrophobic core and of the hydrophilic shell. It was also observed that the effect of the star-block copolymers depended on the fragrance molecule. For example, H40-(PCL)₁₀-(PAA)₇₀ retarded most effectively the evaporation of decanal, whereas H40-(PBMA)₃₇-(PPEGMA)₃₉ was more efficient for benzyl acetate (Figure VIII.3). In the case of geraniol, no significant differences were observed. For Vertenex®, evaporation was slower with H40-(PBMA)₃₇-(PPEGMA)₃₉ up to 90 minutes under the conditions of the measurement, but after 90 minutes H40-(PCL)₁₀-(PAA)₇₀ contained more residual Vertenex®.

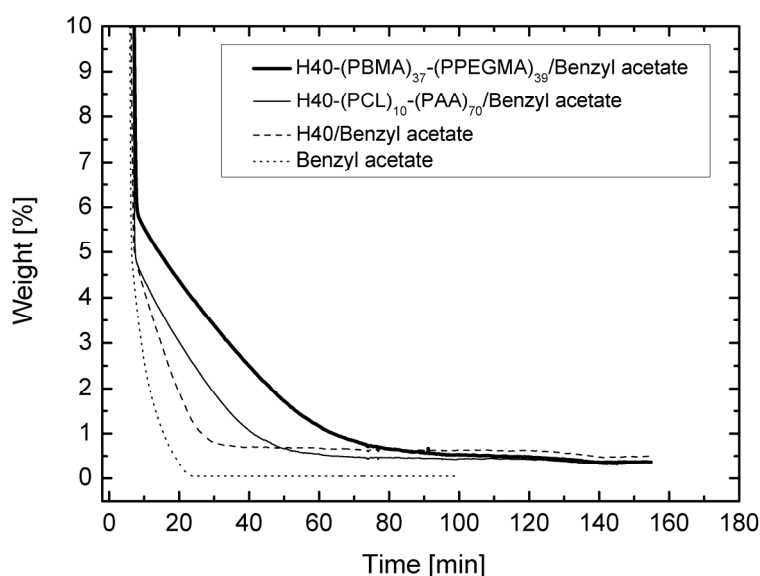


Figure VIII.2 Evaporation of benzyl acetate in the presence of different star-block copolymers

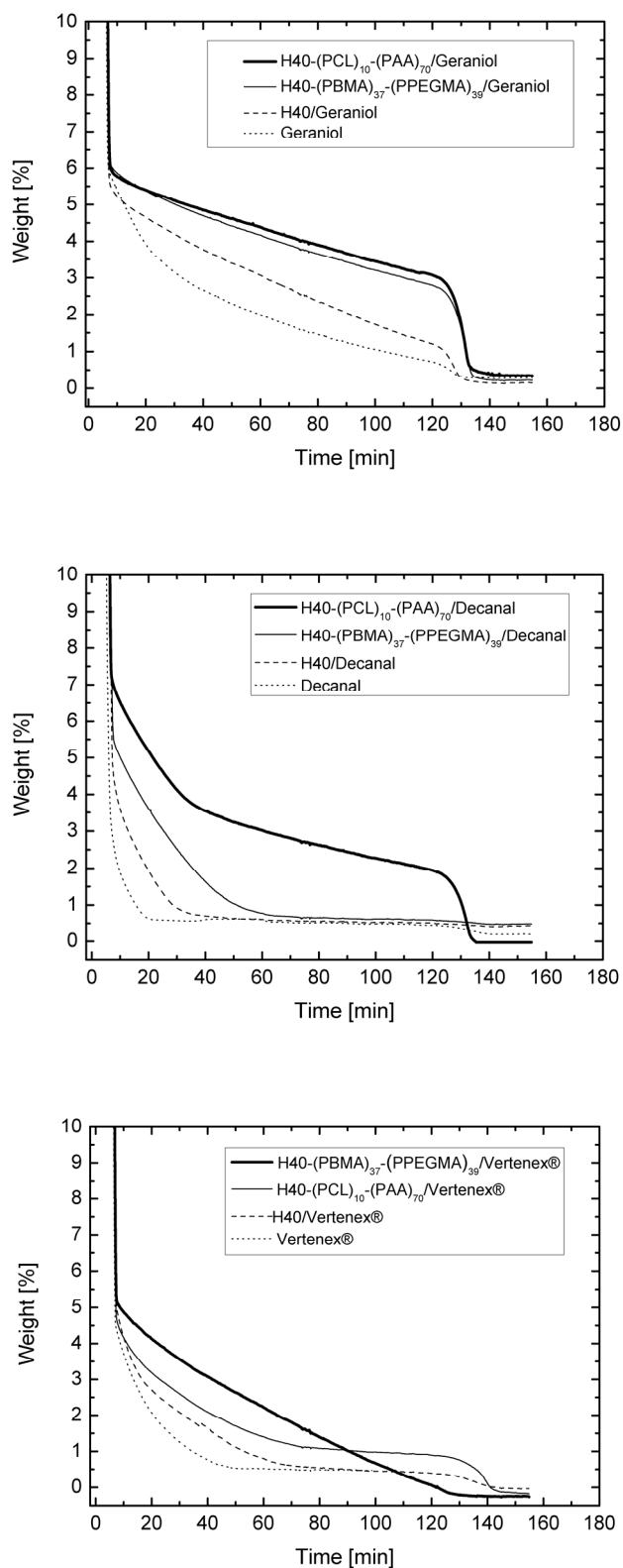


Figure VIII.3 Evaporation of decanal, Vertenex® and geraniol in the presence of H40-(PBMA)₃₇-(PPEGMA)₃₉ or H40-(PCL)₁₀-(PAA)₇₀

To illustrate further the effect of the amphiphilic star-block copolymers on the retention of the fragrance compounds, the difference between the weight of the fragrance compound (in %) in the presence of one of the amphiphilic star-block copolymers (H40-(PCL)₁₀-(PAA)₇₀ or H40-(PBMA)₃₇-(PPEGMA)₃₉ and the H40 reference) and the weight of the fragrance compound in the absence of polymer has been tabulated after an arbitrary time of 80 min at 50 °C, as given in Table VIII.1.

Table VIII.1 Increase in the retention of fragrance molecules in the presence of amphiphilic star-block copolymer with respect to values measured for the fragrance molecule alone

Increase in weight [%] of the retention after 80 min at 50 °C of fragrance molecules			
	Boltorn® H40	H40-(PCL)₁₀-(PAA)₇₀	H40-(PBMA)₃₇-(PPEGMA)₃₉
Geraniol	+0.93	+2.48	+2.23
Decanal	+0.03	+2.10	+0.13
Benzyl acetate	+0.64	+0.46	+0.65
Vertenex®	+0.06	+0.60	+0.91

In the case of benzyl acetate, the increase of retention in the presence of H40-(PCL)₁₀-(PAA)₇₀ or H40-(PBMA)₃₇-(PPEGMA)₃₉ was lower than (or equal to) in the presence of the H40 reference after 80 minutes. However there was still improved retention between 10 and 40 minutes for H40-(PCL)₁₀-(PAA)₇₀ and between 10 and 70 minutes for H40-(PBMA)₃₇-(PPEGMA)₃₉.

After 80 minutes at 50 °C the retention of geraniol was observed to be greater in comparison with the other fragrance molecules investigated. This may be explained by the low volatility of geraniol (93 µg L⁻¹). In the presence of the star-block copolymers geraniol evaporation was linear with time (after the ethanol had evaporated). Its evaporation rate was not significantly influenced by the chemical nature of the star-block copolymers (Figure VIII.3).

The evaporation of decanal was significantly delayed by H40-(PCL)₁₀-(PAA)₇₀ (Figure VIII.3 and Table VIII.1) after 130 minutes at 50 °C, it was not completely evaporated. This was not true for H40-(PBMA)₃₇-(PPEGMA)₃₉ and the H40 reference, which no longer contained decanal after 60 and 40 minutes respectively.

Vertenex® evaporation was apparently sensitive to the nature of the star-block copolymer (Figure VIII.3). In the presence of H40-(PBMA)₃₇-(PPEGMA)₃₉, the evaporation of Vertenex® was significantly delayed but the rate of evaporation remained relatively fast compared with the rate of evaporation observed with H40-(PCL)₁₀-(PAA)₇₀. Evaporation was linear up to 125 minutes in the former case, after which no fragrance compound was detected. With H40-(PCL)₁₀-(PAA)₇₀, after 100 minutes at 50 °C the sample weight changed little with time (appearance of a plateau) although Vertenex® was still present (at least 1 % (w/w)).

Hence, in the presence of H40-(PCL)₁₀-(PAA)₇₀ the evaporation of decanal, geraniol and Vertenex® showed comparable behavior, with the “stabilization” of the evaporation of the respective fragrance molecules and the presence of a plateau, particularly in the case of Vertenex®. For benzyl acetate, on the other hand, the plateau was never observed, presumably due to its high volatility. The evaporation behavior of the fragrances is therefore sensitive to the volatility of the fragrance compounds even in the presence of the polymer.

H40-(PBMA)₃₇-(PPEGMA)₃₉ caused a significant decrease in the evaporation rate in all cases. The effect was more pronounced with benzyl acetate and geraniol, for which the evaporation times, for benzyl acetate, being increased threefold, and the retention of geraniol is double after 80 minutes. A retention effect was also detected for decanal and Vertenex® but was less pronounced.

The TGA measurements are not directly correlated with the fragrance loading in the polymer due to the difference in the encapsulation technique in the NMR measurement (Chapter VII) and in the present release measurement with the large presence of ethanol. TGA results illustrate that it is apparently easier to delay evaporation of weakly volatile fragrance molecules (i.e. geraniol) than highly volatile fragrance molecules (i.e. benzyl acetate). The efficiency of the star-block copolymers is nevertheless clearly demonstrated by TGA under

conditions that mimic those in fine perfumery applications and no significant conclusions may be established in terms of the charges present at the surface of the nanocapsules in the present conditions.

In certain cases a shift in the weight (%) measured occurred at the end of the measurement, depending on the fragrance compounds and the star-block copolymers used. This shift was due to evaporation of the fragrance molecules before the oven temperature was stable (the beginning of the measurement).

II. Release monitored by dynamic headspace analysis

Another parameter that is of great importance is the human olfactory threshold.^[297] Even if the evaporation of the fragrances is delayed in the presence of the polymer it is important to know whether the corresponding concentrations are above or below the human olfactory threshold. In the TGA experiments, the discussion was based essentially on qualitative results. To gain a more quantitative idea of the effect of the star-block copolymers under application conditions, headspace analysis has been undertaken, as will be described in the present section.

II.1. What is headspace analysis?

Headspace analysis is a technique that quantifies the volatile components present in the gas space above a sample that contains the compound(s) of interest. Headspace gas chromatography is used for the analysis of volatiles and semi-volatile organics in solid, liquid and gas samples. The main variants of headspace sampling are described in the literature^[298] and range from static headspace (SHS)^[299] to headspace solid phase microextraction (HS-SPME)^[300] through purge and trap (P&T-HS)^[301] or static and trapped headspace (S&T-HS).^[302] In the present work, purge and trap headspace, commonly named “dynamic headspace” has been used. This consists of continuously stripping the sample by air or gas flow. The volatiles are then trapped by an adsorbent, from which they are subsequently

thermally desorbed. This procedure allows the collection of greater amount of volatiles than those present at equilibrium (as in static headspace). An advantage of using dynamic headspace analysis in fragrance industry is the possibility of measuring the evaporation kinetics of several different fragrance compounds simultaneously and under exactly the same conditions as in the real application.

The popularity of these techniques has grown over recent years and they have now gained worldwide acceptance for analyses of alcohols in blood^[303, 304] and residual solvents in pharmaceutical products.^[305-307] Other common applications include industrial analyses of monomers in polymers and plastic,^[308] flavor compounds in beverages and food products^[309-311], and fragrance compounds in perfumes and cosmetics.^[298, 312, 313]

II.2. A fine perfumery application

The measurement was carried out with and without the amphiphilic star-block copolymer in order to investigate the effect of the polymer on the evaporation of the fragrance compound. Two star-block copolymers were used, i.e. H40-(PCL)₁₀-(PAA)₇₀ and H40-(PBMA)₃₇-(PPEGMA)₃₉. The sample was prepared by mixing the star-block copolymer (2 % (w/w)) with the perfume (composition given in Chapter IV.IV.2.1) (5 % (w/w)) in ethanol/water (85/8 % (w/w)) solution. 2 μL of the mixture was placed in a headspace sampling cell thermostatted at 25 °C and exposed to a constant air flow under humidity control. The fragrance compounds were continuously adsorbed onto cartridges for 60 minutes desorbed thermally and then analyzed with a gas chromatography (GC) equipped with a flame ionization detector (FID). The concentration (ng L^{-1}) of the fragrance molecules was determined as a function of time (min). The physico-chemical properties of the fragrance molecules considered here for the perfume composition are give in Appendix 5.

II.2.1 Behavior of the volatiles

The profiles of the evaporation curves of the individual fragrances differ as a function of their volatilities. Evaporation profiles of compounds with volatility higher than $500 \mu\text{g L}^{-1}$ (such as pipol, 3,5,5-trimethylhexanal, dimetol, acetophenone, ethyl (*E*)-2,4-dimethyl-2-pentenoate, benzyl acetate, jasmonitrile, and decanal) follow an exponential decay from $t = 0$ to $t = 60$ min, as shown in Figure VIII.4. For compounds with lower volatilities, (i.e. benzylacetone, 2-pentylcyclopentanol, geraniol, 4-cyclohexyl-2-methyl-2-butanol, 10-undecenal, Vertenex®, allyl 3-cyclohexylpropanoate) the evaporation profile is discontinuous. The amount of compound increases to a maximum after 15 minutes and then decays exponentially as shown in Figure VIII.5. The polarity of the substrate i.e. the affinity between the fragrance molecules and the substrate, the solvent and the temperature may also influence the profiles.

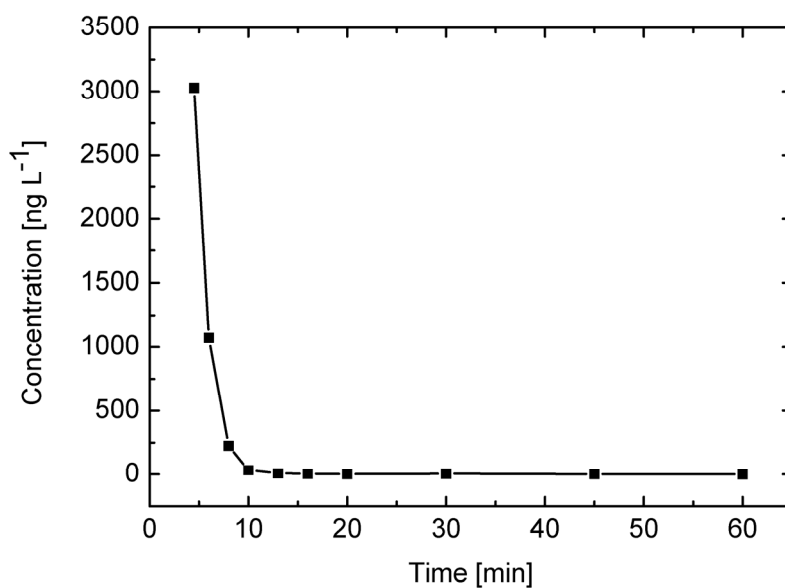


Figure VIII.4 Representative evaporation profile for highly volatile compounds: benzyl acetate

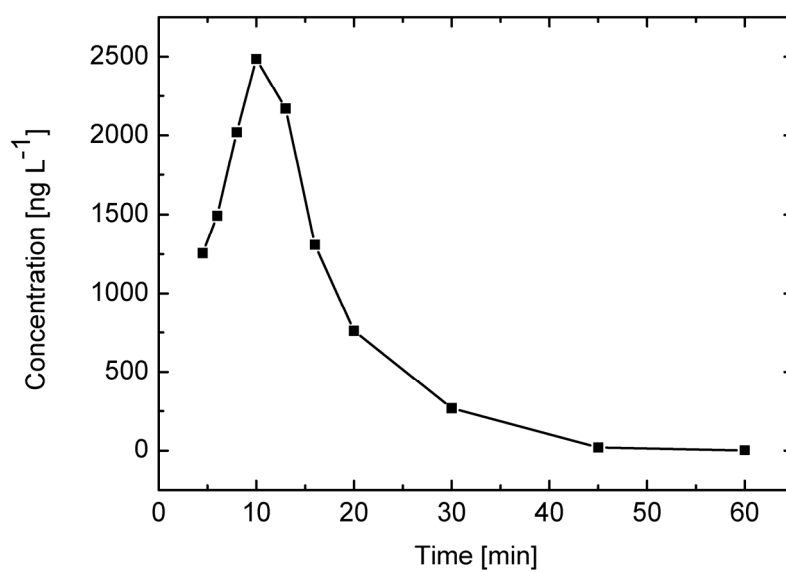


Figure VIII.5 Representative evaporation profile for low volatile compounds: geraniol

II.2.2 Behavior of the volatiles in the presence of the star-block copolymer

The evaporation profiles of benzyl acetate, decanal, Vertenex® and geraniol in the presence of H40-(PBMA)₃₇-(PPEGMA)₃₉ and of H40-(PCL)₁₀-(PAA)₇₀ are given in Figure VIII.6 to Figure VIII.9. In both cases, the evaporation of the fragrance compounds was delayed in the presence of the star-block copolymers and the evaporation profiles of each volatile remained qualitatively unchanged. The maximum concentrations for Vertenex® and geraniol in the presence of the star-block copolymers were lower ($C_{max \text{ Vertenex}^\circledast} = 4250 \text{ ng L}^{-1}$ and $C_{max \text{ geraniol}} = 1800 \text{ ng L}^{-1}$) with H40-(PBMA)₃₇-(PPEGMA)₃₉, for example, than the maximum concentrations measured in the absence of polymer ($C_{max \text{ Vertenex}^\circledast} = 5000 \text{ ng L}^{-1}$ and $C_{max \text{ geraniol}} = 2750 \text{ ng L}^{-1}$). This illustrates the effectiveness of the polymer at the beginning of the measurement. However, the kinetic curves measured in the presence and in the absence of the polymer crossed each other after a certain time, demonstrating the long-lastingness effect of the polymer in such conditions.

For the comparison of the data, the time to reach an arbitrary chosen headspace concentration of 50 ng L^{-1} was determined for H40-(PCL)₁₀-(PAA)₇₀ and H40-(PBMA)₃₇-(PPEGMA)₃₉. The data summarized in Table VIII.2 were obtained for each fragrance compound in the perfume sample.

Table VIII.2 Description of the effect of the polymer in headspace analysis experiment

Name of fragrance compound	Time required to reach a headspace concentration of 50 ng L ⁻¹ [min]		
	no copolymer	H40-(PCL) ₁₀ -(PAA) ₇₀	H40-(PBMA) ₃₇ -(PPEGMA) ₃₉
Pipol	4.5	*)	5.8
3,5,5-Trimethylhexanal	7.9	5.0	12
Dimetol	6.7	8.1	8.4
Acetophenone	5.5	7.2	8.1
Ethyl (<i>E</i>)-2,4-dimethyl-2-pentenoate	*)	6.2	5.9
Benzyl acetate	8.7	21.2	13.5
Jasmonitrile	10	19	13
Decanal	15.2	21.0	19
Benzylacetone	13.5	25.0	22.2
2-Pentylcyclopentanol	25.5	41.1	31.7
Geraniol	36.2	49	45.2
4-Cyclohexyl-2-methyl-2-butanol	29.7	45	34.4
10-Undecenal	24.3	32	28.7
Vertenex®	19.1	32.7	24.0
Allyl 3-cyclohexylpropanoate	26.8	46.2	33

*) headspace concentration always below 50 ng L⁻¹

For each fragrance compound the time to reach the concentration of 50 ng L⁻¹ in the headspace cell was longer in the presence of the star-block copolymer, indicating retarding effect of the copolymer on evaporation. Both types of star-block copolymers influenced the fragrance compound evaporation, although the differences were generally small. The apparently higher concentrations measured in the presence of H40-(PCL)₁₀-(PAA)₇₀ for the majority of the fragrances may be due to its thermal properties. At 25 °C, the PAA outer shell of H40-(PCL)₁₀-(PAA)₇₀ is in the glassy state (T_g around 110 °C). The restricted motion may retain the fragrance compounds. In H40-(PBMA)₃₇-(PPEGMA)₃₉, on the other hand, the PBMA core and the outer PPEGMA shell are in the rubbery state owing to the low T_{gs} (around -64 and 12 °C). However, H40-(PBMA)₃₇-(PPEGMA)₃₉ remains effective in extending the time over which the fragrances evaporate (Figure VIII.6). To compare further the star-block copolymers, the kinetic curve from 0 to 60 minutes must be considered. Under

the present conditions, no significant differences were observed (Figure VIII.6 to Figure VIII.9) illustrating that not only thermal properties but also other parameters (solubility in water, affinity with surface deposition) influence the release of fragrances.

Human olfactory thresholds have been used to assess the effect of the polymer on the release of fragrance molecules. Human olfactory thresholds are available for benzyl acetate and decanal.^[314] In the case of decanal, as shown in Figure VIII.7, the presence of H40-(PBMA)₃₇-(PPEGMA)₃₉ and H40-(PCL)₁₀-(PAA)₇₀ increased the human perception time from 40 minutes (for decanal alone) to more than 60 minutes under the conditions of the measurement. In the case of benzyl acetate (Figure VIII.6), the human perception time was increased from 5.6 minutes to 8.1 and 8.8 minutes in the presence of H40-(PCL)₁₀-(PAA)₇₀ and H40-(PBMA)₃₇-(PPEGMA)₃₉ respectively. These experiments confirm the efficiency of the star-block copolymers, in terms of a criterion of direct relevance to the application.

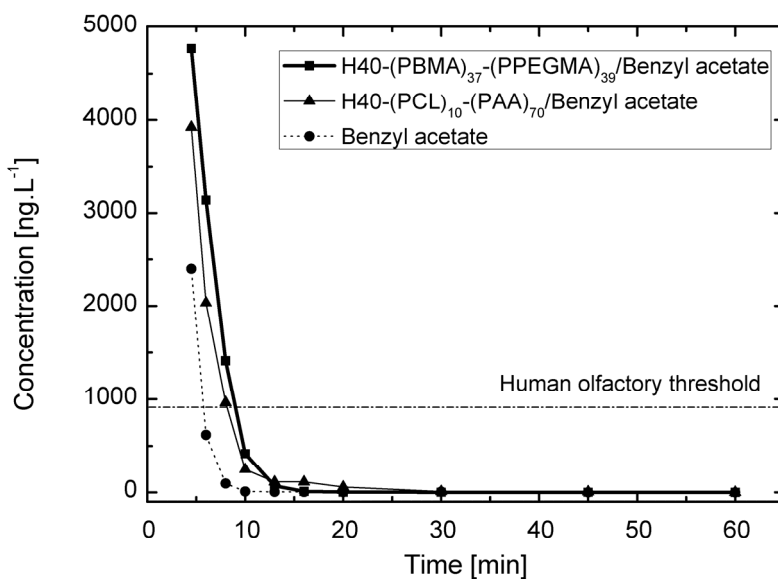


Figure VIII.6 Release of benzyl acetate in the presence of H40-(PCL)₁₀-(PAA)₇₀ or H40-(PBMA)₃₇-(PPEGMA)₃₉ and comparison with the release of benzyl acetate alone

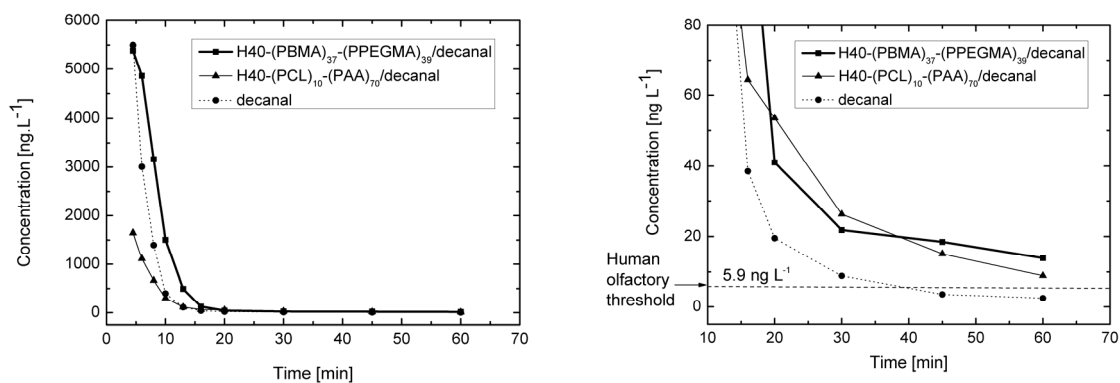


Figure VIII.7 Release of decanal in the presence of H40-(PBMA)₃₇-(PPEGMA)₃₉ or H40-(PCL)₁₀-(PAA)₇₀ and comparison with the release of decanal alone (left). Detail with an indication of the human olfactory threshold (right)

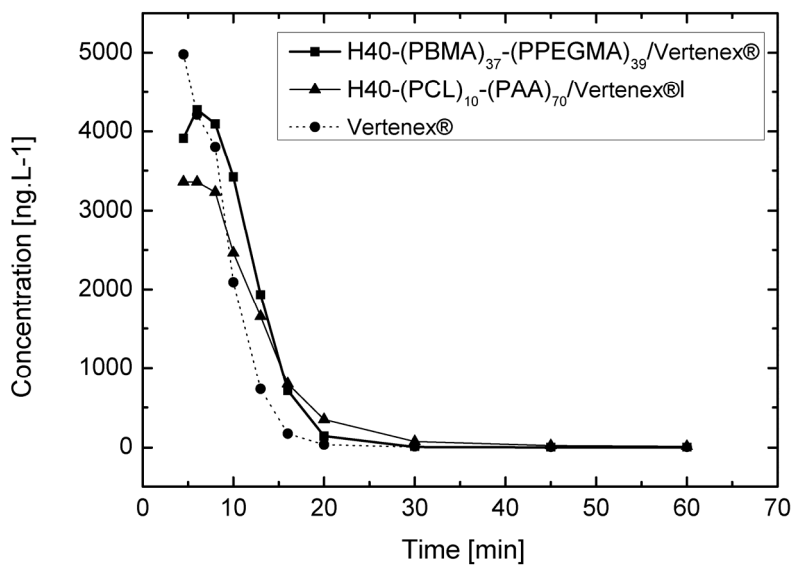


Figure VIII.8 Release of Vertenex® in the presence of H40-(PBMA)₃₇-(PPEGMA)₃₉ or H40-(PCL)₁₀-(PAA)₇₀ and comparison with the release of Vertenex® alone

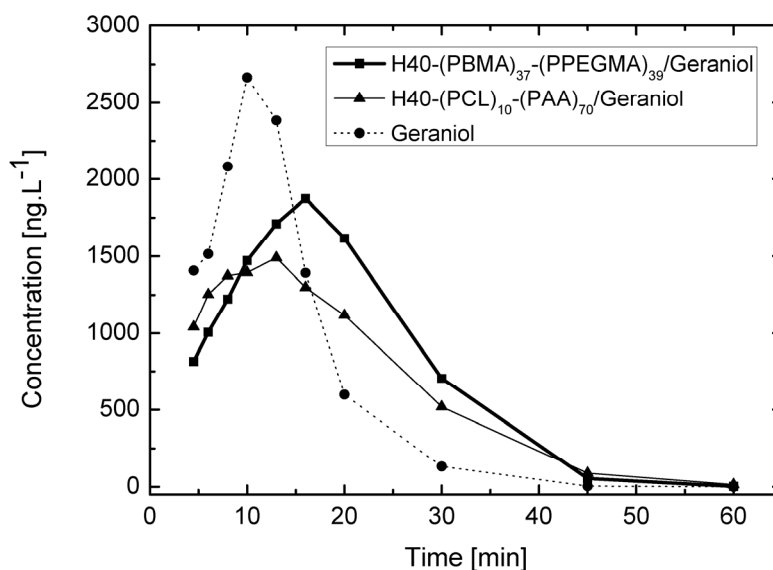


Figure VIII.9 Release of geraniol in the presence of H40-(PBMA)₃₇-(PPEGMA)₃₉ or H40-(PCL)₁₀-(PAA)₇₀ and comparison with the release of geraniol alone

II.3. A fabric softener application

The behavior of the pH-dependent star-block copolymer in a softener base is important for the protection of the fragrance molecule during storage (at low pH) as well as for its release once deposited on the target surface (after an increase of the pH at the end of the washing cycle).

A towel was immersed in a water solution that contained a softener and the perfume/star-block copolymer mixture or the perfume alone. In this case the perfume was composed of an equimolar amount of four fragrance compounds: benzyl acetate, benzylacetone, 4-cyclohexyl-2-methyl-2-butanol and allyl-3-cyclohexylpropanoate as it was detailed in the experimental section (Chapter IV.IV.2.2). After wringing, the towel was placed in the headspace sampling cell thermostatted at 25 °C and exposed to a constant air flow under humidity control. The fragrance compounds were for 5 minutes each 50 minutes adsorbed onto cartridges which were then desorbed thermally in a desorber and analyzed with

a GC equipped with a FID detector. The concentration (ng L^{-1}) of the fragrance molecule was determined as a function of time (min).

Figure VIII.10 compares the release of benzyl acetate in the H40-(PBMA)₃₇-(PPEGMA)₃₉ or H40-(PCL)₁₀-(PAA)₇₀. The release of benzyl acetate in the absence of the copolymers is also shown. At the beginning of the measurement a higher headspace concentration were measured in the absence of the amphiphilic star-block copolymer. Nevertheless, at the end of the experiment all headspace concentrations were higher in the presence of the copolymer, demonstrating the desired improvement in long-lastingness of the fragrance compound. However, the concentrations of benzyl acetate detected under the conditions of the measurement were always below the human olfactory threshold (around 912.0 ng L^{-1}). This effect could be explained by the relative humidity. It has been observed that the loss of volatiles increases with increasing humidity owing to the increase in mobility and in diffusion coefficient.^[90] Moreover, the partial solubility of benzyl acetate in water contributes to its fast release (under the conditions of the measurement the towel was initially immersed in 600 mL water and the fabric softener also contained more than 83 % water). This explanation is support by the results obtained in the case of allyl 3-cyclohexylpropanoate ($\log P$ value of 3.85 as opposed to 1.96 for benzyl acetate). The initial concentration of allyl 3-cyclohexylpropanoate was five times greater than that of benzyl acetate.

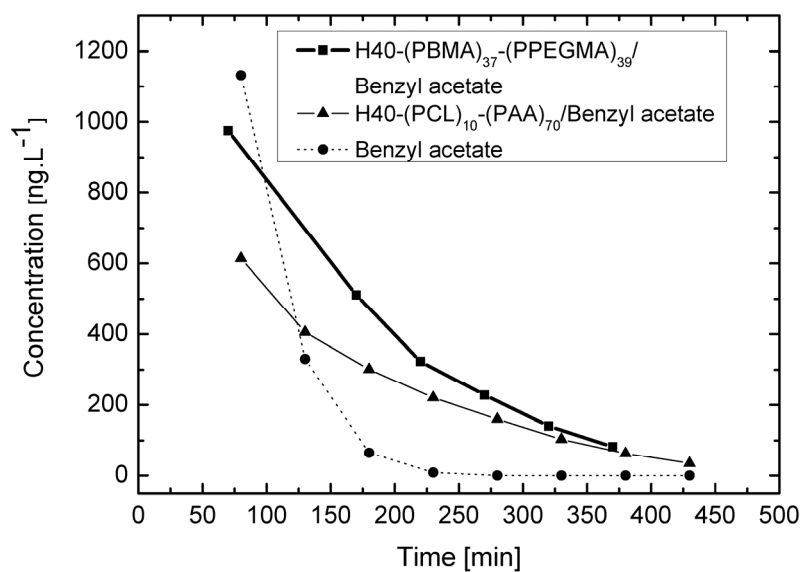


Figure VIII.10 Release of benzyl acetate in a fabric softener in the presence of the amphiphilic star-block copolymers and without the copolymer

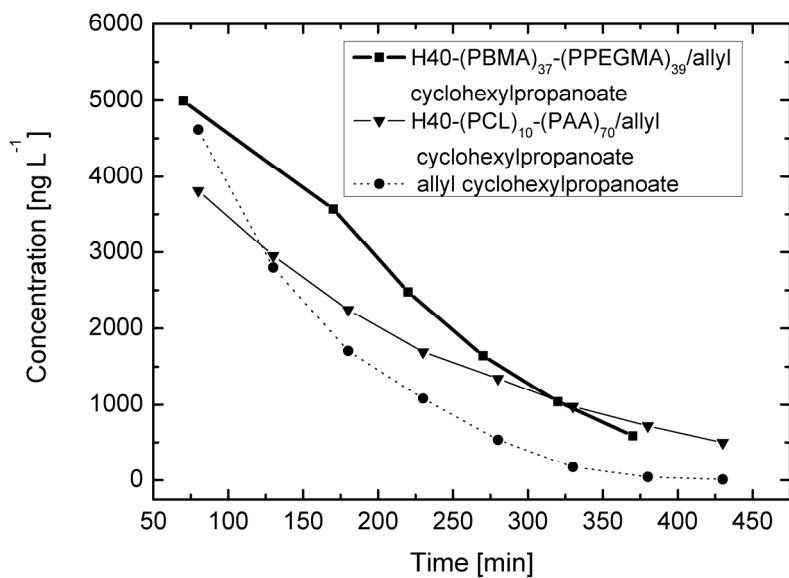


Figure VIII.11 Release of allyl 3-cyclohexylpropanoate in a fabric softener in the presence of the amphiphilic star-block copolymers and without the copolymer

To compare the data, the concentration of each fragrance compound present in the perfume was determined after 370 minutes for H40-(PCL)₁₀-(PAA)₇₀ and H40-(PBMA)₃₇-(PPEGMA)₃₉ (Table VIII.3). The concentration of each fragrance compound was generally higher in the presence of the star-block copolymers after 370 min, illustrating the long-lastingness effect of the star-block copolymer in a fabric softener application. After 370 minutes, the concentration of benzyl acetate, benzyl acetone and 4-cyclohexyl-2-methyl-2-butanol are higher in the presence of H40-(PBMA)₃₇-(PPEGMA)₃₉ in comparison with H40-(PCL)₁₀-(PAA)₇₀. After the immersion of the towel in water, the H40-(PCL)₁₀-(PAA)₇₀ nanocapsules are partially ionized inducing partially desorption of the polymer from the cotton towel. The conformational change of the polymer in aqueous solutions may explained the lower volatiles concentrations in the case of H40-(PCL)₁₀-(PAA)₇₀.^[273]

Table VIII.3 Headspace concentration measured after 370 minutes equilibration in the presence and the absence of H40-(PCL)₁₀-(PAA)₇₀ and of H40-(PBMA)₃₇-(PPEGMA)₃₉

	without polymer [ng L ⁻¹]	in the presence of H40-(PCL) ₁₀ -(PAA) ₇₀ [ng L ⁻¹]	in the presence of H40-(PBMA) ₃₇ -(PPEGMA) ₃₉ [ng L ⁻¹]
Benzyl acetate	0.0	70.0	82.1
Benzylacetone	150.0	147.0	298.2
4-cyclohexyl-2-methyl-2-butanol	180.0	500.0	837.2
Allyl-3-cyclohexylpropanoate	60.0	770.0	588.1

II.4. Olfactory panel

To take into account further the human olfactory threshold, an olfactory panel for fine perfumery was set up. A perfume solution (composed of 15 olfactory compounds) provided by Firmenich SA and adapted for this kind of measurement was investigated with and without H40-(PCL)₁₀-(PAA)₁₁₅ in the following proportions: 10 wt % perfume, 1 wt % polymer, 80 wt % ethanol and 9 wt % water. 4 days after the deposition of one droplet of each solution on two different blades of glass, 17 panellists smelt the two samples successively. In

16 cases, perception of the perfume was significantly stronger in the sample that contained the polymer. This test is another very encouraging result which corroborates the TGA and headspace analyses, and confirms the interest of these new star-block copolymers for fragrance applications.

III. Conclusions

Controlled release depends on the kind of the application. Some times it is important to have a blooming effect just after introducing the capsules into a medium, and sometimes not. In this work the emphasis has been on attaining constant release rates over extended periods of time. The aim is to prolong perception throughout the duration of the application.

The evaporation of fragrance molecules in a fine perfumery or a fabric softener application, in the presence of the star-block copolymers, is significantly delayed in comparison with the measurements in the presence of H40 precursor or in the absence of polymer. In the fine perfumery application, no significant differences in the release of the fragrance molecules were observed for H40-(PBMA)₃₇-(PPEGMA)₃₉ and H40-(PCL)₁₀-(PAA)₇₀. In the case of the softener application, lower concentrations were detected in the presence of pH-responsive nanocapsules (H40-(PCL)₁₀-(PAA)₇₀) owing to structural changes in the polymer structure.

The efficiency of the star-block copolymer is clearly demonstrated in the case of decanal whose concentration remains above the human olfactory threshold throughout the measurements. Olfactory panels, which only use human olfactory threshold, confirmed the practical interest of the star-block copolymers.

Chapter IX. Conclusions and future work

In this work, amphiphilic multi-arm star-block copolymers $\text{HBP-(PCL)}_p\text{-(PAA)}_q$ and $\text{H40-(PBMA)}_{37}\text{-(PPEGMA)}_{39}$ have successfully been synthesized using hyperbranched polyester polyol polymers, H30 and H40, with 26 and 36 functional groups respectively. These highly branched block copolymers were obtained by the combination of ROP and ATRP for $\text{HBP-(PCL)}_p\text{-(PAA)}_q$ or by two consecutive ATRP of methacrylate monomers, in the case of $\text{H40-(PBMA)}_{37}\text{-(PPEGMA)}_{39}$. A 2-bromoisobutyryl bromide was used as the macroinitiator for the ATRP, which allowed the preparation of star polymers with good control of the molecular weight distribution. In the case of $\text{HBP-(PCL)}_p\text{-(PAA)}_q$, *tert*-butyl acrylate monomer was polymerized by ATRP, and then the *tert*-butyl groups were hydrolyzed to form an amphiphilic $\text{HBP-(PCL)}_p\text{-(PAA)}_q$, which was dispersible in water after deprotonation of the carboxylic acid with sodium hydrogenocarbonate. The core-shell architecture resulted in a microphase separated structure, with a dense core in aqueous solution, and a highly mobile hydrophilic shell in both $\text{HBP-(PCL)}_p\text{-(PAA)}_q$ and $\text{H40-(PBMA)}_{37}\text{-(PPEGMA)}_{39}$.

The capacity of these star-block copolymers to encapsulate fragrance molecules in aqueous solution has been demonstrated by different types of NMR measurement. Encapsulation in water is shown to correspond to a dynamic equilibrium between the free molecules and the host-guest complex. The fragrance molecules are preferentially localized in the hydrophobic block of the core-shell polymer to an extent that depends on the octanol-water partition coefficient, $\log P$. Loadings of up to 30 wt% of fragrance molecules have been measured in the polymers in aqueous dispersion, depending on the affinity between the hydrophobic block and the fragrance compound, as reflected by solubility parameter analysis. However, the various factors that influence the fragrance loadings in the polymer ($\log P$, the volatility of the fragrance molecules, the water solubility of the polymer, the affinity between the polymer and the fragrance, the temperature, the concentration etc.) are interdependent, making it difficult to identify general trends.

The amphiphilic star-block copolymers are nevertheless shown to influence strongly the release of the fragrance compounds under conditions representative of a fine perfumery and a softener application, as determined by TGA and headspace analysis (Figure IX.1). The release of fragrance molecules in the fine perfumery application appears relatively insensitive to the choice of star-block copolymer, whereas in the softener base application slight differences were observed, which may be explained by the particular property of the pH-responsive polymer.

Finally, a panel of 17 panellists, reported their impression after smelling a perfume in the presence and the absence of the polymer and confirmed the capacity of the amphiphilic star-block copolymer to delay and prolong the human perception of a mixture of fragrance compounds, consistent with the analytical results.

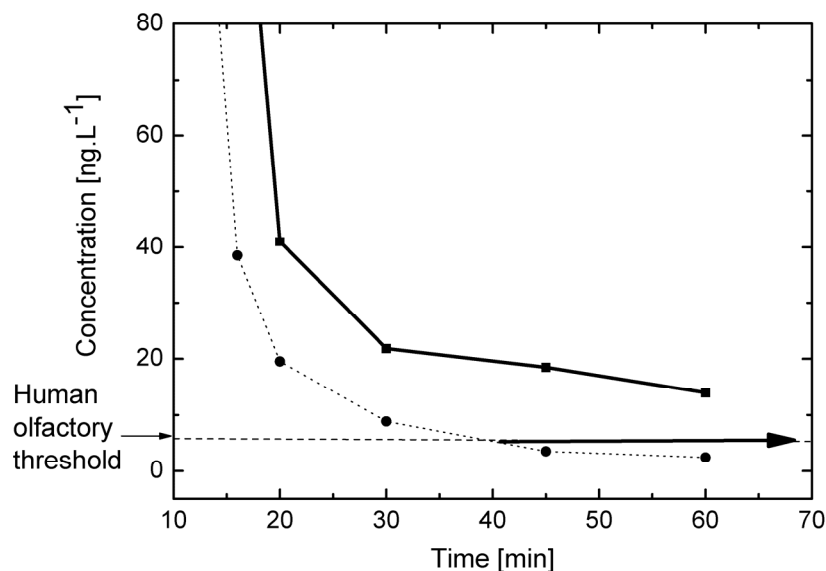


Figure IX.1 As a function of the human olfactory threshold (---): Efficient controlled release of decanal in the presence of H40-(PBMA)₃₇-(PPEGMA)₃₉ (—) in comparison with decanal alone (...) (headspace analysis result)

Given that the solubility parameter approach is shown to be useful in predicting the host guest affinity, the hydrophobic core may in principle be tailored according to the guest to be encapsulated, offering considerable promise for developing systems that target specific volatiles. However, the results also show that it is difficult to prolong evaporation of highly volatile fragrance molecules with the present systems, even in the presence of a glassy shell, as in HBP-(PCL)_p-(PAA)_q, and many other factors may need to be taken into account, including not only the volatility of the fragrances, but also the humidity and surfactant concentration, the phase behaviour of the polymer, and the polymer-substrate interactions. Cross-linking of the PAA blocks may be one possible way of increasing the barrier properties of the nanocapsules with respect to volatile guest molecules.

With regard to potential applications, the star-block copolymers prepared in the present work may also be useful in stabilizing commercial formulations in a similar manner to conventional surfactants. Moreover, their high functionality renders them extremely adaptable

to specific conditions through suitable end-group modification. Thus, whatever the perfumery application (softener, detergent, lotion, cream etc.), the star-block copolymers may in principle act both as stabilizers and encapsulants. Indeed, the absence of the surfactant micelles in practical formulations may improve the retention of the volatiles in the star-block copolymer, increasing the long-lastingness effect. Finally, the relatively low raw materials costs and straightforward chemistry means the present concept can provide cost effective solutions for industry, which represents a considerable advantage vis-à-vis dendrimer-based technologies, for example.

Chapter X. Appendix

Appendix 1

Encapsulation techniques used until now

Spray drying, spray chilling, spray cooling and fluidized bed methods consist of forming an emulsion between the active substance (flavor, fragrance...) and an aqueous solution of the polymer. The emulsion is dried by atomization in an enclosure equipped with an air flow. The nomenclature depends on the air flow temperature: spray drying ($T = 180\text{-}200\text{ }^{\circ}\text{C}$), spray cooling ($T = 45\text{-}122\text{ }^{\circ}\text{C}$), spray chilling ($T = 32\text{-}42\text{ }^{\circ}\text{C}$). A fine powder between 20-100 μm is obtained. The fluidized bed method is based on the same principle, but with a second particle agglomeration step that gives large uniform particles between 200-2000 μm in diameter. 20 to 50 % loads are typically obtained with atomization techniques. The emulsion quality, the type of polymer, the drying conditions are important parameters. It has been demonstrated that spray drying gives good results with a wide variety of polymers. Moreover it may be used with a wide variety of active molecules and is relatively cheap. However, the lack of protection against oxidation leads to short life times.^[68]

The coacervation method consists of the precipitation of the polymer induced by solid particles of the active molecules. In “complex coacervation”, micro-particles are formed using two polymers and in complex coacervation with pH adjustment two polymers with opposite charges are used. The load is between 25 and 97 %. This technique is not expensive and the resulting particles have long lifetimes. However, their size is not well controlled and is relatively large (20-1000 μm), which can induce instability. Use of crosslinking agent can be considered as a means to improve stability of the particles.

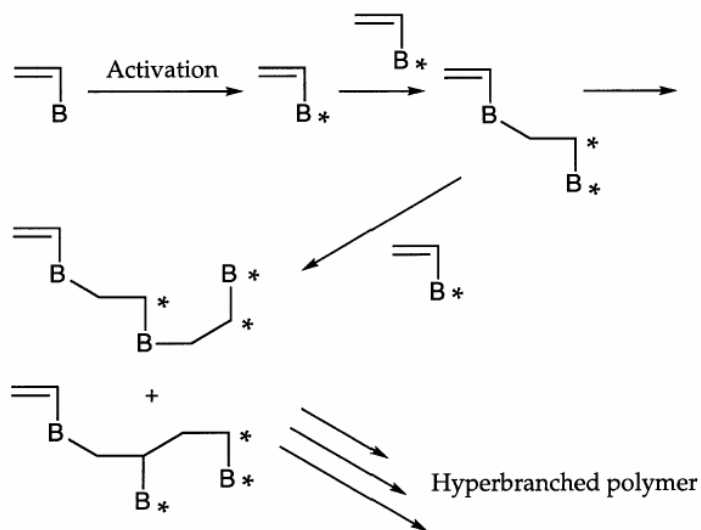
Extrusion consists of mixing polymers and flavors (essential oils) and then passing them through an extrusion die into a bath that contains a non solvent for the polymer. After a rapid solidification, the extrudates are cut into 1 mm long granules. The main advantage of this technique is that the flavors are totally protected by the polymer. The lifetime of the particles is long, with good protection against oxidation. However, only 8 to 10 % loading is possible. This method was developed for the encapsulation of citrus oil^[3] and is very often used for drinks and lyophilized foods that have to be solubilized in water before use.

Appendix 2

Two other methods used for the preparation of hyperbranched polymers

Self condensing vinyl polymerization

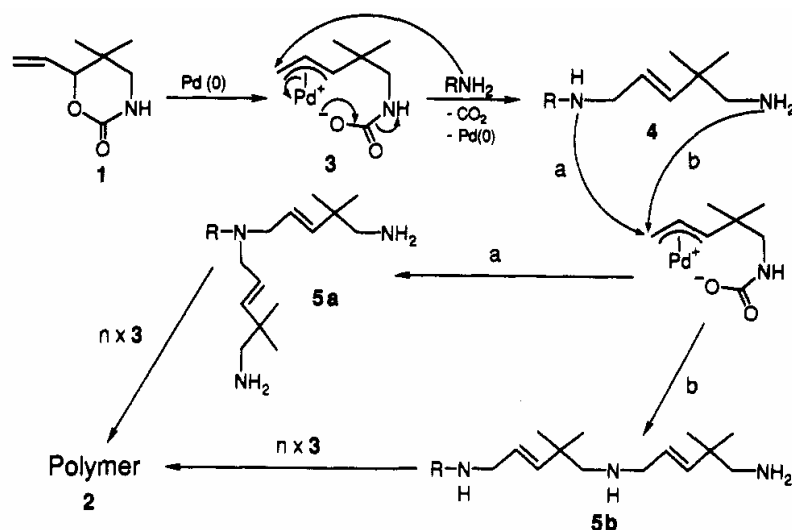
Self-condensing vinyl polymerization of an AB^* type monomers as been developed by Fréchet et al.^[315] in 1995. This consists of the activation of a group associated with a double bond, which reacts with the double bond of a second AB^* monomer to give a covalent bond and a new active site on the carbon of the double bond. This second activated site creates branching as illustrated below. Poly(styrene) and poly(meth)acrylate hyperbranched polymers have been obtained by this technique.



Self-condensing vinyl polymerization of an AB^* monomer^[113]

Multi-branching ring-opening polymerization

The present strategy for the preparation of HBPs was developed by Suzuki in 1992, who synthesized hyperbranched poly(amine) from cyclic carbamate^[316] by ring-opening multi-branch polymerization (ROMBP). Branch points are generated through the propagation step. The reaction is induced by the addition of an initiator to the latent AB_x monomer. Cyclic carbamate, epoxide, oxetane and caprolactone have been used for the preparation of HBPs by this method.



Ring-opening multi-branch polymerization for the preparation of hyperbranched poly(amine)^[316]

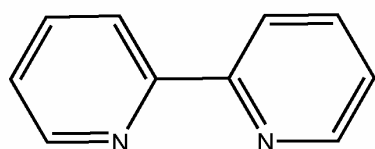
Appendix 3

Schematic representation of the ligands used in ATRP process

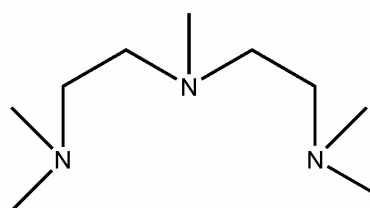
PMDETA: pentamethyl diethylene triamine

HMTETA: hexamethyl triethylene tetramine

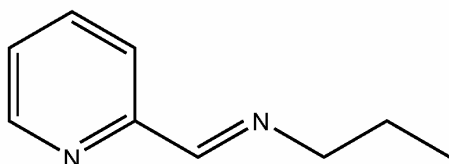
Me₆ TREN: tris-2-dimethyl aminoethyl amine



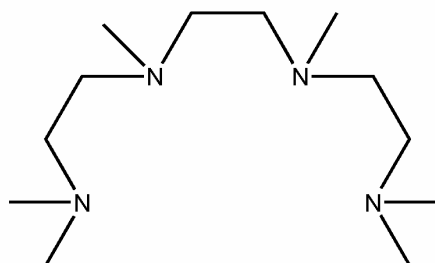
2,2'-bipyridyl



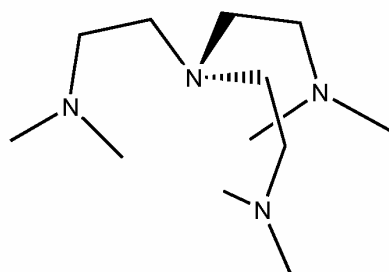
PMDETA



N-propyl-2- pyridylmethanimine



HMTETA

Me₆TREN

Appendix 4

Procedure for the polymerization of n-butyl methacrylate and poly(ethylene glycol methyl ether methacrylate) on H40 based hyperbranched polymer

Polymerization of n-butyl methacrylate using H40-Br as macroinitiator to give H40-(PBMA)_p
A flask equipped with a nitrogen inlet was charged with the macroinitiator H40-Br, toluene, n-butyl methacrylate, CuBr and N-propyl-2-pyridylmethanimine. The mixture was subsequently deoxygenated by three freeze pump-thaw cycles. Polymerization was carried out in a thermostatically controlled oil bath at 60 °C. After 140 min, the reaction mixture was cooled in an ice bath. The catalyst complex was removed by suction filtration of the reaction mixture through a layer of silica gel (ca. 3 cm) using a small quantity of toluene to rinse the column. The resulting polymer solution was partially evaporated and finally precipitated into methanol (20 times the volume of the reaction mixture). The precipitate was dried under vacuum.

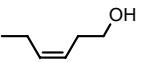
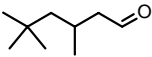
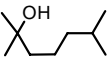
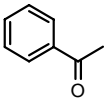
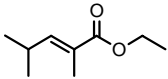
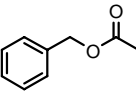
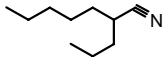
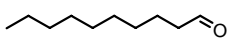
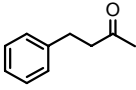
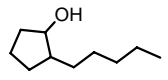
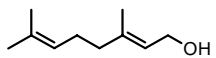
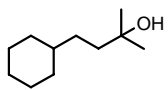
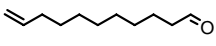
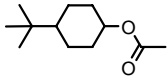
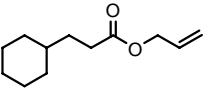
Polymerization of n-butyl methacrylate using H40-(PBMA)_p-Br as macroinitiator to give H40-(PBMA)_p-(PPEGMA)_q

A flask equipped with a nitrogen inlet was charged with CuBr and poly(ethylene glycol) methyl ether methacrylate (PEGMA). After degassing by bubbling nitrogen through the mixture for 30 minutes, N-propyl-2-pyridylmethanimine was added and degassing was continued for another 15 min. After that, a previously degassed solution of H40-(PBMA)_p in toluene was added, and nitrogen purging was continued for 15 min. Finally, the reaction flask was placed in a thermostatically controlled oil bath at 60 °C. After 5 h, the polymerization was stopped by cooling the reaction mixture to 0 °C. The catalyst was removed by suction filtration through a layer of silica gel (~ 3 cm) using toluene to rinse the column. Subsequently, toluene was evaporated from the resulting polymer solution. The polymer was isolated and purified by repeated precipitation into diethyl ether (20 times the volume of the reaction mixture). Further purification was carried out by dialysis in water (molecular weight cut off = 10,000 g mol⁻¹).

Appendix 5

Physico chemical properties of the fragrance molecules used in headspace analysis

The values were calculated by J.-Y. de Saint Laumer (Firmenich SA) using the EPIwin v 3.10 program (US Environmental Protection Agency, 2000)

Name	Structure	LogP	Vapor pressure at 20 °C (Pa)	Volatility ($\mu\text{g L}^{-1}$)
Pipol		1.49	283.27	4100.3
3,5,5-Trimethylhexanal		3.35	251.52	6393.8
Dimetol		3.14	137.71	3023.6
Acetophenone		1.74	43.8	583.1
Ethyl (<i>E</i>)-2,4-dimethyl-2-pentenoate		3.24	-	-
Benzyl acetate		1.96	24.9	500
Jasmonitrile		4.84	27.6	546.7
Decanal		3.76	31.3	528
Benzylacetone		1.89	8.4	107.9
2-Pentylcyclopentanol		3.38	1.3	-
Geraniol		3.47	2.1	93
4-Cyclohexyl-2-methyl-2-butanol		3.75	1.3	174.9
10-Undecenal		4.12	9.9	188.3
Vertenex®		4.42	9.1	200
Allyl 3-cyclohexylpropanoate		3.85	3.5	67.2

Chapter XI. References

- [1] F. Basset, C. Chavigny, *Encapsulation des parfums Une croissance exponentielle*, Parfums cosmétiques actualités, **2003**, 86
- [2] L. Brannon-Peppas, *Controlled Release in the Food and Cosmetics Industries in Polymeric Delivery Systems, Properties and Applications* (Eds.: M. A. El-Nokaly, D. M. Piatt, B. A. Charpentier), ACS Symposium Series, San Francisco, **1993**
- [3] B. F. Gibbs, S. Kermasha, I. Alli, C. N. Mulligan, *Encapsulation in the food industry: a review*, International Journal of Food Science and Nutrition, **1999**, 50, 213
- [4] C. Quellet, M. Schudel, R. Ringgenberg, *Flavors and Fragrance Delivery Systems*, Chimia, **2001**, 55, 421
- [5] S.-J. Park, R. Arshady, *Microcapsules for Fragrances and Cosmetics*, Microspheres, Microcapsules, Liposomes, **2003**, 6, 157
- [6] R. Duncan, *The dawning era of polymer therapeutics*, Nature Reviews Drug Discovery, **2003**, 2, 347
- [7] A. J. M. D'Souza, E. M. Topp, *Release from polymeric prodrugs: Linkages and their degradation*, Journal of Pharmaceutical Sciences, **2004**, 93, 1962
- [8] Y. Tang, S. Y. Liu, S. P. Armes, N. C. Billingham, *Solubilization and Controlled Release of a Hydrophobic Drug Using Novel Micelle-Forming ABC Triblock Copolymers*, Biomacromolecules, **2003**, 4, 1636

-
- [9] H. M. Aliabadi, A. Mahmud, A. D. Sharifabadi, A. Lavasanifar, *Micelles of methoxy poly(ethylene oxide)-b-poly(L-lactide) as vehicles for the solubilization and controlled delivery of cyclosporine A*, Journal of Controlled Release, **2005**, *104*, 301
- [10] S. A. Hagan, A. G. A. Coombes, M. C. Garnett, S. E. Dunn, M. C. Davies, L. Illum, S. S. Davis, S. E. Harding, S. Purkiss, P. R. Gellert, *Poly(lactide)-Poly(ethylene glycol) Copolymers as Drug Delivery System. I Characterization of Water Dispersible Micelle-Forming Systems*, Langmuir, **1996**, *12*, 2153
- [11] K. Kataoka, G. S. Kwon, M. Yokoyama, T. Okano, Y. Sakurai, *Block copolymer micelles as vehicles for drug delivery*, Journal of Controlled Release, **1993**, *24*, 119
- [12] M.-H. Dufresne, E. Fournier, M.-C. Jones, M. Ranger, J.-C. Leroux, *Block copolymer micelles-engineering versatile carriers for drugs and biomacromolecules*, Bull. Tech. Gattefosse, **2003**, *96*, 87
- [13] L. Tao, K. E. Uhrich, *Novel amphiphilic macromolecules and their in vitro characterization as stabilized micellar drug delivery systems*, Journal of Colloid and Interface Science, **2006**, *298*, 102
- [14] G. R. Newkome, C. N. Moorefield, F. Vögtle, *Dendrimers and Dendrons - Concepts, Syntheses, Applications*, Wiley-VCH, Weinheim, **2001**
- [15] *Dendrimers and Other Dendritic Polymers*, (Eds.: J. M. J. Fréchet, D. A. Tomalia), Wiley Series in Polymer Science, Wiley, Chichester, **2001**
- [16] M. Krämer, J.-F. Stumbé, H. Türk, S. Krause, A. Komp, L. Delineau, S. Prokhorova, H. Kautz, R. Haag, *pH-Responsive Molecular Nanocarriers Based on Dendritic Core-Shell Architectures*, Angewandte Chemie International Edition, **2002**, *41*, 4252
- [17] A. W. Bosman, H. M. Janssen, E. W. Meijer, *About Dendrimers: Structure, Physical Properties, and Applications*, Chemical Reviews, **1999**, *99*, 1665
- [18] G. R. Newkome, C. N. Moorefield, G. R. Baker, M. J. Saunders, S. H. Grossman, *Unimolecular Micelles*, Angewandte Chemie International Edition, **1991**, *30*, 1178
- [19] C. J. Hawker, K. L. Wooley, J. M. J. Fréchet, *Unimolecular Micelles and Globular Amphiphiles: Dendritic Macromolecules as Novel Recyclable Solubilization Agents*, Journal of the Chemical Society Perkin Transaction 1, **1993**, 1287
- [20] H. Liu, A. Jiang, J. Guo, K. E. Uhrich, *Unimolecular Micelles: Synthesis and Characterization of Amphiphilic Polymer Systems*, Journal of Polymer Science, Part A: Polymer Chemistry, **1999**, *37*, 703
-

-
- [21] C. N. Moorefield, G. R. Newkome, *Unimolecular micelles: supramolecular use of dendritic constructs to create versatile molecular containers*, *Comptes Rendus Chimie*, **2003**, *6*, 715
- [22] M. A. R. Meier, J.-F. Gohy, C.-A. Fustin, U. S. Schubert, *Combinatorial Synthesis of Star-Shaped Block Copolymers: Host-Guest Chemistry of Unimolecular Reversed Micelles*, *Journal of the American Chemical Society*, **2004**, *126*, 11517
- [23] J. Zou, Y. Zhao, W. Shi, *Encapsulation mechanism of molecular nanocarriers based on unimolecular micelle forming dendritic core-shell structural polymers*, *Journal of Physical Chemistry B*, **2006**, *110*, 2638
- [24] J.-T. Simonnet, P. Richart, *Nanocapsules based on dendritic polymers*, **2002**, US 6,379,683 B1
- [25] M. W. P. L. Baars, E. W. Meijer, *Host-Guest Chemistry of Dendritic Molecules*, *Topics in Current Chemistry*, **2000**, *210*, 131
- [26] M. Liu, K. Kono, J. M. J. Fréchet, *Water-soluble dendritic unimolecular micelles: Their potential as drug delivery agents*, *Journal of Controlled Release*, **2000**, *65*, 121
- [27] M. T. Morgan, M. A. Carnahan, C. E. Immoos, A. A. Ribeiro, S. Finkelstein, S. J. Lee, M. W. Grinstaff, *Dendritic Molecular Capsules For Hydrophobic Compounds*, *Journal of the American Chemical Society*, **2003**, *125*, 15485
- [28] H. Namazi, M. Adell, *Dendrimers of citric acid and poly (ethylene glycol) as the new drug-delivery agents*, *Biomaterials*, **2005**, *26*, 1175
- [29] D. K. Smith, F. Diederich, *Supramolecular Dendrimer Chemistry: A Journey Through the Branched Architecture*, *Topics in Current Chemistry*, **2000**, *210*, 183
- [30] S. C. Zimmerman, L. J. Lawless, *Supramolecular Chemistry of dendrimers*, *Topics in Current Chemistry*, **2001**, *217*, 95
- [31] S. E. Stiriba, H. Frey, R. Haag, *Dendritic Polymers in Biomedical Applications: From Potential to Clinical Use in Diagnostics and Therapy*, *Angewandte Chemie International Edition*, **2002**, *41*, 1329
- [32] J. J. Fréchet, R. H. Ihre, *Dendritic support or carrier macromolecule*, **2002**, WO0226867
- [33] M. Jikei, M.-A. Kakimoto, *Hyperbranched polymer: a promising new class of materials*, *Progress in Polymer Science*, **2001**, *26*, 1233
-

-
- [34] C. R. Yates, W. Hayes, *Synthesis and applications of hyperbranched polymers*, European Polymer Journal, **2004**, *40*, 1257
- [35] C. J. G. Plummer, L. Garamszegi, Y. Leterrier, M. Rodlert, J. A. E. Månson, *Hyperbranched Polymer Layered Silicate Nanocomposites*, Chemistry of Materials, **2002**, *14*, 486
- [36] C. J. G. Plummer, L. Garamszegi, T. Q. Nguyen, M. Rodlert, J.-A. E. Månson, *Templating Porosity in Polymethylsilsesquioxane Coatings using Trimethylsilylated Hyperbranched Polymers*, Journal of Materials Science, **2002**, *37*, 4819
- [37] R. Mezzenga, A. Luciani, J. A. E. Månson, *Phase Separation and Gelation of Epoxy Resin/Hyperbranched Polymer Blends*, Polymer Engineering and Science, **2002**, *42*, 249
- [38] M. Rodlert, H. J. M. Grünbauer, C. J. G. Plummer, J. A. E. Månson, *Hyperbranched Polymer/Clay nanocomposites*, Advanced Engineering Materials, **2004**, *6*, 715
- [39] M. Rodlert, C. J. G. Plummer, L. Garamszegi, Y. Leterrier, H. J. M. Grünbauer, J.-A. E. Månson, *Hyperbranched polymer/montmorillonite clay nanocomposites*, Polymer, **2004**, *45*, 949
- [40] M. Rodlert, C. J. G. Plummer, Y. Leterrier, J. A. E. Månson, H. J. M. Grünbauer, *Rheological behavior of hyperbranched polymer/montmorillonite clay nanocomposites*, Journal of Rheology, **2004**, *48*, 1049
- [41] E. Malmström, M. Johansson, A. Hult, *Hyperbranched Aliphatic Polyesters*, Macromolecules, **1995**, *28*, 1698
- [42] C. J. Hawker, R. Lee, J. M. J. Fréchet, *One-step synthesis of hyperbranched dendritic polyesters*, Journal of the American Chemical Society, **1991**, *113*, 4583
- [43] L. Garámszegi, T. Q. Nguyen, C. J. G. Plummer, J.-A. E. Månson, *Characterization of Hyperbranched Aliphatic Polyesters and Their Trimethylsilylated Derivatives by GPC-Viscometry*, Journal of Liquid Chromatography and Related Technologies, **2003**, *26*, 203
- [44] A. Luciani, C. J. G. Plummer, T. Q. Nguyen, L. Garamszegi, J.-A. E. Månson, *Rheological and physical properties of aliphatic hyperbranched polyesters*, Journal of Polymer Science, Part B: Polymer Physics, **2004**, *42*, 1218
- [45] C. J. G. Plummer, A. Luciani, T. Q. Nguyen, L. Garamszegi, M. Rodlert, J.-A. E. Månson, *Rheological characteristics of hyperbranched polyesters*, Polymer Bulletin, **2002**, *49*, 77
-

-
- [46] C. Ternat, G. Kreutzer, C. J. G. Plummer, T. Q. Nguyen, A. Herrmann, L. Ouali, H. Sommer, W. Fieber, M. I. Velazco, H.-A. Klok, J.-A. E. Månson, *Amphiphilic Multi-arm Star-Block Copolymers for Encapsulation of Fragrance Molecules*, *Macromolecular Chemistry and Physics*, **2007**, *208*, 131
- [47] L. Ouali, A. Herrmann, C. Ternat, C. J. G. Plummer, H.-A. Klok, G. Kreutzer, J.-A. E. Månson, H. Sommer, M. I. Velazco, *Amphiphilic Star Block copolymers*, **2006**, WO 2006/038110 A2
- [48] G. Kreutzer, C. Ternat, T. Q. Nguyen, C. J. G. Plummer, J.-A. E. Månson, V. Castelletto, I. W. Hamley, F. Sun, S. S. Sheiko, A. Herrmann, L. Ouali, H. Sommer, W. Fieber, M. I. Velazco, H.-A. Klok, *Water-soluble, Unimolecular Containers Based on Amphiphilic Multiarm Star Block Copolymers*, *Macromolecules*, **2006**, *39*, 4507
- [49] K. Hoste, K. D. Winne, E. Schacht, *Polymeric prodrugs*, *International Journal of Pharmaceutics*, **2004**, *277*, 119
- [50] D. Berthier, A. Trachsel, C. Fehr, L. Ouali, A. Herrmann, *Amphiphilic polymethacrylate- and polystyrene-based chemical delivery systems for damascones*, *Helvetica Chimica Acta*, **2005**, *88*, 3089
- [51] R. Göller, J. P. Vors, A. M. Caminade, J. P. Majoral, *Phosphorous dendrimers as new tools to deliver active substances*, *Tetrahedron Letters*, **2001**, *42*, 3587
- [52] G. R. Newkome, Z. Q. Yao, G. R. Baker, V. K. Gupta, *Cascade Molecules: A New Approach to Micelles.*, *Journal of Organic Chemistry*, **1985**, *50*, 2003
- [53] D. A. Tomalia, H. Baker, J. Dewald, M. Hall, G. Kallos, J. R. Martin, J. Ryder, P. Smith, *A new Class of Polymers-Starbust-Dendritic Macromolecules*, *Polymer Journal*, **1985**, *17*, 117
- [54] S. J. Risch, G. A. Reineccius, *Encapsulation and Controlled release of Food Ingredients*, (Eds.:S. J. Risch, G. A. Reineccius), ACS Symposium Series, Chicago, **1995**
- [55] W. M. McKernan, *Microencapsulation in the flavour industry*, *Flavour Industry*, **1972**, *3*, 596
- [56] F. Shahidi, X.-Q. Han, *Encapsulation of Food Ingredients*, *Critical Reviews in Food Science and Nutrition*, **1993**, *33*, 501
- [57] B. Green, **1956**, U.S. 2,730,456
- [58] A. M. Van Herk, A. L. German, *Microencapsulated pigments and fillers, Microspheres, Microcapsules, Liposomes*, **1999**, *1*, 457
-

-
- [59] K. Rogers, *Controlled Release Technology and Delivery Systems*, Cosmetics and Toiletries, **1999**, 114, 53
- [60] I. Z. MacKenzie, *Prostaglandins. Has the initial promise been realised?*, Drugs, **1983**, 25, 1
- [61] C. Thies, *Microcapsules as drug delivery devices*, Critical Reviews in Biomedical Engineering, **1982**, 8, 355
- [62] S. D. Bruck, *Medical applications of polymeric materials*, Medical Progress through Technology, **1982**, 9, 1
- [63] R. Langer, M. Karel, *Controlled Release Technology: Polymers in medicine, food, and agriculture*, Polymer News, **1981**, 7, 250
- [64] M. Malmsten, *Soft drug delivery systems*, Soft Matter, **2006**, 2, 760
- [65] A. Madene, M. Jacquot, J. Scher, S. Desobry, *Flavour encapsulation and controlled release - a review*, International Journal of Food Science and Technology, **2006**, 41, 1
- [66] S. J. Rish, *Encapsulation: Overview of Uses and Techniques* in Encapsulation and Controlled release of Food Ingredients (Eds.: S. J. Risch, G. A. Reineccius), ACS Symposium Series, Chicago, **1995**
- [67] D. Fairhurst, M. Mitchnick, *Submicron Encapsulation of Organic Sunscreens*, Cosmetics and Toiletries, **1995**, 110, 47
- [68] J. Uhlemann, B. Schleifenbaum, H.-J. Bertram, *Flavor Encapsulation Technologie: An Overview Including Recent Developments*, Perfumer and Flavorist, **2002**, 27, 52
- [69] G. A. Reineccius, *Liposomes for Controlled Release in the Food Industry* in Encapsulation and Controlled release of Food Ingredients (Eds.: S. J. Risch, G. A. Reineccius), ACS Symposium Series, Chicago, **1995**
- [70] A. R. Hedges, W. J. Shieh, C. T. Sikorski, *Use of Cyclodextrins for Encapsulation in the Use and Treatment of Food Products* in Encapsulation and Controlled release of Food Ingredients (Eds.: S. J. Risch, G. A. Reineccius), ACS Symposium Series, Chicago, **1995**
- [71] B. Martel, M. Morcellet, D. Ruffin, F. Vinet, M. Weltrowski, *Capture and controlled release of fragrances by CD finished textiles*, Journal of Inclusion Phenomena, **2002**, 44, 439
- [72] C. X. Wang, S. L. Chen, *Fragrance-release property of β -cyclodextrin inclusion compounds and their application in aromatherapy*, Journal of Industrial Textiles, **2005**, 34, 157
-

-
- [73] T. Ooya, J. Lee, K. Park, *Effects of ethylene glycol-based graft, star-shaped, and dendritic polymers on solubilization and controlled release of paclitaxel*, Journal of Controlled Release, **2003**, 93, 121
- [74] F. Ahmed, D. E. Discher, *Self-porating polymersomes of PEG-PLA and PEG-PCL: hydrolysis-triggered controlled release vesicles*, Journal of Controlled Release, **2004**, 96, 37
- [75] H. Ritter, *Green polymer synthesis in water with help of cyclodextrins: Structures mechanism and applications*, Polymer Preprints, **2003**, 44, 605
- [76] Y.-Y. Liu, X.-D. Fan, *Synthesis, properties and controlled release behaviors of hydrogel networks using cyclodextrin as pendant groups*, Biomaterials, **2005**, 26, 6367
- [77] D. Benczédi, A. Blake, *Encapsulation and the Controlled Release of flavours*, Leatherhead Food RA Food Industry Journal, **1999**, 2, 36
- [78] K. Susuki, Y. Saito, Y. Tokuoka, M. Abe, T. Sato, *Poly(ethylene oxide)/Poly(propylene)/Poly(ethylene oxide) Triblock Copolymer as a Sustained-release Carrier for perfume Compounds*, Journal of American Organic Chemical Society (JAOCS), **1997**, 74, 55
- [79] K. E. Uhrich, S. M. Cannizzaro, R. S. Langer, K. M. Shakesheff, *Polymeric Systems for Controlled Drug Release*, Chemical Reviews, **1999**, 99, 3181
- [80] M. N. V. R. Kumar, N. Kumar, A. J. Domb, M. Arora, *Pharmaceutical Polymeric Controlled Drug Delivery Systems*, Advances in Polymer Science, **2002**, 160, 45
- [81] J. P. Jain, S. Modi, A. J. Domb, N. Kumar, *Role of polyanhydrides as localized drug carriers*, Journal of Controlled Release, **2005**, 103, 541
- [82] C. Perez, A. Sanchez, D. Putnam, D. Ting, R. Langer, M. J. Alonso, *Poly(lactic acid)-poly(ethylene glycol) nanoparticles as new carriers for the delivery of plasmid DNA*, Journal of Controlled Release, **2001**, 75, 211
- [83] J. G. Eley, P. P. Tirumalasetty, *Release characteristics of polymethacrylate nanospheres containing coumarin-6*, Journal of microencapsulation, **2003**, 20, 653
- [84] J. Wen, G. J. A. Kim, K. W. Leong, *Poly(D,L-lactide-co-ethyl ethylene phosphate)s as new drug carriers*, Journal of Controlled Release, **2003**, 92, 39
- [85] N. Csaba, L. Gonzalez, A. Sanchez, M. J. Alonso, *Design and characterisation of new nanoparticulate polymer blends for drug delivery*, Journal of Biomaterials Science, Polymer Edition, **2004**, 15, 1137

-
- [86] I. Ydens, P. Degée, C. Nouvel, E. Dellacherie, J.-L. Six, P. Dubois, "Surfactant-free" stable nanoparticles from biodegradable and amphiphilic poly(*E*-caprolactone)-grafted dextran copolymers, *e-Polymers*, **2005**, 46, 1
- [87] A. Rösler, G. W. M. Vandermeulen, H.-A. Klok, *Advanced drug delivery devices via self-assembly of amphiphilic block copolymers*, *Advanced Drug Delivery Reviews*, **2001**, 53, 95
- [88] C. Whorton, *Factors Influencing Volatile Release from Encapsulation Matrices* in *Encapsulation and Controlled release of Food Ingredients* (Eds.: S. J. Risch, G. A. Reineccius), ACS Symposium Series, Chicago, **1995**
- [89] S. A. Stern, S. Trohalaki, *Fundamentals of Gas Diffusion in Rubbery and Glassy Polymers* in *Barrier Polymers and Structures* (Eds.: W. J. Koros), American Chemical Society, Washington, D.C., **1990**
- [90] O. O. Omatete, C. J. King, *Volatiles Retention During Rehumidification of Freeze Dried Food Models*, *Journal of Food Technology*, **1978**, 13, 265
- [91] Y. Teng, M. E. Morrison, P. Munk, S. E. Webber, K. Prochazka, *Release kinetics studies of aromatic molecules into water from block polymer micelles*, *Macromolecules*, **1998**, 31, 3578
- [92] S. Labrousse, Y. Roos, M. Karel, *Collapse and Crystallization in Amorphous Matrices with Encapsulated Compounds*, *Sciences des Aliments*, **1992**, 12, 757
- [93] Y.-I. Jeong, J.-B. Cheon, S.-H. Kim, J.-W. Nah, Y.-M. Lee, Y.-K. Sung, T. Akaike, C.-S. Cho, *Clonazepam release from core-shell type nanoparticles in vitro*, *Journal of Controlled Release*, **1998**, 51, 169
- [94] K. B. Thurmond II, T. Kowalewski, K. L. Wooley, *Water-soluble Knedel-like structures: The preparation of shell-cross-linked small particles*, *Journal of the American Chemical Society*, **1996**, 118, 7239
- [95] T. Sanji, Y. Nakatsuka, S. Ohnishi, H. Sakurai, *Preparation of nanometer-sized hollow particles by photochemical degradation of polysilane shell cross-linked micelles and reversible encapsulation of guest molecules*, *Macromolecules*, **2000**, 33, 8524
- [96] V. Büttin, N. C. Billingham, S. P. Armes, *Synthesis of shell cross-linked micelles with tunable hydrophilic/hydrophobic cores [6]*, *Journal of the American Chemical Society*, **1998**, 120, 12135
-

-
- [97] J. Ding, G. Liu, *Polystyrene-block-poly(2-cinnamoyl ethyl methacrylate) Nanospheres with Cross-Linked Shells*, *Macromolecules*, **1998**, *31*, 6554
- [98] S. Stewart, G. Liu, *Hollow nanospheres from polyisoprene-block-poly(2-cinnamoyl ethyl methacrylate)-block-poly(tert-butyl acrylate)*, *Chemistry of Materials*, **1999**, *11*, 1048
- [99] Q. Zhang, E. E. Remsen, K. L. Wooley, *Shell Cross-Linked Nanoparticles Containing Hydrolytically Degradable, Crystalline Core Domains*, *Journal of the American Chemical Society*, **2000**, *122*, 3642
- [100] J. Ding, G. Liu, *Water-soluble hollow nanospheres as potential drug carriers*, *Journal of Physical Chemistry B*, **1998**, *102*, 6107
- [101] K. S. Murthy, Q. Ma, C. G. J. Clark, E. E. Remsen, K. L. Wooley, *Fundamental design aspects of amphiphilic shell-crosslinked nanoparticles for controlled release applications*, *Chemical Communication*, **2001**, 773
- [102] D. A. Tomalia, *Birth of a new macromolecular architecture: Dendrimers as quantized building blocks for nanoscale synthetic polymer chemistry*, *Progress in Polymer Science*, **2005**, *30*, 294
- [103] P. J. Flory, *Molecular Size Distribution in Three Dimensional Polymers. I. Gelation*, *Journal of the American Chemical Society*, **1941**, *63*, 3083
- [104] E. Buhleier, W. Wehner, F. Vögtle, *"Cascade"- and "Nonskid-Chain-like" Syntheses of Molecular Cavity Topologies*, *Synthesis*, **1978**, 155
- [105] C. J. Hawker, J. M. J. Fréchet, *Preparation of polymers with controlled molecular architecture. A new convergent approach to dendritic macromolecules*, *Journal of the American Chemical Society*, **1990**, *112*, 7638
- [106] P. E. Froehling, *Dendrimers and dyes- a review*, *Dyes and Pigments*, **2001**, *48*, 187
- [107] K. L. Wooley, C. J. Hawker, J. M. J. Fréchet, *Hyperbranched Macromolecules via a Novel Double-Stage Convergent Growth Approach*, *Journal of the American Chemical Society*, **1991**, *113*, 4252
- [108] T. Kawaguchi, K. L. Walker, C. L. Wilkins, J. S. Moore, *Double Exponential Dendrimer Growth*, *Journal of the American Chemical Society*, **1995**, *117*, 2159
- [109] R. Spindler, J. M. J. Fréchet, *Two-step Approach towards the Accelerated Synthesis of Dendritic Macromolecules*, *Journal of the Chemical Society Perkin Transaction 1*, **1993**, 913
-

-
- [110] F. Zeng, S. C. Zimmerman, *Rapid Synthesis of Dendrimers by an Orthogonal Coupling Strategy*, Journal of the American Chemical Society, **1996**, *118*, 5326
- [111] P. J. Flory, *Principles of polymer chemistry*, Cornell University Press, New York, **1952**
- [112] Y. H. Kim, O. W. Webster, *Water-Soluble Hyperbranched Polyphenylene: "A Unimolecular Micelle"?*, Journal of the American Chemical Society, **1990**, *112*, 4592
- [113] A. Hult, M. Johansson, E. Malmstrom, *Hyperbranched polymers*, Advances in Polymer Science, **1999**, *143*, 1
- [114] K. Inoue, *Functional dendrimers, hyperbranched and star polymers*, Progress in Polymer Science, **2000**, *25*, 453
- [115] C. Gao, D. Yan, *Hyperbranched polymers: from synthesis to applications*, Progress in Polymer Science, **2004**, *29*, 183
- [116] E. Malmstrom. In *Polymer Technology*, Royal Institute of Technology: Stockholm, 1996,
- [117] D. Hölder, A. Burgath, H. Frey, *Degree of branching in hyperbranched polymers*, Acta Polymerica, **1997**, *48*, 30
- [118] D. Hölder, H. Frey, *Degree of branching in hyperbranched polymer.2. Enhancement of the DB: Scope and limitations*, Acta Polymerica, **1997**, *48*, 298
- [119] R. Hanselmann, D. Hölder, H. Frey, *Hyperbranched Polymers Prepared via the Core-Dilution/Slow Addition Technique: Computer Simulation of Molecular Weight Distribution and Degree of Branching*, Macromolecules, **1998**, *31*, 3790
- [120] T. H. Mourey, S. R. Turner, M. Rubinstein, J. M. J. Fréchet, C. J. Hawker, K. L. Wooley, *Unique behavior of dendritic macromolecules. Intrinsic viscosity of polyether dendrimers*, Macromolecules, **1992**, *25*, 2401
- [121] S. R. Turner, B. I. Voit, T. H. Mourey, *All-aromatic hyperbranched polyesters with phenol and acetate end groups: synthesis and characterization*, Macromolecules, **1993**, *26*, 4617
- [122] S. R. Turner, F. Walter, B. I. Voit, T. H. Mourey, *Hyperbranched Aromatic Polyesters with Carboxylic Acid Terminal Groups*, Macromolecules, **1994**, *27*, 1611
- [123] J. M. J. Fréchet, *Fuctional polymers and Dendrimers: Reactivity, Molecular Architecture, and Interfacial Energy*, Science, **1994**, *263*, 1710
-

-
- [124] P. J. Farrington, C. J. Hawker, J. M. J. Fréchet, M. E. Mackay, *The melt viscosity of dendritic poly(benzyl ether) macromolecules*, *Macromolecules*, **1998**, *31*, 5043
- [125] K. L. Wooley, C. J. Hawker, J. M. Pochan, J. M. J. Fréchet, *Physical properties of dendritic macromolecules: A study of glass transition temperature*, *Macromolecules*, **1993**, *26*, 1514
- [126] C. J. Hawker, F. Chu, *Hyperbranched Poly(ether ketones): Manipulation of Structure and Physical Properties*, *Macromolecules*, **1996**, *29*, 4370
- [127] E. Malmström, M. Johansson, A. Hult, *The effect of terminal alkyl chains on hyperbranched polyesters based on 2,2-bis(hydroxymethyl)propionic acid*, *Macromolecular Chemistry and Physics*, **1996**, *197*, 3199
- [128] E. Malmström, A. Hult, U. W. Gedde, F. Liu, R. H. Boyd, *Relaxation processes in hyperbranched polyesters: Influence of terminal groups*, *Polymer*, **1997**, *38*, 4873
- [129] Y. H. Kim, O. W. Webster, *Hyperbranched Polyphenylenes*, *Macromolecules*, **1992**, *25*, 5561
- [130] D. Schmaljohann, L. Häubler, P. Pötschke, B. Voit, T. J. A. Loontjens, *Modification with alkyl chains and the influence on thermal and mechanical properties of aromatic hyperbranched polyesters*, *Macromolecular Chemistry and Physics*, **2000**, *201*, 49
- [131] H. Magnusson, E. Malmström, A. Hult, M. Johansson, *The effect of degree of branching on the rheological and thermal properties of hyperbranched aliphatic polyethers*, *Polymer*, **2002**, *43*, 301
- [132] F. Vögtle, S. Gestermann, R. Hesse, H. Schwierz, B. Windisch, *Functional dendrimers*, *Progress in Polymer Science*, **2000**, *25*, 987
- [133] D. K. Smith, A. R. Hirst, C. S. Love, J. G. Hardy, S. V. Brignell, B. Huang, *Self-assembly using dendritic building blocks - Towards controllable nanomaterials*, *Progress in Polymer Science (Oxford)*, **2005**, *30*, 220
- [134] F. Aulenta, W. Hayes, S. Rannard, *Dendrimers: A new class of nanoscopic containers and delivery devices*, *European Polymer Journal*, **2003**, *39*, 1741
- [135] A. D'Emanuele, D. Attwood, *Dendrimer-drug interactions*, *Advanced Drug Delivery Reviews*, **2005**, *57*, 2147
- [136] S. Svenson, D. A. Tomalia, *Dendrimers in biomedical applications - Reflections on the field*, *Advanced Drug Delivery Reviews*, **2005**, *57*, 2106
-

-
- [137] J. M. J. Fréchet, *Dendrimers and Other Dendritic Macromolecules: From Building Blocks to Functional Assemblies in Nanoscience and Nanotechnology*, Journal of polymer science: Part A: Polymer chemistry, **2003**, *41*, 3713
- [138] M. Maciejewski, *Concepts of Trapping Topologically by Shell Molecules*, Journal of the Macromolecules Science Chemistry: Part A, **1982**, *17A*, 689
- [139] K. Uhrich, *Hyperbranched Polymer for Drug Delivery*, Trends Polymer Science, **1997**, *5*, 388
- [140] M. Liu, J. M. J. Fréchet, *Designing dendrimers for drug delivery*, Pharmaceutic Science and Technology Today, **1999**, *2*, 393
- [141] R. Esfand, D. A. Tomalia, *Poly(amidoamine)(PAMAM) dendrimers: from biomimicry to drug delivery and biomedical applications*, DTT a researcher, **2001**, *6*, 427
- [142] A. K. Patri, I. J. Majoros, J. R. Baker, *Dendritic polymer macromolecular carriers for drug delivery*, Current Opinion in Chemical Biology, **2002**, *6*, 466
- [143] R. Duncan, L. Izzo, *Dendrimer biocompatibility and toxicity*, Advanced Drug Delivery Reviews, **2005**, *57*, 2215
- [144] L. Y. Qiu, Y. H. Bae, *Polymer architecture and drug delivery*, Pharmaceutical Research, **2006**, *23*, 1
- [145] D. A. Tomalia, A. M. Naylor, W. A. Goddard, *Starburst dendrimers: Molecular-Level Control of Size, Shape, Surface Chemistry, Topology, and Flexibility from Atoms to Macroscopic Matter*, Angewandte Chemie International Edition, **1990**, *29*, 138
- [146] H. R. Ihre, O. L. P. D. Jesus, F. C. Szoka, J. M. J. Fréchet, *Polyester Dendritic Systems for Drug Delivery Applications: Design, Synthesis, and Characterization*, Bioconjugate Chemistry, **2002**, *13*, 443
- [147] U. Gupta, H. B. Agashe, A. Asthana, N. K. Jain, *Dendrimers: Novel polymeric nanoarchitectures for solubility enhancement*, Biomacromolecules, **2006**, *7*, 649
- [148] H. Yang, W. J. Kao, *Dendrimers for pharmaceutical and biomedical applications*, Journal of Biomaterials Science, Polymer Edition, **2006**, *17*, 3
- [149] J. F. G. A. Jansen, E. M. M. DeBrabander-VanDenBerg, E. W. Meijer, *Encapsulation of Guest Molecules into a Dendritic Box*, Science, **1994**, *266*, 1226
- [150] J. F. G. A. Jansen, E. W. Meijer, *The Dendritic Box: Shape-Selective Liberation of Encapsulated Guests*, Journal of the American Chemical Society, **1995**, *117*, 4417
-

-
- [151] S. Stevelmans, J. C. M. V. Hest, J. F. G. A. Jansen, D. A. F. J. V. Boxtel, E. M. M. DeBrabander-VanDenBerg, E. W. Meijer, *Synthesis, Characterization, and Guest-Host Properties of Inverted Unimolecular Dendritic Micelles*, Journal of the American Chemical Society, **1996**, *118*, 7398
- [152] M. W. P. L. Baars, P. E. Froehling, E. W. Meijer, *Liquid-liquid extractions using poly(propylene imine)dendrimers with an apolar periphery*, Chemical Communication, **1997**, 1959
- [153] A. I. Cooper, J. D. Londono, G. Wignall, J. B. McClain, E. T. Samulski, J. S. Lin, A. Dobrynin, M. Rubinstein, A. L. C. Burke, J. M. J. Fréchet, J. M. Desimone, *Extraction of a hydrophilic compound from water into liquid CO₂ using dendritic surfactants*, Nature, **1997**, *389*, 368
- [154] V. Chechik, M. Zhao, R. M. Crooks, *Self-Assembled Inverted micelles Prepared from a Dendrimer Template: Phase Transfert of Encapsulated Guests*, Journal of the American Chemical Society, **1999**, *121*, 4910
- [155] A. Sunder, M. Krämer, R. Hanselmann, R. Mülhaupt, H. Frey, *Molecular Nanocapsule Based on Amphiphilic Hyperbranched Polyglycerols*, Angewandte Chemie International Edition, **1999**, *38*, 3552
- [156] S. E. Stiriba, H. Kautz, H. Frey, *Hyperbranched Molecular Nanocapsule: Comparison of the hyperbranched architecture with the Perfect Linear Analogue*, Journal of the American Chemical Society, **2002**, *124*, 9698
- [157] T. Satoh, M. Tamaki, Y. Kitajyo, T. Maeda, H. Ishihara, T. Imai, H. Kaga, T. Kakuchi, *Synthesis of unimolecular reversed micelle consisting of a poly(L-lactide) shell and hyperbranched D-mannan core*, Journal of Polymer Science, Part A: Polymer Chemistry, **2006**, *44*, 406
- [158] Y. Pan, W. T. Ford, *Dendrimers with Both Hydrophilic and Hydrophobic Chains at Every End*, Macromolecules, **1999**, *32*, 5468
- [159] A. Fishman, M. E. Farrah, J.-H. Zhong, S. Paramanatham, C. Carrera, E. Lee-Ruff, *Synthesis and Investigation of Novel Branched PEG-Based Soluble Polymer Supports*, Journal of Organic Chemistry, **2003**, *68*, 9843
- [160] B. W. Barry, D. I. D. Eini, *Solubilization of hydrocortisone, dexamethasone, testosterone and progesterone by long-chain polyoxyethylene surfactants*, Journal of Pharmacokinetics and Pharmacodynamics, **1976**, *28*, 210
-

-
- [161] S. Zalipsky, *Chemistry of polyethylene glycol conjugates with biologically active molecules*, *Advanced Drug Delivery Reviews*, **1995**, *16*, 157
- [162] S. Herman, G. Hooftman, E. Schacht, *Poly(Ethylene Glycol) with Reactive Endgroups: I. Modification of Proteins*, *Journal of Bioactive and Compatible Polymers*, **1995**, *10*, 145
- [163] Z. Sideratou, D. Tsiourvas, C. M. Paleos, *Solubilization and release properties of PEGylated diaminobutane poly(propylene imine) dendrimers*, *Journal of Colloid and Interface Science*, **2001**, *242*, 272
- [164] H. Yang, J. J. Morris, S. T. Lopina, *Polyethylene glycol-polyamidoamine dendritic micelle as solubility enhancer and the effect of the length of polyethylene glycol arms on the solubility of pyrene in water*, *Journal of Colloid and Interface Science*, **2004**, *273*, 148
- [165] M. W. P. L. Baars, R. Kleppinger, M. H. J. Koch, S.-L. Yeu, E. W. Meijer, *The Localization of Guest in Water-Soluble Oligoethyleneoxy-Modified Poly(propylene imine) Dendrimers*, *Angewandte Chemie International Edition*, **2000**, *39*, 1285
- [166] M. Liu, K. Kono, J. M. J. Fréchet, *Water-Soluble Dendrimer-Poly(ethylene glycol) Starlike Conjugates as Potential Drug Carriers*, *Journal of polymer science: Part A: Polymer chemistry*, **1999**, *37*, 3492
- [167] C. Kojima, K. Kono, K. Maruyama, T. Takagishi, *Synthesis of polyamidoamine dendrimers having poly(ethylene glycol) grafts and their ability to encapsulate anticancer drugs*, *Bioconjugate Chemistry*, **2000**, *11*, 910
- [168] A. M. Naylor, W. A. Goddard, G. E. Kiefer, D. A. Tomalia, *Starburst Dendrimers .5. Molecular Shape Control*, *Journal of the American Chemical Society*, **1989**, *111*, 2339
- [169] D. M. Watkins, Y. Sayed-Sweet, J. W. Klimash, N. J. Turro, D. A. Tomalia, *Dendrimers with Hydrophobic Cores and the Formation of Supramolecular Dendrimer-Surfactant Assemblies*, *Langmuir*, **1997**, *13*, 3136
- [170] J. F. Kukowska-Latallo, A. U. Bielinska, J. Johnson, R. Spindle, D. A. Tomalia, J. R. Baker, *Efficient transfer of genetic material into mammalian cells using starburst polyamidoamine dendrimers*, *Proceedings of the National Academy of Sciences of the United States of America*, **1996**, *93*, 4897
- [171] M. X. Tang, C. T. Redemann, F. C. Szoka, *In vitro gene delivery by degraded polyamidoamine dendrimers*, *Bioconjugate Chemistry*, **1996**, *7*, 703
-

-
- [172] G. Pistolis, A. Malliaris, D. Tsiourvas, C. M. Paleos, *Poly(propyleneimine) Dendrimers as pH-Sensitive Controlled-Release Systems*, *Chemistry A European Journal*, **1999**, *5*, 1440
- [173] Z. Sideratou, D. Tsiourvas, C. M. Paleos, *Quaternarized Poly(propylene imine) Dendrimers as Novel pH-Sensitive Controlled-Release Systems*, *Langmuir*, **2000**, *16*, 1766
- [174] L. Brunsveld, B. J. B. Folmer, E. w. Meijer, R. P. Sijbesma, *Supramolecular Polymers*, *Chemical Reviews*, **2001**, *101*, 4071
- [175] S. Mattei, P. Seiler, F. Diederich, V. Gramlich, *Dendrophanes: Water-soluble dendritic receptors*, *Helvetica Chimica Acta*, **1995**, *78*, 1904
- [176] P. Wallimann, P. Seiler, F. Diederich, *Dendrophanes: Novel steroid-recognizing dendritic receptors: Preliminary communication*, *Helvetica Chimica Acta*, **1996**, *79*, 779
- [177] P. Wallimann, S. Mattei, P. Seiler, F. Diederich, *New Cyclophanes as Initiator Cores for the Construction of Dendritic Receptors: Host-Guest Complexation in Aqueous Solutions and Structures of Solid-State Inclusion Compounds*, *Helvetica Chimica Acta*, **1997**, *80*, 2368
- [178] S. Mattei, P. Wallimann, B. Kenda, W. Amrein, F. Diederich, *Dendrophanes: Water-Soluble Dendritic Receptors as Models for Buried Recognition Sites in Globular Proteins*, *Helvetica Chimica Acta*, **1997**, *80*, 2391
- [179] G. R. Newkome, L. A. Godinez, C. N. Moorefield, *Molecular recognition using b-cyclodextrin-modified dendrimers: Novel building blocks for convergent self-assembly*, *Chemical Communications*, **1998**, 1821
- [180] C. M. Cardona, S. Mendoza, A. E. Kaifer, *Electrochemistry of encapsulated redox centers*, *Chemical Society Reviews*, **2000**, *29*, 37
- [181] C. M. Cardona, T. D. McCarley, A. E. Kaifer, *Synthesis, electrochemistry, and interactions with b-cyclodextrin of dendrimers containing a single ferrocene subunit located 'off-center'*, *Journal of Organic Chemistry*, **2000**, *65*, 1857
- [182] J.-F. Nierengarten, L. Oswald, J.-F. Eckert, J.-F. Nicoud, N. Armaroli, *Complexation of fullerenes with dendritic cyclotrimeratrylene derivatives*, *Tetrahedron Letters*, **1999**, *40*, 5681
- [183] M. Numata, A. Ikeda, C. Fukuhara, S. Shinkai, *Dendrimers can act as a host for [60]fullerene*, *Tetrahedron Letters*, **1999**, *40*, 6945

-
- [184] G. R. Newkome, B. D. Woosley, E. He, C. N. Moorefield, R. Güther, G. R. Baker, G. H. Escamilla, J. Merrill, H. Luftmann, *Supramolecular chemistry of flexible, dendritic-based structures employing molecular recognition*, Chemical Communication, **1996**, 2737
- [185] D. K. Smith, F. Diederich, *Dendritic hydrogen bonding receptors: Enantiomerically pure dendroclefts for the selective recognition of monosaccharides*, Chemical Communications, **1998**, 2501
- [186] T. Nagasaki, M. Ukon, S. Arimori, S. Shinkai, *Crowned Arborols*, Journal of the Chemical Society-Chemical Communications, **1992**, 608
- [187] C. C. Mak, N. Bampos, J. K. M. Sanders, *Metalloporphyrin dendrimers with folding arms*, Angewandte Chemie - International Edition, **1998**, 37, 3020
- [188] J. J. Michels, M. W. P. L. Baars, E. W. Meijer, J. Huskens, D. N. Reinhoudt, *Well-defined assemblies of adamantyl-terminated poly(propylene imine) dendrimers and α -cyclodextrin in water*, Journal of the Chemical Society. Perkin Transactions 2, **2000**, 1914
- [189] R. Castro, I. Cuadrado, B. Alonso, C. M. Casado, M. Moran, A. E. Kaifer, *Multisite inclusion complexation of redox active dendrimer guests*, Journal of the American Chemical Society, **1997**, 119, 5760
- [190] C. Valerio, J.-L. Fillaut, J. Ruiz, J. Guittard, J.-C. Blais, D. Astruc, *The dendritic effect in molecular recognition: Ferrocene dendrimers and their use as supramolecular redox sensors for the recognition of small inorganic anions*, Journal of the American Chemical Society, **1997**, 119, 2588
- [191] Y. C. Lee, R. T. Lee, *Carbohydrate-Protein Interactions: Basis of Glycobiology*, Accounts of Chemical Research, **1995**, 28, 321
- [192] T. D. James, H. Shinmori, M. Takeuchi, S. Shinkai, *A saccharide 'sponge'. Synthesis and properties of a dendritic boronic acid*, Chemical Communications, **1996**, 705
- [193] W. H. Carothers, *Studies on polymerization and ring formation. I. An introduction to the general theory of condensation polymers*, Journal of the American Chemical Society, **1929**, 51, 2548
- [194] P. J. Flory, *Principles of polymer chemistry*, Cornell University Press, New York, **1953**
- [195] G. Odian, *Principles of Polymerization, Fourth Edition*, John Wiley & Sons, Inc., Hoboken, New Jersey, **2004**
- [196] M. Szwarc, *Living Polymers*, Nature, **1956**, 178, 1168
-

-
- [197] M. Fontanille, Y. Gnanou, *Chimie et physico-chimie des polymères*, Dunod, Paris, **2002**
- [198] K. Matyjaszewski, *Controlled/living radical polymerization: State of the art in 2002*, ACS Symposium Series, **2003**, 854, 2
- [199] P. G. Griffiths, E. Rizzardo, D. H. Solomon, *Quantitative Studies on Free-Radical Reactions with the Scavenger 1,1,3,3-Tetramethylisoindolyl-2-Oxy*, Tetrahedron Letters, **1982**, 23, 1309
- [200] M. Kato, M. Kamigaito, M. Sawamoto, T. Higashimura, *Polymerization of methyl methacrylate with the carbon tetrachloride/dichlorotris-(triphenylphosphine)ruthenium(II)/methylaluminum bis(2,6-di-tert-butylphenoxide) initiating system: possibility of living radical polymerization*, Macromolecules, **1995**, 28, 1721
- [201] J.-S. Wang, K. Matyjaszewski, *Controlled/"living" radical polymerization. Atom transfer radical polymerization in the presence of transition-metal complexes*, Journal of the American Chemical Society, **1995**, 117, 5614
- [202] K. Matyjaszewski, J. Xia, *Atom Transfer Radical Polymerization*, Chemical Reviews, **2001**, 101, 2921
- [203] M. Kamigaito, T. Ando, M. Sawamoto, *Metal-Catalyzed Living Radical Polymerization*, Chemical Reviews, **2001**, 101, 3689
- [204] J. Chiefari, Y. K. Chong, F. Ercole, J. Krstina, J. Jeffery, T. P. T. Le, R. T. A. Mayadunne, G. F. Meijs, C. L. Moad, G. Moad, E. Rizzardo, S. H. Thang, *Living free-radical polymerization by reversible addition - Fragmentation chain transfer: The RAFT process*, Macromolecules, **1998**, 31, 5559
- [205] D. P. Curran, *The Design and Application of Free-Radical Chain Reactions in Organic-Synthesis.2*, Synthesis-Stuttgart, **1988**, 489
- [206] T. E. Patten, K. Matyjaszewski, *Atom Transfer Radical Polymerization and the Synthesis of Polymeric Materials*, Advanced Materials, **1998**, 10, 901
- [207] C. Yoshikawa, A. Goto, T. Fukuda, *Quantitative comparison of theory and experiment on living radical polymerization kinetics. 2. Atom transfer radical polymerization*, Macromolecules, **2003**, 36, 908
- [208] A. K. Nanda, K. Matyjaszewski, *Effect of [bpy]/[Cu(I)] ratio, solvent, counterion, and alkyl bromides on the activation rate constants in atom transfer radical polymerization*, Macromolecules, **2003**, 36, 599
-

-
- [209] K. Matyjaszewski. In *ACS Symposium Series*, 1998, Vol. 685, pp 2
- [210] K. Matyjaszewski, *Transformation of "Living" Carbocationic and other Polymerizations to Controlled/"Living" Radical Polymerization*, *Macromolecular Symposia*, **1998**, *132*, 85
- [211] J. Xia, S. G. Gaynor, K. Matyjaszewski, *Controlled/"Living" Radical Polymerization. Atom Transfer Radical Polymerization of Acrylates at ambient Temperature*, *Macromolecules*, **1998**, *31*, 5958
- [212] K. A. Davis, B. Charleux, K. Matyjaszewski, *Preparation of Block Copolymers of Polystyrene and Poly(*t*-butyl acrylate) of Various Molecular Weights and Architectures by Atom Transfer Radical Polymerization*, *Journal of polymer science: Part A: Polymer chemistry*, **2000**, *38*, 2274
- [213] K. Matyjaszewski, J.-L. Wang, T. Grimaud, D. A. Shipp, *Controlled/"living" atom transfer radical polymerization of methyl methacrylate using various initiation systems*, *Macromolecules*, **1998**, *31*, 1527
- [214] J.-L. Wang, T. Grimaud, K. Matyjaszewski, *Kinetic study of the homogeneous atom transfer radical polymerization of methyl methacrylate*, *Macromolecules*, **1997**, *30*, 6507
- [215] K. A. Davis, H.-J. Paik, K. Matyjaszewski, *Kinetic investigation of the atom transfer radical polymerization of methyl acrylate*, *Macromolecules*, **1999**, *32*, 1767
- [216] Z. Shen, Y. Chen, E. Barriau, H. Frey, *Multi-Arm Star Polyglycerol-block-poly(*tert*-butyl acrylate) and the Respective Multi-Arm Poly(acrylic acid) Stars*, *Macromolecular Chemistry and Physics*, **2006**, *207*, 57
- [217] K. Matyjaszewski, *The synthesis of functional star copolymers as an illustration of the importance of controlling polymer structures in the design of new materials*, *Polymer International*, **2003**, *52*, 1559
- [218] J. L. Hedrick, M. Trollsås, C. J. Hawker, B. Atthoff, H. Claesson, A. Heise, R. D. Miller, D. Mecerreyes, R. Jérôme, P. Dubois, *Dendrimer-like Star Block and Amphiphilic Copolymers by combination of Ring Opening and Atom Transfer Radical Polymerization*, *Macromolecules*, **1998**, *31*, 8691
- [219] A. Heise, C. Nguyen, R. Malek, J. L. Hedrick, C. W. Frank, R. D. Miller, *Starlike polymeric architectures by Atom Transfer Radical Polymerization: Templates for the Production of Low Dielectric Constant Thin Films*, *Macromolecules*, **2000**, *33*, 2346
-

-
- [220] A. Heise, J. L. Hedrick, M. Trollsås, R. D. Miller, C. W. Frank, *Novel Starlike Poly(methyl methacrylate)s by Controlled Dendritic Free Radical Initiation*, *Macromolecules*, **1999**, *32*, 231
- [221] S. Maier, A. Sunder, H. Frey, R. Mülhaupt, *Synthesis of poly(glycerol)-block-poly(methyl acrylate) multi- arm star polymers*, *Macromolecule Rapid Communication*, **2000**, *21*, 226
- [222] Y. Zhao, X. Shuai, C. Chen, F. Xi, *Synthesis of novel dendrimer-like star block copolymers with definite numbers of arms by combination of ROP and ATRP*, *Chemical Communication*, **2004**, *14*, 1608
- [223] Z. Jia, Y. Zhou, D. Yan, *Amphiphilic star-block copolymers based on a hyperbranched core: Synthesis and supramolecular self-assembly*, *Journal of Polymer Science, Part A: Polymer Chemistry*, **2005**, *43*, 6534
- [224] S. Angot, K. S. Murthy, D. Taton, Y. Gnanou, *Scope of the Copper Halide/Bipyridyl System Associated with Calixarene-Based Multihalides for the Synthesis of Well-Defined Polystyrene and Poly(meth)acrylate stars*, *Macromolecules*, **2000**, *33*, 7261
- [225] S. Angot, K. S. Murthy, D. Taton, Y. Gnanou, *Atom Transfer Radical Polymerization of Styrene Using a Novel Octafunctional Initiator: Synthesis of Well-Defined Polystyrene Stars*, *Macromolecules*, **1998**, *31*, 7218
- [226] J. Ueda, M. Kamigaito, M. Sawamoto, *Calixarene-Core Multifunctional Initiators for the Ruthenium-Mediated Living Radical Polymerization of Methacrylates*, *Macromolecules*, **1998**, *31*, 6762
- [227] A. Heise, J. L. Hedrick, C. W. Frank, R. D. Miller, *Starlike Block Copolymers with Amphiphilic Arms as Models for Unimolecular Micelles*, *Journal of the American Chemical Society*, **1999**, *121*, 8647
- [228] Y. M. Chen, G. Wulff, *ABA and star amphiphilic block copolymers composed of polymethacrylate bearing a galactose fragment and poly(caprolactone)*, *Macromolecular Rapid Communications*, **2002**, *23*, 59
- [229] X. Yu, X. Tang, C. Pan, *Synthesis, characterization and self-assembly behavior of six-armed star block copolymers with triphenylene core*, *Polymer*, **2005**, *46*, 11149
- [230] J. Chen, H. Zhang, J. Chen, X. Wang, X. Wang, *Synthesis of star-shaped poly(caprolactone)-b-poly(styrene) block copolymer by combining ring-opening*
-

-
- polymerization and atom transfer radical polymerization*, Journal of Macromolecular Science - Pure and Applied Chemistry, **2005**, 42 A, 1247
- [231] K. Ohno, B. Wong, D. M. Haddleton, *Synthesis of Well-Defined Cyclodextrin-Core Star Polymers*, Journal of Polymer Science, Part A: Polymer Chemistry, **2001**, 39, 2206
- [232] D. M. Haddleton, D. Kukulj, E. J. Kelly, C. Waterson, *Glucose derived star polymers by atom transfer polymerization*, Journal of Polymer Science and Engineering, **1999**, 80, 145
- [233] D. M. Haddleton, K. Ohno, *Well -Defined Oligosaccharide-Terminated Polymers from Living Radical Polymerization*, Biomacromolecules, **2000**, 1, 152
- [234] L. Bes, S. Angot, A. Limer, D. M. Haddleton, *Sugar-Coated Amphiphilic Block Copolymer Micelles from Living Radical Polymerization: Recognition by Immobilized Lectins*, Macromolecules, **2003**, 36, 2493
- [235] D. Mecerreyes, R. Jérôme, P. Dubois, *Novel macromolecular architectures based on aliphatic polyesters: Relevance of the "coordination-insertion" ring-opening polymerization* in Advances in Polymer Science (Eds.: **1999**)
- [236] S. Penczek, A. Duda, R. Szymanski, T. Biela, *Macromolecular Symposia*, **2000**, 153, 1
- [237] H. Sugimoto, S. Inoue, *Polymerization by metalloporphyrin and related complexes*, Advances in Polymer Science, **1999**, 146, 41
- [238] H. R. Kricheldorf, M. Berl, N. Scharnagl, *Poly(lactones). 9. Polymerization Mechanism of Metal Alkoxide Initiated Polymerizations of Lactide and Various Lactones*, Macromolecules, **1988**, 21, 286
- [239] M. Myers, E. F. Connor, T. Glauser, A. Möck, G. Nyce, J. L. Hedrick, *Phosphines: Nucleophilic organic catalysts for the controlled ring-opening polymerization of lactides*, Journal of polymer science: Part A: Polymer chemistry, **2002**, 40, 844
- [240] M. Möller, R. Kånge, J. L. Hedrick, *$\text{Sn}(\text{OTf})_2$ and $\text{Sc}(\text{OTf})_3$: Efficient and Versatile Catalysts for the Controlled Polymerization of Lactones*, Journal of polymer science: Part A: Polymer chemistry, **2000**, 38, 2067
- [241] H. R. Kricheldorf, C. Boettcher, K.-U. Tönnes, *Poly(lactones): 23. Polymerization of racemic and meso D,L-lactide with various organotin catalyst-stereochemical aspects*, Polymer, **1992**, 33, 2817
- [242] M. Möller, F. Nederberg, L. S. Lim, R. Kånge, C. J. Hawker, J. L. Hedrick, Y. Gu, R. Shah, N. L. Abbott, *Stannous(II) Trifluoromethane Sulfonate: A Versatile Catalyst for the*
-

-
- Controlled Ring-Opening Polymerization of Lactides: Formation of Stereoregular Surfaces from Polylactide "Brushes"*, Journal of polymer science: Part A: Polymer chemistry, **2001**, 39, 3529
- [243] J. Liu, L. Liu, *Ring-opening Polymerization of ϵ -caprolactone Initiated by Natural Amino Acids*, Macromolecules, **2004**, 37, 2674
- [244] H. R. Kricheldorf, C. Boettcher, K.-U. Tönnes, *Polylactones: 23. Polymerization of racemic and meso D,L-lactide with various organotin catalyst-stereochemical aspects*, Polymer, **1992**, 33, 2817
- [245] H. R. Kricheldorf, M. Berl, N. Scharnagl, *Poly(lactones). 9. Polymerization Mechanism of Metal Alkoxide Initiated Polymerizations of Lactide and Various Lactones*, Macromolecules, **1988**, 21, 286
- [246] H. Kricheldorf, I. Kreiser-Saunders, C. Boettcher, *Poly(lactones) .31.Sn(II)octoate-initiated polymerization of L-lactide - A mechanistic study*, Polymer, **1995**, 33, 1253
- [247] A. Kowalski, A. Duda, S. Penczek, *Kinetics and mechanism of cyclic esters polymerization initiated with tin(II) octoate. 3. Polymerization of L,L-dilactide*, Macromolecules, **2000**, 33, 7359
- [248] M. Trollsås, J. L. Hedrick, D. Mecerreyes, P. Dubois, R. Jérôme, H. Ihre, A. Hult, *Highly Functional Branched and Dendri-Graft Aliphatic Polyesters through Ring Opening Polymerization*, Macromolecules, **1998**, 31, 2756
- [249] C. Nouvel, P. Dubois, E. Dellacherie, J.-L. Six, *Controlled Synthesis of Amphiphilic Biodegradable Polylactide-Grafted Dextran Copolymers*, Journal of polymer science: Part A: Polymer chemistry, **2004**, 42, 2577
- [250] S. Penczek, A. Duda, R. Szymanski, *Macromolecular Symposia*, **1998**, 132, 441
- [251] M. Trollsås, J. L. Hedrick, D. Mecerreyes, P. Dubois, R. Jérôme, H. Ihre, A. Hult, *Versatile and Controlled Synthesis of Star and Branched Macromolecules by Dendritic Initiation*, Macromolecules, **1997**, 30, 8508
- [252] M. Trollsås, C. J. Hawker, J. F. Remenar, J. L. Hedrick, M. Johansson, H. Ihre, A. Hult, *Highly Branched Radical Block Copolymers via Dendritic Initiation of Aliphatic Polyesters*, Journal of Polymer Science, Part A: Polymer Chemistry, **1998**, 36, 2793
- [253] B. S. Lele, J.-C. Leroux, *Synthesis of novel amphiphilic star-shaped poly(ϵ -caprolactone)-block-poly(N-(2-hydroxypropyl)methacrylamide) by combination of ring-opening and chain transfer polymerization*, Polymer, **2002**, 43, 5595
-

-
- [254] H. Claesson, E. Malmström, M. Johansson, A. Hult, *Synthesis and characterisation of star branched polyesters with dendritic cores and the effect of structural variations on zero shear rate viscosity*, *Polymer*, **2002**, *43*, 3511
- [255] M. Trollsås, J. L. Hedrick, *Dendritic-Like Star polymers*, *Journal of the American Chemical Society*, **1998**, *120*, 4644
- [256] A. Würsch, M. Möller, T. Glauser, L. S. Lim, S. B. Voytek, J. L. Hedrick, *Dendritic-Linear AxBx Block Copolymers prepared via Controlled Ring-opening Polymerization of lactones from Orthogonally Protected Multifunctional Initiator*, *Macromolecules*, **2001**, *34*, 6601
- [257] D. M. Haddleton, D. Kukulj, D. J. Duncalf, A. M. Heming, A. J. Shooter, *Low-temperature living "radical" polymerization (atom transfer polymerization) of methyl methacrylate mediated by copper(I) N-alkyl-2-pyridylmethanimine complexes*, *Macromolecules*, **1998**, *31*, 5201
- [258] *Perstorp*, Perstorp product data sheet Boltorn, <http://www.perstorp.com>,
- [259] E. Malmström, A. Hult, *Kinetics of formation of hyperbranched polyesters based on 2,2-bis(methylol)propionic acid*, *Macromolecules*, **1996**, *29*, 1222
- [260] A. Burgath, A. Sunder, H. Frey, *Role of cyclization in the synthesis of hyperbranched aliphatic polyesters*, *Macromolecular Chemistry and Physics*, **2000**, *201*, 782
- [261] H. Magnusson, E. Malmström, A. Hult, *Structure Buildup in Hyperbranched Polymers from 2,2-Bis(hydroxymethyl)propionic Acid*, *Macromolecules*, **2000**, *33*, 3099
- [262] H. Komber, A. Ziemer, B. Voit, *Etherification as Side Reaction in the Hyperbranched Polycondensation of 2,2-Bis(hydroxymethyl)propionic Acid*, *Macromolecules*, **2002**, *35*, 3514
- [263] E. Zagar, M. Zigon, *Characterization of a commercial Hyperbranched Aliphatic Polyester Based on 2,2-Bis(methylol)propionic Acid*, *Macromolecules*, **2002**, *35*, 9913
- [264] E. Zagar, M. Zigon, *Molar mass distribution of a commercial aliphatic hyperbranched polyester based on 2,2-bis(methylol)propionic acid*, *Journal of Chromatography A*, **2004**, *1034*, 77
- [265] W. Li, J. Amos, S. Jordan, A. Theis, C. Davis, *Selecting the optimum silicone particle size/cationic polymer structure to maximize shampoo conditioning performance*, *Journal of Cosmetic Science*, **2006**, *57*, 178
-

-
- [266] J. V. Gruber, B. R. Lamoureux, N. Joshi, L. Moral, *The use of x-ray fluorescent spectroscopy to study the influence of cationic polymers on silicone oil deposition from shampoo*, *Journal of Cosmetic Science*, **2001**, 52, 131
- [267] J. V. Gruber, B. R. Lamoureux, N. Joshi, L. Moral, *Influence of cationic polysaccharides on polydimethylsiloxane (PDMS) deposition onto keratin surfaces from a surfactant emulsified system*, *Colloids and Surfaces B-Biointerfaces*, **2000**, 19, 127
- [268] A. Sunder, R. Hanselmann, H. Frey, R. Mülhaupt, *Controlled Synthesis of Hyperbranched Polyglycerols by Ring-Opening Multibranching Polymerization*, *Macromolecules*, **1999**, 32, 4240
- [269] A. Sunder, R. Mülhaupt, H. Frey, *Hyperbranched Polyether-Polyols Based on Polyglycerol: Polarity Design by block Copolymerization with Propylene Oxide*, *Macromolecules*, **2000**, 33, 309
- [270] X. Zhang, H. Yang, Q. Liu, Y. Zheng, H. Xie, Z. Wang, R. Cheng, *Synthesis and Characterization of Biodegradable Triblock Copolymers Based on Bacterial Poly[(R)-3-hydroxybutyrate] by Atom Transfer Radical Polymerization*, *Journal of Polymer Science, Part A: Polymer Chemistry*, **2005**, 43, 4857
- [271] S. Huijser, B. B. P. Staal, J. Huang, R. Duchateau, C. E. Koning, *Chemical composition and topology of poly(lactide-co-glycolide) revealed by pushing MALDI-TOF MS to its limit*, *Angewandte Chemie - International Edition*, **2006**, 45, 4104
- [272] K. R. M. Vidts, B. Dervaux, F. E. Du Prez, *Block, blocky gradient and random copolymers of 2-ethylhexyl acrylate and acrylic acid by atom transfer radical polymerization*, *Polymer*, **2006**, 47, 6028
- [273] K. Nakashima, Y. Fujimoto, T. Anzai, J. Dong, H. Sato, Y. Ozaki, *Fluorescence and FTIR Studies on the pH-Dependent Conformational Change of Poly(methacrylic acid) in Aqueous Solutions*, *Bulletin of the Chemical Society of Japan*, **1999**, 72, 1233
- [274] J. K. Wolterink, J. v. Male, M. A. C. Stuart, L. K. Koopal, E. B. Zhulina, O. V. Borisov, *Annealed Star- Branched Polyelectrolytes in Solution*, *Macromolecules*, **2002**, 35, 9176
- [275] S. Karanam, H. Goossens, B. Klumperman, P. Lemstra, *Controlled Synthesis and Characterization of Model Methyl Methacrylate/ tert-Butyl Methacrylate Triblock Copolymers via ATRP*, *Macromolecules*, **2003**, 36, 3051
-

-
- [276] K. Matyjaszewski, P. J. Miller, J. Pyun, G. Kickelbick, S. Diamanti, *Synthesis and characterization of star polymers with varying arm number, length, and composition from organic and hybrid inorganic/organic multifunctional initiators*, *Macromolecules*, **1999**, *32*, 6526
- [277] K. A. Davis, K. Matyjaszewski, *Atom Transfer Radical Polymerization of tert-Butyl Acrylate and Preparation of Block Copolymers*, *Macromolecules*, **2000**, *33*, 4039
- [278] K. Matyjaszewski, Y. Nakagawa, C. B. Jasieczek, *Polymerization of n-Butyl Acrylate by Atom Transfer Radical Polymerization. Remarkable Effect of Ethylene Carbonate and Other Solvents*, *Macromolecules*, **1998**, *31*, 1535
- [279] C. Burguière, C. Chassenieux, B. Charleux, *Characterization of aqueous micellar solutions of amphiphilic block copolymers of poly(acrylic acid) and polystyrene prepared via ATRP. Toward the control of the number of particles in emulsion polymerization*, *Polymer*, **2003**, *44*, 509
- [280] H. Mori, D. C. Seng, H. Lechner, M. Zhang, A. H. E. Müller, *Synthesis and characterization of branched polyelectrolytes. 1. Preparation of hyperbranched poly(acrylic acid) via self-condensing atom transfer radical copolymerization*, *Macromolecules*, **2002**, *35*, 9270
- [281] F. A. Plamper, H. Becker, M. Lanzendörfer, M. Patel, A. Wittemann, M. Ballauff, A. H. E. Müller, *Synthesis, Characterization and Behavior in Aqueous Solution of Star-Shaped Poly(acrylic acid)*, *Macromolecular Chemistry and Physics*, **2005**, *206*, 1813
- [282] Y. Shen, F. Zeng, S. Zhu, R. Pelton, *Novel cationic macromonomers by living anionic polymerization of (dimethylamino)ethyl methacrylate*, *Macromolecules*, **2001**, *34*, 144
- [283] D. Paneva, L. Mespouille, N. Manolova, P. Degee, I. Rashkov, P. Dubois, *Comprehensive study on the formation of polyelectrolyte complexes from (quaternized) poly[2-(dimethylamino)ethyl methacrylate] and poly(2-acrylamido-2-methylpropane sodium sulfonate)*, *Journal of Polymer Science, Part A: Polymer Chemistry*, **2006**, *44*, 5468
- [284] X. Zhang, J. Xia, K. Matyjaszewski, *Controlled/"Living" Radical Polymerization of 2-(Dimethylamino)ethyl Methacrylate*, *Macromolecules*, **1998**, *31*, 5167
- [285] N. Pantoustier, S. Moins, M. Wautier, P. Degée, P. Dubois, *Solvent-free synthesis and purification of poly[2-(dimethylamino)ethyl methacrylate] by atom transfer radical polymerization*, *Chemical Communication*, **2003**, 340
-

-
- [286] F. Zeng, Y. Shen, s. Zhu, R. Pelton, *Synthesis and Characterization of Comb-Branched Polyelectrolytes. 1.Preparation of Cationic Macromonomer of 2-(Dimethylamino)ethyl Methacrylate by Atom Transfer Radical Polymerization*, *Macromolecules*, **2000**, *33*, 1628
- [287] G. Bo, B. Wesslén, K. B. Wesslén, *Amphiphilic comb-shaped polymers from poly(ethylene glycol) macromonomers*, *Journal of Polymer Science, Part A: Polymer Chemistry*, **1992**, *30*, 1799
- [288] E. Nunez, C. Ferrando, E. Malmström, H. Claesson, P.-E. Werner, U. W. Gedde, *Crystal structure, melting behaviour and equilibrium melting point of star polyesters with crystallisable poly(*ε*-caprolactone) arms*, *Polymer*, **2004**, *45*, 5251
- [289] H. Kaneyoshi, Y. Inoue, K. Matyjaszewski, *Synthesis of Block and Graft Copolymers with Linear Polyethylene Segments by Combination of Degenerative Transfer Coordination Polymerization and Atom Transfer Radical Polymerization*, *Macromolecules*, **2005**, *38*, 5425
- [290] A. Leo, C. Hansch, D. Elkins, *Partition Coefficients and Their Uses*, *Chemical Reviews*, **1971**, *71*, 525
- [291] O. A. Raevsky, *Physicochemical descriptors in property-based drug design*, *Mini-Reviews in Medicinal Chemistry*, **2004**, *4*, 1041
- [292] G. Klopman, H. Zhu, *Recent methodologies for the estimation of *n*-octanol/water partition coefficients and their use in the prediction of membrane transport properties of drugs*, *Mini-Reviews in Medicinal Chemistry*, **2005**, *5*, 127
- [293] H. Tang, M. Mayersohn, *A global examination of allometric scaling for predicting human drug clearance and the prediction of large vertical allometry*, *Journal of Pharmaceutical Sciences*, **2006**, *95*, 1783
- [294] W. Fieber, A. Herrmann, L. Ouali, M. I. Velazco, G. Kreutzer, H.-A. Klok, C. Ternat, C. J. G. Plummer, J.-A. E. Månson, H. Sommer, *NMR Diffusion and Relaxation Studies to Investigate the Encapsulation of Fragrances into Amphiphilic Multiarm Star Block Copolymers*, *Macromolecules*, **2006**, submitted
- [295] D. W. Van Krevelen, *Properties of Polymers: Their correlation with chemical structure; their numerical estimation and prediction from additive group contributions*, Elsevier Science Publishers, **1990**
- [296] H. Gygas, H. Koch, *The measurement of odors*, *Chimia*, **2001**, *55*, 401
-

-
- [297] M. Devos, F. Patte, J. Rouault, P. Laffort, L. J. van Gemert, *Standardized Human Olfactory Thresholds*, Oxford university, **1990**
- [298] A. Chaintreau, *Sample Preparation, Headspace Techniques* in Encyclopedia of Analytical Chemistry (Eds.: R. A. Meyers), John Wiley & Sons, Chichester, **2000**
- [299] B. Kolb, *Static Headspace-Gas Chromatography: Theory and Practice*, John Wiley, New York, **1997**
- [300] J. Pawliszyn, *Solid Phase Microextraction: Theory and Practice*, John Wiley, New York, **1997**
- [301] S. M. Abeel, A. K. Vickers, D. Decker, *Trends in Purge and Trap*, Journal of chromatography science, **1994**, 32, 328
- [302] A. Chaintreau, A. Grade, R. Munoz-Box, *Determination of partition coefficients and quantitation of headspace volatile compounds*, Analytical Chemistry, **1995**, 67, 3300
- [303] T. Kumazawa, H. Seno, X.-P. Lee, A. Ishii, O. Suzuki, K. Sato, *Detection of ethanol in human body fluids by headspace solid-phase micro extraction (SPME)/capillary gas chromatography*, Chromatographia, **1996**, 43, 393
- [304] X.-P. Lee, T. Kumazawa, K. Sato, H. Seno, A. Ishii, O. Suzuki, *Improved extraction of ethanol from human body fluids by headspace solid-phase microextraction with a Carboxen-polydimethylsiloxane-coated fiber*, Chromatographia, **1998**, 47, 593
- [305] R. L. Barnes, *Headspace Analysis of Pharmaceuticals*, Journal of chromatographic science, **1990**, 90, 149
- [306] S. Ulrich, *Solid-phase microextraction in biomedical analysis*, Journal of Chromatography A, **2000**, 902, 167
- [307] C. Bicchi, D. Joulain, *Headspace-gas Chromatographic Analysis of Medicinal and Aromatic Plants and Flowers*, Flavour and Fragrance Journal, **1990**, 5, 131
- [308] A. Hagman, S. Jacobsson, *Quantitative Determination of Volatiles in Polyolefins by Dynamic Headspace/Capillary Gas Chromatography/Mass Spectroscopy*, Journal of High Resolution Chromatography, **1988**, 11, 830
- [309] H. Kataoka, H. L. Lord, J. Pawliszyn, *Applications of solid-phase microextraction in food analysis*, Journal of Chromatography A, **2000**, 880, 35
- [310] P. Comuzzo, L. Tat, A. Tonizzo, F. Battistutta, *Yeast derivatives (extracts and autolysates) in winemaking: Release of volatile compounds and effects on wine aroma volatility*, Food Chemistry, **2006**, 99, 217
-

- [311] R. L. Rouseff, K. R. Cadwallader, *Headspace Analysis of Foods and Flavors: Theory and Practice*, Klumer Academic Publishers, New York, **2001**
- [312] T. G. Hartman, J. Lech, K. Karmas, J. Salinas, R. T. Rosen, C. T. Ho, *Flavor Characterization Using Adsorbent Trapping/Thermal Desorption or Direct Thermal Desorption/Gas Chromatography and Gas Chromatography/Mass Spectroscopy*, (Eds.:C. T. Ho, C. H. Manley, M. Dekker), New York, **1993**
- [313] A. Herrmann, C. Debonneville, V. Laubscher, L. Aymard, *Dynamic Headspace analysis of the light-induced controlled release of perfumery aldehydes and ketones from α -keto esters in bodycare and household applications*, Flavour and Fragrance Journal, **2000**, *15*, 415
- [314] *Standardized Human Olfactory Thresholds*, (Eds.:M. Devos, F. Patte, J. Rouault, P. Laffort, L. J. V. Gemert), Oxford University Press, Oxford, **1990**
- [315] J. M. J. Fréchet, M. Henmi, I. Gitsov, S. Aoshima, M. R. Leduc, R. B. Grubbs, *Self-Condensing Vinyl Polymerization: An Approach to Dendritic Materials*, Science, **1995**, *269*, 1080
- [316] M. Suzuki, A. Ii, T. Saegusa, *Multibranching polymerization: Palladium-catalyzed ring-opening polymerization of cyclic carbamate to produce hyperbranched dendritic polyamine*, Macromolecules, **1992**, *25*, 7071

Céline Ternat

Born on October 3rd, 1977
French, single

Current position

Dec.2002-Feb.2007: PhD. Student in polymer science

Ecole Polytechnique Fédérale de Lausanne (EPFL)

Laboratoire de Technologie des Composites et Polymères (LTC)

Industrial partner: Firmenich (Geneva)

Research field: “Design of amphiphilic nanocapsules based on hyperbranched star-block copolymers for the encapsulation and the controlled release of olfactory compounds”

Advisors: Prof. Jan-Anders Månson, Dr. Christopher J.G. Plummer

Competences and experience

- “Living” Free Radical Polymerization techniques
- Chemical modification of mono-functional and multi-arm polymers
- Polymer characterization: spectroscopy (NMR, FT-IR) and chromatography analysis, thermal properties (thermogravimetry analyser and differential scanning calorimetry)
- Analysis and quantification of encapsulated fragrances with industrial and spectroscopic techniques

Biographical information

2001-2002: D.E.A. Functional polymers (post graduate diploma taken before completing a PhD)

Université Paris XII (Paris, Fr.), obtained with distinction

Research field: “Design of a macromolecular vector based on a biodegradable polymer for therapeutic applications”

Laboratoire de Recherche sur les Polymères LRP, UMR/CNRS 7581 (Thiais, Fr.) in collaboration with the Université de Pharmacie (Paris V, F)

Advisors: Prof. Philippe Guérin, Dr. Estelle Renard, Dr. Valérie Langlois

1999-2001: M.S.T. in Biology and Biochemistry

Université Paris XII (Paris, Fr.) obtained with distinction

Research field: “Chemical modifications of Bacterial polymers”

Laboratoire de Recherche sur les Polymères LRP, UMR/CNRS 7581 (Thiais, F)

Advisors: Prof. Philippe Guérin, Dr. Estelle Renard

1997-1999: DEUG in Biology and chemistry

Université Paris XII (Paris, F), obtained with distinction

Research field: "Study of chemical and enzymatique polymerization of poly(β -malic acid)"
Laboratoire de Recherche sur les Polymères LRP, UMR/CNRS 7581
(Thiais, F)
Advisor: Prof. Philippe Guérin

Conferences

- Warwick 2006: International Conference on Polymer Synthesis, Warwick (UK), July 31st- August 3rd, 2006
- European Polymer Federation EUPOC 2006: Branched Macromolecular Structures, Gargnano, (Italy), May 7-12, 2006
- Polymer Science in Suisse Romande
Neuchâtel, Switzerland, November 18, 2005, poster presentation

Publications

Ternat, C., Plummer, C. J. G., Kreutzer, G., Klok, H.-A., Herrmann, A., Ouali, L., Sommer, H., Fieber, W., Velazco, M. I. and Månson, J.-A.; Physical properties of the amphiphilic star-block copolymers and encapsulation of guest molecules 2007, *in progress*

Ternat, C.; Kreutzer, G.; Plummer, C. J. G.; Nguyen, T. Q.; Ouali, L.; Herrmann, A.; Sommer, H.; Fieber, W.; Velazco, M. I.; Klok, H.-A.; Månson, J.-A. E., Amphiphilic Multi-arm Star-Block Copolymers for Encapsulation of Fragrance Molecules. *Macromolecular Chemistry and Physics* 2007, 208, 131-145.

Fieber, W., Herrmann, A., Ouali, L., Velazco, M. I., Kreutzer, G., Klok, H.-A., **Ternat, C.**, Plummer, C. J. G., Månson, J.-A. E. and Sommer, H.; NMR Diffusion and Relaxation Studies to Investigate the Encapsulation of Fragrances into Amphiphilic Multiarm Star Block Copolymers. *Macromolecules* 2007, *accepted*

Kreutzer, G.; **Ternat, C.**; Nguyen, T. Q.; Plummer, C. J. G.; Månson, J.-A. E.; Castelletto, V.; Hamley, I. W.; Sun, F.; Sheiko, S. S.; Herrmann, A.; Ouali, L.; Sommer, H.; Fieber, W.; Velazco, M. I.; Klok, H.-A., Water-soluble, Unimolecular Containers Based on Amphiphilic Multiarm Star Block Copolymers. *Macromolecules* 2006, 39, 4507-4516.

Renard, E.; **Ternat, C.**; Langlois, V.; Guerin, P., Synthesis of graft bacterial polyesters for nanoparticles preparation. *Macromolecular Bioscience* 2003, 3, (5), 248-252.

Patent

Ouali, L.; Herrmann, A.; **Ternat, C.**; Plummer, C. J. G.; Klok, H.-A.; Kreutzer, G.; Månson, J.-A. E.; Sommer, H.; Velazco, M. I. Amphiphilic Star Block copolymers. WO 2006/038110 A2, 13 April 2006, 2006.

Languages

- French: mother tongue
- English: written and spoken
- Spanish: basic understanding

Interests

- Swimming, running, skiing, hiking